Waste and Biomass Valorization
https://doi.org/10.1007/s12649-023-02355-6

ORIGINAL PAPER

TiO_2 Nanoparticles Derived from *Capparis Zeylanica*: An Effective Treatment for Diabetic and Food Borne Infections

M. Nilavukkarasi[1] · S. Vijayakumar[1] · Pradnya Jagtap[2] · Vaishali Undale[3] · Nilambari Gurav[4] · Shailendra Gurav[5] · R. Mythili[6] · Sandhanasamy Devanesan[7] · Mohamad S. Alsalhi[7] · Woong Kim[8]

Received: 1 September 2023 / Accepted: 14 November 2023

Abstract
The current work is concerned with the fabrication of titanium dioxide (TiO_2) nanoparticles (NPs) employing *Capparis zeylanica* leaf extract, as well as the investigation of the antidiabetic potential of the synthesized nanoparticles in relation to food-borne infections. Various spectroscopic and microscopic approaches were used to characterize the biosynthesized TiO_2 NPs. Synthesized TiO_2 NPs were tested for their antimicrobial activity against various microbial pathogens using the agar well diffusion technique and demonstrated effective growth inhibition. Furthermore, the dyslipidemia status of alloxan-induced diabetic rats supplemented TiO_2 NPs significantly improved. It also reduced blood glucose levels and revealed substantial changes in the liver and pancreatic profiles over the days. Therefore, the synthesized TiO_2 NPs showed potential antidiabetic and antimicrobial potential, indicating a good alternative for environmental and biological applications.

Keywords Green Synthesis · *Capparis Zeylanica* · TiO_2 NPs · Antimicrobial Activity · Food Borne Infections

Introduction

Nanomaterials exhibit atom-like behavior when split to near atomic size due to their enormous surface area and greater wide band gap between the covalent and conduct bands, resulting in increased surface energy. The global nanotechnology trend is expected to influence various biomedical research fields, including drug delivery, bioimaging, and cancer treatment. There have been several reports of metal oxide nanoparticles. Among them, Titanium dioxide (TiO_2) is an abundantly available metal oxide that comes in three distinct forms: anatase, brookite, and rutile. TiO_2NPs are white-coloured n-type semiconductors with outstanding thermal stability, optical and dielectric attributes, biocompatibility, and nontoxicity. Every year, four million tons of TiO_2 are consumed across the world. In addition, TiO_2 is one of the top five nanoparticles used in consumer products, accounting for 70% of global pigment manufacturing volume. TiO_2 can be found in paints, coatings, plastics, papers,

✉ S. Vijayakumar
svijaya_kumar2579@rediff.com

✉ Shailendra Gurav
shailendra.gurav@nic.in

[1] PG and Research Department of Botany, A.V.V.M. Sri Pushpam College, Bharathidasan University, Poondi 613053, India

[2] PDEA's S. G. R. S. College of Pharmacy, Saswad, Pune, Maharashtra, India 412 301

[3] Dr. D. Y. Patil Institute of Pharmaceutical Sciences and Research, Pune, Maharashtra, India

[4] PES's Rajaram and Tarabai Bandekar College of Pharmacy, Goa University, Ponda 403401, Goa, India

[5] Department of Pharmacognosy, Goa College of Pharmacy, Goa University, Panaji 403 001, Goa, India

[6] Department of Pharmacology, Saveetha Institute of Medical and Technical Sciences, Saveetha Dental College, Saveetha University, Chennai 600077, India

[7] Department of Physics and Astronomy, College of Science, King Saud University, P. O. Box 2455, Riyadh 11451, Saudi Arabia

[8] Department of Environmental Engineering, Kyungpook National University, Daehakro, Buk-gu, Daegu 41566, South Korea

Published online: 21 December 2023

inks, medications, pharmaceuticals, food, cosmetics, toothpaste etc.

Chronic Metabolic (CM) is a disorder that impairs glucose homeostasis, causes pancreatic-cell dysfunction, and impairs insulin production in peripheral tissues, primarily skeletal muscle and adipose tissue [1]. A 2017 study also showed that diabetes prevalence was greater in cities, with a predicted increase to 642 million by 2040, with an average of three people diagnosed per second [2]. To manage diabetes, various oral anti-hyperglycemic medicines are available on the market. However, it remains a problem for the scientific community to relieve it with minor or no adverse effects. On the other hand, plants have high performance with little or no side effects, especially regarding metabolic problems, because their efficiency derives from a combination of active chemicals evoking simultaneously [3]. Therefore, this study examined the food-born infectious microorganism and antidiabetic efficacy of *C. zeylanica*-mediated TiO_2 nanoparticles on streptozotocin-induced diabetes by *in-vivo* models.

Materials and Methods

One of the scholars gathered the *C. zeylanica* plant in the Poondi area of Thanjavur, India (10.7870^0 N, 79.1378°E). Techno Scientific Company Pvt Ltd., Trichirappalli, India, provided Titanium oxy sulphate, NaOH, and Whatman filter paper, Grade-1. The chemicals utilized in the testing were all analytical grade and had not been further refined. Deionized water was used to make all suspensions and solutions. All glassware was cleansed in mild nitric acid and dried in the oven before use.

Plant Extract Formulation, Biogenesis and Characterization of Biosynthesized TiO_2 NPs

Preparation of plant extract, biosynthesis and characterization of TiO_2 NPs were already published in our previous paper [4].

Antimicrobial Properties

The antimicrobial properties of TiO_2 NPs were determined using the conventional diffusion method technique. Pathogenic organisms like *Staphylococcus aureus* and *Staphylococcus epidermidis*, *Enterococcus faecalis* [Gram positive],, *E. coli, Shigella dysenteriae* [Gram negative], and *Candida albicans, Aspergillus niger*, and *Alternaria alternata* [fungi] cultures were evaluated, which were supplied by MTCC, Chandigarh, India. MHA (Muller Hinton Agar) and SDA (Sabouraud dextrose agar) mediums were subcultured. Then, using a micropipette, 20 µL of material was pipetted into each plate's well. As a positive control for bacteria and fungi. A 6 mm well was bored into the MHA and SDA plates. Gentamycin (5 µg) and Nystatin (50 µg) were used as a standard drug. Only distilled water was employed as a negative control. The bacterial and fungal colonies were cultivated for 24 h at 30 ± 2 °C and 37 ± 2 °C for 72 h, respectively. The tests' diameters were measured in millimetres, and each experiment was performed in triplicate [5–8].

Antidiabetic Activity Using Wister Rats

For this investigation, 200–250 g Wistar male rats were examined. Animals were given standard laboratory chow with unrestricted access to water and kept under well-ventilated settings with 12 h day and 12 h night cycles. Before starting the tests, the animals were given time to adjust to laboratory circumstances. The Institutional Research Ethics Committee of Seth Govind Raghunath Sable College of Pharmacy, Saswad, India approved the protocols, which followed agreements and rules. The animals were cared for in accordance with industry standards for lab animals. Before receiving streptozotocin injections (STZ) (70 mg/kg 1, i.p.), rats were permitted to fast for 12 h. In rats, this dosage of streptozotocin causes diabetes. Fasting blood glucose levels of more than 150 $nmolL^{-1}$ were declared diabetes five days later. Each experimental group had ten rats: (1) a normal control group, (2) a diabetic control group, (3) a diabetic group that was given metformin, (4) a diabetic group that was treated with synthesized TiO_2 NP at a dose 100 mg/kg, and (5) a diabetic group that was treated with synthesized TiO_2 NPs 200 mg /kg. The NPs were administered to diabetic Wistar rats orally every day for 28 days. Blood glucose level was measured on days 7, 14, 21 and 28 days with Glucose strips (Accucheck). On the 29th day, the rats were humanly euthanized with CO_2 in a CO_2 chamber. The pancreas and liver were isolated for histopathological investigations.

Results and Discussion

Antimicrobial Properties

The present study aimed to evaluate the antimicrobial properties of synthesized TiO_2 NPs against the selected microbial species, namely *S. aureus* and *S. epidermidis* [Gram positive], *E. faecalis, E. coli, S. dysenteriae* [Gram negative], *C. albicans, A. niger*, and *A. alternata*. The plant extract-mediated TiO_2NPs showed potent antimicrobial efficacy against *S. epidermidis* (27 mm), *S. aureus* (26 mm), *E.*

faecalis (25 mm), *E.coli* (24 mm), *S. dysenteriae* (24 mm), *C. albicans* (22 mm), *A. alternata* (21 mm), and *A. niger* (19 mm) (Table 1). As a positive control, the conventional antibiotic Gentamycin and Nystatin were utilized.

Because of the presence of hydroxyl groups, titanium nanoparticles can disintegrate the outer membranes of bacteria, resulting in the organisms' death [9]. Gram-positive bacteria were more resistant to the antibacterial impact than Gram-negative bacteria. Gram-negative bacteria's thin cell wall, which contains several layers of lipopolysaccharide and a few layers of peptidoglycan, was linked to their low antibacterial activity [5]. On the other hand, Gram-positive bacteria have a peptidoglycan cell wall that is made up of many layers. There is yet to be a reliable explanation of TiO_2 NPs' antibacterial mechanism. Punitha et al., [10] reported that TiO_2's bactericidal activity is primarily attributed to the destruction of bacterial outer membranes by Reactive Oxygen Species (ROS), mainly hydroxyl radicals (-OH), which causes phospholipid peroxidation and, finally, cell death.

Effect of Test Drugs in STZ-Induced Diabetic Rats

TiO_2 NPs have been evaluated in STZ-induced diabetes in rats. The involvement of free radicals generation and the resulting alteration of endogenous scavengers of these reactive species have been reported in STZ diabetogenicity [11]. Blood glucose levels were measured to assess the effect of NPs on glycemic control blood glucose levels every week for 28 days. On day 0 of the study in diabetic Wistar rats significant increase ($p < 0.0001$) in all the diabetic groups (DC, STD, 100 mg/kg, and 200 mg/kg) was observed as compared to the normal control group as seen in Fig. 1 (a). Also, the groups' DC, STD, 100 mg/kg, and 200 mg/kg showed non-significant differences (ns), indicating that all the groups had similarly elevated blood glucose levels. A similar study conducted by Selvan, 2008 that after 24 h treatment with STZ, the fasting blood glucose level was significantly changed in the range of 300–350 mg/dl. It was significantly ($p < 0.001$) reduced by 14 days of treatment with methanolic extract of *Artanema sesamoides* [12].

After starting the treatment in the study groups, a decrease in blood glucose levels in treatment groups (STD, 100 mg/kg and 200 mg/kg) was observed compared to the diabetic control group. However, a reduction in the blood glucose level has initiated on day 7; as observed in Fig. 1 (b), it is statistically non-significant. This might be because of the time required for NP to reach optimum effective concentration at the site of action. On days 14, 21 and 28 of the study, as seen in Fig. 1 (c, d, e) significant ($p < 0.001$) reduction in blood glucose levels in all the treatment groups (STD, 100 mg/kg and 200 mg/kg) as compared to DC was observed. No significant difference between STD and the 100 mg/kg and 200 mg/kg was observed, indicating the treatment of 100 and 200 mg/kg produces a similar reduction in blood glucose levels. A consistent decrease in the glucose level in NP treated group signifies NP's antidiabetic potential, which might be due to the antioxidant property of NP. Also, the NP shows a non-significant difference compared to STD (metformin-treated group) directing toward hypoglycemic action of NP similar as well proven and widely used OHA. Therefore, TiO_2 NP is ameliorating the glycemic parameter signifying the antidiabetic potential of the NP. Similarly, Nagaraja et al., [13] reported that 200 and 400 mg/kg dosages displayed a much greater activity level than a conventional drug.

Figure 1(f) shows the blood glucose level reduction on days 0, 7, 14, 21, and 28 cumulatively. On days 0 and 7, a comparable reduction in blood glucose was not observed, signifying although the treatment had started, a significant reduction had not been produced. While from day 14 to 28 consistent decrease in blood level followed, which is almost close to the normal control group's blood glucose level. Ogbonnia et al., [14] has reported a significant reduction in Blood glucose level in STZ-induced diabetes by extracts of *T. africana* leaves and *B. pinnatum* plants and their mixture, in an equal proportion,

Table 1 Antimicrobial activity of eco-synthesized TiO_2NPs using *C. zeylanica*

S.No	Name of the Organisms	Zone of inhibition (ug/ml^{-1})				
		Plant extract	$TiOSO_4$	TiO_2	Positive Control	Negative Control
1.	***S. aureus***	08 ± 1.24	12 ± 1.30	26 ± 2.04	15 ± 1.55	0
2.	***S. epidermidis***	08 ± 1.33	13 ± 1.33	27 ± 2.05	16 ± 1.67	0
3.	***E. faecalis***	07 ± 1.24	11 ± 1.32	25 ± 1.54	14 ± 1.35	0
4.	***E. coli***	07 ± 1.09	09 ± 1.23	24 ± 1.49	13 ± 1.32	0
5.	***S. dysenteriae***	05 ± 0.88	10 ± 0.19	23 ± 1.37	12 ± 1.27	0
6.	***C. albicans***	08 ± 1.05	12 ± 0.18	22 ± 0.93	10 ± 1.05	0
7.	***A. niger***	06 ± 0.98	11 ± 1.3	19 ± 1.56	09 ± 0.67	0
8.	***A. alternate***	05 ± 0.88	10 ± 0.93	21 ± 1.86	11 ± 0.98	0

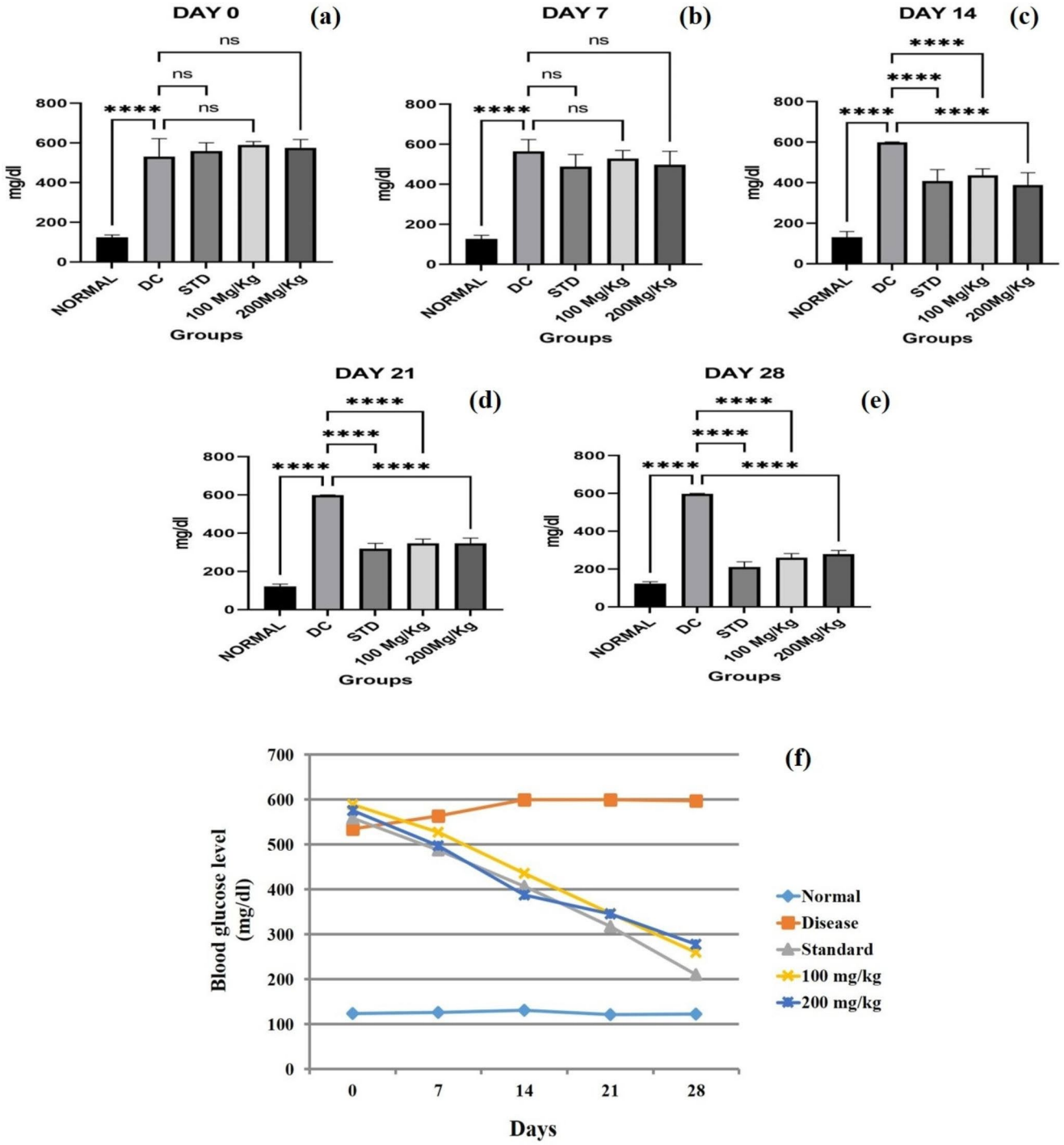

Fig. 1 All values are expressed as Mean ± SEM. n = 6. All data are subjected to One Way ANOVA followed by Bonferroni's multiple comparison test. DC: Diabetic control is compared with the Normal control group, STD: standard drug-treated group, 100 mg/kg and 200 mg/kg: Herbal drug treatment groups compared with the Diabetic control group.* ***$p < 0.0001$, ns :Not Significant

Effect of Test Drugs on Histology of Pancreas in STZ-Induced Diabetic Rats

The histopathological studies showed more than 75% pathological changes in the pancreas (Fig. 2) in DC compared to normal control indicating the pancreatic cells were damaged due to the action of STZ. The treatment groups Std,100 mg/kg, and 200 mg/kg showed fewer pathological changes (50%) compared to DC, suggesting that treatment with the test drug reduces pancreatic tissue damage and,

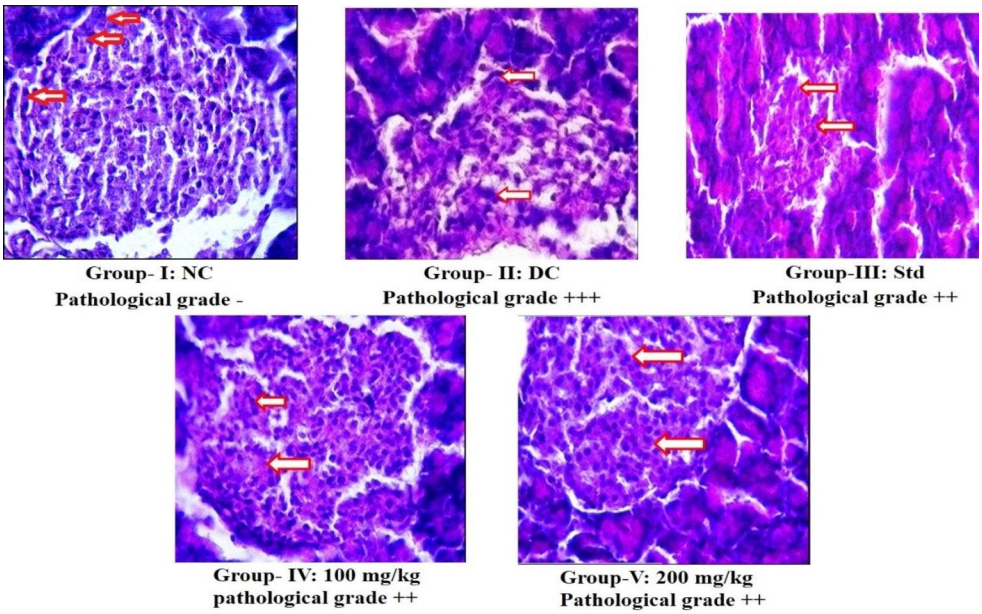

Fig. 2 Pancreas was observed for the following findings under 400X after staining with hematoxylin stain. i) Beta cells (slightly elongated cells red arrow) **Pathological grade**: Grade: -- no injury; Grade: +++ severe injury; Grade: ++ moderate injury; Grade: + mild injury

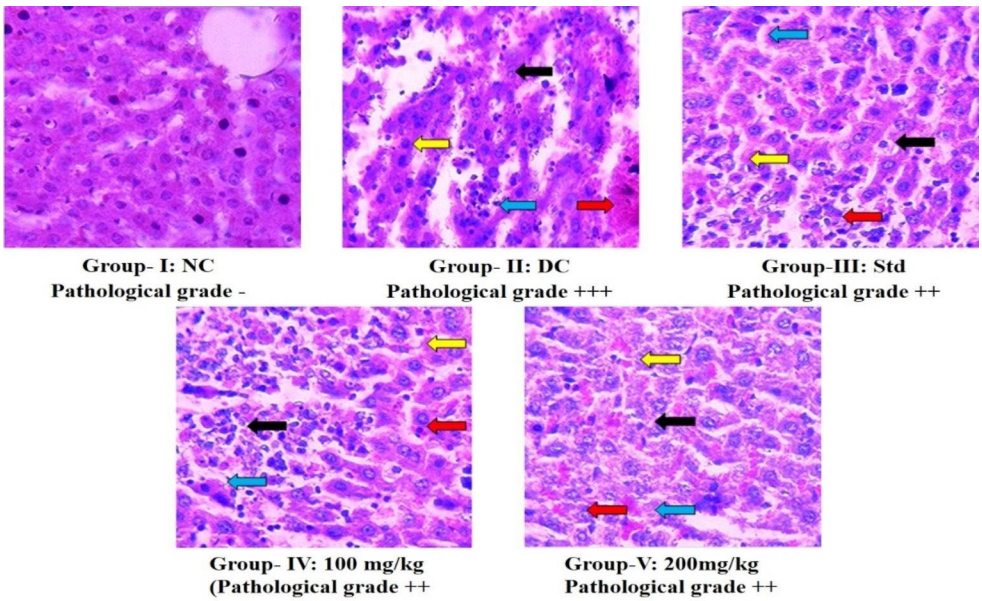

Fig. 3 Liver tissue was observed for the following findings under 400X after staining with hematoxylin stain. i) Swelling of hepatocytes (yellow arrow), ii) Congestion & hemorrhages (red arrow), iii) Necrosis of hepatocytes (black arrow), iv) Leucocytic infiltration (blue arrow) **Pathological grade**: Grade: -- no injury; Grade: +++ severe injury; Grade: ++ moderate injury; Grade: + mild injury

thereby, beta cells correlating with its antidiabetic potential. Furthermore, the study showed that zinc oxide nanoparticles significantly reduced blood glucose in diabetic rats. In inference, the nanoparticles of zinc oxide act as proponents' antidiabetic agent [15].

When type 2 diabetes (T2D) is still in its early stages, the excess fat in the cells can be removed, restoring normal function to the pancreatic beta cells that are not producing enough insulin. A study by Selvan et al. [12] reported the histopathological changes in the liver and kidney in diabetic control groups while restoration of the histopathological changes in the pancreas in groups treated with methanolic extract of *Artanema sesamoids.*

Effect of Test Drugs on Histology of the Liver in STZ-Induced Diabetic Rats

The liver plays a vital role in the metabolism and elimination of drugs and their metabolites. Therefore, the histopathology of liver tissue was carried out to confirm the deleterious effect of NPs on the liver, if any. The histopathological studies showed more than 75% pathological changes in liver (Fig. 3) in DC rats compared to normal control rats. On the other hand, the treatment groups Std, 100 mg/kg, and 200 mg/kg showed fewer pathological changes (50%) compared to DC, suggesting that treatment with the NPs protects against liver tissue damage compared to the STZ-treated

group. The histopathological studies after treatment with a polyhedral formulation, ESF/AY/500 in streptozotocin-induced diabetic male Albino rats has been reported no pathological changes in the histology of liver, kidney, and pancreas as compared to a diabetic control group [16].

Conclusion

Based on the findings, we deduced that this work's green manufacture of TiO_2 NPs using *C. zeylanica* leaf extracts might effectively cure food-borne illnesses and diabetes. It was discovered that the TiO_2 NPs significantly reduced the growth of both bacterial and fungal strains. TiO_2's bactericidal action is generally ascribed to Reactive Oxygen Species (ROS), particularly hydroxyl radicals (-OH), which break down the outer membranes of bacteria, leading to phospholipid peroxidation and ultimately cell death. The glycemic parameter, which indicates the NP's capacity to prevent diabetes, is being improved by TiO_2 NP. These results may contribute to the creation of a practical nanoparticle platform for drug discovery studies aimed at treating food-borne infections and diabetes.

Acknowledgements We express our gratitude to the management of A.V.V.M. Sri Pushpam College (Autonomous), Poondi, for providing us with the necessary support and research facilities to complete this work. This research was funded by DST-FIST (SR/FST/ College- 222/2014), DBT- STAR (HRD-11011/18/2022-HRD-DBT). The authors express their sincere appreciation to the Researchers Supporting Project Number (RSP2023R398) King Saud University, Riyadh, Saudi Arabia.

Declarations

Ethics approval and consent to participate All the biological studies were performed following the Committee for the Purpose of Control and Supervision of Experiment on Animals (CPCSEA) guidelines and with prior approval (PES's RTBCOP/IAEC/2021/R-90) of the Institutional Animal Ethics Committee (Registration No. 1659/PO/RE/S/12/CPCSEA). We hereby confirm that the study is reported following ARRIVE guidelines (https://arriveguidelines.org).

Conflict of Interest The authors declared no conflict of interest.

References

1. Vijayan, M., Jose, R., Jose, S., Abraham, S., Joy, J.: Study on quality of Life Assessment in Diabetic Retinopathy among patients with type 2 Diabetes. Asian J. Pharm. Clin. Res. **10**, 116–119 (2017)
2. Zou, Q., Qu, K., Luo, Y., Yin, D., Ju, Y., Tang, H.: Predicting Diabetes Mellitus with Machine Learning techniques. Front. Genet. **9**, 515 (2018)
3. Guo, Y., Jiang, N., Zhang, L., Yin, M.: Green synthesis of gold nanoparticles from Fritillaria Cirrhosa and its anti-diabetic activity on Streptozotocin induced rats. Arab. J. Chem. **13**, 5096–5106 (2020)
4. Nilavukkarasi, M., Vijayakumar, S., Kalaskar, M., Nilambari, G., Shailendra, G., Praseetha, P.K.: Capparis Zeylanica L. conjugated TiO2 nanoparticles as bio-enhancers for antimicrobial and chronic wound repair. Biochem. Biophys. Res. Commun. **623** (2020)
5. Vembu, S., Vijayakumar, S., Nilavukkarasi, M., Vidhya, E., Punitha, V.N.: Phytosynthesis of TiO_2 nanoparticles in diverse applications: What is the exact mechanism of action? J. Sens. **3**, 100161 (2022)
6. Khashayar, S., Majid, B., Ran, W., Mohammad, R.K.: Distribution of antimicrobial resistance genes and integrons among Shigella spp. isolated from water sources. J. Glob Antimicrob. Resist. **19**, 122–128 (2019)
7. Khashayar, S., Lili, Z., Abbas, S.D., Majid, K., Abolghasem, H., Hongduo, B., Mohadeseh, B., Mojtaba, M., Maoda, P., Tao, H., Majid, B., Ran, W.: Effective control of Shigella contamination in different foods using a novel six-phage cocktail. LWT **144** (2021)
8. Majedeh, B., Akbar, H.N., Hesam, A.B., Sepideh, H., Issa, A., Farzaneh, F.: An overview of modified sensors with focus on electrochemical sensing of sulfite in food samples. Eurasian Chem. Commun. **3**, 116–138 (2021)
9. Subhapriya, S., Gomathipriya, P.: Green synthesis of titanium dioxide (TiO_2) nanoparticles by Trigonella foenum-graecum extract and its antimicrobial properties. Microb. Pathog. **116**, 215–220 (2018)
10. Punitha, V.N., Vijayakumar, S., Sakthivel, B., Praseetha, P.K.: Protection of neuronal cell lines, antimicrobial and photocatalytic behaviours of eco-friendly TiO_2 nanoparticles. J. Environ. Chem. Eng. **104343** (2020)
11. Srinivasan, K., Ramarao, P.: Animal models in type 2 Diabetes research: An overview. Indian J. Med. Res. **125**, 451–472 (2007)
12. Selvan, V.T., Manikandan, L., Senthil Kumar, G.P., Suresh, R., Kakoti, B.B., Gomathi, P.: Antidiabetic and antioxidant effect of methanol extract of Artanema sesamoides in streptatozocin-induced diabetic rats. Int. J. Appl. Res. Nat. Prod., 25–33 (2008)
13. Nagaraja, S., Ahmed, S.S., Goudanavar, P., Fattepur, S., Meravanige, G., Shariff, A., Shiroorkar, P.N., Habeebuddin, M.: Green Synthesis and characterization of silver nanoparticles of Psidium guajava Leaf Extract and evaluation for its antidiabetic activity. Molecules. **27**, 4336 (2022)
14. Ogbonnia, S., Odimegwu, J., Enwuru, V.: Evaluation of hypoglycaemic and hypolipidaemic effects of aqueous ethanolic extracts of Treculia africana Decne and Bryophyllum pinnatum, Lam. And their mixture on streptozotocin (STZ)-induced diabetic rats. Afr. J. Biotech. **7**, 2935–2939 (2008)
15. Neha, S., Reena, L.: Anti-diabetic property of Green Synthesized Zinc-Oxide nanoparticles from Leaf Extract of *Chrysanthemum indicum* Plant. Rasayan J. Chem. **13**, 570–573 (2020)
16. Sajeeth, C.I., Manna, P.K., Manavalan, R., Jolly, C.I.: Antidiabetic activity of a polyherbal formulation, ESF/AY/500 in streptozotocin induced diabetic male albino rats: A Research. Int. J. Drug Dev. Res. **1**, 311–322 (2010)

ISSN 2231–5683 (Print)
2231–5691 (Online)
DOI: 10.52711/2231-5691.2024.00012

Vol. 14 | Issue-01|
January – March | 2024

Available online at
www.anvpublication.org

Asian Journal of Pharmaceutical Research (AJPRes.)
Home page *www.asianjpr.com*

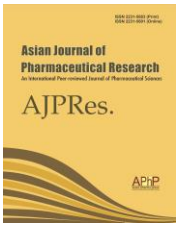

REVIEW ARTICLE

Pathophysiology, Diagnosis and Management of Cataract

Vaishnavi Pradeep More[1]*, Pradnya Nilesh Jagtap[2], Sumit Kailas Musale[3], Ankita Mahadeo Kadam[4], Shweta Shivaling Bobade[5], Komal Dattatray Pol[6]

[1]Master of Pharmacy, Department of Pharmacology,
PDEA's Seth Govind Raghunath Sable College of Pharmacy, Saswad, Pune, India.
[2]Head of Department of Pharmacology,
PDEA's Seth Govind Raghunath Sable College of Pharmacy, Saswad, Pune, India.
[3]Assistant Professor, Department of Pharmacology,
PDEA's Seth Govind Raghunath Sable College of Pharmacy, Saswad, Pune, India.
[4]Master of Pharmacy, Department of Pharmacology,
PDEA's Seth Govind Raghunath Sable College of Pharmacy, Saswad, Pune, India.
[5]Master of Pharmacy, Department of Pharmacology,
PDEA's Seth Govind Raghunath Sable College of Pharmacy, Saswad, Pune, India.
[6]Master of Pharmacy, Department of Pharmacology,
PDEA's Seth Govind Raghunath Sable College of Pharmacy, Saswad, Pune, India
*Corresponding Author E-mail: **morevaishnavi1203@gmail.com**

ABSTRACT:

In order to properly focus light onto the retina for the best image quality, the human lens and cornea must first refract light. The human lens changes physically, biochemically, and morphologically as we age, which causes opacification. Cataract, which is opacity within the clear lens of the eye, is the primary factor in blindness globally. Modification, aggregation and precipitation of crystallins are the main mechanisms underlying cataract development. Most cataracts are caused by age-related degeneration; however, cataract can also develop secondary to trauma or as a consequence of another disease. Cataract rarely occurs in children. Oxidative damage to the eye lens is believed to be a key factor in the beginning and development of cataracts, even if the nosogenesis of cataract is unclear. Different kinds of cataract formation are linked to a number of highly reactive oxygen species (ROS), including hydrogen peroxide (H_2O_2), superoxide anion (O_2), nitric oxide (NO), and hydroxyl radicals (OH^-). Surgery is the only option for treating cataracts. However, the lack of surgical facilities in underdeveloped and developing nations as well as post-operative difficulties drive researchers to discover alternative cataract treatment options. This review article provides details on anatomy and physiology of lens, different cataract types i.e., diabetic, pediatric, age-related cataract as well as the management of cataract including surgical and pharmacological treatments.

KEYWORDS: Opacity, Crystallins, Oxidative damage, Post-operative, Aggregation, Opacification, Blindness.

INTRODUCTION:

The most common reason for blindness in older individuals worldwide, particularly in developing nations, is cataract[1]. An estimated 20 million people worldwide are blinded as a result of aging-related cataracts. When cataracts interfere with daily life, surgery to replace the hazy lens with an artificial lens has emerged as the gold standard for treating the condition[2].

Received on 09.05.2023 Modified on 18.07.2023
Accepted on 28.09.2023
Asian J. Pharm. Res. 2024; 14(1):77-82.
DOI: 10.52711/2231-5691.2024.00012

However, the operation is not always an accessible medical option, particularly in low- and middle-income nations. Additionally, cataract surgery can have a negative impact on patients' quality of life and lay a heavy burden on healthcare systems by increasing the likelihood of vision-related concerns including posterior capsule opacification, particularly in newborns and young children[3-5].

Uncorrected refractive error was the main global cause of moderate to severe visual impairment, followed by cataract, and cataract was the leading global cause of blindness overall. From 1990 through 2010, this frequency-based ranking remained constant. However, when the causes of blindness were examined regionally, significant disparities became clear. Cataract-related blindness rates in 2010 ranged from 15% or less in high socioeconomic areas to >40% or more in south and southeast Asia and Oceania[6,7]. Similar to blindness, wealthier socioeconomic regions had the lowest percentage of moderate to severe vision impairment brought on by cataract (13.0–13.8%), whereas south and southeast Asia had the highest incidence (both >20%).

Oxidative damage to the eye lens is believed to be a key factor in the beginning and development of cataracts, even if the nosogenesis of cataract is unclear[8]. Different kinds of cataract formation have been linked to a number of highly reactive oxygen species (ROS), including hydrogen peroxide (H_2O_2), superoxide anion (O_2), nitric oxide (NO), and hydroxyl radicals (OH^-). Therefore, a lot of work has gone into finding potent antioxidative pharmacological drugs[9].

On the level of public health, doctors and ophthalmologists view cataract-related blindness as a challenging problem. Surgery is the only way to treat it, which places a heavy financial strain on society. Therefore, strategies have been developed to lessen the impact of this problem by identifying and maybe altering elements that will result in the prevention of the disease, or at the at least, delay it (up to 10 years). This was observed to result in a 45% or more reduction in the frequency of procedures[10]. Therefore, when it comes to cataract, attempts have been made to concentrate on preventive medicine.

Various types of cataracts:

1. Pediatric cataract:

One of the most significant surgically curable causes of infant blindness is pediatric cataract. Treatment of pediatric cataract has a significant social impact since it can prevent "lost years of blindness." There are many known morphological types, but zonular has the best visual prognosis.

The morphology of the cataract is significant for a number of reasons, including the age at which it first appears, heredity, and causation, as well as its potential significance for visual prognosis. Lamellar cataracts and posterior lenticonus fare better than other morphological forms, although thick central cataracts perform very poorly. Trisomy 21, acute metabolic cataracts, and congenital rubella all cause total cataracts that almost completely cover the lens, but they can also occur in familial or sporadic cases.

The outer zones of the lens liquefy while the nucleus of congenital Morgagnian cataracts is unaffected. The nucleus can now descend by gravity in any direction, depending on where the head is located. The final step of the lens' re-absorption is represented by membrane cataracts, which either leave a disc of lens material or merged anterior and posterior capsules. It is frequent in PFV, trauma, congenital rubella, and PFV. The most typical kind of congenital cataract is the zonular cataract. It affects one or more lens zones or layers. These cataracts are typically inherited as an autosomal dominant trait or idiopathic.

They often consist of a layer of tiny white dots in one or more layers of the lens and are bilateral but slightly asymmetrical. Although occasionally involving the foetal nucleus and having clear I, cortex outside of them, the embryonic nucleus is spared. There is frequently significant intra- and inter-ocular variation. Morphologically, a cataract is frequently incomplete and may have what are referred to as "riders" on the edges. The visual prognosis is better than in many other morphological kinds, particularly in partial cataract.

A specific variety of zonular cataract known as a sutural cataract is marked by opacities that surround or involve the sutures. The variations, which are frequently familial, range from an increased suture density to a variety of whitish or cerulean dots grouped around one or both sutures. If they don't reach the nuclear stage, they are visibly unimportant. The anomalies of lens vesicle detachment are anterior polar and anterior pyramidal cataracts. Compared to anterior polar cataracts, anterior pyramidal cataracts are more likely to progress and be visually prominent. They could separate, creating an anterior chamber foreign body. The condition known as anterior lenticonus can be spontaneous or connected to other diseases. Alport's syndrome is characterised by bilateral anterior lenticonus. It can be a symptom of a problem with the basement membrane. About 10% of young children with it have a congenital condition, although its prevalence might rise to 30% over time.

The posterior lens capsule thins and bows in the back due to posterior lenticonus, which can be unilateral, bilateral, or asymmetrical. The patient may either lack a

cataract or have a high degree of astigmatism, which is frequently irregular. If cataracts are present, they could be localised or progressive. Unlike anterior lenticonus, it rarely has any systemic illness associated with it. It may be autosomal dominant, sporadic, or X linked.[11]

There are various cataract types and causes in children.

- A child's cataracts may be acquired or congenital (existing at birth) (develop as an infant, child, or adolescent).
- One or both of the eyes may develop cataracts. One cataract may be worse than the other when there are two.
- Cataracts can range in size from microscopic spots to dense clouds and can occur in various locations on the lens.
- Cataracts can be brought on by genetics, metabolic conditions including diabetes, and ocular trauma.[12]

2. Age related cataract:

Age-related cataract, also known as senile cataract, is a cataract that develops in adults over 50 without being caused by recognised mechanical, chemical, or radiation stress. In the aged, it worsens and occurs more frequently[13]. It is classified as:

a. Nuclear cataract:

As the lens ages, additional layers of fibres are added, the lens nucleus is compressed and hardened (a condition known as nuclear sclerosis cataract), and the lens also turns yellower as a result. Nuclear sclerosis develops gradually over many years. In other situations, it has only a minor impact on vision or results in a myopic shift, also known as second sight because reading glasses may no longer be required. Further advancement can lead to loss of eyesight, usually more at a distance than up close, as well as loss of color differentiation.

b. Cortical cataract:

The most recent lens fibres make up the cortex of the lens. With age, no fibres are lost, and new fibres are introduced to the lens' exterior, hidden beneath the lens' outer coating or capsule. When the visual axis or the entire cortex is affected, the lens turns white and is referred to as mature. Discrete opacities (cortical spokes) can form within the lens cortex with age but usually do not cause any visual symptoms.

c. Posterior sub capsular cataract:

Granular opacities known as cataracts mostly affect the central posterior cortex, right behind the posterior capsule. They can occur in younger individuals, are frequently accompanied by glare complaints, such as when driving at night, and tend to impair near vision more so than far vision.[14]

The lens will become thicker and heavier as it ages, which are the most noticeable changes. With age, a diffusion barrier forms between the lens nucleus and the nutrients and endogenous antioxidants that are given by the lens cortex and epithelium due to the lens nucleus' ongoing expansion. Existing cells are not biodegraded as a result of the absence of protein turnover, and lens proteins, especially the older ones found in the nucleus, are susceptible to PTMs like deamidation, glycation, phosphorylation, loss of bound water, cross-linking, and protein aggregation. Additionally, if the coloration is sufficiently dense, it might lead to an age-related nuclar cataract. This coloration of the lens is caused by the accumulation of chromophores and fluorophores.[15]

3. Diabetic cataract:

The prevalence of diabetes mellitus (DM), a chronic systemic disease, has risen over time. All ocular structures may be impacted by DM, with cataract being the most frequent ocular complication. The most common reason for blindness in the world is cataract. The incidence of cataract formation is higher in the diabetic population due to a number of causes.

a. Pathway for polyol:

A hyperosmotic effect caused by the increased intracellular sorbitol buildup causes hydropic lens fibres to degenerate and produce cataract. Compared to non-diabetic patients, diabetes patients produce sorbitol more quickly than the enzyme sorbitol dehydrogenase can break it down into fructose. Because sorbitol is polar, diffusion-based intracellular clearance of the substance is also avoided. When sorbitol builds up and fluid is infused, the consequence is a hyperosmotic reaction. The production of lens opacities is caused by the liquefaction of lens fibres caused by the intracellular accumulation of polyols.

b. Oxidative and osmotic stress:

Another contributing factor in the rapid development of cataracts, particularly in young individuals with type 1 DM, is osmotic stress brought on by the considerable swelling of the cortical lens fibres. The major location of protein synthesis, the endoplasmic reticulum (ER), is stressed by osmotic stress brought on by the buildup of sorbitol, which creates free radicals. An unfolded protein response that results in reactive oxygen species and damages lens fibres under oxidative stress is another factor that can lead to stress in the ER. Additionally, elevated glucose levels in the aqueous humour can cause lens proteins to glycate, which creates advanced glycation end products. Hydroxyl radicals (OH-) are also generated after entering the lens as a result of Fenton reactions brought on by high levels of hydrogen peroxide (H_2O_2) in diabetics' aqueous humor. Free radical nitric oxide (NO•), which may promote peroxynitrite generation and contribute to cell damage due to its

oxidising capabilities, is another component that is raised in the lens and aqueous humour of diabetes patients. However, because of their reduced antioxidant capacity, diabetic lenses are more vulnerable to oxidative stress. The most prevalent antioxidant enzyme in the lens that converts superoxide radicals (O_2-) into H_2O_2 and oxygen is called superoxide dismutase (SOD).[16]

Diagnosis of cataract:

An eye exam that may include the following investigations can determine the degree of visual deterioration that represents the asperity of the cataract.

- **Refraction test:** This test determines whether wearing glasses can improve vision.
- **Visual acuity test:** A visual awareness eye test is the same as the yearly eye exams that an ophthalmologist performs on everyone. The ability to read letters of gradually smaller sizes is tested individually for each eye using a viewing device or an eye chart. The doctor can determine how much the cataract has impacted vision using this technique. Visual aptitude is a gauge of how well someone can see.
- **Testing of contrast sensitivity:** Tests for visual acuity and contrast sensitivity are similar, but contrast sensitivity testing more clearly demonstrates how cataracts reduce image contrast due to light glare and scattering. This test is based on the ability to distinguish between different shades of grey because a cataract may impair this ability.
- **Testing for color vision:** Aids in identifying acquired color vision defects that may be present in cataract patients.
- **Testing for glare:** Different lighting conditions, such as at night and in blazing sunshine, can alter vision. By having a patient read the chart twice, once with and once without bright lights, these marks can be determined under various types of lighting.
- **Potential acuity testing:** A test that provides a rough idea of what the vision will be like after cataract surgery and is interpreted as the eye's vision power in the absence of a cataract.
- **Spectacular photographic microscopy:** A specialized microscope is used to take a picture of the endothelial layer of the cornea. This is typically done in advance of cataract surgery to assess the endothelium's condition, which could have an impact on the procedure's outcome.
- **Retinal examination:** Eye drops are used to dilate the pupils prior to the retinal examination so that the retina can be seen more clearly. To detect cataracts, macular degeneration, glaucoma, and other issues with the optic nerves and retina that may be the source of vision loss, an ophthalmoscope or slit-lamp is used.
- **Slit-lamp examination:** Conducted using a specialized microscope called a slit-lamp that shines a powerful, thin beam of light into the eye to provide an enhanced three-dimensional view of the interior of the eye. The structures at the front of the eye, such as the iris, cornea, and lens, as well as the region between the cornea and iris, can all be examined in section by manual detection in order to look for any abnormalities.
- **Tonometry:** Using a specialized instrument, a test can be performed to determine the intraocular pressure (IOP), or pressure inside the eye. Injected eye drops are an option.[17]

Management of cataract:

When a cataract affects visual function, it is necessary to replace the clouded crystalline lens with an IOL that has the right refractive power in order to restore the transparency of the optical pathway. Due to our ability to measure the optical parameters of the eye, sophisticated technologies to remove the cataract, and ongoing advancements in IOL design, current surgical techniques achieve these goals with accuracy, reproducibility, and safety. The majority of the surrounding clear lens capsule is preserved during extracapsular cataract surgery in order to support the IOL indefinitely. To suspend and support the lens, zonules (microscopic ligaments) affix and insert circumferentially onto the lens capsular equator. The large, firm lens nucleus and the softer surrounding cortex are removed following creation of a central opening in the anterior capsule. The IOL is then positioned anterior to the remaining clear posterior capsule within the vacated capsular bag.

- **Various surgical techniques:**

1. Phacoemulsification:

In order to break up the rigid lens nucleus, phacoemulsification uses ultrasonic energy to vibrate a titanium needle at high frequencies. The resulting emulsate is aspirated from the eye at the same time. Phacoemulsification was first developed by Charles Kelman in the late 1960s. The advantage of using phacoemulsification over only manual techniques is the ability to remove the large nucleus through a 3.0mm-long incision. Then, through this small incision (which is typically not necessary to be stitched) foldable IOLs are implanted. Surgery can now be performed through 2.2 mm mini-incisions or 1.8 mm micro-incisions thanks to advancements in equipment and needles. However, using micro-incisions necessitates the use of unique IOLs. Smaller incisions have many benefits, including the ability to use topical anaesthesia rather than local injection anaesthesia, especially if the incision is made in the peripheral cornea, better intraocular environment control, increased safety should the patient move, quick restoration of the incision's structural integrity, reduced post-operative physical restraints, and a reduced risk of corneal shape changes. Phacoemulsification has been the industry standard in developed nations for more than 20

years due to its ability to reduce astigmatism and speed up physical and visual rehabilitation. Cost and other factors influence the prevalent use of manual techniques in developing nations. Phacoemulsification and other surgical technology advancements have increased the safety and reproducibility of small incision cataract surgery, though they do not replace a surgeon's unique surgical skill. The nuclei of the most advanced cataracts, which have larger and harder nuclei, are a case in point. The development of surgical microscopes has been crucial, as with any microsurgery. Additionally, improvements are made in viscoelastics, transparent viscous gels the surgeon uses to shield the intraocular structures from trauma during surgery. The risk of corneal decompensation (corneal oedema brought on by the corneal endothelium's inability to keep the cornea relatively dehydrated) has decreased as a result of improved viscoelastics. The advantages of using femtosecond laser technology to automate some surgical procedures are being assessed. The majority of IOLs are made of silicone or acrylic plastic, which allows the lens to be folded. The initial goal of IOL research was to create the safest design. To further improve the optical properties, more developments were made. Modern IOLs prevent secondary posterior capsule opacification, reduce unwanted optical spherical aberration, and block UV light. IOLs are available in a variety of refractive powers, just like other corrective lenses. Toric lenses and multifocal lenses are two new IOL designs that address astigmatism and presbyopia to lessen the need for glasses. Surgery to remove cataracts has become one of the most popular refractive procedures thanks to modern technology and IOLs. Other tools, such as iris retractors, pupil expansion rings, capsule retractors, and capsular tension rings, help difficult eyes with smaller pupils or abnormal zonules undergo successful surgery. Finally, the success rate with mature white cataracts has increased thanks to dyes that stain and make the anterior capsule more visible.

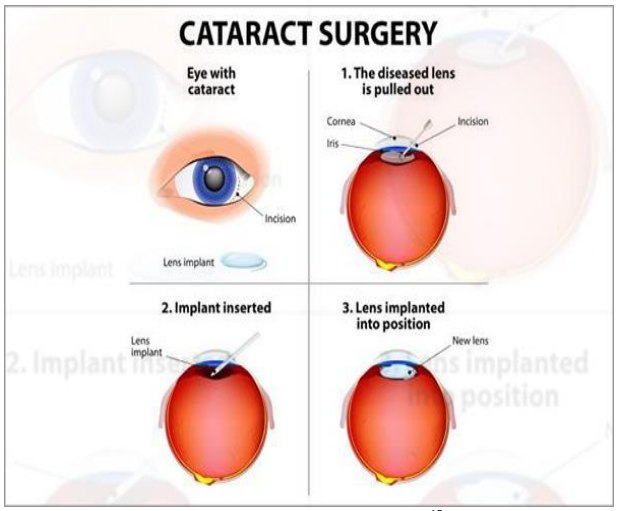

Fig. No. 1 Phacoemulsification[18]

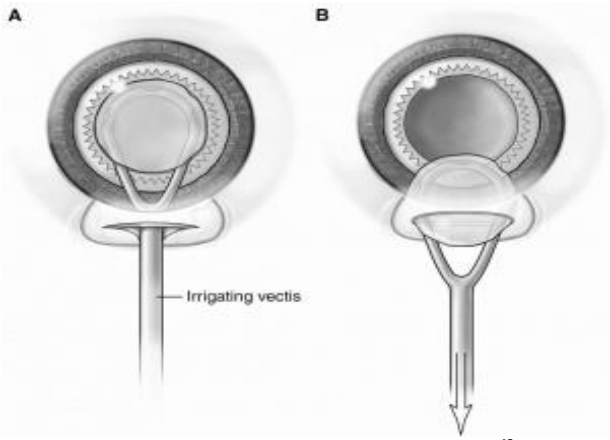

Fig.No. 2 MSICS as well as modified MSICS [19]

2. Msics as well as modified msics:

In the developed world, phacoemulsification is the gold standard for cataract removal. However, using it in societies that are less developed economically raises a number of problems. Compared to manual methods, it requires a significant initial investment in the phacoemulsification equipment and much higher ongoing costs for medical supplies. In developing nations, the expense and level of expertise required for equipment maintenance is also a concern. Additionally, phacoemulsification requires more time and effort to learn than manual cataract surgery, and developing nations may not have the necessary teaching resources or facilities. Last but not least, the manual technique is preferable for treating hard and mature cataracts, which are more prevalent in underprivileged populations.

As a result, alternative surgical methods for cataract surgeries in developing nations have been developed. A sutureless M-SICS technique is the most widely used. Sutureless large incision manual cataract extraction (SLIMCE) is one of the MSICS technique modifications that is becoming more and more popular, particularly in China. All of these adjustments make use of a longer, sutureless scleral tunnel incision to reduce astigmatism and quicken the physical and visual recovery, as well as a larger incision to increase the safety of cataract removal. Compared to phacoemulsification, MSICS produces excellent results at a lower cost and faster surgical time. Aside from being quick and inexpensive, MSICS is also simpler to learn for novice surgeons and, in their hands, is safer for advanced mature cataracts. Additionally, MSICS rarely results in dropped nuclei, a serious side effect of cataract surgery that involves the nucleus dislocating onto the retina. If this complication is not properly managed by a vitreoretinal specialist, a rare subspecialty in many developing nations, it has a poor prognosis. Phacoemulsification and MSICS are both risk-free and offer superior visual results.[20]

- **Pharmacological treatments:**

Table no.1: Pharmacological treatments of cataract[21]

Pharmacological group	Advantages	Disadvantages
Aspirin/aspirin-like drugs, for example, aspirin, ibuprofen and paracetamol	Antidenaturating agents by acetylation of lens proteins Weak antioxidants and plasma sugar lowering properties Effective both systemically and topically	Major systemic side effects, for example, gastric ulcer and renal impairment Ocular side effects, for example, stinging and corneal disorders Further investigations and clinical trials yet to be done on different cataract models
Protein stabilizers/protectors, for example, bendazac and hydroxy bendazac	Inhibit protein aggregation and Denaturation delays post-translational modifications Effective both systemically and topically	Long-term safety on ocular tissues is understudied Not supported by large groups clinical trials
Opioid growth factor antagonist, for example, naltrexone	Maintaining lens epithelial density Protecting against dry-eye induced cataractogenesis Enhancing transport of endogenous antioxidants and precursors to the lens nucleus	Over-activation of lens fibres could prompt building up of the diffusion barrier to lens nucleus Lens opacity due to over-expression of ascorbic acid transporters Not supported by research or clinical trials
Flavonoids, for example, quercetin, diosmin and curcumin	Antioxidant properties Aldose reductase inhibitors	Poor water solubility Chemically unstable Not supported by large groups clinical trials
N-acetyl carnosine	Antioxidant properties Antiglycating properties reverse cataractous lenses	Not supported by large groups clinical trials One-centre studies

CONFLICT OF INTEREST:

The authors have no conflicts of interest regarding this investigation**.**

ACKNOWLEDGMENT:

We are thankful to PDEA's Seth Govind Raghunath College of Pharmacy, Saswad, Pune, Maharashtra, India for providing laboratory facility for this research work.

REFERENCES:

1. Congdon NG, Friedman DS, Lietman T. Important causes of visual impairment in the world today. JAMA. 2003; 290(15): 2057-60. doi: 10.1001/jama.290.15.2057.
2. Lamoureux EL, Fenwick E, Pesudovs K, Tan D. The impact of cataract surgery on quality of life. Curr Opin Ophthalmol. 2011; 22(1): 19-27. doi: 10.1097/ICU.0b013e3283414284.
3. Apple DJ, Solomon KD, Tetz MR, Assia EI, Holland EY, Legler UF, Tsai JC, Castaneda VE, Hoggatt JP, Kostick AM. Posterior capsule opacification. Surv Ophthalmol. 1992; 37(2): 73-116. doi: 10.1016/0039-6257(92)90073-3
4. Apple DJ, Peng Q, Visessook N, Werner L, Pandey SK, Escobar-Gomez M, Ram J, Whiteside SB, Schoderbeck R, Ready EL, Guindi A. Surgical prevention of posterior capsule opacification. Part 1: Progress in eliminating this complication of cataract surgery. J Cataract Refract Surg. 2000; 26(2): 180-7. doi: 10.1016/s0886-3350(99)00353-3.
5. Hodge WG. Posterior capsule opacification after cataract surgery. Ophthalmology. 1998; 105(6): 943-4. doi: 10.1016/S0161-6420(98)96040-7.
6. Li EY, Liu Y, Zhan X, Liang YB, Zhang X, Zheng C, Jhanji V, Xu P, Chang DF, Lam DS. Prevalence of blindness and outcomes of cataract surgery in Hainan Province in South China. Ophthalmology. 2013; 120(11): 2176-83. doi: 10.1016/j.ophtha.2013.04.003. Epub 2013 May 25.
7. Pascolini D, Mariotti SP. Global estimates of visual impairment: 2010. Br J Ophthalmol. 2012; 96(5): 614-8. doi: 10.1136/bjophthalmol-2011-300539. Epub 2011 Dec 1.
8. Spector A. Review: Oxidative stress and disease. J Ocul Pharmacol Ther. 2000; 16(2): 193-201. doi: 10.1089/jop.2000.16.193.
9. Babizhayev MA, Deyev AI, Linberg LF. Lipid peroxidation as a possible cause of cataract. Mech Ageing Dev. 1988; 44(1): 69-89. doi: 10.1016/0047-6374(88)90080-2.
10. Kupfer C. Bowman lecture. The conquest of cataract: a global challenge. Trans Ophthalmol Soc U K (1962). 1985; 104 (Pt 1): 1-10.
11. Medsinge A, Nischal KK. Pediatric cataract: challenges and future directions. Clin Ophthalmol. 2015; 9: 77-90. doi: 10.2147/OPTH.S59009.
12. Available from https://www.aao.org/eye-health/diseases/what-are-pediatric-cataracts
13. Gupta VB, Rajagopala M, Ravishankar B. Etiopathogenesis of cataract: an appraisal. Indian J Ophthalmol. 2014; 62(2): 103-10. doi: 10.4103/0301-4738.121141.
14. Asbell PA, Dualan I, Mindel J, Brocks D, Ahmad M, Epstein S. Age-related cataract. Lancet. 2005; 365(9459): 599-609. doi: 10.1016/S0140-6736(05)17911-2.
15. Abdelkader H, Alany RG, Pierscionek B. Age-related cataract and drug therapy: opportunities and challenges for topical antioxidant delivery to the lens. J Pharm Pharmacol. 2015; 67(4): 537-50. doi: 10.1111/jphp.12355. Epub 2015 Feb 3.
16. Kiziltoprak H, Tekin K, Inanc M, Goker YS. Cataract in diabetes mellitus. World J Diabetes. 2019; 10(3): 140-153. doi: 10.4239/wjd.v10.i3.140.
17. Anjal K, Bhavya. K Bharathan, Hanan Hussain, Nirmala P S, Swathy M, Different Techniques for Cataract Detection, International Research Journal of Engineering and Technology. 2017: 4(2).
18. Available from https://www.eye-care-hospital.com/micro-incision-cataract-surgery
19. Available from https://eyewiki.aao.org/Manual_Small_Incision_Cataract_Surgery
20. Lam, D., Rao, S., Ratra, V. et al. Cataract. Nature Reviews Disease Primers. 2015; 1(1): 1-15. http://intjmi.com/files/site1/user_files_1e3831/admin-A-10-1-392-f516a32.pdf
21. Abdelkader H, Alany RG, Pierscionek B. Age-related cataract and drug therapy: opportunities and challenges for topical antioxidant delivery to the lens. J Pharm Pharmacol. 2015; 67(4): 537-50. doi: 10.1111/jphp.12355. Epub 2015 Feb 3

International Journal of Pharmaceutics: X 7 (2024) 100257

Contents lists available at ScienceDirect

International Journal of Pharmaceutics: X

journal homepage: www.sciencedirect.com/journal/international-journal-of-pharmaceutics-x

QbD-guided phospholipid-tagged nanonized boswellic acid naturosomal delivery for effective rheumatoid arthritis treatment

Poonam Usapkar [a,1], Suprit Saoji [b,1], Pradnya Jagtap [c], Muniappan Ayyanar [d], Mohan Kalaskar [e], Nilambari Gurav [f], Sameer Nadaf [g], Satyendra Prasad [b], Damiki Laloo [h], Mohd Shahnawaz Khan [i], Rupesh Chikhale [j], Shailendra Gurav [a,*]

[a] Department of Pharmacognosy, Goa College of Pharmacy, Panaji, Goa University, Goa-403 001, India
[b] Department of Pharmaceutical Sciences, R. T. M. Nagpur University, Nagpur, Maharashtra- 440 033, India
[c] Department of Pharmacology, PDEA's S. G. R. S. College of Pharmacy, Saswad, Maharashtra-412 301, India
[d] Department of Botany, A.V.V.M. Sri Pushpam College (Autonomous), (Affiliated to Bharathidasan University), Poondi 613 503, India
[e] Department of Pharmacognosy, R.C. Patel Institute of Pharmaceutical Education and Research, Shirpur, Maharashtra- 425 405, India
[f] Department of Pharmacognosy, PES's Rajaram and Tarabai Bandekar College of Pharmacy, Ponda, Goa University, Goa-403401, India
[g] Bharati Vidyapeeth College of Pharmacy, Palus 416310, Maharashtra, India
[h] Department of Pharmacognosy, Girijananda Institute of Pharmaceutical Science, Girijananda Chowdhury University, Azara, Guwahati 781017, India
[i] Department of Biochemistry, College of Science, King Saud University, Riyadh, Saudi Arabia
[j] UCL School of Pharmacy, 29–39 Brunswick Square, London WC1N 1AX, United Kingdom

ARTICLE INFO

Keywords:
Boswellia serrata
Rheumatoid arthritis
Phytosome
Phospholipid-complex
TNF- α

ABSTRACT

Studies have reported the potential role of Boswellic acids (BAs), bioactive pentacyclic triterpenes from *Boswellia serrata* (BS), in treating rheumatoid arthritis (RA). However, poor water solubility and limited oral absorption are restricting factors for its better therapeutic efficacy. Based on these assumptions, the current study aimed to develop naturosomal delivery of BAs to boost their extremely low bioavailability, colloidal stability, and water solubility. Nanonized naturosomes were developed and subsequently analyzed to show their physicochemical and functional features employing the quality-by-design approach. The solubility analysis of Boswellic acid naturosomes revealed a 16 times improvement in aqueous solubility compared to BS extract (BSE). The zeta potential and dynamic light scattering findings of BSE naturosomes (BSENs) have demonstrated their colloidal stability with regulated nano-size particles. Additionally, compared to BSE (~31%), *in-vitro* dissolution experiments showed that >99% of pentacyclic triterpenes were released from BSENs. Studies on *ex-vivo* permeation showed that BSENs' permeation (>79%) significantly improved over BSE's (~20%). *In-vivo* efficacy studies using CFA-prompted arthritis in rodents showed a critical expansion in body wt and an undeniable reduction in paw thickness, paw volume, and TNF-α treated with BSEN compared to the arthritis control and BSE-treated group. These findings suggest that BSENs can help treat RA drugs by demonstrating their efficacy in further clinical research to validate the significant improvements.

1. Introduction

A chronic, inflammatory, and autoimmune condition known as rheumatoid arthritis (RA) is thought to affect 0.24 to 1% of people worldwide. It is characterized by discomfort, articular cartilage degeneration, and edema and inflammation around the joints (Majeed et al., 2021). Nonsteroidal anti-inflammatory drugs (NSAIDs), corticosteroids, anti-rheumatic drugs, and biological response modifiers are used in the clinical management of RA. Still, their toxicities, iatrogenic reactions, and side effects compromise the therapeutic process. As a result, there has been a lot of interest in herbs that have anti-RA activity as possible safe alternatives to or supplements to anti-inflammatory drugs (Khayyal et al., 2018).

A branching tree known as *Boswellia serrata* Roxb. (BS), a member of Burseraceae, thrives in the arid parts of India and the Middle East. The plant has a variety of uses, including those in food, medicine, materials,

* Corresponding author at: Department of Pharmacognosy, Goa College of Pharmacy, Panaji, Goa University, Goa- 403 001, India.
E-mail address: shailendra.gurav@nic.in (S. Gurav).
[1] Equal Contribution and can be treated as First Author.

https://doi.org/10.1016/j.ijpx.2024.100257
Received 8 January 2024; Received in revised form 14 May 2024; Accepted 15 May 2024
Available online 19 May 2024

and cosmetics. An olibanum or frankincense-like gum resin is found in these trees. These gum resins have a long history of treating many bacterial and inflammatory illnesses (Khayyal et al., 2018; Suther et al., 2022). Di Lorenzo et al. (2013) have reported BS as one of the plant food supplements used to treat inflammatory conditions. Based on their pilot study, Italiano et al. (Italiano et al., 2020) have proposed BS-containing food supplements to improve the quality of life of osteoarthritic patients. The extract of BS gum resin (BSE) has shown anti-RA properties. Additionally, BSE has also been demonstrated to have anti-inflammatory cytokine inhibition potential. In rat models of collagen-induced arthritis, it decreased interleukin-1 (IL − 1), tumour necrosis factor (TNF), and interferon (IFN) and boosted interleukin-10 (IL − 10) production. These cytokines are critical in persistent inflammation and tissue destruction during the progression of RA (Kumar et al., 2019).

The oleo gum resins of *Boswellia* species include triterpenes known as boswellic acids (BAs). There are about twelve distinct pentacyclic triterpenes (BAs) known. 3-acetyl−11-keto-beta-boswellic acid (AKBBA) and beta-boswellic acid (BBA) have attracted much pharmacological attention. AKBBA inhibits the leukotriene-mediated inflammatory pathways and 5-lipoxygenases (5-LO). AKBBA also lowers the activity of cyclooxygenase−1 in human platelets, NF-κB induction, inflammation-promoting cytokines, and leukotriene inhibition (Roy et al., 2019). A preliminary pharmacokinetic test revealed a poor bioavailability observed with one of the pentacyclic triterpenes of BAs, particularly 3-acetyl−11-keto-boswellic acid (AKBA). The systemic bioavailability of BAs is restricted since they are steroidal (lipophilic) and cannot dissolve into an intestinal fluid (Sharma et al., 2010). Commercially accessible boswellic acid extracts can be found in pharmaceutical and nutraceutical products. However, there is currently no research on the extract's low water solubility, nor are there any methods to increase the solubility and bioavailability regarding the treatment of RA.

Several strategies have been proposed to address phytoactives' poor solubility and bioavailability, including innovative formulations such as emulsions, liposomes, nanoparticles, chemical structural modification, and prodrug delivery. A possible method for enhancing phytoactives' bioavailability is a naturosomal drug delivery, i.e., a phospholipid carrier technique. Compared to traditional herbal medications or extracts, naturosomes are more readily absorbed due to the nanonized complex tagged with phospholipid, thus increasing the bioavailability, reducing the dose, and sustaining the duration of action. Recent studies have also demonstrated the efficacy of complexing phytoactives with dietary phospholipids to boost their bioavailability and, thus, therapeutic efficacy (Gurav et al., 2022; Metkari et al., 2023; Saoji et al., 2017; Saoji et al., 2022; Saoji et al., 2016b). BSE is, therefore, a suitable option for the development of naturosomes.

Given this, the current study aimed to determine if the anti-inflammatory effect of nanonized BSE would be enhanced by naturosomal drug delivery in an animal model of RA produced by Freund's Complete Adjuvant (FCA). A Quality by design (QbD) strategy optimized the formulated BSE naturosomes (BSENs) and subjected them to their physicochemical, functional, and pharmacological attributes.

2. Materials and methods

2.1. Materials

Natural Remedies Ltd., Bangalore, India, provided the standardized BSE, which included ~30% AKBA. Analysis using high-performance liquid chromatography (HPLC) verified the BSE's identification. The German company Lipoid, Ludwigshafen, graciously donated hydrogenated soy phosphatidylcholine (Phospholipon® 90H).

2.2. Analysis of the 3-acetyl−11-keto-boswellic acid (AKBA) present in BSE

The concentrations of AKBA in BSE were determined using a modified reverse-phase (RP) HPLC method (Mannino et al., 2016). The HPLC system (Shimadzu, Japan) with LC solution software was employed, equipped with a manual rheodyne sample injector, an SPD-M20A detector, and an LC-20 CE HPLC pump with gradient elution. The mobile phase was made up of (a) Water: Methanol (50:50) containing 5 mM ammonium acetate and (b) Methanol: 1-Propanol (80:20) containing 5 mM ammonium acetate (25:75, *v*/v), at a flow rate of 200 µL/min. With a detector wavelength of 250 nm at room temperature, a Micra-NPS RP18 column (33 × 8 mm, 1.5 µ porous silica) was utilized as the stationary phase. The AKBA calibration curve was generated by analyzing the concentration of the AKBA standard solution and then graphing the peak regions against concentration.

2.3. Preparation of BSEN

The BSEN was developed by slightly tweaking the solvent evaporation process described in our previous studies (Gurav et al., 2022; Saoji et al., 2017; Saoji et al., 2016b) and employing the QbD methodology. In a circular bottom flask measuring 100 mL, different ratios of Phospholipon®90H and BSE were used, such as 0.5:1, 2:1, or 3.5:1, and the mixture was supplemented with 40 mL of ethanol. A water bath was used to control and sustain the reaction at various temperatures, such as 30, 40, or 50 °C. Different periods, i.e., 1, 2, or 3 h, were used to conduct the reaction. A surplus of n-hexane was added while stirring to ensure a clear solution, which had been dried up to 2–3 mL. The dispersion was filtered and vacuum-dried after it had formed to eliminate any leftover solvents. The resultant BSENs were kept at room temperature for additional analysis in amber-coloured glass vials that had been nitrogen flushed.

2.4. QbD approach

Currently, the QbD technique is employed to create high-quality products. QbD refers to a factual, prospect-based, comprehensive, and proactive strategy for developing pharmaceuticals that begins with fixed objectives and focus on understanding the products and processes, using sound science and excellent risk management, with better control process (Dias et al., 2022; Halarnekar et al., 2023; Rarokar et al., 2021; Rodrigues et al., 2020; Rodrigues et al., 2022). With the help of a QbD-based strategy and 17 experimental trials (Design-Expert software Version 13.0- Stat-Ease Inc., Minneapolis, USA), we investigated how changing the phospholipid-to-drug ratio (X_1, w:w), the reaction temperature (X_2, °C), and the reaction duration (X_3, h) affected the product's Critical Quality Attribute (CQA), and entrapment efficiency (EE) (Gurav et al., 2022). A statistical model (Eq. (1)) with interaction and polynomial components was applied to investigate the effect of independent variables on response.

$$Y = b_0 + b_1X_1 + b_2X_2 + b_3X_3 + b_{11}X_1^2 + b_{22}X_2^2 + b_{33}X_3^2 + b_{12}X_1X_2 + b_{23}X_2X_3 + b_{13}X_1X_3 \quad (1)$$

Where B_i is the estimated coefficient for the factor Xi, b_0 is the arithmetic mean response of the 17 runs, and Y is the dependent variable. The principal effects (X_1, X_2, and X_3) indicated the typical outcome of the incremental rise in each factor. The three variables were adjusted concurrently, and the interaction terms (X_1X_2, X_2X_3, and X_1X_3) demonstrated how the response changed. The polynomial terms (X_{12}, X_{22}, and X_{32}) were added to analyze on-linearity. Tables S1 and S2 (Supplementary File) provided information about the central composite design (CCD) batches.

2.5. EE of BSEN

The EE, measured as the amount of AKBA trapped by the BSEN, was determined using a reported method (Tan et al., 2012). Briefly, 10 mL of chloroform was mixed with precisely weighed (100 mg) BSEN powder

and analyzed using HPLC, as mentioned in Section 2.2. Eq. (2) was used to determine the prepared BSEN's EE.

$$EE\ (\%) = C_t - C_f / C_t \times 100 \quad (2)$$

Where C_t = A complete concentration of BSE, C_f = BSE found in the filtrate.

2.6. Determination of AKBA content in BSEN

AKBA content in prepared BSEN was determined using the reported HPLC method as specified above and computed using the following Eq. (3);

$$\text{Drug content} = \text{amount of drug in the BSEN/Amount of BSEN} \times 100\% \quad (3)$$

2.7. Physicochemical characterization of BSEN

2.7.1. Photomicroscopy

In order to conduct a microscopic examination, a suspension made up of approximately 100 mg of the BSEN was transferred to a glass tube and diluted with 10 mL of phosphate buffer saline (pH 7.4). When the suspended vesicles were put on a transparent glass slide, a microscope (Model: DM 2500, Leica Microsystems, Germany) took photomicrographs at 20× magnification (Saoji et al., 2022).

2.7.2. Scanning electron microscopy (SEM)

Briefly, the BSEN was layered on double-sided carbon tape and a brass stub. With the help of the fine auto coater, palladium was coated onto the surface powder. Using SEM (Model: JFC1600, Jeol Ltd., Tokyo, Japan) with a digital camera and an increasing voltage of 10 KV, palladium-coated samples were examined (Rarokar et al., 2021; Andrade et al., 2024).

2.7.3. Transmission electron microscopy (TEM)

A small amount of the BSEN was placed on a grid made of copper and negatively smeared with 2% uranic acid for the TEM examination (Make: Jeol, Model: JEM 2100) (Gurav et al., 2022).

2.7.4. Fourier transform infrared spectroscopy (FTIR)

An FTIR spectrophotometer with an attenuated total reflectance (ATR) accessory (Model: IR Prestige-21, Shimadzu, Japan) was used to obtain the infrared spectra of BSE, Phospholipon®90H, and BSEN. The materials were vacuum-dried to presumably eliminate the influence of any remaining moisture before any spectra were taken. For each sample analysis, 45 scans were performed at a resolution of 4 cm^{-1} from 4500 to 400 cm^{-1} (Rarokar et al., 2021).

2.7.5. Differential scanning calorimetry (DSC)

Using a differential scanning calorimeter, the tested substances (BSE, Phospholipon®90H, and BSEN) were thermally analyzed (Model: Q20, TA Instruments, Inc., New Castle, DE, USA). Dry nitrogen gas purged the area during the analysis (50 mL/min). The instrument's heat capacity and flow were calibrated using high-purity indium. Using a crimper, the samples (2.5–5 mg) were packed in aluminum pans with their covers. Each sample went through a single cycle of heating from 0 to 400 °C at a rate of 10 °C/min. The Universal Analysis program version 4.5 A, build 4.5.0.5, was used to analyze the peak transition onset temperatures of the samples (TA Instruments, Inc., New Castle, DE, USA) (Rodrigues et al., 2022).

2.7.6. Powder X-ray diffraction (PXRD)

PXRD (Model: D2 Phaser, Bruker AXS, Inc., Madison, WI, USA) with a Bragg-Brentano geometry (θ/2θ) optical setup was used to assess the polymorphic state of the materials (SBE and BN). As the diffraction angle increased from 2° to 90°, 2θ angle, the samples were scanned with a step-angle of 0.2° 2θ and a count time of 0.5 s (Saoji et al., 2017).

2.7.7. Particle size and zeta potential analysis

The BSEN was subjected to a photon correlation spectroscopy (PCS) study of particle size utilizing dynamic light scattering on a Zetasizer® nano (Model: Zen 3600, Malvern Instruments, Malvern, UK) fitted with a 5 mW Helium-Neon laser with an output wavelength of 633 nm. Measurements were conducted at 25 °C, a 90° angle, and a runtime of at least 40 to 80s. Based on the electrophoretic mobility of naturosomes, the zeta potential was calculated using Smoluchowski's equation (Gracias et al., 2023).

2.8. Functional evaluation of BSEN

2.8.1. Apparent solubility analysis

Apparent solubility tests were conducted using the stated method (Gurav et al., 2022). In brief, 10 mL of water or n-Octanol was added to an excess of BSE, a physical mixture of BSE and Phospholipon®90H (PM) and BSEN in a sealed glass vial and kept at room temperature (25 ± 0.5 °C). The mixture was then stirred for 24 h, followed by centrifugation at 4000 rpm for 30 min. The supernatant was filtered using a 0.45 µm membrane filter, followed by proper dilutions with the mobile phase and subsequent analysis using the previously mentioned HPLC technique.

2.8.2. Drug dissolution study

An *in-vitro* dissolution study of test drugs, i.e., BSE, PM, and BSEN, was conducted using USP type-II dissolution apparatus (Electrolab, India, TDT-06 T). Initially, a weighed amount of BSEN equivalent to 50 mg of BSE was added to the agitated dissolution medium (900 mL phosphate buffer, pH 6.8) and stirred at 100 rpm, maintaining the temperature at 37 ± 0.5 °C. 10 mL of the sample was periodically removed and replaced with an equivalent amount of fresh dissolution medium to maintain the sink condition. Finally, the withdrawn samples were filtered using a 0.45 µm membrane filter and analyzed using the reported HPLC method. DDSolver®, an add-on program, was utilized to compare the dissolution profiles (Rarokar et al., 2023).

2.8.3. Ex-vivo permeability

An adult male Wistar rat (220–250 g) was given a lethal dose of thiopental (35 mg/kg, i.v.) before being cervically dislocated to harvest its intestine for experimental purposes. Per the reported procedure, *ex-vivo* permeability studies were conducted using a Franz diffusion cell and everted intestine (Dixit et al., 2012). The everted intestine was loaded with BSEN at a predetermined concentration and placed in a small pool of receptor media (50 mL). The cellular material was agitated at 37 ± 0.5 °C using a magnetic stirrer. An aliquot of 5 mL was taken at predetermined intervals for up to 8 h to determine the drug concentration, and each withdrawal was replaced with an equivalent amount of the same diffusion medium.

2.9. Evaluation of in-vivo anti-arthritic activity

2.9.1. Animals

The selection of male Wistar rats weighing 220–250 g and all animal experiments were carried out with the prior approval (SGRS/IAEC/08/2019–20) of the Institutional Animal Ethics Committee registered under the Committee for the Purpose of Control and Supervision of Experiments on Animals, Government of India (Registration No. 311/PO/ReBi/S/2000/CPCSEA). All experiments were performed per the U. K. Animals Act (1986) and its accompanying recommendations, as detailed in the ARRIVE guidelines.

2.9.2. Induction of adjuvant arthritis

The evaluation of their anti-arthritic potential was conducted as per the reported method by Gautam et al. (2019). Rats were induced with

adjuvant arthritis using the documented procedure (Pearson, 1956). The animals were divided into five groups of six rats each ($n = 6$) and injected with 0.1 mL of FCA into the sub-plantar region of the left hind paw on day 0:

Group I - Normal control,

Group II - Arthritic control (FCA-induced arthritis),

Group III - FCA-induced arthritis + Indomethacin as a reference drug (3 mg/kg),

Group IV - FCA-induced arthritis + BSE (180 mg/kg),

Group V - FCA-induced arthritis + BSEN (equivalent to 180 mg/kg BSE).

Each test dosage was given orally 1 h before adjuvant injection and once daily for 22 days (from day 0 to day 21). By assessing the biophysical parameters, such as the paw thickness and paw volume at days 0, 11, and 22, the anti-arthritic potential of the formulated BSEN against pure BSE was evaluated.

2.9.3. Measurement of body weight

On days 0, 11, and 22 of the experiment, the body weights of the animals were noted. To measure the changes in body weight across all the tested groups, the difference in body weights on days 11 and 22 was calculated (Gautam et al., 2019).

2.9.4. Measurement of paw thickness

On days 0, 11, and 22, the paw's thickness was measured to evaluate the inflammation as an acute lesion on an injected limb. According to the specified formula (4), the following percentage inhibition of paw thickness was determined:

$$\text{Percentage inhibition} = (\text{Tc} - \text{Tt}) \times 100/\text{Tc} \quad (4)$$

Where Tc- Mean change in paw thickness of the arthritis control group, Tt- Mean change in paw thickness of the treated group.

2.9.5. Measurement of paw volume

The injected limb's paw volume of the animal was measured on days 0, 11, and 22 by positioning it vertically in the plethysmometer up to the level of the lateral malleolus (Gautam et al., 2019). The difference in the initial and final paw volumes measured the paw volume reduction.

2.9.6. Measurement of TNF-α

All tested groups' blood samples were collected on days 11 and 22 via the retro-orbital route. Blood was centrifuged at 1000 rpm for 10 min to separate the serum, which was further evaluated for the TNF-α concentration using an ELISA (enzyme-linked immunosorbent assay) kit (Akhtar et al., 2021).

2.9.7. Histopathological study

Following blood collection, the rats were sacrificed by cervical dislocation while being anesthetized with diethyl ether. Arthritic and inflamed joints were removed from the hind paw and preserved in 10% formalin for histological examination. The joints were decalcified with 10% formic acid for 30 days (Shabbir et al., 2014, 2016). The tissues were finally encased in paraffin. Haematoxylin and eosin staining was performed on the joint segment (5 μm). The histopathological alterations in the joints, including inflammatory cells, bone erosion, and cartilage destruction, were recorded.

2.9.8. Statistical analysis

One-way analysis of variance (ANOVA) was used to analyze the statistical significance of the result obtained from the FCA-induced arthritis model. Then, the Bonferroni multiple comparisons test was performed. The outcomes were reported as mean ± SEM and were deemed significant at $p < 0.05$.

3. Results and discussion

3.1. Preparation of BSEN

Our previous studies successfully developed naturosomal delivery of hesperetin, *Withania somnifera*, *Centella asiatica*, and *Bacopa monnieri* with their enhanced aqueous solubility and therapeutic efficacy (Gurav et al., 2022; Saoji et al., 2017; Saoji et al., 2022; Saoji et al., 2016b).

According to the preliminary examination of the influence of numerous factors, the phospholipid-to-drug ratio, reaction temperature, and reaction duration significantly impacted the generated naturosomes' capacity to entrap molecules. Table 1 displays the results of the EE (%). The experimental trial's measured values showed the EE between 88.09 and 96.33%. The responses Y (R^2: 0.9824 & PRESS: 13.71) best fit the quadratic model. This demonstrates that the proposed model can correctly forecast the 98.24% variations in responses Y. Utilizing ANOVA, the model's effectiveness was assessed (Supplementary File-Table S2).

The F-value for the model, which denotes its significance, was found to be 43.39. In this instance, EE was significantly impacted by X_1, X_2, and the quadratic terms of X_1, X_2, and X_3. For response Y, the difference between the expected R^2 of 0.8798 and the adjusted R^2 of 0.9597 is <0.2, indicating reasonable agreement. The polynomial Eq. (5) illustrates the relationship between independent and dependent variables as mentioned below:

$$\text{EE\%} = +89.58 + 0.4760 \times {}_1 + 0.4330 \times {}_2 + 0.2400 \times {}_3 - 0.0175\, X_1X_2 + 0.0875\, X_1X_3 + 0.1925\, X_2X_3 + 3.68 \times {}_1{}^2 + 2.64 \times {}_2{}^2 - 0.8001 \times {}_3{}^2 \quad (5)$$

CCD response surfaces and contour plots are shown in Fig. 1, which displays the variation in EE for different X_1, X_2, and X_3 values. Response surface and contour plots showed that the investigated factors X_1, X_2, and X_3 had a significant impact on the effectiveness of EE. It was discovered that the higher EE was best suited under settings when X_1, X_2, and X_3 levels were increasing. Based on these findings and the results of the multiple regression model, it was determined that the X_1, X_2, and X_3 should all be set at their optimal values, which were 3.473:1, 49.72 °C, and 2.872 h, respectively.

3.2. Validation of the model

A further batch of BSEN was prepared to validate the developed model. X_1, X_2, and X_3 values of 3.473:1, 49.72 °C, and 2.872 h generated this validation batch, which uses the model's optimal settings for the

Table 1
CCD formulation batches with %EE.

Batches	X_1	X_2	X_3	Entrapment efficiency*
	w/w	°C	H	%
F1	+1	−1	+1	95.46 ± 1.16
F2	0	0	+1	89.05 ± 0.84
F3	0	0	−1	88.09 ± 1.30
F4	−1	0	0	92.53 ± 1.12
F5	+1	+1	+1	96.33 ± 1.20
F6	0	0	0	89.69 ± 1.32
F7	0	0	0	89.98 ± 1.06
F8	+1	+1	−1	95.4 ± 1.30
F9	0	+1	0	93.16 ± 1.24
F10	−1	−1	−1	94.52 ± 1.18
F11	0	0	0	89.94 ± 1.14
F12	+1	0	0	93.57 ± 0.84
F13	−1	−1	+1	94.33 ± 0.94
F14	+1	−1	−1	95.32 ± 1.23
F15	−1	+1	+1	95.25 ± 1.1
F16	0	−1	0	90.87 ± 1.06
F17	−1	+1	−1	94.69 ± 0.82

* Values represent mean ± standard deviation ($n = 3$).

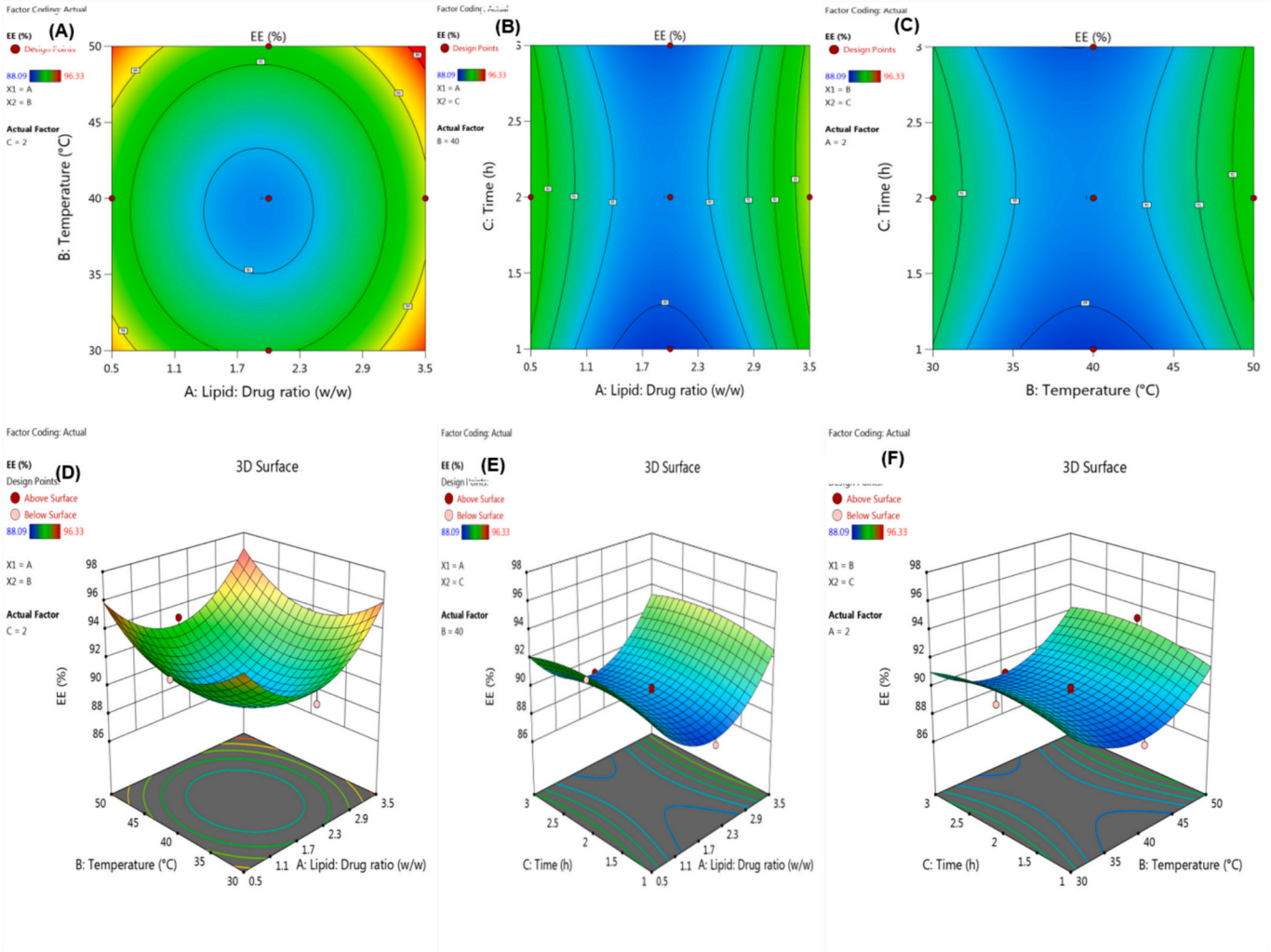

Fig. 1. The response surface plots and the con$_t$our plots of entrapment efficiency (Y, %) as a function of the ratio of Phospholipid and BSE (X_1, w:w), the reaction temperature (X_2, °C), and the reaction time (X_3, h).

formulation and process variables. Table S3 (Supplementary File) shows the actual EE attained with the provided formulation and the anticipated efficiency of the BSEN obtained using the model. It was discovered that the typical AKBA entrapment effectiveness in naturosomes synthesized under ideal conditions was 94.87 ± 1.29%. These findings demonstrated good concordance with the model's predicted value, i.e., 96.34%, signifying the applicability and reliability of the created model. The model's relative robustness was shown by the bias (%), which was determined using Eq. (6) below and found to be <3% (1.53%) (Qin et al., 2010).

$$Bias\ (\%) = predicted\ value – observed\ value \times 100\ predicted\ value \quad (6)$$

3.3. Drug content

Estimating the drug concentration in the finished product is a crucial component of drug-entrapped systems since it highlights the differences between formulations made under various circumstances. The drug quantity in an optimally prepared BSEN was 98.93 ± 0.78%.

3.4. Physico-chemical characterization of the prepared BSEN

3.4.1. Photomicroscopy

The microscopic inspection of Figs. 2A and B revealed the presence of the complex's spherical structures. The portrayed structures looked like vesicles with the drug inside. Specifically, BSE intercalated in the lipid layers of Phospholipon®90H. The drug particles' surface shape showed that they are linked to phospholipids, which form complexes of variable sizes (Gurav et al., 2022).

3.4.2. SEM

The complex was irregularly shaped and had rough surface morphology in the SEM images (Figs. 2C and D). The drug was utterly transformed into the phyto-phospholipid complex, where Phospholipon®90H physically confined it. As a result, crystals were no longer present in the complex since they had an amorphous nature (Gurav et al., 2022).

3.4.3. TEM

The BSEN complex was seen on TEM images (Figs. 2E and F). A TEM investigation revealed the development of vesicular structures that looked spherical (Gurav et al., 2022).

3.4.4. FTIR

Fig. 3A displays the findings from the FTIR examinations of the BSE, Phospholipon®90H, and the produced BSEN. The phenolic -OH stretching vibration (hydroxyl group) showed a visible peak in the FTIR spectra of BSE at 3462.22 cm^{-1}. The alkyl C—H stretch in the BSE was responsible for the peak at 2922.16 cm^{-1}. C═O stretching (carboxyl group) peaked at 1697.36 cm^{-1}. On the other hand, the peak at 1452.40

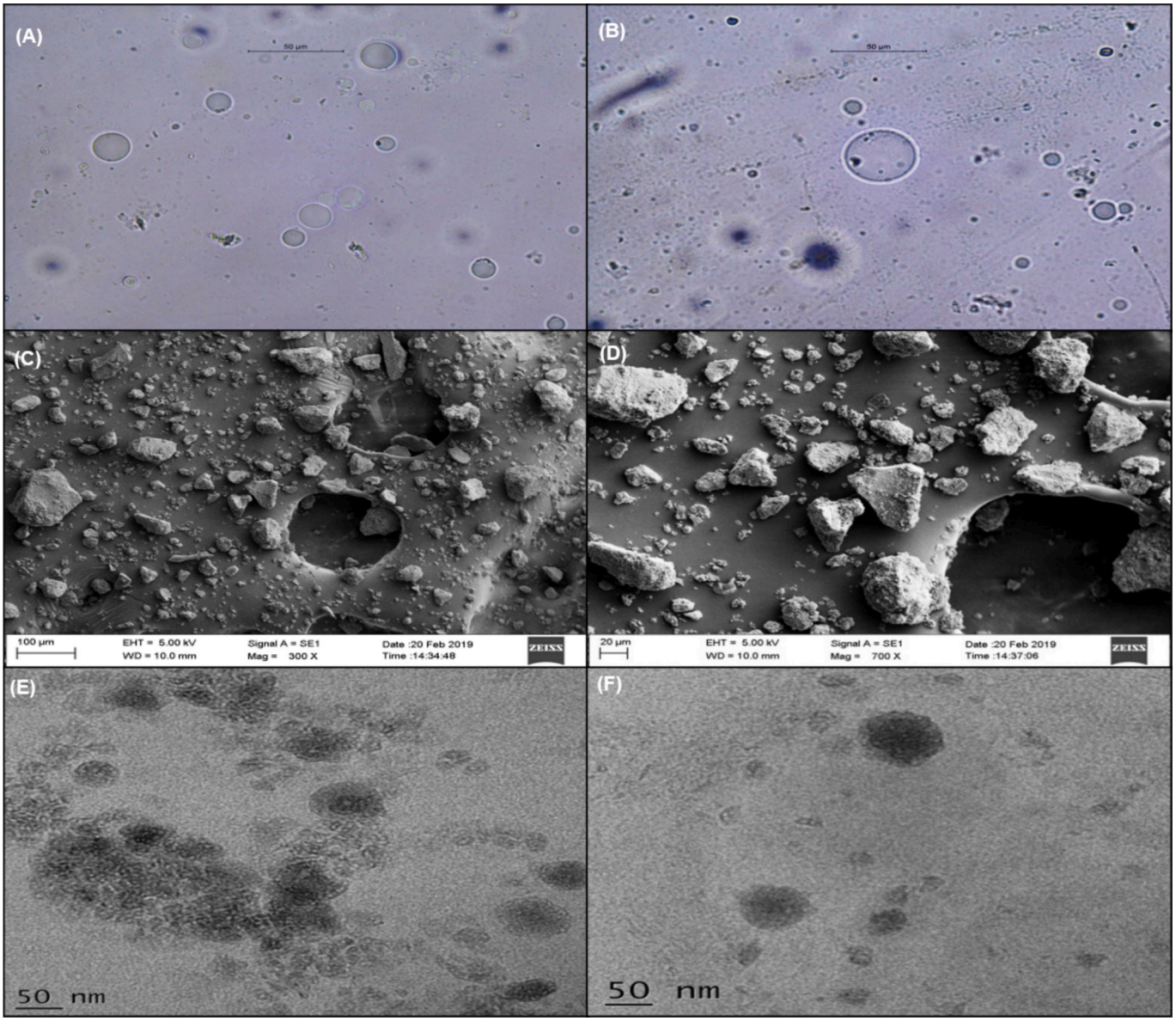

Fig. 2. Photo microscopic images of BSEN. (A and B), SEM images of BSEN (C and D), and TEM images of BSEN (E and F).

cm^{-1} was due to the presence of C═C aromatic bending.

The typical C—H stretching signal in the long fatty acid chain was detected in Phospholipon®90H's FTIR spectra at 2918 cm^{-1} and 2850 cm^{-1}, respectively. The spectrum also bears several stretching bands, including a C═O stretching band in the fatty acid ester at 1738 cm^{-1}, a P═O stretching band at 1236 cm^{-1}, a P-O-C stretching band at 1091 cm^{-1}, and a -N+$(CH_3)_3$ stretching band at 970 cm^{-1}.

Strong hydrogen bonds were formed between the -OH groups of the phospholipids and BSE in the BSEN, as evidenced by the absorption peak of hydroxyl (-OH) in the FTIR spectra of the produced BSEN, which had a broad peak with stretching moved to a lower wave number (at 3319.49 cm^{-1}). Long-chain fatty acids do not play a role in naturosome formation, as evidenced by the band of the two long aliphatic chains of the fatty acids in the phospholipid molecule remains unaltered in the BSEN spectra. The P-O-C stretching vibrations altered to a lower wave number, and the P═O absorption band of phospholipids shifted to a higher wave number, respectively, confirming the development of naturosome (Gurav et al., 2022; Jena et al., 2014; Saoji et al., 2022).

3.4.5. DSC

DSC is a popular tool for analyzing the interactions between various formulation components. It is common to see these interactions as the disappearance of endothermic peaks, the advent of new peaks, changes to the peak's commencement and shape, peak temperature or melting point, relative peak area, or enthalpy (Maiti et al., 2007). The DSC thermograms of pure BSE, Phospholipon®90H, and BSEN are displayed in Fig. 3B. The pure BSE showed a prominent endothermic peak at about 165.78 °C. The sharp endothermic peak for Phospholipon®90H was observed at 150.18 °C and 242.05 °C, respectively. The melting of the phospholipid most likely generated the first peak (at 150.18 °C). At 242.05 °C, a second peak is seen, possibly due to a transition from a gel to a liquid-crystalline state. Added isomeric or crystal changes to the phospholipid's carbon chain are possible (Semalty et al., 2010). Broad, partially fused endothermic peaks are visible on the thermogram of the BSEN at a temperature of 100.09 °C. The peaks of BSE and Phospholipon®90H were distinct from these. The drug's improved solubility and diminished crystallinity may be explained by decreased melting and enthalpy (Singh et al., 2013). Thus, BSEN formation was evident as the initial peaks of BSE and Phospholipon®90H disappeared from the BSEN

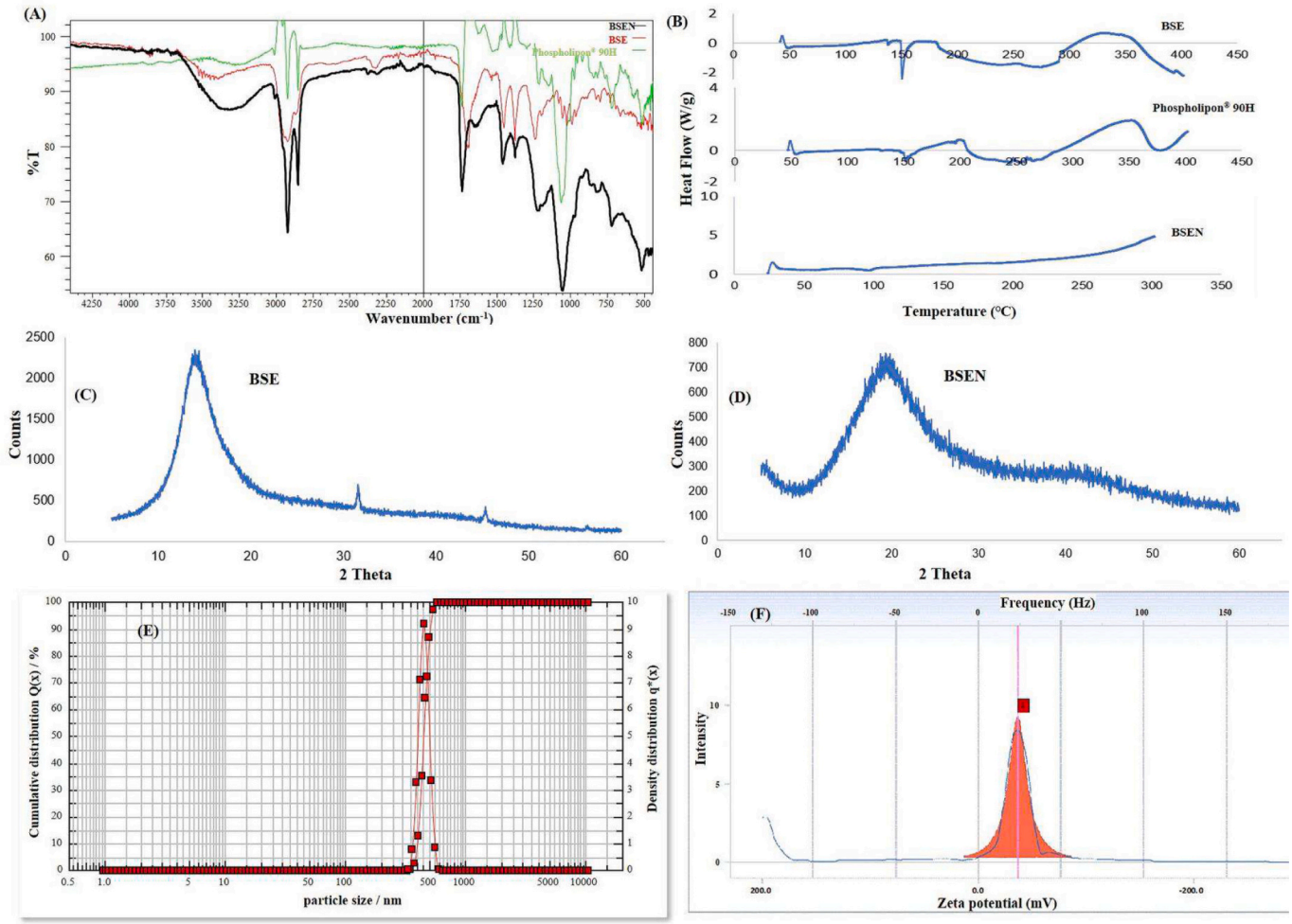

Fig. 3. (A) FTIR spectral overlain of BSE, Phospholipon®90H, and BSEN, (B) DSC thermograms of BSE, Phospholipon®90H and BSEN, (C) X-ray diffractograms of BSE (D) (C) X-ray diffractograms of BSEN, (E) Particle size distribution of BSEN, and (F) Zeta potential analysis of BSEN.

thermogram and the lower phase transition temperature than Phospholipon®90H. These results are consistent with those found in the earlier reports of Gurav et al. (Gurav et al., 2022). DSC thermograms further suggest that the interaction between the BSE and Phospholipon®90H results from a combination of forces, including hydrogen bonds and van der Waals interactions. This interaction may indicate drug amorphization and/or complex formation (Singh et al., 2014; Zhang et al., 2010). The BSE may have interacted with the polar region of Phospholipon®90H and then been trapped in the long-chain hydrocarbon tail of the phospholipid molecule. As a result, the phase transition temperature dropped, leading to a subsequent decrease in phospholipid hydrocarbon chains and the disappearance of Phospholipon®90H's second endothermic peak (Maiti et al., 2007).

3.4.6. PXRD

The PXRD patterns of BSE and BSEN are depicted in Fig. 3C and D. Sharp crystalline peaks can be seen in the BSE diffractogram. The BSEN's diffractogram showed that most of the crystalline peaks connected to the BSE had vanished. These findings corroborated earlier research in which the disappearance of drug peaks was linked to the development of drug-phospholipid complexes (Saoji et al., 2016b; Singh et al., 2014). This proved that the BSEN was formed when the BSE crystalline peaks vanished. Consequently, it can be concluded that the BSE in the Phospholipon®90H matrix may exist in either a molecularly distributed or an amorphous condition (Semalty et al., 2010).

3.4.7. Particle size and zeta potential analysis

Figs. 3E and F depict the prepared BSEN's average particle size and zeta potential values. The average particle size of BSEN was 441.12 ± 32 nm. Most particles have a surface area to volume (SA/V) ratio inversely related to size. The entrapped medication is thus more readily released from the naturosome via diffusion and surface erosion when the BSEN particle is smaller and has a higher SA/V. Additionally, they benefit from allowing the drug-entrapped naturosomes to pass through physiological drug barriers. Endocytosis allows particles smaller than 500 nm to enter cells across the plasma membrane (LeFevre et al., 1978; Savic et al., 2003). However, the lymphatic system is used to uptake bigger particles (> 5 mm).

Another vital metric frequently utilized to evaluate naturosomal stability is zeta potential. The zeta potential of the prepared BSEN was −36.35 ± 1.19 mV. These findings concur with earlier research stating that zeta potential values greater than or equal to −30 mV are acceptable and indicate solid physical stability (Halarnekar et al., 2023; Sze et al., 2003).

3.5. Functional evaluation of BSEN

3.5.1. Apparent solubility

Table S4 (Supplementary File) displays the findings from measurements of the apparent solubilities of pure BSE, PM, and a manufactured BSEN. Pure BSE was found to be poorly soluble in water (~12 µg/ mL) but significantly more soluble in n-Octanol (~355 µg/mL), showing that

the medication has a lipophilic nature. In terms of n-octanol and aqueous solubility, PM showed no appreciable change. On the other hand, the BSEN demonstrated a substantial increase (over 16-fold) in the aqueous solubility. The drug's partial amorphization (lower molecular crystallinity) and the naturosome's overall amphiphilic character could contribute to the produced complexes' increased solubility (Singh et al., 2013; Xia et al., 2013).

3.5.2. *In-vitro drug release (dissolution)*

Fig. 4A displays the outcomes of *in-vitro* drug release experiments. The pure BSE demonstrated the slowest dissolution rate, with only about 31% *w*/w of BSE being dissolved at the end of the 12 h dissolution in the phosphate buffer (pH -6.8). At the end of the dissolution period, the prepared BSEN showed a noticeably faster release of BSE. Over 99% w/w BSE was seen to be released from the BSEN at the end of 12 h, indicating that the BSEN's dissolution profile followed a zero-order release. The wettability and crystal morphology of the solids have a significant impact on the dissolution rate, and the enhanced solubility and partially disrupted crystalline phase (amorphous form) in the produced naturosome may be responsible for the improved dissolution rate of BSE from the BSEN (Freag et al., 2013; Semalty et al., 2010). The increased amorphous state and enhanced water solubility of naturosomes might have contributed to the gradual accumulation of drug release.

3.5.3. *Ex-vivo permeability*

Fig. 4B displays the outcomes of the *ex-vivo* permeability research on pure BSE and the produced BSEN using the everted intestinal method. The examined samples' permeability seems to correspond to the patterns found in the *in-vitro* release investigation. After the three-hour investigation, it was found that just 20% by weight of the pure BSE had passed through the everted intestine. However, the prepared BSEN showed a noticeably enhanced ability to pass BSE via the everted intestine. Over 79% w/w of BSE from BSEN was discovered to have permeated the biological barrier after the 3 h of testing. The amphiphilic character of the phospholipids may function as a surfactant and boost the permeability of the medication through the membrane (Li et al., 2015). This drug-phospholipid complexation technique presents itself as a viable formulation strategy for enhancing BSE delivery to the physiology due to the reported better solubility, higher dissolution rate, and observed more excellent permeability of the BSE in the produced BSEN. Our present results are coherent with Hüsch et al. (2013) study, suggesting that the poor bioavailability, absorption, and permeability of administering BSE or BAs can be enhanced by formulating into a phospholipid complex (Hüsch et al., 2013).

3.6. *Anti-arthritic study*

3.6.1. *Effect on body weight*

Compared to normal control rats, the body weight of arthritis-affected control rats dramatically reduced ($p < 0.01$ and $p < 0.001$) from day 11 to day 22 (Fig. 4C). When compared to rats with arthritis, rats treated with indomethacin 3 mg/kg (the reference medicine) and BSEN (equivalent to 180 mg/kg BSE) showed a substantial increase in body weight ($p < 0.05$, $p < 0.01$ and $p < 0.001$) from days 11 to 22. However, this difference was not seen in the BSE (180 mg/kg) treatment group. The effects of BSEN and indomethacin on body weight gain were comparable ($p > 0.05$), whereas BSEN was more effective in terms of body weight gain when compared to pure BSE ($p < 0.05$). Wendt et al. (2019) showed that under arthritic situations, the body weights of the rats were significantly lower in the control group (arthritic rats) than in healthy or treated rats (Wendt et al., 2019). This may be linked to cachexia, a condition in which there is a decrease in food intake and a loss of muscle mass (lipolysis) that inhibits the accumulation of body mass. According to studies, cachexia in arthritic rats results from metabolic changes brought on by systemic inflammation as well as anorexia (Evans et al., 2008; Fonseca et al., 2011). Our study aligns with

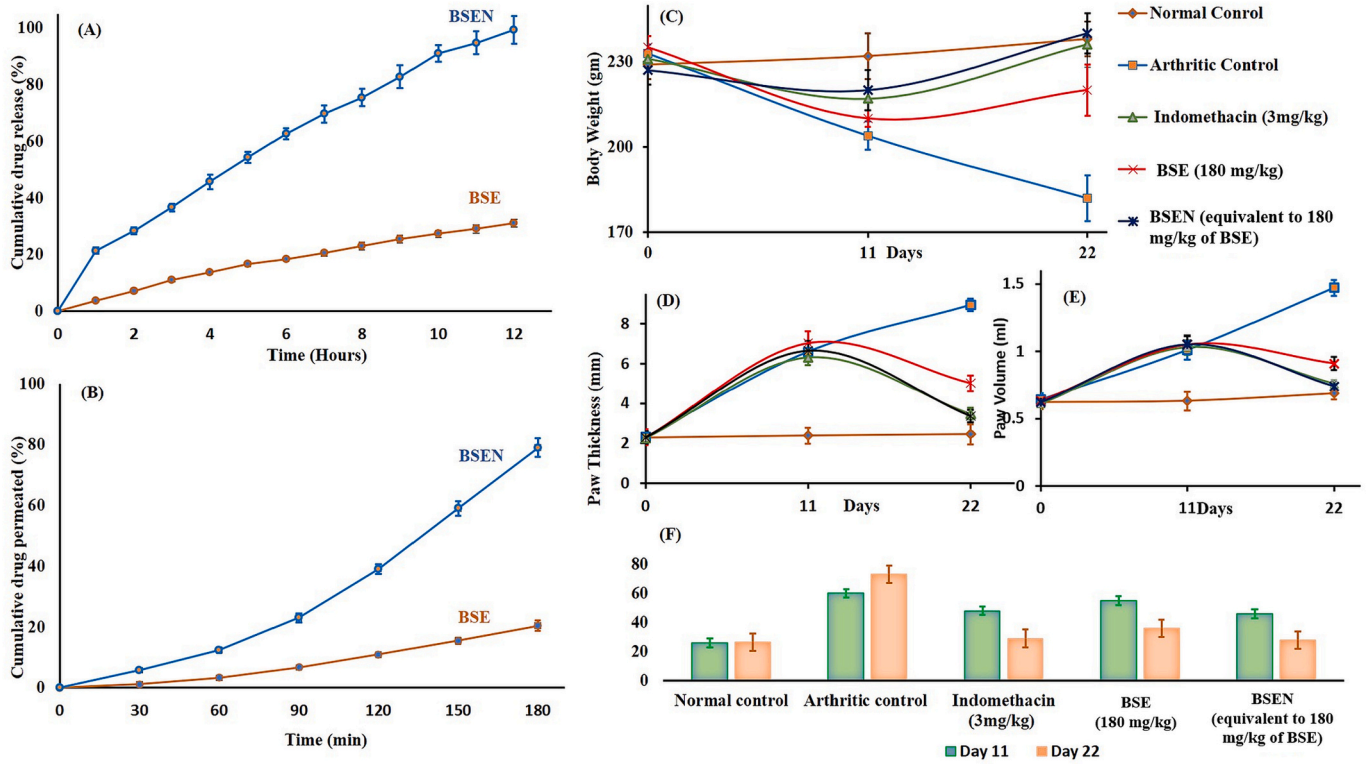

Fig. 4. (A) In-vitro dissolution profiles of BSE and BSEN, (B) *Ex-vivo* permeability profiles of BSE and BSEN, (C) Body weight, (D) Paw Thickness, (E) Paw Volume, (F) TNF-α measurement in mice. Animals were treated with vehicle (control), Arthritic control (FCA-induced arthritis), indomethacin (3 mg/kg), pure BSE (180 mg/kg), and the BSEN (equivalent to BSE 180 mg/kg). Data expressed as mean ± SEM.

these reports, and treatment with BSENs ameliorated the cachexia condition, leading to improved body mass.

3.6.2. Effect on paw thickness

In animals, the CFA-induced arthritis paradigm simulates chronic inflammation accompanied by multiple systemic changes, including synovial hyperplasia (Mbiantcha et al., 2017). Rats that had been given CFA (groups 2 to 5) to make them arthritic had statistically considerably ($p < 0.01$ and $p < 0.001$) thicker paws than the normal control group. When compared to BSE (180 mg/kg) in the arthritis-induced group, the indomethacin (3 mg/kg) and BSEN (equivalent to 180 mg/kg BSE) treatments dramatically ($p < 0.05$ and $p < 0.01$) reduced the paw thickness (Fig. 4D). Interestingly, the decreased in rat paw thickness was also reported with similar effects produced by the formulating BSEN in carrageenan-induced paw edema model (Sharma et al., 2010). This indicates that BAs developed in phytosomal delivery have dramatic anti-inflammatory benefits, which aligns with our results.

3.6.3. Effect on paw volume

On day 0 before CFA injection, each rat's left hind paw volume in each group was assessed and considered as baseline values (Fig. 4E). On days 11 and 22, compared to day 0, there was a slight increase in the paw volume of the normal control. On day 11 compared to day 0, all CFA-induced arthritic groups (group 2 to 5) paw volume measurements showed a substantial increase ($p < 0.01$ and $p < 0.001$). Following medication administration, BSE (180 mg/kg) had no discernible impact on the edema, whereas BSEN (equivalent to 180 mg/kg BSE) at the same dosing level reduced the edema volume similarly as indomethacin (3 mg/kg) ($p < 0.05$ and $p < 0.001$). The decline in CFA-induced paw inflammation measures the anti-inflammatory potential of the test drug (Kshirsagar et al., 2014).

3.6.4. Effect on TNF-α

After receiving a CFA injection, the rat footpad becomes inflamed around the ligaments and joint capsules. During the initial phases of inflammation, edema brought on by CFA gradually appears and persists for two weeks. Significant leukocyte infiltration, an increase in chemokine and cytokine levels, such as IL-1 and TNF-, the production of reactive oxygen species, the breakdown of cartilage and bone, and swelling and deformation are the main contributing factors (Mbiantcha et al., 2017). TNF-α is an inflammatory cytokine encoded within the major histocompatibility complex as a trimeric protein. Patients with RA have high levels of TNF-α in their blood and synovial fluid, suggesting that this may be one of the causes of RA (Farrugia and Baron, 2016). On day 11, TNF-α levels in the CFA-induced arthritic rats were higher ($p < 0.01$ and $p < 0.001$) than in the normal control group (Fig. 4F). As an inflammatory marker, TNF-α encourages inflammation and leads to the deterioration of joint tissue when its levels get elevated. When day 22 readings were compared to day 11 values, the arthritic control group's TNF-α levels increased noticeably. TNF-α levels were significantly

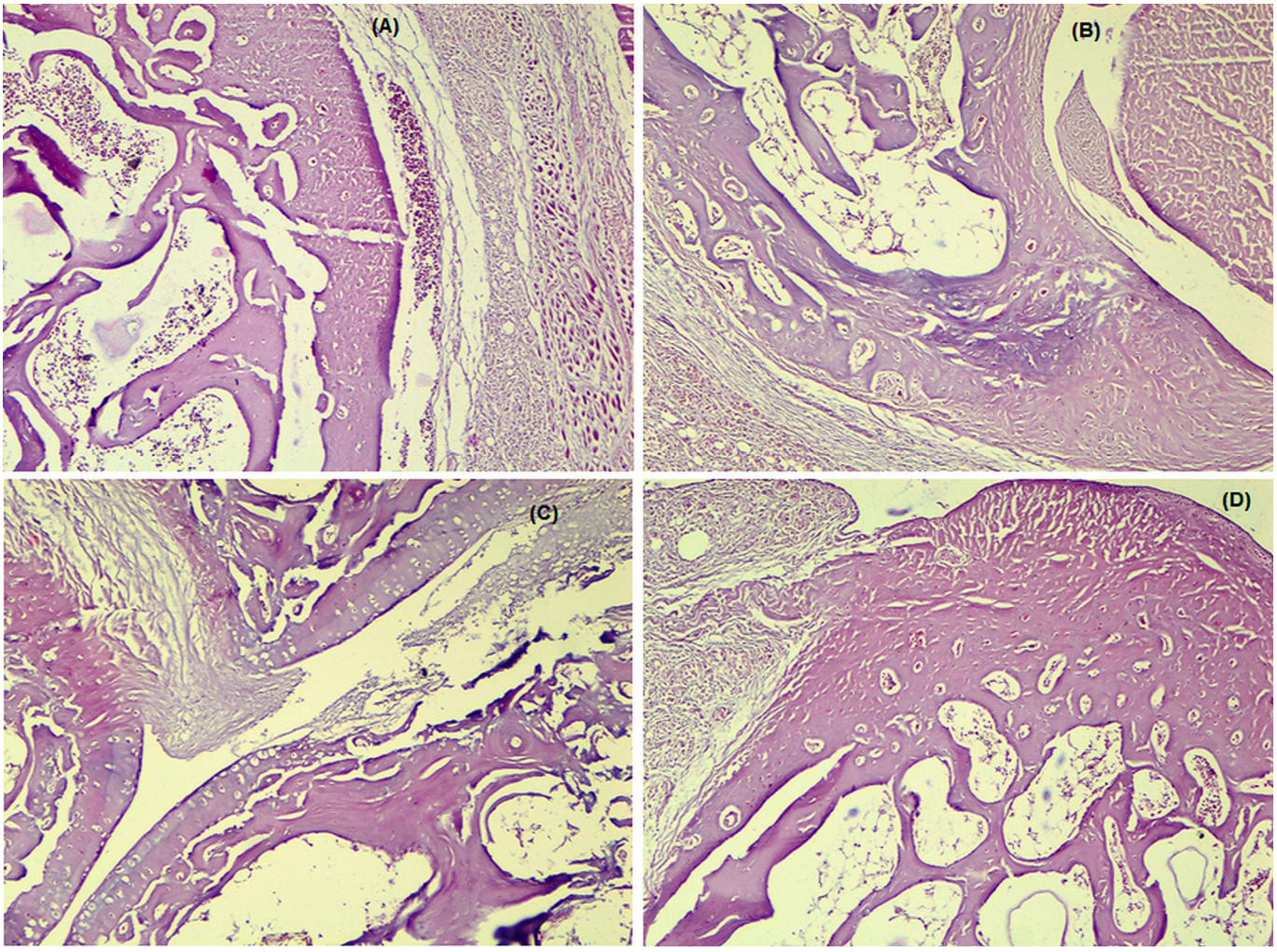

Fig. 5. Histopathological images of the cartilage tissue of the joint sections of an inflamed hind limb. (A) Arthritic control (FCA-induced arthritis), (B) indomethacin (3 mg/kg), (C) pure BSE (180 mg/kg) and (D) the BSEN (equivalent to BSE 180 mg/kg) treated rats.

reduced in the groups treated with indomethacin and BSEN ($p < 0.05$ and $p < 0.001$) but not in the groups treated with BSE, compared to the rats with arthritis in the control group. Literature has suggested that boswellic acid exhibits potential anti-inflammatory and anti-arthritic properties in both *in-vitro* and *in-vivo* models. The molecular target of its inhibitory activity on kappa B kinases was shown to have anti-inflammatory effects, which led to an inhibition of NF-κB activation and TNF-α release from activated monocytes (Nema et al., 2022). These findings align with our study, which suggested that boswellic acid given alone or in the form of naturosome produces potential effects in alleviating the inflammatory cascade in RA condition.

3.6.5. Histopathological analysis

An arthritic control inflamed hind limb's joint sections' histological findings (Fig. 5A) revealed degenerative cartilage and bone tissue alterations. The cartilage tissue displayed focal areas with an uneven surface that may have been damaged or eroded. Additionally, the joint tissue showed focal infiltration of inflammatory cells. Arthritis and the degenerative characteristics of bone and cartilage were linked to pathological alterations in the cartilage tissue. Rats treated with indomethacin (3 mg/kg) (Fig. 5B) or BSEN (equivalent to 180 mg/kg BSE) (Fig. 5D) displayed normal cellular histomorphology in the bone tissue and surrounding muscle tissue in the joint sections. The bone tissue and cartilage both seemed consistent and intact. Joint tissue slices exhibited relatively fewer pathogenic or inflammatory alterations.

Rats treated with BSE (180 mg/kg) demonstrated negligible cartilage and bone tissue degeneration in the joint tissue (Fig. 5C). Only one focus with bone deterioration characteristics was visible in the cartilage tissue.

Pure BSE has limited bioavailability because of its lipophilic makeup, which may explain why it had no discernible effects on body weight, paw thickness, paw volume, or TNF-α inhibition in the current investigation. However, the same amount of BSE supplied in phospholipid nanocarrier form, i.e., BSEN, considerably raised body weight, decreased the thickness of the paw and the volume of paw edema, and inhibited TNF-α in serum, demonstrating a significantly greater bioavailability of BSE via naturosomal nano drug delivery system.

Even though both BSE and BSEN treatment showed anti-arthritic potential, BSEN appeared more effective than BSE in treating FCA-induced arthritis. The following elements may be responsible for improving BSEN's relative absorption after oral administration: BSE has a dissolving rate restriction because of its lipophilic nature, which limits its absorption and bioavailability. Interactions between the non-polar fatty acid portion of the phospholipid and the BSE may have improved BSEN's total hydrophilicity and solubility (Khan et al., 2013). As a result, the BSEN's ability to dissolve more quickly may have enhanced.

Additionally, the reduced particle size of the produced BSEN might have increased the percentage of BSE absorption following oral administration. A longer duration of effect and increased bioavailability may be brought about by the prolonged release of BSE from BSEN and a reduced metabolism (Tan et al., 2012). As noted in earlier research, intestinal transport and absorption mechanisms may have contributed to the increased BSEN oral bioavailability (Metkari et al., 2023; Saoji et al., 2016a; Yanyu et al., 2006).

3.7. Proposed mechanism in naturosome formation

Phospholipids are critical components of cell membranes, with a distinct structure that aids in naturosome synthesis. A phospholipid molecule comprises one hydrophilic head group and two hydrophobic fatty acid tails. In water, phospholipids spontaneously form bilayers, with hydrophilic heads facing the aqueous environment and hydrophobic tails facing inward, insulated from water. Because of their amphiphilic nature, phospholipids can form stable structures like micelles, which enclose hydrophobic compounds (Metkari et al., 2023; Saoji et al., 2017; Saoji et al., 2016b).

In the context of naturosome complex formation, the amphiphilic nature of phospholipids enables them to interact with hydrophobic bioactive compounds/extracts derived from plants. These interactions involve the hydrophobic tails of phospholipids associating with the hydrophobic regions of the bioactive compounds while the hydrophilic heads remain exposed to the surrounding medium (Gurav et al., 2022; Saoji et al., 2017; Saoji et al., 2022). This results in the formation of complexes where the bioactive compounds are encapsulated within the phospholipid bilayers. Additionally, the self-assembly properties of phospholipids contribute to the stability and uniform dispersion of the complexes (Khan et al., 2013).

In our investigation, the spectroscopic data confirmed that the interaction of phospholipid with bioactive is due to the formation of hydrogen bonds between the polar head and the polar functionalities of the active ingredient. In a nutshell, the interactions between active constituents and phospholipids occur via hydrogen bonds to generate intermolecular force rather than chemical or hybrid bonds.

4. Conclusion

The present investigation attempted fabrication and anti-arthritic assessment of naturosomal nanocarriers in FCA-induced arthritis. The central composite design gave the optimal conditions for preparing naturosomes by combining several rational combinations of drug: phospholipid, reaction time, and reaction temperature. As a result, naturosomal delivery of BAs enhanced their aqueous solubility (a major constraint in the therapeutic application) and dissolution rate, potentially amplifying their total therapeutic efficacy. The aforementioned findings were further confirmed by the enhanced permeability of BSEN than BAE. Also, *in-vivo* studies using the FCA-induced arthritic animal model demonstrated significantly more activity of BSEN. Further, more research examining pharmacokinetic characteristics must support the higher bioavailability and greater absorption hypotheses.

Supplementary data to this article can be found online at https://doi.org/10.1016/j.ijpx.2024.100257.

CRediT authorship contribution statement

Poonam Usapkar: Writing – original draft, Validation, Software, Methodology, Investigation. **Suprit Saoji:** Writing – review & editing, Software, Resources, Investigation, Formal analysis, Data curation. **Pradnya Jagtap:** Software, Methodology, Investigation, Formal analysis, Data curation. **Muniappan Ayyanar:** Writing – review & editing, Validation, Software, Methodology, Investigation, Formal analysis, Data curation. **Mohan Kalaskar:** Writing – review & editing, Software, Resources, Methodology, Formal analysis, Data curation. **Nilambari Gurav:** Writing – review & editing, Visualization, Methodology, Formal analysis, Data curation. **Sameer Nadaf:** Writing – review & editing, Validation, Software, Methodology, Formal analysis, Data curation. **Satyendra Prasad:** Writing – review & editing, Software, Resources, Methodology, Formal analysis, Data curation. **Damiki Laloo:** Writing – review & editing, Software, Resources, Methodology, Formal analysis, Data curation. **Mohd Shahnawaz Khan:** Writing – review & editing, Validation, Resources, Funding acquisition, Formal analysis, Data curation. **Rupesh Chikhale:** Writing – review & editing, Visualization, Software, Methodology, Funding acquisition, Formal analysis, Data curation. **Shailendra Gurav:** Writing – original draft, Methodology, Investigation, Data curation, Conceptualization.

Declaration of competing interest

The authors declare no competing interests.

Data availability

Data will be made available on request.

Acknowledgments

The authors acknowledge the generous support from the Research Supporting Project (RSP2024R352) by King Saud University, Riyadh, Kingdom of Saudi Arabia.

References

Akhtar, M.F., Khan, K., Saleem, A., Baig, M.M.F.A., Rasul, A., Abdel-Daim, M.M., 2021. Chemical characterization and anti-arthritic appraisal of Monotheca buxifolia methanolic extract in complete Freund's adjuvant-induced arthritis in Wistar rats. Inflammopharmacology 29, 393–408.

Andrade, F., Jenipher, C., Gurav, N., Nadaf, S., Khan, M.S., Mahajan, N., Bhagwat, D., Kalaskar, M., Chikhale, R., Bhole, R., Lalsare, S., 2024. Endophytic fungi-assisted biomass synthesis of eco-friendly formulated silver nanoparticles for enhanced antibacterial, antioxidant, and antidiabetic activities. J. Drug Deliv. Sci. Technol. 97, 105749.

Di Lorenzo, C., Dellagli, M., Badea, M., Dima, L., Colombo, E., Sangiovanni, E., Restani, P., Bosisio, E., 2013. Plant food supplements with anti-inflammatory properties: a systematic review (II). Crit. Rev. Food Sci. Nutr. 53, 507–516.

Dias, C., Ayyanar, M., Amalraj, S., Khanal, P., Subramaniyan, V., Das, S., Gandhale, P., Biswa, V., Ali, R., Gurav, N., 2022. Biogenic synthesis of zinc oxide nanoparticles using mushroom fungus *Cordyceps militaris*: Characterization and mechanistic insights of therapeutic investigation. J. Drug Deliv. Sci. Technol. 73, 103444.

Dixit, P., Jain, D.K., Dumbwani, J., 2012. Standardization of an ex vivo method for determination of intestinal permeability of drugs using everted rat intestine apparatus. J. Pharmacol. Toxicol. Methods 65, 13–17.

Evans, W.J., Morley, J.E., Argilés, J., Bales, C., Baracos, V., Guttridge, D., Jatoi, A., Kalantar-Zadeh, K., Lochs, H., Mantovani, G., 2008. Cachexia: a new definition. Clin. Nutr. 27, 793–799.

Farrugia, M., Baron, B., 2016. The role of TNF-α in rheumatoid arthritis: a focus on regulatory T cells. J Clin. Transl. Res. 2, 84.

Fonseca, E.A.I., de Oliveira, M.A., de Souza Lobato, N., Akamine, E.H., Colquhoun, A., de Carvalho, M.H.C., Zyngier, S.B., Fortes, Z.B., 2011. Metformin reduces the stimulatory effect of obesity on in vivo walker-256 tumor development and increases the area of tumor necrosis. Life Sci. 88, 846–852.

Freag, M.S., Elnaggar, Y.S., Abdallah, O.Y., 2013. Lyophilized phytosomal nanocarriers as platforms for enhanced diosmin delivery: optimization and ex vivo permeation. Int. J. Nanomedicine 2385–2397.

Gautam, R.K., Gupta, G., Sharma, S., Hatware, K., Patil, K., Sharma, K., Goyal, S., Chellappan, D.K., Dua, K., 2019. Rosmarinic acid attenuates inflammation in experimentally induced arthritis in Wistar rats, using Freund's complete adjuvant. Int. J. Rheum. Dis. 22, 1247–1254.

Gracias, S., Ayyanar, M., Peramaiyan, G., Kalaskar, M., Redasani, V., Gurav, N., Nadaf, S., Deshpande, M., Bhole, R., Khan, M.S., 2023. Fabrication of chitosan nanocomposites loaded with biosynthetic metallic nanoparticles and their therapeutic investigation. Environ. Res. 234, 116609.

Gurav, S., Usapkar, P., Gurav, N., Nadaf, S., Ayyanar, M., Verekar, R., Bhole, R., Venkataramaiah, C., Jena, G., Chikhale, R., 2022. Preparation, characterization, and evaluation (in-vitro, ex-vivo, and in-vivo) of naturosomal nanocarriers for enhanced delivery and therapeutic efficacy of hesperetin. PLoS One 17, e0274916.

Halarnekar, D., Ayyanar, M., Gangapriya, P., Kalaskar, M., Redasani, V., Gurav, N., Nadaf, S., Saoji, S., Rarokar, N., Gurav, S., 2023. Eco synthesized chitosan/zinc oxide nanocomposites as the next generation of nano-delivery for antibacterial, antioxidant, antidiabetic potential, and chronic wound repair. Int. J. Biol. Macromol. 242, 124764.

Hüsch, J., Bohnet, J., Fricker, G., Skarke, C., Artaria, C., Appendino, G., Schubert-Zsilavecz, M., Abdel-Tawab, M., 2013. Enhanced absorption of boswellic acids by a lecithin delivery form (Phytosome®) of Boswellia extract. Fitoterapia 84, 89–98.

Italiano, G., Raimondo, M., Giannetti, G., Gargiulo, A., 2020. Benefits of a food supplement containing Boswellia serrata and bromelain for improving the quality of life in patients with osteoarthritis: a pilot study. J. Altern. Complement. Med. 26, 123–129.

Jena, S.K., Singh, C., Dora, C.P., Suresh, S., 2014. Development of tamoxifen-phospholipid complex: novel approach for improving solubility and bioavailability. Int. J. Pharm. 473, 1–9.

Khan, J., Alexander, A., Saraf, S., Saraf, S., 2013. Recent advances and future prospects of phyto-phospholipid complexation technique for improving pharmacokinetic profile of plant actives. J. Control. Release 168, 50–60.

Khayyal, M.T., El-Hazek, R.M., El-Sabbagh, W.A., Frank, J., Behnam, D., Abdel-Tawab, M., 2018. Micellar solubilisation enhances the antiinflammatory activities of curcumin and boswellic acids in rats with adjuvant-induced arthritis. Nutrition 54, 189–196.

Kshirsagar, A.D., Panchal, P.V., Harle, U.N., Nanda, R.K., Shaikh, H.M., 2014. Anti-inflammatory and antiarthritic activity of anthraquinone derivatives in rodents. Int. J. Inflamm. 2014.

Kumar, R., Singh, S., Saksena, A.K., Pal, R., Jaiswal, R., Kumar, R., 2019. Effect of Boswellia serrata extract on acute inflammatory parameters and tumor necrosis factor-α in complete Freund's adjuvant-induced animal model of rheumatoid arthritis. Int. J. Appl. Basic Med. Res. 9, 100.

LeFevre, M., Olivo, R., Vanderhoff, J., Joel, D., 1978. Accumulation of latex in Peyer's patches and its subsequent appearance in villi and mesenteric lymph nodes. Proc. Soc. Exp. Biol. Med. 159, 298–302.

Li, J., Wang, X., Zhang, T., Wang, C., Huang, Z., Luo, X., Deng, Y., 2015. A review on phospholipids and their main applications in drug delivery systems. Asian J. Pharm. Sci. 10, 81–98.

Maiti, K., Mukherjee, K., Gantait, A., Saha, B.P., Mukherjee, P.K., 2007. Curcumin–phospholipid complex: preparation, therapeutic evaluation and pharmacokinetic study in rats. Int. J. Pharm. 330, 155–163.

Majeed, M., Nagabhushanam, K., Lawrence, L., Nallathambi, R., Thiyagarajan, V., Mundkur, L., 2021. *Boswellia serrata* Extract containing 30% 3-acetyl-11-keto-boswellic acid attenuates inflammatory mediators and preserves extracellular matrix in collagen-induced arthritis. Front. Physiol. 1578.

Mannino, G., Occhipinti, A., Maffei, M.E., 2016. Quantitative determination of 3-O-acetyl-11-keto-β-boswellic acid (AKBA) and other boswellic acids in Boswellia sacra Flueck (syn. B. Carteri Birdw) and Boswellia serrata Roxb. Molecules 21, 1329.

Mbiantcha, M., Almas, J., Shabana, S.U., Nida, D., Aisha, F., 2017. Anti-arthritic property of crude extracts of *Piptadeniastrum africanum* (Mimosaceae) in complete Freund's adjuvant-induced arthritis in rats. BMC Complement. Altern. Med. 17, 1–16.

Metkari, V., Shah, R., Salunkhe, N., Gurav, S., 2023. QBD approach for the design, optimization, development, and characterization of naringenin-loaded phytosomes to enhance solubility and oral bioavailability. J. Pharm. Innov. 18, 2083–2097.

Nema, N.K., Chaudhary, S.K., Kar, A., Bahadur, S., Harwansh, R.K., Haldar, P.K., Sharma, N., Mukherjee, P.K., 2022. Bioactive leads for skin aging—current scenario and future perspectives. In: Evidence-Based Validation of Herbal Medicine. Elsevier, pp. 185–222.

Pearson, C.M., 1956. Development of arthritis, periarthritis and periostitis in rats given adjuvants. Proc. Soc. Exp. Biol. Med. 91, 95–101.

Qin, X., Yang, Y., Fan, T.-T., Gong, T., Zhang, X.-N., Huang, Y., 2010. Preparation, characterization and in vivo evaluation of bergenin-phospholipid complex. Acta Pharmacol. Sin. 31, 127–136.

Rarokar, N., Gurav, S., Khedekar, P., 2021. Meloxicam encapsulated nanostructured colloidal self-assembly for evaluating antitumor and anti-inflammatory efficacy in 3D printed scaffolds. J. Biomed. Mater. Res. A 109, 1441–1456.

Rarokar, N., Agrawal, R., Yadav, S., Khedekar, P., Ravikumar, C., Telange, D., Gurav, S., 2023. Pteroyl-γ-l-glutamate/pluronic® F68 modified polymeric micelles loaded with docetaxel for targeted delivery and reduced toxicity. J. Mol. Liq. 369, 120842.

Rodrigues, K., Gurav, S., Joshi, A., Krishna, M., Bhandarkar, A., 2020. Porous polymeric carrier system for modified drug release of boswellic acid. Chem. Sci. J. 11, 1–12.

Rodrigues, K., Nadaf, S., Rarokar, N., Gurav, N., Jagtap, P., Mali, P., Ayyanar, M., Kalaskar, M., Gurav, S., 2022. QBD approach for the development of hesperetin loaded colloidal nanosponges for sustained delivery: in-vitro, ex-vivo, and in-vivo assessment. OpenNano 7, 100045.

Roy, N.K., Parama, D., Banik, K., Bordoloi, D., Devi, A.K., Thakur, K.K., Padmavathi, G., Shakibaei, M., Fan, L., Sethi, G., 2019. An update on pharmacological potential of boswellic acids against chronic diseases. Int. J. Mol. Sci. 20, 4101.

Saoji, S.D., Belgamwar, V.S., Dharashivkar, S.S., Rode, A.A., Mack, C., Dave, V.S., 2016a. The study of the influence of formulation and process variables on the functional attributes of simvastatin–phospholipid complex. J. Pharm. Innov. 11, 264–278.

Saoji, S.D., Raut, N.A., Dhore, P.W., Borkar, C.D., Popielarczyk, M., Dave, V.S., 2016b. Preparation and evaluation of phospholipid-based complex of standardized centella extract (SCE) for the enhanced delivery of phytoconstituents. AAPS J. 18, 102–114.

Saoji, S.D., Dave, V.S., Dhore, P.W., Bobde, Y.S., Mack, C., Gupta, D., Raut, N.A., 2017. The role of phospholipid as a solubility-and permeability-enhancing excipient for the improved delivery of the bioactive phytoconstituents of Bacopa monnieri. Eur. J. Pharm. Sci. 108, 23–35.

Saoji, S.D., Rarokar, N.R., Dhore, P.W., Dube, S.O., Gurav, N.S., Gurav, S.S., Raut, N.A., 2022. Phospholipid based colloidal nanocarriers for enhanced solubility and therapeutic efficacy of withanolides. J. Drug Deliv. Sci. Technol. 70, 103251.

Savic, R., Luo, L., Eisenberg, A., Maysinger, D., 2003. Micellar nanocontainers distribute to defined cytoplasmic organelles. Science 300, 615–618.

Semalty, A., Semalty, M., Singh, D., Rawat, M., 2010. Preparation and characterization of phospholipid complexes of naringenin for effective drug delivery. J. Incl. Phenom. Macrocycl. Chem. 67, 253–260.

Shabbir, A., Shahzad, M., Ali, A., Zia-ur-Rehman, M., 2014. Anti-arthritic activity of N′-[(2, 4-dihydroxyphenyl) methylidene]-2-(3, 4-dimethyl-5, 5-dioxidopyrazolo [4, 3-c][1,2] benzothiazin-1 (4H)-yl) acetohydrazide. Eur. J. Pharmacol. 738, 263–272.

Shabbir, A., Shahzad, M., Ali, A., Zia-ur-Rehman, M., 2016. Discovery of new benzothiazine derivative as modulator of pro-and anti-inflammatory cytokines in rheumatoid arthritis. Inflammation 39, 1918–1929.

Sharma, A., Gupta, N.K., Dixit, V.K., 2010. Complexation with phosphatidyl choline as a strategy for absorption enhancement of boswellic acid. Drug Deliv. 17, 587–595.

Singh, D., Rawat, M., Semalty, A., Semalty, M., 2013. Chrysophanol–phospholipid complex: a drug delivery strategy in herbal novel drug delivery system (HNDDS). J. Therm. Anal. Calorim. 111, 2069–2077.

Singh, C., Bhatt, T.D., Gill, M.S., Suresh, S., 2014. Novel rifampicin–phospholipid complex for tubercular therapy: synthesis, physicochemical characterization and in-vivo evaluation. Int. J. Pharm. 460, 220–227.

Suther, C., Daddi, L., Bokoliya, S., Panier, H., Liu, Z., Lin, Q., Han, Y., Chen, K., Moore, M.D., Zhou, Y., 2022. Dietary Boswellia serrata acid alters the gut microbiome and blood metabolites in experimental models. Nutrients 14, 814.

Sze, A., Erickson, D., Ren, L., Li, D., 2003. Zeta-potential measurement using the Smoluchowski equation and the slope of the current–time relationship in electroosmotic flow. J. Colloid Interface Sci. 261, 402–410.

Tan, Q., Liu, S., Chen, X., Wu, M., Wang, H., Yin, H., He, D., Xiong, H., Zhang, J., 2012. Design and evaluation of a novel evodiamine-phospholipid complex for improved oral bioavailability. AAPS PharmSciTech 13, 534–547.

Wendt, M.M., de Oliveira, M.C., Franco-Salla, G.B., Castro, L.S., Parizotto, Â.V., Silva, F. M.S., Natali, M.R., Bersani-Amado, C.A., Bracht, A., Comar, J.F., 2019. Fatty acids

uptake and oxidation are increased in the liver of rats with adjuvant-induced arthritis. Biochim. Biophys. Acta Mol. basis Dis. 1865, 696–707.
Xia, H.-J., Zhang, Z.-H., Jin, X., Hu, Q., Chen, X.-Y., Jia, X.-B., 2013. A novel drug–phospholipid complex enriched with micelles: preparation and evaluation in vitro and in vivo. Int. J. Nanomedicine 545–554.
Yanyu, X., Yunmei, S., Zhipeng, C., Qineng, P., 2006. The preparation of silybin–phospholipid complex and the study on its pharmacokinetics in rats. Int. J. Pharm. 307, 77–82.
Zhang, Y., Huo, M., Zhou, J., Zou, A., Li, W., Yao, C., Xie, S., 2010. DDSolver: an add-in program for modeling and comparison of drug dissolution profiles. AAPS J. 12, 263–271.

Contents lists available at UGC-CARE

International Journal of Pharmaceutical Sciences and Drug Research

[ISSN: 0975-248X; CODEN (USA): IJPSPP]

journal home page : http://ijpsdr.com/index.php/ijpsdr

Research Article

Design and Development of Some Pyrimidine Analogues as an Anthelmintic Agent

Smita J. Pawar*, **Rahul Dorugade, Amol P. Kale, Dhanashri Zope**

PDEA's Department of Pharmaceutical Chemistry, Seth Govind Raghunath Sable College of Pharmacy, Pune, Maharashtra, India.

ARTICLE INFO

Article history:

Received: 07 September, 2023

Revised: 26 December, 2023

Accepted: 30 December, 2023

Published: 30 January, 2024

Keywords:

Anthelmintics, Pyrimidine, Aldehydes, Microparasitic diseases, Molecular docking, Earthworms, Nematode, Trematode, Cestode.

DOI:

10.25004/IJPSDR.2024.160102

ABSTRACT

Anthelmintic drugs are used to treat parasitic infections and acknowledge the challenge in developing effective anthelmintics due to the significant homology between parasites and their hosts. Despite the existence of various anthelmintic drugs in the market, the emergence of drug resistance necessitates the continuous development of new and more efficient drugs to combat parasitic infections. The development of anthelmintic drugs involves a multi-faceted process that aims to create effective treatments against parasitic infections. Pyrimidines have been investigated for their potential anthelmintic activity. Therefore, the present study involves the synthesis of derivatives based on pyrimidine. The series of 4-amino-2-hydroxy-6-substituted phenyl pyrimidine-5-carbonitrile was synthesized by treating substituted benzaldehyde with malononitrile and urea. The synthesized compounds were subsequently screened for their anthelmintic efficacy. The chemical structures were confirmed by infrared (IR) and proton nuclear magnetic resonance (^{1}H-NMR) spectroscopy. The anthelmintic activity was performed on the adult Indian earthworm *Pheretima posthuma*. *In-vitro* anthelmintic studies revealed that, among all the screened compounds, compound 1f demonstrated significant or appreciable anthelmintic properties. Molecular docking was conducted on quinol-fumarate reductase to elucidate potential interactions between the newly synthesized pyrimidine derivatives and the specific cavity of the quinol-fumarate reductase enzyme. This analysis aimed to gain insights into the binding interactions and the possible mechanism of action of the synthesized compounds.

Introduction

Anthelmintics are pharmaceuticals used to treat and prevent microparasitic diseases like parasitic nematode, trematode, and cestode infections in humans as well as animals.[1,2] Our capacity to disrupt the life cycles of these parasites has been hampered by the lack of efficient vaccinations and poor sanitation in some endemic places.[3,4] High costs and small global markets for antiparasitic medications and chemicals are barriers to the development of novel anthelmintics. For animals and people, the expenses of developing new medications are expected to be $400 million and over $800 million, respectively. According to estimates, there is a $12 billion global market for antiparasitic medications and chemicals for plant pathogens, a $11 billion market for livestock and companion animals, and a $0.5 billion industry for human health.[5] The market offers a wide range of anthelmintics or anthelmintic medications to eliminate such parasitic worms from the body by either killing or stunning them without significantly harming the host cell.[6, 7] Due to the persistence of the recurring establishment of resistance, well-known marketing pyrimidine-derived medicines pyrantel and morantel are frequently employed as anthelmintic medications with broad-spectrum activity and high cure rates.[8] But utilizing currently available medications, some infectious disorders that are already present cannot be entirely cured in humans.[9] Parasites can develop resistance to anthelmintic drugs.[10]

However, 4- (1H-benzimidazol-2-yl)-6- (2-chloroquinolin-3-yl) pyrimidine-2-amine derivatives showed good anthelmintic activity against *Pheretima posthuma* using albendazole as a standard.[11] The presence of

***Corresponding Author:** Dr. Smita J. Pawar

Address: PDEA's Department of Pharmaceutical Chemistry, Seth Govind Raghunath Sable College of Pharmacy, Pune, Maharashtra, India.

Email ✉**:** sjpawar4477@gmail.com

Tel.: +91-9970705513

Relevant conflicts of interest/financial disclosures: The authors declare that the research was conducted in the absence of any commercial or financial relationships that could be construed as a potential conflict of interest.

various substitutions such as hydroxy, methoxy, and nitro groups on the aromatic ring of 4,6-disubstituted pyrimidine-2-one derivatives provides significant activity.[12] 2-methyl/propyl4 (2 (substitutedbenzylidene) hydrazinyl)5,6,7,8 tetrahydrobenzo[4,5]thieno[2,3] pyrimidines were synthesized and evaluated for anthelminthic activity against adult Indian earthworms (*P. posthuma*). Compounds with propyl group at the 2-position of the thieno[2,3-d] pyrimidine scaffold found to be favorable for the anthelminthic activity of the exhibiting mean paralytic time of 2.5, 2.81 minutes and helminthicidal time of 21, 20.03 minutes, respectively, at the same concentration (100 µg/ml, 259.7 µM).[13] 2- (N, N-dimethyl guanidinyl)-4,6-diaryl pyrimidines exhibited good anthelmintic activity inducing paralysis in 36 to 48 minutes and death in 40 to 51 minutes as compared to the standard drug albendazole.[14] Anthelmintics, a category of antiparasitic medications, often present significant challenges for individuals infected with parasites. Anti-parasitic drugs effectively eliminate parasitic worms without harming the host. David I Ugwu *et al.* (2018) synthesized new pyrimidine analogs bearing carboxamide and sulphonamide moieties and tested them for anthelmintic activity. Among all compounds (44) exhibited satisfactory anthelmintic activity (Paralyzing time: 37, 26 and 19 minutes) compared to that of albendazole (Paralyzing time: 28, 20 and 10 minutes). The increased activity could potentially be attributed to the existence of both the nitrophenyl and pyrimidine scaffold.[15] Based on literature findings suggesting the potential anthelmintic properties of pyrimidine, we undertook the design and synthesis of 4-Amino-2-hydroxy-6-substitutedphenylpyrimidine-5-carbonitrile and conducted an evaluation of its efficacy against parasites. The chemical structures were confirmed by infrared (IR) and proton nuclear magnetic resonance (^{1}H-NMR). The molecular docking was performed on quinol-fumarate reductase to gain insight into the possible interactions between newly synthesized pyrimidine derivatives and the selected cavity of quinol-fumarate reductase enzyme.

Materials And Method

The chemicals utilized in the synthesis were all of laboratory-grade quality. The determination of melting points was carried out using an open capillary equipped with the Veego electronic apparatus (model: VMP-D). The IR spectra of the synthesized compounds were obtained using a Shimadzu 8400-S fourier-transform infrared spectroscopy (FTIR) spectrophotometer with potassium bromide. The ^{1}H-NMR spectra were recorded in $CDCl_3$ and DMSO using an NMR BRUKER 500 MHz instrument, and the chemical shift values were expressed in parts per million, referenced downfield from tetramethyl silane (TMS) as the internal standard. Thin layer chromatography (TLC) was conducted on precoated aluminum sheets (Silica gel 60F254, 6x2.5 cm) employing a solvent mixture of chloroform: ethyl acetate (4:1). The spots were visualized under ultraviolet light. To assess the purity of the synthesized compounds, Rf values were calculated for each compound using the following formula:

RF= Distance travelled by the compound/Distance travelled by the solvent front

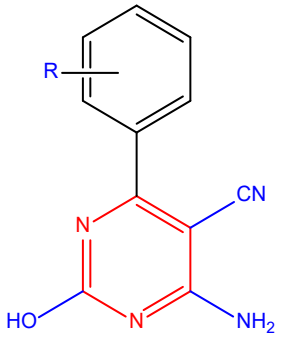

Scheme 1: Phenyl derivative of pyrimidine-5-carbonitrile

Scheme of Synthesis

The target derivatives of pyrimidine were synthesized by treating equimolar quantity of malononitrile, sodium ethoxide and substituted benzaldehyde (Scheme 1). The mixture was acidified with glacial acetic acid and the product was separated. The detailed procedure is as follows.

Procedure for synthesis of 4-amino-2-hydroxy-6-substituted phenylpyrimidine-5-carbonitrile (1a-f)

A solution of 0.01 mole of sodium ethoxide, the equimolar quantity of malononitrile 0.01 mole of substituted benzaldehyde and 0.015 mole of urea was stirred and heated under reflux until the reaction completes. Following this, the reaction mixture was cooled by pouring it onto crushed ice, and 3 to 4 drops of glacial acetic acid were introduced. The resulting solid was separated by filtration, and dried, and the crude product was further purified by recrystallization using aqueous ethanol.

- *4-Amino-2-hydroxy-6-phenylpyrimidine-5-carbonitrile* 1a

Yield: 82%. m.p.: 179–180°C. FTIR: OH (3564.57), NH (3495.13), ArCH (3093.92), CN (2314.66), C=N (1647.27), C=C (1543.10), C-N (1219.21); ^{1}H-NMR (500 MHz, $CDCl_3$) δ: 7.733–7.747 Ar-CH (d, 2H), 7.726–7.730 Ar-CH (t, 1H),7.952–7.961 Ar-CH (d, 2H), 5.108 NH_2 (s, 2H), 8.559 OH (s, 1H).

- *4-Amino-6- (4-chlorophenyl)-2-hydroxypyrimidine-5-carbonitrile* 1b

Yield: 68%. m.p.: 162–164°C. FTIR: OH (3371.68), NH (3302.24), ArCH (3032.20), CN (2229.79), C=N (1581.33), C=C (1496.81), C-N (1095), C-Cl (825.56); ^{1}H-NMR (500 MHz, $CDCl_3$) δ: 7.723–7.737 Ar-CH (d, 2H), 7.947–7.952 Ar-CH (d, 2H), 5.108 NH_2 (s, 2H), 8.559 OH (s, 1H).

- *4-Amino-2-hydroxy-6- (4-nitroyphenyl)pyrimidine-5-carbonitrile* 1c

Yield: 78%. m.p.: 221–223°C. FTIR:OH (3363.97), NH (3209.30) ArCH (3035.91), CN (2206.64), C=N (1635.69), C=C (1519.96), N-O (1257.63), C-N (1126.47); ^{1}H-NMR (500 MHz, $CDCl_3$) δ: 7.615–7.723 Ar-CH (d, 2H), 7.923–7.934 Ar-CH (d, 2H), 5.108 NH_2 (s, 2H), 8.559 OH (s, 1H).

- *4-Amino-2-hydroxy-6- (4-hydroxyphenyl)pyrimidine-5-carbonitrile* 1d

Yield: 61%. m.p.: 173-175°C. FTIR:OH (3402.54), NH (3302.24), ArCH (3032.20), CN (2229.79), C=N (1566.25), C=C (1450.52), C-N (1296.21; ^{1}H-NMR (500 MHz, $CDCl_3$) δ: 7.723-7.737 Ar-CH (d, 2H), 7.947-7.952 Ar-CH (d, 2H), 8.455 OH (s, 1H) 5.108 NH_2 (s, 2H), 8.559 OH (s, 1H).

- *4-Amino-6- (3-bromophenyl)-2-hydroxypyrimidine-5-carbonitrile* 1e

Yield: 81%. m.p.: 178–180°C. FTIR:OH (3402.54), NH (3302.24), ArCH (3032.20), CN (2229.79), C=N (1597.11), C=C (1512.34), C-N (1242.20), C-Br (840.99); ^{1}H-NMR (500 MHz, $CDCl_3$) δ: 7.723–7.737 Ar-CH (d, 2H), 7.947–7.952 Ar-CH (d, 2H), 8.455 OH (s, 1H) 5.108 NH_2 (s, 2H), 8.559 OH (s, 1H).

- *4-Amino-6- (4-fluorophenyl)-2-hydroxypyrimidine-5-carbonitrile* 1f

Yield: 91%. m.p.: 226–228°C. FTIR:OH (3379.40), NH (3333.10) ArCH (3066.21),CN (2206.64), C=N (1604.83), C=C (1527.67), C-N (1350.22), C-F (1111.03); ^{1}H-NMR (500 MHz, $CDCl_3$) δ: 7.739–7.745 Ar-CH (d, 2H), 7.937–7.942 Ar-CH (d, 2H), 5.110 NH_2 (s, 2H), 8.549 OH (s, 1H).

Biological Evaluation

Experimental animal

The anthelmintic activity was evaluated in vitro using adult earthworms (*P. posthuma*). Earthworms were collected from moist soil and subsequently cleansed with normal saline to eliminate any fecal matter or debris adhering to their bodies. Earthworms measuring 6–8 cm in length and 0.3–0.5 cm in width were utilized for the anthelmintic activity test. The identification of the earthworms was conducted at the Department of Zoology, Waghire College, Saswad. *P. posthuma* was chosen as a model for anthelmintic activity due to its similarity in anatomy and physiology to the intestinal roundworm parasites found in humans. Before the commencement of the experiment, the earthworms underwent a washing process using normal saline. [16,17]

The inclusion criteria for the study were as follows:

- Healthy earthworms within the length range of 6–8 cm were included.
- Earthworms of the same species were selected to prevent errors in the study results.

Anthelmintic activity on P. posthuma

The anthelmintic activity was evaluated on adult Indian earthworms (*P. posthuma*) due to their physiological resemblance to the intestinal roundworm parasites found in humans. To prepare the samples, synthesized compounds (100 mg) were triturated with Tween 80 (0.5%) and distilled water, followed by stirring using a mechanical stirrer for 30 minutes. A suspension of the reference drug, albendazole, was also prepared at the same concentration using a similar method.

Three sets of *P. posthuma* of almost identical sizes (2 inches in length) were placed in 4-inch diameter petri plates containing 10 mL suspensions of the test samples and reference drug at concentrations of 50, 100, and 150 mg/mL, maintained at room temperature. Additionally, another set of *P. posthuma* was kept as a control in a 10 mL suspension of distilled water and Tween 80.

The paralyzing and death times of the earthworms were recorded, and the mean values were calculated for triplicate sets. The determination of death time involved placing the earthworms in warm water (50°C) to stimulate movement; if there was no movement, it indicated that the worm had died.

The results obtained from the test samples were compared with those treated with the standard drug, albendazole, to assess and compare the anthelmintic activity.

Molecular Docking

The molecular docking procedure involved utilizing Vlife MDS 4.6 software with the grid batch docking method.

The structures of all the compounds were initially constructed using ChemDraw Ultra 8.0 software. These structures underwent further adjustments, including the addition or removal of hydrogens. Subsequently, the geometries of these compounds were optimized utilizing the Merck molecular force field (MMFF). To explore the conformational space, various conformers of the six-compound set were generated through a systematic conformational search option.

For the receptor, the structure of the quinol-fumarate reductase protein (PDB: 3VR8) was retrieved from the protein data bank (http://www.rcsb.org). This protein structure served as the target for the molecular docking simulations.

Receptor Representation

The receptor representation involved the retrieval of the PDB file from the RCSB protein data bank. The protein initially comprised numerous side chains, which were refined to create a monomer by eliminating chains other than chain A along with ligands. Additionally, water molecules were removed from this monomeric form of the protein structure.

Hydrogens were then added to the protein molecule, and subsequent energy minimization was carried out utilizing the MMFF to optimize the structure and minimize potential energy interactions within the protein.

Generation of Conformers

The generation of conformers involved creating various 3D optimized structures for individual ligands using a systematic conformational search method. In this approach, a predefined set of rotatable bonds within the ligands was identified. For each of these bonds, the software explored all feasible conformations in relation to one another.

The optimization of the generated conformers was carried out utilizing the MMFF force field, which is a commonly used force field for molecular mechanics calculations, to refine and optimize the geometries of these conformers. This process allowed for the exploration of the different possible spatial arrangements or conformations of the ligands.

Docking

The docking procedure involved batch grid docking by generating conformers of the test compounds. Cavity number 1 was selected as the target binding site, and the docking simulations were executed utilizing the Biopredicta program. Following the docking simulations, the resulting docked conformations were subjected to scoring using a scoring function, presumably, the dock score. This score likely assessed and ranked the interactions or binding affinities of the compounds within the binding site of the enzyme. Moreover, the binding energy of the complex formed between the compound and the enzyme was also considered as an important parameter for the evaluation of the interactions and potential affinity of the compound with the enzyme.

Protein Complex Optimization

The process of protein complex optimization involves allowing the ligand to adopt a minimum energy pose within the active site cavity of the protein. This optimization is achieved by merging the docked molecule (ligand) into the protein structure. Subsequently, the ligand-enzyme complex undergoes another round of minimization, refining the arrangement and interactions between the ligand and the enzyme. During this complex optimization, particular attention is paid to observing and noting the interactions of the compounds with the amino acid residues present in the cavity of the protein. This analysis aims to understand the specific interactions between the ligand and the active site residues, shedding light on the binding mode and potential mechanisms of action within the protein's active site.

Binding energy = Optimized docked complex energy – (energy of optimized apo receptor without ligand + energy of optimized ligand

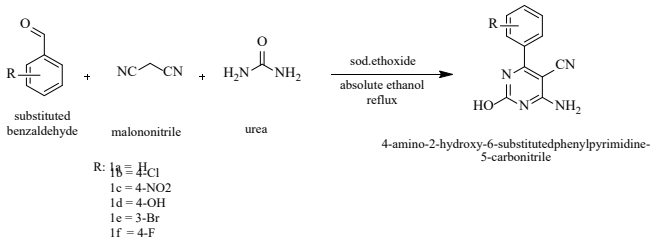

Scheme 2: Synthesis of 4-amino-2-hydroxy-6-substitutedphenylpyrimidine-5-carbonitrile (1a-f)

Results

The new derivatives, 4-Amino-2-hydroxy-6-substituted phenylpyrimidine-5-carbonitrile (1a-f), were successfully synthesized by reacting pyrimidine, malononitrile, and urea with selected benzaldehydes in absolute ethanol according to Scheme 2. The IR spectrum of synthesized compounds showed the NH stretch between 3301 to 3495 cm^{-1}. The broad stretch of hydroxyl OH was observed between 3564 to 3402 cm^{-1}

Anthelmintic activity was observed in a dose-dependent manner. Compound 1f exhibited the highest anthelmintic activity at concentrations of 50, 100, and 150 mg/mL, surpassing the standard drug albendazole (10 mg/mL). Compounds 1b, 1d, and 1e also demonstrated modest yet significant activity at a concentration of 150 mg/mL against the *P. posthuma* worm. Statistical analysis using 'Dunnett's test' with one-way ANOVA showed significant differences ($p < 0.001$) compared to both the control and standard group. Table 1, Figs 1, and 2 summarize the anthelmintic activity results.

Molecular docking was performed for the synthesized compounds using mitochondrial quinol-fumarate reductase enzyme, referencing pyrental. The interactions were compared, and satisfactory results were obtained, providing insight into the binding interactions of the synthesized compounds with the mitochondrial quinol-fumarate reductase enzyme of *P. posthuma*. Table 2 summarizes the dock score and binding energies of all compounds and the standard. Figs 3 and 4 illustrate the interactions of compound 1f and the standard, respectively.

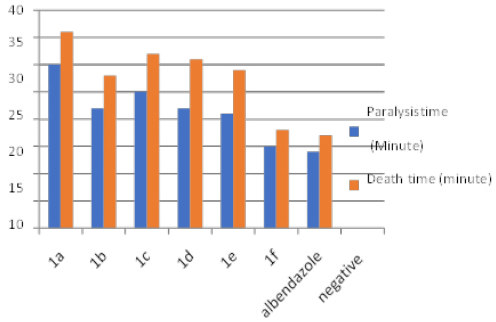

p-value =0.00027, (p value ≤ 0.05 is significant.)

Fig. 1: Graph showing paralysis time and death time for synthesized compounds showing anthelmintic activity

Table 1: Anthelmintic activity of the synthesized compounds

S. No.	*Compounds*	*Dose (mg/mL)*	*Paralysis time (minute)*	*Death time (minute)*
			Means ± S.E.M	*Mean ± S.E.M*
1	1a	50	32 ± 0.5	38 ± 0.41
		100	31 ± 0.65	37 ± 0.32
		150	30 ± 0.45	36 ± 0.96
2	1b	50	25 ± 0.529	32 ± 0.36
		100	23 ± 0.26	31 ± 0.54
		150	22 ± 0.74	28 ± 0.32
3	1c	50	30 ± 0.763	34 ± 0.61
		100	28 ± 0.341	32 ± 0.38
		150	25 ± 0.23	32 ± 0.54
4	1d	50	27 ± 0.76	38 ± 0.8
		100	25 ± 0.95	35 ± 0.56
		150	22 ± 0.16	31 ± 0.43
5	1e	50	25 ± 0.36	35 ± 0.72
		100	23 ± 0.04	32 ± 0.56
		150	21 ± 0.69	29 ± 0.403
6	1f	50	20 ± 1.2	25 ± 0.78
		100	18 ± 0.56	22 ± 0.62
		150	15 ± 0.75	18 ± 0.12
8	Albendazole	50	17 ± 1.1	21 ± 2.1
		100	16 ± 1.2	20 ± 0.78
		150	14 ± 0.8	17 ± 0.62

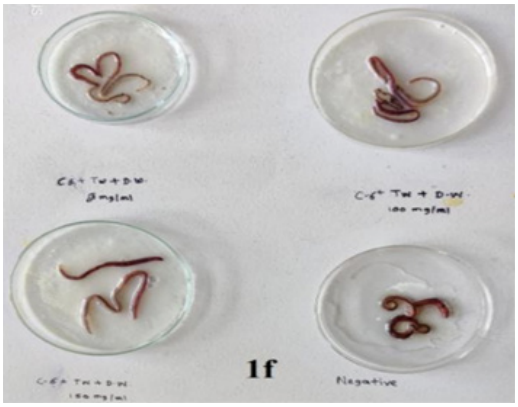

Fig. 2: Anthelmintic activity of compound 1f

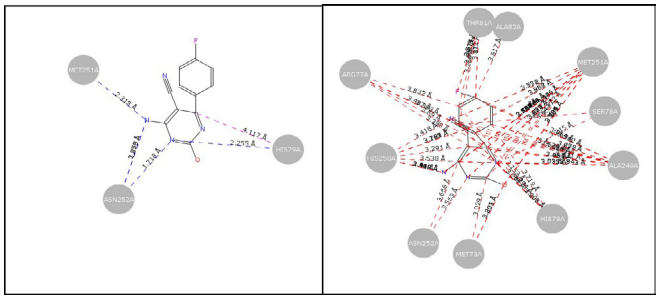

Fig. 3: Interactions of compound1fwith mitochondrial quinol-fumarate reductase enzyme

Table 2: Dock score and different binding interactions of target compounds with *Homo sapien dhfr*

Compound	*No of conformer*	*Conformer No.*	*Dock score*	*Binding energy (kcal/mol)*	*Interactions*
1a	122	C96	-3.5915	-98.83	HB-SER78A, HIS79A HP-HIS79A VDW-MET73A, ARG77A, SER78A, HIS79A, THR80A, ALA249A, HIS250A, MET251A, ASN252A
1b	122	C2	-3.2552	-21.87	HB-ALA82A HP- HIS79A VDW-MET73A, ARG77A, SER78A, HIS79A, THR81A, THR247A, ALA249A, HIS250A, MET251A
1c	122	C10	-3.4920	-68.70	HB- HIS79A, ASN252A HP-HIS79A, MET73A, ARG77A, SER78A, HIS79A, ALA249A, HIS250A, MET251A, ASN252A
1d	122	C122	-3.8572	-24.68	HB-HIS79A, ASN252A, ASN252A HP-HIS79A VDW-MET73A, ARG77A, HIS79A, ALA249A, HIS250A, MET251A, ASN252A
1e	122	C92	-3.7800	-56.59	HB-ALA82A HP- HIS79A VDW-MET73A, ARG77A, SER78A, HIS79A, THR81A, ALA82A, ALA249A, HIS250A, MET251A,
1f	122	C28	-3.8958	-96.83	HB- ASN252A, MET251A, HIS79A HP-HIS79A VDW-MET73A, ARG77A, SER78A, HIS79A, THR80A, ALA249A, HIS250A, MET251A, ASN252A
Pyrantel	130	C57	-3.4009	-24.62	HB-HIS79A HP-LYS72A, MET73A, SER78A, ALA249A VDW-LYS72A, ARG77A, SER78A, HIS79A, THR248A, ALA249A, HIS250A, MET251A

HB-Hydrogen bond interaction, HP-Hydrophobic interaction, VDW-Vander Waal's interaction.

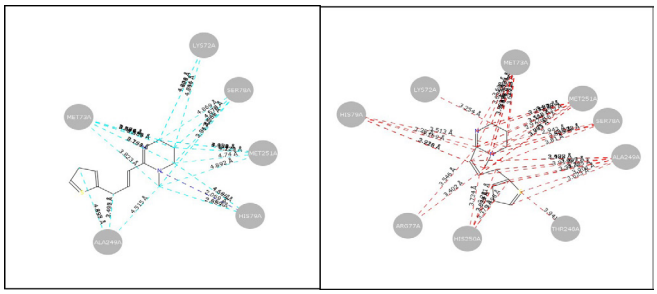

Fig. 4: The interaction of pyrantel with mitochondrial quinol-fumarate reductase enzyme.

Discussion

All synthesized compounds underwent thorough characterization using IR and ^{1}H-NMR spectroscopy. The biological data, expressed as mean ± SEM, was statistically analyzed using One-way ANOVA. The results indicated that the test compounds exhibited significant activity comparable to the standard drug, Albendazole. Among the series of synthesized compounds, compound 1f, characterized by fluoro substitution on the phenyl ring of the pyrimidine structure, demonstrated promising results. Its activity was notably similar to that of the standard drug, albendazole. This suggests the potential of compound 1f as an effective anthelmintic agent. Comparative molecular docking studies were conducted to assess the interactions between the synthesized compounds (1a-f) and the reference drug pyrantel with the mitochondrial quinol-fumarate reductase enzyme. Compound 1f, distinguished by fluoro substitution on the phenyl ring of the pyrimidine structure, displayed the highest dock score compared to the standard drug, pyrantel. These interactions were characterized by hydrophobic interactions, indicating the potential contribution of aromatic rings to the compounds' anthelmintic activity. Additionally, strong hydrogen bonding further highlighted the high affinity of compound 1f with the mitochondrial quinol-fumarate reductase enzyme.

Overall, the study suggests that compound 1f, specifically with fluoro substitution on the phenyl ring of the pyrimidine

structure, holds promise as a potent anthelmintic agent. Its interactions with the target enzyme further support its potential as a candidate for further investigation and development in the field of anthelmintic therapy.

Conclusion

The synthesized series of 4-amino-2-hydroxy-6-substituted phenyl pyrimidine-5-carbonitrile derivatives underwent in-vitro evaluation for their pharmacological activity. Among all the synthesized compounds, compound 1f demonstrated significant anthelmintic properties, showing promising activity in this study. Comparative molecular docking studies were conducted to analyze the interactions between the synthesized compounds and the standard drug, pyrantel, using the mitochondrial quinol-fumarate reductase enzyme. Notably, compound 1f, distinguished by fluoro substitution on the phenyl ring of the pyrimidine structure, exhibited the highest dock score compared to the standard drug pyrantel. These docking results aligned with the observed biological activity, indicating a correlation between the docking predictions and the compounds' actual anthelmintic properties.

In conclusion, the study highlights compound 1f, with its fluoro substitution on the phenyl ring of the pyrimidine structure, as a promising candidate with appreciable anthelmintic activity. The correlation observed between the results of molecular docking studies and biological evaluations strengthens the potential of compound 1f as a significant lead compound warranting further exploration and development in the realm of anthelmintic research and drug discovery.

Acknowledgement

The authors gratefully acknowledge the support received from Pune district Education Association's Seth Govind Raghunath Sable College of Pharmacy, Saswad (Maharashtra) 412301.

References

1. Nixon SA, Welz C, Woods DJ, Costa-Junior L, Zamanian M, Martin RJ. Where are all the Anthelmintics? Challenges and Opportunities on the Path to New Anthelmintics. Int J Parasitol Drugs Drug Resist. 2020; 14: 8–16. Available from: doi: 10.1016/j.ijpddr.2020.07.001
2. Abongwa M, Martin RJ, Robertson AP. A Brief Review on the Mode of Action of Antinematodal Drugs. Acta Vet (Beogr). 2017; 67(2):137–152. Available from: doi: 10.1515/acve-2017-0013
3. Hu Y, Ellis BL, Yiu YY, Miller MM, Urban JF, Shi LZ. An Extensive Comparison of the Effect of Anthelmintic Classes on Diverse Nematodes. Plos One. 2013; 8(7):70702. Available from: DOI: 10.1371/journal.pone.0070702
4. Martin RJ. Modes of action of anthelmintic drugs. Vet J. 1997; 154(1):11–34. doi.org/10.1016/S1090-0233(05)80005-X
5. Shelke PS, Jagtap PN, Tanpure PR. *In-vitro* Anthelmintic Activity of *Boswellia serrata* and *Aloe barbadensis* Extracts on *Pheretima posthuma*: Indian earthworm. Int J Res Med Sci. 2020; 8(5):1843. DOI: https://doi.org/10.18203/2320-6012.ijrms20201939
6. Mottier L, Alvarez L, Ceballos L, Lanusse C. Drug Transport Mechanisms in Helminth Parasites: Passive Diffusion of Benzimidazole Anthelmintics. Exp Parasitol 2006; 113(1): 49-57. DOI: 10.1016/j.exppara.2005.12.004
7. Shruthi N, Poojary B, Kumar V, Bhat M, Joshi H, Revanasiddappa BC. Synthesis, molecular properties and evaluation of anthelmintic activity of new thiazolopyrimidine derivatives. J Chem Pharm Res. 2015; 7(6):181-191.
8. Dixit A, Tanaka A, Greer JM, Donnelly S. Novel Therapeutics for Multiple Sclerosis Designed by Parasitic Worms. Int J Mol Sci. 2017; 18(10):2141. doi: 10.3390/ijms18102141
9. Yadav P, Singh R. A Review on Anthelmintic Drugs and their Future Scope. Int J Pharm Pharm Sci. 2011; 3(3):17-21.
10. Madawali IM, Das K, Gaviraj EN, Navanath V, Shivakumar KB. Synthesis and Evaluation of 4-(1H-Benzimidazol-2-Yl)-6-(2 Chloroquinolin-3- Yl) Pyrimidin-2-Amines as Potent Anthelmintic Agents. J Chem Pharm Res. 2019; 10(11):76–83.
11. Sudha Rani K, Lakshmi Durga J, Srilatha M, Sravani M, Sunand V. Synthesis, Characterization, Anthelmintic and *In-silico* Evaluation of 4,6-Disubstituted Pyrimidine-2- One Derivatives. Pharma Chem. 2018; 10(8):57–61.
12. Chitikina SS, Buddiga P, Deb PK, Mailavaram RP, Venugopala KN, Nair AB. Synthesis and Anthelmintic Activity of some Novel (E)-2-methyl/propyl-4-(2- (substitutedbenzylidene)hydrazinyl)-5,6,7,8-tetrahydrobenzo[4,5]thieno[2,3-d]pyrimidines. Med Chem Res. 2020; 29(9):1600–10. doi.org/10.1007/s00044-020-02586-5
13. Kumarachari R, Peta S, Surur A, Mekonnen Y. Synthesis, Characterization and *In-silico* Biological Activity of Some 2-(N,N-dimethylguanidinyl)-4,6-diarylpyrimidines. J Pharm Bioallied Sci. 2016; 8(3):181-187. DOI: 10.4103/0975-7406.171678
14. Mohanram I, Meshram J. Design, Synthesis, and Evaluation of Isoniazid Derivatives Acting as Potent Anti-Inflammatory and Anthelmintic Agents via Betti Reaction. Med Chem Res. 2014; 23:939–947. DOI:10.1007/s00044-013-0693-2
15. Bolade G, Adeyemi AA. Anthelmintic Activities of Three Medicinal Plants from Nigeria. Fitoterapia. 2008; 79(3): 223-225. DOI: 10.1016/j.fitote.2007.11.023
16. Shaikh A, Meshram J. Novel 1,3,4-Oxadiazole Derivatives of Dihydropyrimidinones:Synthesis, Anti-Inflammatory, Anthelmintic, and Antibacterial Activity Evaluation. J Hetero Chem. 2015; 53(4): 1176-1182. doi.org/10.1002/jhet.2377
17. Deodhar MN, Khopade PL, Varat MG. Sulfonamide Based β -Carbonic Anhydrase Inhibitors: 2D QSAR Study. Med Chem. 2013; 1–8. Available from: doi.org.10.1155/2013/107840

HOW TO CITE THIS ARTICLE: Pawar SJ, Dorugade R, Kale AP, Zope D. Design and Development of Some Pyrimidine Analogues as an Anthelmintic Agent. Int. J. Pharm. Sci. Drug Res. 2024;16(1):9-15. **DOI:** 10.25004/IJPSDR.2024.160102

Contents lists available at UGC-CARE

International Journal of Pharmaceutical Sciences and Drug Research

[ISSN: 0975-248X; CODEN (USA): IJPSPP]

journal home page : http://ijpsdr.com/index.php/ijpsdr

Research Article

In-silico Studies of Heterocyclic Benzoxazole Derivatives as an Anticancer Agent: Molecular Docking, 2D and 3D QSAR

Smita J. Pawar*, **Dhanashri Zope, Amol P. Kale**

PDEA's Department of Pharmaceutical Chemistry, Seth Govind Raghunath Sable College of Pharmacy, Pune, Maharashtra, India.

ARTICLE INFO

Article history:

Received: 05 September, 2023

Revised: 20 October, 2023

Accepted: 27 October, 2023

Published: 30 November, 2023

Keywords:

Benzoxazole, Docking, Thymidylate synthase, 2D QSAR, 3D QSAR, Anticancer, MLR, kNN MFA.

DOI:

10.25004/IJPSDR.2023.150612

ABSTRACT

In-silico molecular docking studies and QSAR study of benzoxazole derivatives synthesized by Kakkar *et al*. was done. Comparative studies of docking of 5-flurouracil and 20 compounds revealed considerable interactions, indicating the affinity of newly synthesized compounds for thymidylate synthase. The statistically significant 2D-QSAR models were developed using a molecular design suite (VLifeMDS 4.6). The study was performed with 20 compounds (data set) using sphere exclusion (SE) algorithm, random selection and manual selection methods used for the division of the data set into training and test set. Multiple linear regression [MLR] methodology with stepwise (SW) forward-backward variable selection method was used for building the QSAR models. The results of the 2D-QSAR models were further compared with 3D-QSAR models generated by k-Nearest Neighbor Molecular Field Analysis (kNN-MFA), investigating the substitutional requirements for the favorable anticancer activity against HCT 116 cell line and providing useful information in the characterization and differentiation of their binding sites. The results may be useful for further designing benzoxazole derivatives as anticancer agents prior to synthesis.

INTRODUCTION

Cancer is the leading cause of death in developed countries and the second leading cause of death in developing countries.[1] The risk of recurrence is still very significant even though surgical resection may be curative. In addition to surgical resection, adjuvant or neoadjuvant use of chemotherapeutic drugs alone or in conjunction with radiotherapy continues to be the mainstay of treatment regimens for high-risk patients. Unfortunately, only a modest drop in mortality is seen when the aforementioned standard therapy procedures are used, and the probability of developing a disease recurrence is still very significant.[2] The main issues in treating cancer are cytotoxicity and genotoxicity of anticancer medications against normal cells, which increase the risk of subsequent malignancy. One of the standard drugs for treatment of colorectal cancer is 5-fuorouracil (5-FU). However, it is associated with many side effects as it affects the cancer cells and the normal cells. In order to overcome the undesirable side effects of available anticancer agents, novel chemotherapeutic agents are needed for more effective cancer treatment. Therefore, finding and developing medications that can effectively trigger apoptosis while having the least negative effects on cancer cells is of significant interest.[3]

Chemotherapy is still a crucial component of cancer treatment since it kills cancer cells without harming healthy cells, and it has had great success thanks to the development of numerous new medications. As a result, various therapeutic attack kinds have been researched.[4-8] Drugs that perturb microtubule/tubulin dynamics are used widely in cancer chemotherapy. Despite of this progress, the discovery of most potent anticancer agents is a challenging issue in cancer chemotherapy for future generations. Therefore, there is a critical need to research and create innovative anticancer drugs with various

***Corresponding Author:** Dr. Smita Pawar

Address: PDEA's Department of Pharmaceutical Chemistry, Seth Govind Raghunath Sable College of Pharmacy, Pune, Maharashtra, India.

Email ✉**:** sjpawar4477@gmail.com

Tel.: +91-9970705513

Relevant conflicts of interest/financial disclosures: The authors declare that the research was conducted in the absence of any commercial or financial relationships that could be construed as a potential conflict of interest.

modes of action. Creating drug molecules with specified features has long been a prized objective for chemists, especially when developing novel medicines for improved medical care.[9]

Benzoxazole moiety is a medicinally relevant scaffold and is identified as a pharmacophore structure. The benzoxazole nucleus can be found in molecules used in research to assess new products with promising biochemical activity, including anticancer activities,[10-12] and they serve as a topoisomerase-I poison[13] and show antibacterial,[14] antifungal,[15] antimicrobial,[16] and anti-measles virus activities.[17] Benzoxazole ring occurs in a number of natural products such as salvianen and pseudosalvianen.[19,20] Derivatives of benzoxazole have gained much importance because of its wide applications in the medicinal sector. In nature, benzoxazole and their derivatives are widely distributed and are known to have significant physiological effects. Benzoxazole derivatives can bind to a variety of targets with strong affinity.[21,22] It is particularly crucial as a building block for synthesizing numerous physiologically active natural compounds. Kakkar *et al.* designed and synthesized benzoxazole-based derivatives and evaluated their anticancer activity. All the synthesized compounds showed remarkable anticancer activity against HCT 116 human cancer cell line.[23]

The two conventional core pillars of the drug discovery process are empirical research technique and fortuitous chance. Trial-and-error synthesis techniques and random screening for biological activity take a lot of time and are not cost-effective. Additionally, health risks and therapeutic effects are evaluated using various *in-vivo* techniques and tests, with animal models for these purposes involving many ethical problems.[24-25] The long-term goal of employing computer tools to speed up the drug discovery process was made possible by the development of computer technology to calculate the characteristics of molecules. The QSAR method saves us in this situation. Without the inconveniences of trial-and-error synthesis and random screening for activity and toxicity issues, quantitative structure-activity relationship modeling enables us to develop predictive biological activity models as a function of molecular and structural data of the target therapeutic molecules. The QSAR method correlates the biological properties of a compound to molecular descriptors obtained from the molecule's chemical properties. It is a mathematical correlation between the activity profile and the chemical structures of the molecule that has been statistically validated.[26-29]

Drug exerts its biological activity by binding to the pocket of receptor molecule, usually protein. In their binding conformations, the molecules exhibit geometric and chemical complementarily, both of which are essential for successful drug activity. The computational process of searching for a ligand that is able to fit both geometrically and energetically into the binding site of a protein is called molecular docking. Molecular docking helps study drug/ligand or receptor/protein interactions by identifying the suitable active sites in the protein, obtaining the best geometry of ligand-receptor complex and calculating the energy of interaction for different ligands to design more effective ones. The target or receptor is either experimentally known or theoretically generated through knowledge-based protein modeling or homology modeling. The molecular docking tool has been developed to obtain a preferred geometry of interaction of ligand-receptor complexes having minimum interaction energy based on different scoring functions.[30]

Traditional computer-assisted quantitative structure-activity relationship (QSAR) studies, which were invented by C. Hansch *et al.* in 1962 which helps to correlate the bioactivity of compounds with structural descriptors and also have been proven to be one of the useful techniques for accelerating the drug design process. We have used multiple linear regression methodology (MLR) to conduct 2D QSAR on benzoxazole derivatives in order to gain additional insights into the structure-activity relationships of these derivatives and comprehend the mechanism of their substitutional specificity. Cross-validation tests, randomization tests, and external test set prediction were used to determine the significance of the QSAR models. Before synthesizing new anticancer drugs, the robust 2D models may be helpful in further designing new candidates.[31]

Three-dimensional quantitative structure-activity relationship (3D QSAR) facilitates the evaluation of three-dimensional molecular fields around molecules and generates a relationship of these fields' values with the activity. One technique for establishing a connection between activity and molecular field is the k-nearest neighbor (kNN) method, which interprets the findings and offers suggestions for developing new compounds. For Molecular Field Analysis (kNN-MFA), a set of molecules must be properly aligned. A typical rectangular grid is then created, enclosing the molecules. Using the methyl probe of charge+1, the steric and electrostatic energies are calculated at the grid's lattice points. For relationship generation utilizing the kNN approach, these interaction energy levels at the grid points are taken into account. We developed a 3D QSAR model using the kNN approach, and this model generated additional leads for the synthesis of effective anticancer drugs.[32,33]

In the present research work, a data set of 20 molecules showing good inhibitory activity against HCT 116 human cancer cell line was subjected to docking, 2D and 3D QSAR analyses, in search of newer and potent anticancer agents. Significant models were generated statistically, and the most robust models for 2D and 3D QSAR were obtained using MLR and stepwise variable selection kNN-MFA approach, respectively using V-Life Molecular Design Suite software version 4.6.

Materials and Methods

Selection of Data Set

Table 1 lists a set of 20 selected compounds from a series of novel benzoxazole analogs reported by Kakkar *et al.*, 2019.[23] To make it more suited for QSAR studies, the biological activities reported in IC_{50} (µg/mL) for anticancer activity were transformed to algorithmic IC_{50} values. These derivatives were substituted with different groups (like hydrogen, fluorine, chlorine, methyl, and alkyl chain, methoxy many more) on different positions and every group has its own contribution in the physicochemical characteristics and biological activities of the designed compounds.[34]

Sketching of Molecules

The construction of the molecular structures is the next step in constructing a model. V- Life MDS software was used to sketch the structures, which were also energy reduced. Through using same software, the energy-minimized structures were used to generate molecular descriptors such as electronic, geometric, hydrophobic, and topological features.[35] Table 1 shows the substitution, IC_{50} and -log (IC_{50})values of the compound chosen for the MLR model.

Docking Study

Molecular docking techniques consist in finding the low-energy binding modes of a ligand within the active site of a macromolecule and evaluating the binding energy with a score.[36] Explanation of the selectivity of small sets of ligands has been attempted with accurate but time-consuming techniques.[37-39] Otherwise, automated docking methods may be used to estimate the thymidylate synthase affinity for large molecular databases. The objective of this work had been to use structural information of the target to confirm the binding affinity of synthesized molecules to thymidylate synthase as well as study binding nature. Docking studies were carried out in Vlife molecular docking suite 4.6 by using Biopredicta.

Optimization of Protein

Docking studies were carried out using thymidylate synthase. The 3H9K isoform of human thymidylate synthase was downloaded from Protein Data Bank website. The tetramer is converted into the monomer. Water molecules, cofactors, and heme were deleted from protein. The reference molecule was extracted. Hydrogens were added in molecule and energy was minimized using Merck molecular force field (MMFF).

Optimization of Ligand

3D structure is optimized, conformers were generated (Monte Carlo method), and the least energy conformers were selected. For the preparation of ligand, the structures of all the compounds used against HCT 116 human cancer cell line in *in-vitro* assay were energy minimized using MMFF.

Table 1: The chemical structures, IC_{50} and -log (IC_{50}) of compounds used for QSAR studies

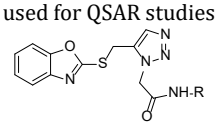

S. No	*Substitutions (R)*	*IC_{50}*	*-log IC_{50}*
1	3-nitrophenyl	97.5	-1.989
2	4-nitrophenyl	73.1	-1.864
3	4-methoxyphenyl	108.7	-2.036
4	2-chloro-4-nitrophenyl	22.5	-1.352
5	2,4,5-trichlorophenyl	85.3	-1.931
6	2-methyl-3-chlorophenyl	84.6	-1.927
7	2-methyl-3-chlorophenyl	72.0	-1.857
8	4-ethylphenyl	254.2	-2.405
9	2,4-dimethylphenyl	66.1	-1.820
10	2-chlorophenyl	175.1	-2.243
11	4-fluorophenyl	130.4	-2.115
12	4-bromophenyl	225.1	-2.352
13	3,4-dichlorophenyl	230.3	-2.362
14	2-bromophenyl	90.0	-1.954
15	3,5-dimethylphenyl	40.7	-1.610
16	3-bromophenyl	38.3	-1.583
17	2,3-dimethylphenyl	177.9	-2.251
18	2-bromophenyl	148.7	-2.172
19	3-chlorophenyl	50.0	-1.699
20	4-chlorophenyl	200.1	-2.301

Docking

Batch docking of optimized molecule was performed on the optimized receptor. Cavity number 1 for the 3H9K receptor was selected where the docking would be performed. The flexible GA batch docking did docking studies.

2D QSAR Analysis

Calculation of descriptors

Numbers of descriptors were calculated after optimization or minimization of the energy of the data set molecules. Various types of physicochemical descriptors were calculated: Individual (Molecular weight, H-Acceptor count, H-Donor count, X log P, slog P, SMR, Polarizability, etc.), Element count (N, C, S count etc.), Distance based topological (DistTopo, Connectivity Index, Wiener Index, Balaban Index), Estate numbers ($SsCH_3$count, $SdCH_2$count, $SssCH_2$count, StCH count, etc.), Estate contribution ($SsCH_3$-index., $SdCH_2$- index, $SssCH_2$-index , StCH index), and Polar surface area. The invariable descriptors (the descriptors that are constant for all the molecules) were removed, as they do not contribute to QSAR.

Generation of training and test set

In order to evaluate the QSAR model, data set was divided into training and test set using random selection and manual selection method. The training set is used to develop the QSAR model for which biological activity data are known. Test set is used to challenge the QSAR model developed based on the training set to assess the model's predictive power, which is not included in model generation.

Random Selection Method: To construct and validate the QSAR models, internal and external, the data sets were divided into training and test sets randomly. The ratio of 70:30 (training: test) was applied to data set.

Manual data selection method: Data set is divided manually into training and test sets on the basis of the result obtained in random selection method.

Generation of 2D QSAR model by multiple linear regression

Two-dimensional quantitative structure activity relationship (2D QSAR) studies using the multiple linear regression (MLR) method were performed on a series of benzoxazole derivatives as anticancer agents using software VLife MDS. MLR is a method used for modeling linear relationship between a dependent variable Y (Activity) and independent variable X (2D/3D descriptors). MLR is based on least squares. MLR estimates values of regression coefficients (r^2) by applying least squares curve fitting method. The model creates a relationship in the form of a straight line (linear) that best approximates all the individual data points. In regression analysis, the conditional mean of dependant variable (Activity) Y depends on (descriptors) X.

3D QSAR Analysis

We attempted to obtain further insights into the structural requirement of benzoxazole derivatives as anticancer agents by applying 3D-QSAR using kNN-MFA method. Molecular alignment was performed which is useful for studying shape variation with respect to the base structure i.e., benzoxazole moiety selected for alignment. Further, the aligned molecules were used for 3D QSAR studies. The method used for alignment was template based. A template structure was defined and used as a basis for alignment of a set of molecules. The geometries of the aligned molecules were stored in the align molecules subfolder in the align folder. All the aligned molecules were opened from Align Molecules subfolder in the Align folder. The 20 aligned molecules are shown in Fig. 1.

Calculation of descriptors

The 3D QSAR worksheet was launched at the beginning. The subfolder containing all aligned molecules was opened. The data of biological activity (IC_{50}) was inserted in the column. This was followed by the calculation of the molecular local shape field descriptors for finding a relationship with the activity and various parameters for field calculation selected are shown below:

Field Type: Electrostatic, steric, and hydrophobicity

Charge Type: Gasteiger-Marsili

For performing a robust QSAR analysis, descriptors that show variation for all the molecules are important. A descriptor that is constant for all the molecules will not contribute to QSAR and, hence should be removed from the worksheet. Thus, invariable columns were removed.

Data selection of training and test set

The training and test set was selected by manual selection method, ensuring that the molecules have uniform spread (training and test) in terms of both activity and chemical space. The dependent variable selected was biological activity as a negative log of IC_{50}; the remaining variables were considered independent variables.

Generation of 3D QSAR model by kNN MFA model

This method employs a stepwise variable selection procedure combined with kNN to optimize the number of nearest neighbors (k) and the selection of variables from the original pool as described in simulated annealing. The kNN-MFA model was generated using stepwise forward-backward variable selection method. The relative positions of the local fields around aligned molecules that are important for activity variation in the model were observed by clicking the Show Points button in the 'Model Summary' dialog box. The best model was selected on the basis of various statistical parameters. The quality and predictability of the model was estimated from the cross-validated squared correlation coefficient and predicted r^2.

Result and Discussion

Docking Studies

In this comparative docking experiment of benzoxazole compounds with known anticancer drug 5-fluorouracil the dock score was calculated -4.742203 kcal/mole. Van der Waals interactions, H-bond interactions, and hydrophobic interactions are some of the elements considered while predicting the ligand's potency or affinity to the receptor. The higher the affinity of molecule towards the receptor, the more negative the value of the energy of binding. The increased Van der Waals interaction indicates that the ligand structure contains more bulky groups due to

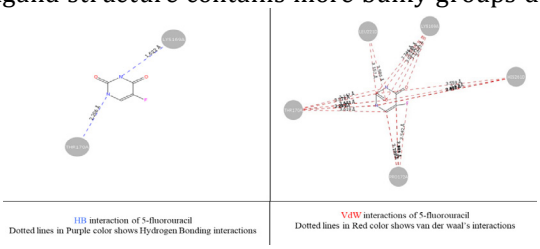

Fig. 1: 2D-view of the reference molecule show the hydrogen bonding and van der waal's interaction with thymidylate synthase.

which Van der Waals interactions were formed. If the charge interactions are present, it assists in determining more appropriate binding and thus exhibits more affinity to the receptor, adding more efficacies. Obtained results were evaluated in terms of docking score into the active site of (3H9K). The software provides facility of the batch docking of the optimized ligand molecules with the simulated receptor. All ligands are docked an active site i.e., cavity for docking of receptor 3H9K. We compared the dock score of each selected molecule and reference molecule, which shows the variation in the docking score, so we predicted that molecules with minimum dock score show more affinity for thymidylate synthase inhibition and Dock score shown in Table 2. Table 2 shows that ligands 4 and 16 have the betterdock scores, or the lowest binding energy in Kcal/mol among all the compounds. These molecules have a higher affinity against the active site of the receptor. It is understandable that molecules with a lower dock score and binding energy confirm more affinity towards the receptor.

Interactions of Ligands with Receptor

Molecule 5-Fluorouracil

This is a reference molecule. It is anticancer agent. The low dock score of this molecule is -4.742203 kcal/mol with thymidylate synthase (3H9K). The ligand showed hydrogen bond interaction with LYS169A and THR170A as well as van der waal's interaction with LYS169A, PRO172A, THR170A, HIS261D and LEU221D. These interactions are important for increased affinity for thymidylate synthase.

Molecule (4)

The low dock score of this ligand is -4.154462 kcal/mol against the binding site of the thymidylate synthase receptor. In Fig. 2 the residual interactions of compound 4 revealed one (1) conventional H-bonds, four (4) hydrophobic, eleven (11) electrostatic (Van Der Waal's) interaction types with different amino acid residues in the active site of the targeted receptor. The NH group attached to the carbonyl group in molecule 04 can interact with the residues of LYS169A with a distance of 2.392 Å. It was also noteworthy that the hydrophobic interaction also existed between the hydrophobic residues of compound 04 and the active site of the ILE168A, LYS169A, THR241A, LEU243A at a distance of 4.884, 4.734, 4.894 and 4.786 Å, respectively. The eleven Van der Waal'sinteraction were formed with THR51D (3.701), ARG50D (3.822), GLY242A (3.364), THR241A (3.716), PRO172A (3.175 Å), ASN171A (3.566 Å), THR170A (3.378 Å), LEU234A (2.965 Å), LYS169A (3.195 Å), ILE240A (3.26 Å), and ILE168A (3.029 Å) at different interaction distances accordingly.

Molecule (16)

The low dock score of this ligand is -4.219219 kcal/mol against binding site of thymidylate synthase receptor. In

Table 2: Docking score of the benzoxazole derivatives with the structure of thymidylate synthase (3H9K)

Compound	*Dock score*	*Binding energy*
1	-3.822572	-640.6586
2	-4.096091	-649.4137
3	-3.322664	-639.9574
4	-4.154462	-651.7083
5	-4.546775	-636.2337
6	-3.849419	-639.9083
7	-3.76660	-636.0455
8	-3.576736	-632.3346
9	-3.939365	-636.845
10	-4.138222	-636.8219
11	-3.772533	-629.5271
12	-3.998726	-631.0459
13	-4.021897	-632.1873
14	-4.144334	-636.521
15	-4.077910	-634.5393
16	-4.219219	-649.9165
17	-4.338950	-640.9052
18	-4.123791	-634.0953
19	-4.035604	-629.9877
20	-4.081383	-630.1479
5-Fluorouracil	-4.742203	-1117.7934

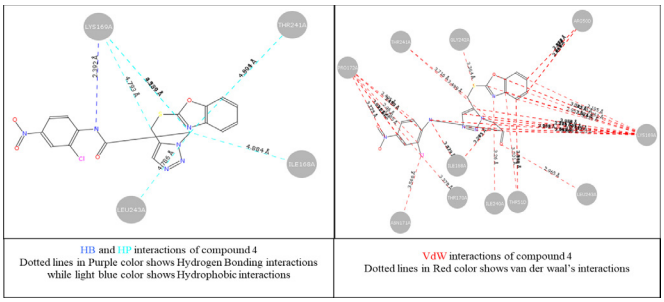

Fig. 2: 2D-view of molecule 4 show the hydrogen bonding, hydrophobic and van der waal's interaction with thymidylate synthase.

Fig. 3 the residual interactions of compound 16 revealed one (1) conventional H-bonds, four (4) hydrophobic, and 12 electrostatic (Van der Waal's) interaction types with different amino acid residues in the active site of the targeted receptor. The NH group attached to the carbonyl group in molecule 16 can interact with the residues of ILE168A with a distance of 2.442 Å. Also, the hydrophobic interaction also existed between the hydrophobic residues of compound 16 and the active site of the LYS169A, THR170A, PRO172A at a distance of 4.8553, 4.582, and 4.88 Å, respectively. The twelve Van der Waal's interaction were formed with THR170A, LEU243A, VAL203A, HIS256D, ASP218D, ARG175E, ILE168A, PRO172A, SER206A, THR241A, LYS169A, and TYR258D at interaction distances of 2.844, 3.181, 2.992, 3.835, 3.496, 2.703, 3.983, 3.385, 3.977, 2.894, 2.835, and 3.782 Å, respectively.

2D QSAR Model

Different sets of 2D-QSAR models were generated using the MLR analysis in conjunction with stepwise forward-backward variable selection method. Different training

and test set were constructed using random and manual selection method. The best QSAR model was selected based on values of r^2 (squared correlation coefficient), q^2 (cross-validated correlation coefficient), pred_r^2 (predicted correlation coefficient for the external test set), F (Fisher ratio) reflects the ratio of the variance explained by the model and the variance due to the error in the regression. The F–test values indicate that the model is statistically significant. The statistical values of the corresponding best model are reported in Table 3.

Test set: 2, 11, 13, 14, 16, 17, 19

The best equation obtained by multiple linear regression is as follows:

Biological activity (IC_{50}) = 0.1071(± 0.0001) T_T_T_4 + 0.1523(0.009) T_C_N_7 -0.2974(0.0166) SssCH_2E-index -0.7617(0.0117) T_N_N_7 -5.4863(1.1947) SAAverage.

Interpretation of the 2D-QSAR model

From equation, 2D-QSAR model explains 99.32% (r^2 = 0.9932) of the total variance in the training set, which means that the model's failure probability is 1 in 10000. This model was considered as the model showed an internal predictive power (q^2: 0.8166) of 81% and a predictivity for the external test set (pred_r^2:0.5828) of about 58%.The descriptors T_T_T_4 and T_C_N_7 indicates the Count of number of any atom separated from any other heteroatom by four bonds distance in a molecule and count of number of carbon atoms (single, double or triple bonded) separated from any nitrogen atom(single, double or triple bonded) by 7 bonds distance in a molecule, respectively. The positive contribution of 40.07 and 18.26% of these descriptors revealed the increase of anticancer activity of benzoxazole with the presence of NO_2 group such as compound 1, 2, and 4. Higher values of these descriptors lead to good anticancer activity while lower values lead to reduced anticancer activity. Moreover, negative coefficient value of descriptors SssCH_2E-index [number of CH_2 group connected with two single bonds], T_N_N_7 [count of number of nitrogen atoms separated from any other nitrogen atom by 7 bonds in a molecule],

Table 3: Statistical results for MLR method

Parameter	*MLR method*
n	13
Degree of freedom	7
r^2	0.9932
q^2	0.8166
F test	203.2395
r^2_se	0.0329
q^2_se	0.1701
pred_r^2	0.5828
pred_r^2se	0.4512
Descriptors (range)	T_T_T_4 (0.1071) T_C_N_7 (+ 0.1523) SssCH_2E-index (-0.2974) T_N_N_7 (-0.7617) SAAverage (-5.4863)

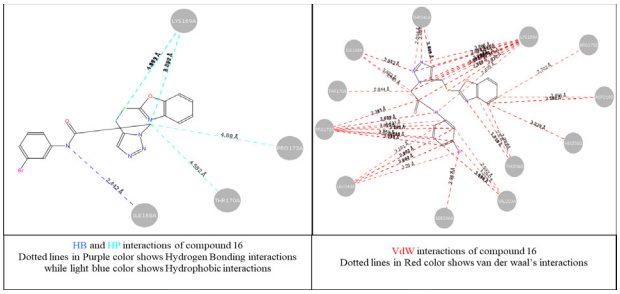

Fig. 3: 2D-view of the molecule 16 show the hydrogen bonding, hydrophobic and van der waal's interaction with thymidylate synthase

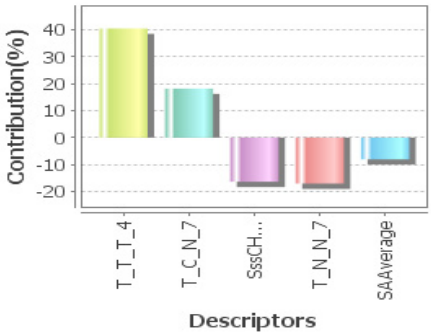

Fig. 4: Contribution chart for 2D-QSAR model showing contribution of different descriptors

SAAverage [average hydrophobicity function value] on the anticancer activity indicated that lower value leads to better anticancer activity whereas higher value leads to decreased anticancer activity. The contribution chart for model is represented in Fig. 4 reveals that the two descriptors T_T_T_4, T_C_N_7 contributed 40.07, 18.26%, respectively. Three more descriptors SssCH2E-index, T_N_N_7, SAAverage, are contributing inversely 16.65, 18.49, and 7.56%, respectively to biological activity.

Predictivity of MLR model

Predictivity of the model was evaluated by predicting the activity of the molecules belonging to the training set (internal predictivity) as well as molecules in the test set (external predictivity) as shown in Table 4. (Red color = test set). Data fitness plot and Graphical representation of the model's predictive power are shown in Figs 5 and 6, respectively.

3D-QSAR Model

3D QSAR models were developed for set of 20 compounds using stepwise kNN MFA method for anticancer activity. The steric and electrostatic descriptors specify the regions, where variation in the structural features of different compounds in training set leads to increase or decrease in activities.

In the present study the benzoxazole nucleus considered as a template and each molecule was superimposed on the template. 3D QSAR model was derived using the kNN descriptors as independent variables and IC_{50}

Table 4: Actual and predicted activities for 20 compounds based on the best 2D-QSAR models

compound	*Observed value*	*Predicted value*	*Residual value*
1	-1.989	-2.104	-0.115
2	-1.864	-2.102	-0.238
3	-2.036	-2.208	-0.172
4	-1.352	-1.654	-0.302
5	-1.931	-1.839	0.092
6	-1.927	-1.758	0.169
7	-1.857	-1.760	0.097
8	-2.405	-2.327	0.078
9	-1.820	-1.778	0.042
10	-2.243	-2.353	-0.11
11	-2.115	-2.272	-0.157
12	-2.352	-2.353	-0.001
13	-2.362	-1.967	0.395
14	-1.954	-1.839	0.115
15	-1.610	-1.694	-0.084
16	-1.583	-1.978	-0.395
17	-2.251	-1.568	0.683
18	-2.172	-2.14	0.032
19	-1.699	-1.839	-1.14
20	-2.301	-2.379	-0.078

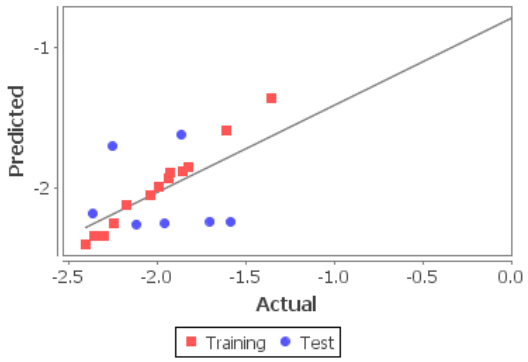

Fig. 5: Data fitness plot for 2D-QSAR model

concentration as a dependent variable. 3D QSAR models were built in V-Life molecular design software using SWkNN method. Various models have been developed by changing training and test set data. Selection of best model was performed based on statistical parameters of the models. The corresponding best model is reported in Table 5.

Test set: 2, 11, 13, 14, 16, 17, 19

Interpretation of 3D QSAR model

The kNN MFA model generated from template-based alignment showed Q2 of 0.8264 with two descriptors, namely S_1120 and E_808. Steric and electrostatic field energy of interaction between template and compounds at their corresponding spatial grid points of 1120 and 808. Which showed relative position and ranges of the corresponding important steric and electrostatic files in the model. As far as S_1120 steric field is concerned, a negative range indicates that negative steric potential was favorable for increased activity; hence, less bulky group

Table 5: Statistical results of kNN molecular field analysis

Parameter	*kNN MFA method*
n	13
Degree of freedom	10
q^2	0.8264
q^2_se	0.1310
pred_r^2	-1.2354
pred_r^2se	0.3913
Descriptors (range)	S_1120 (-0.1268 -0.1166) E_808 (0.0734 0.1147)

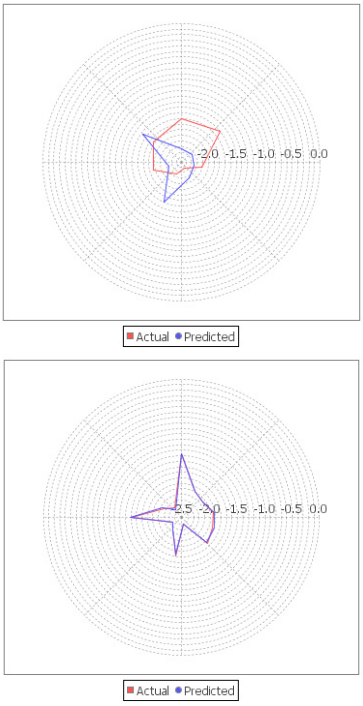

Fig. 6: Graph between actual and predicted biological activity of test and training set for 2D-QSAR model

was preferred in that region. Thus, a green sphere (S_1120) near the benzoxazole ring's substituent suggests a less bulky group is required in this region. One electrostatic descriptor indicated by blue sphere (E_808) is observed in the model and contributes positively, suggesting that more electropositive (electron withdrawing) groups are favorable in this position. Fig. 7 shows the 3D alignment of molecules with the important steric and electrostatic points contributing to the 3D QSAR model.

Predictivity of kNN MFA Model

Predictivity of the model was evaluated by predicting the activity of the molecules belonging to the training set (internal predictivity) as well as molecules in the test set (external predictivity) as shown in Table 6. (Red color = test set). Data fitness plot and Graphical representation of the model's predictive power are shown in Figs. 8 and 9, respectively.

Table 6: Actual and predicted activities for 20 compounds based on the best 3D-QSAR models

Compound	*Observed value*	*Predicted value*	*Residual value*
1	-1.989	-1.839	0.15
2	-1.864	-1.721	0.143
3	-2.036	-2.144	-0.108
4	-1.352	-1.476	-0.124
5	-1.931	-1.919	0.012
6	-1.927	-1.862	0.065
7	-1.857	-1.862	-0.005
8	-2.405	-2.397	0.008
9	-1.820	-1.857	-0.037
10	-2.243	-2.246	-0.003
11	-2.115	-2.288	-0.173
12	-2.352	-2.328	0.024
13	-2.362	-2.164	0.198
14	-1.954	-2.247	-0.293
15	-1.610	-1.559	0.051
16	-1.583	-2.245	-0.662
17	-2.251	-1.643	0.608
18	-2.172	-2.18	-0.008
19	-1.699	-2.244	-0.548
20	-2.301	-2.327	-0.026

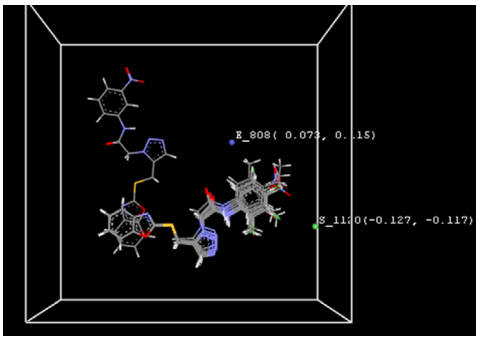

Fig. 7: 3D-alignment of molecules (Ball and stick model) with the important steric and electrostatic points contributing 3D-QSAR model

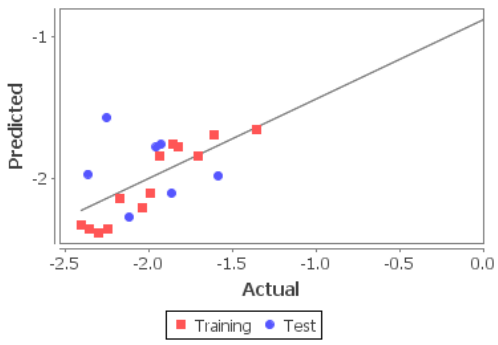

Fig. 8: Data fitness plot for 3D-QSAR model

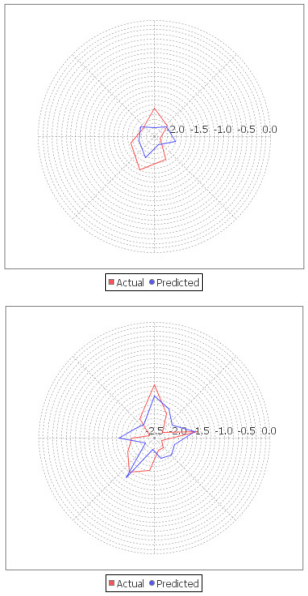

Fig. 9: Graph between actual and predicted biological activity of test and training set for 3D-QSAR model

Conclusion

According to the docking simulation, the hydrophobic Van der Waals, H-bond interactions create stable compounds of ligands with receptors. According to Table 2, the ligands 4 and 16 were shown to have the lowest dock scores of -4.154462 and -4.219219, respectively and the lowest binding energy of -651.7083 and -649.9165 kcal/mol, respectively, indicating that they had a higher affinity for the receptor's active site. It is evident that molecules with a low dock score and binding energy have a greater affinity for the receptor. Statistically significant 2D/3D-QSAR models were generated with the purpose of deriving structural requirements for the anticancer activities of some novel benzoxazole derivatives against HCT 116. The best 2D QSAR models indicate that the descriptors T_T_T_4, T_C_N_7positively participate for the anticancer activity whereas, $SssCH_2E$-index, T_N_N_7 and SAAveragenegatively participate for the anticancer activity. kNN-MFA investigated the substitutional requirements for the receptor-drug interaction and constructed the best 3D-QSAR models by kNN MFA method, providing that negative steric potential i.e., less bulky groups was favorable for increased activity whereas positive electrostatic potential is needed for potential anticancer activity. In conclusion, the information provided by the robust 2D/3D-QSAR models use for the design of new molecules and hence, it helped to identify the lead that could be optimized further for better anticancer potential.

Acknowledgement

The authors acknowledge the support from Pune District Education Association's Seth Govind Raghunath Sable College of Pharmacy, Saswad (Maharashtra) 412301.

References

1. The Global Burden of Disease: 2004 Update; World Health Organization: Geneva, Switzerland, 2008.
2. Wang Z, Shi XH, Wang J, Zhou T, Xu YZ, Huang TT, Li YF, Zhao YL, Yang L, Yang S. Synthesis, Structure-Activity Relationships and Preliminary Antitumor Evaluation of Benzothiazole-2-thiol Derivatives as Potential Anticancer Agents. Bioorg. Med. Chem. Lett. 2011; 21:1907–1101.
3. Garcia M, Jemal A, Ward E. M, Center M. M, Hao Y, Siegel R. L, Thun. M. J. Global cancer facts & Fig.s. American Cancer Society. 2007.
4. Hanahan D, Weinberg RA. The Hallmarks of cancer. Cell. 2000; 100: 57.
5. Stratton MR, Campbell PJ, Futreal PA. The Cancer Genome. Nature. 2009; 458: 719.
6. Hanahan D, Weinberg RA. Hallmarks of Cancer: The Next Generation. Cell. 2011; 144: 646.
7. Boyle FT, Costello GF, Cancer therapy: A Move to the Molecular Level. Chem Soc Rev. 1998; 27: 251.
8. Gibbs JB, Mechanism-based Target Identification and Drug Discovery in Cancer Research. Science. 2000; 287: 1969.
9. Lu Y, Chen YJ, Xiao M, Li W, Miller DD. An Overview of Tubulin Inhibitors that Interact with the Colchicine Binding Site. Pharm Res. 2012; 29: 2943.
10. Don MJ, Shen CC, Lin YL, Syu WJ, Ding YH, Sun CM. Nitrogen Containing Compounds from Salvia Miltiorrhiza. Nat Prod. 2005; 68: 1066.
11. Viirre RD, Evindar G, Batey RA. Copper-catalyzed Domino Annulation Approaches to the Synthesis of Benzoxazoles under Microwave-accelerated and Conventional Thermal Conditions. J Org Chem. 2008; 73: 345.
12. Osmaniye D, Çelikateş BK, Saglık BN,Levent S,Cevik UA,Cavusoglu BK, Ilgın S, Ozkay Y,Kaplancıkli ZA. Synthesis of some New Benzoxazole Derivatives and Investigation of their Anticancer Activities. Eur J Med Chem. 2021; 210: 112979.
13. Cheng CC, Liu DE, Chou TC. Design of Antineoplastic Agents on the Basis of the "2-Phenylnaphthalene-Type" Structural Pattern. I. Synthesis of Substituted 3- Phenylquinazolones, Benzoxazolo[2,3-b] quinazolones and Benzothiazolo[2,3- b]quinazolones. Heterocycles. 1993; 35: 775.
14. Elnima EI, Zubair MU, Al-Badr AA. Antibacterial and antifungal activities of benzimidazole and benzoxazole derivatives. Antimicrobial Agents and Chemotherapy, 1981; 19: 29-32.
15. Kaplancikli Z. A, Turan-Zitouni G, Revial G, Guven K. Synthesis and Study of Antibacterial and Antifungal Activities of Novel 2-[[(benzoxazole/benzimidazole-2- yl)sulfanyl] acetylamino] thiazoles. Archives of Pharmacal. Research. 2004; 27: 1081–1085.
16. Sun LQ, Chen J, Bruce M, Deskus JA, Epperson JR, Takaki K, Johnson G, Iben L, Mahle C. D, Ryan E, Xu C. Synthesis and Structure-activity Relationship of Novel Benzoxazole Derivatives as Melatonin Receptor Agonists. Bioorg. Med. Chem. Lett. 2004; 14: 3799.
17. Ertan T, Yildiz I, Tekiner-Gulbas B, Bolelli K, Temiz-Arpaci O, Yalcin I, Aki E, Ozkan S, Kaynak F. Synthesis, biological evaluation and 2D-QSAR analysis of benzoxazoles as antimicrobial agents. Eur. J Med. Chem. 2000; 44: 501.
18. Alper-Hayta S, Arisoy M, Temiz-Arpaci O, Yildiz I, Aki E, Oezkan S, Kaynak F. Synthesis and Anticancer Activity of New ((Furan-2-yl)-1,3,4-thiadiazolyl)-1,3,4- oxadiazole Acyclic Sugar Derivatives. Eur. J Med. Chem. 2008; 43: 2568.
19. Sun A, Prussia A, Zhan W, Murray EE, Doyle J, Cheng LT, Yoon JJ, Radchenko EV, Palyulin VA, Compans RW, Liotta DC, Plemper RK, Snyder JA. Nonnucleoside Inhibitor of Measles Virus RNA-Dependent RNA Polymerase Complex Activity. J Med. Chem. 2006; 49: 5080.
20. Borrel C, Thoret S, Cachet X, Guenard D, Tillequin F, Koch M, Michel S. New antitubulin derivatives in the combretastatin A4 series: synthesis and biological evaluation. Bioorg. Med. Chem. 2005; 13: 3853.
21. Katritzky A. QSAR modeling, synthesis, and bioassay of diverse leukemia RPMI-8226 cell line active agents. Bioorg. Med. Chem. Lett. 2010; 45: 5183-99.
22. Rapatri V, Chitre T, Bothara K. Novel 4-(morpholin-4-yl)-N-(arylidene) Benzohydrazides: Synthesis, Antimycobacterial activity, and QSAR Investigations. Eur. J Med. Chem. 2009; 44: 3954-60.
23. Kakkar S, Kumar S, Narasimhan B, Lim S. M, Ramasamy K, Mani V, Ali Shah S. A. Design, Synthesis, and Biological Potential of Heterocyclic Benzoxazole Scafolds as Promising Antimicrobial and Anticancer Agents. Chemistry Central Journal. 2018; 12: 96.
24. Sastry MG, Adzhigirey M, Day T, Annabhimoju R, Sherman W. Protein and Ligand Preparation: Parameters, Protocols, and Influence on Virtual Screening Enrichments. J. Comput. Aided Mol. Des. 2013; 27(3): 221-234.
25. Kumar S, Singh J, Narasimhan B, Shah S.A.A, Lim S.M, Ramasamy K, Mani V. Reverse Pharmacophore Mapping and Molecular Docking Studies for Discovery of GTPase HRas as Promising Drug Target for Bis-pyrimidine Derivatives. Chem. Cent. J. 2018; 12: 106.
26. Katritzky A. QSAR modeling, synthesis, and bioassay of diverse leukemia RPMI-8226 cell line active agents. Bioorg. Med. Chem. Lett. 2010; 45: 5183-99.
27. Rapatri V, Chitre T,Bothara K. Novel 4-(morpholin-4-yl)-N-(arylidene) benzohydrazides: Synthesis, Antimycobacterial Activity, and QSAR Investigations. Eur. J Med. Chem. 2009; 44: 3954-60.
28. Karthiga S, Velmurugan D. Molecular modeling, QSAR and pharmacophore studies on anti-viral, anti-malarial and anti-inflammatory bioactive compounds from marine sources. Asian J Pharma Clin Res. 2015; 8: 36-43.
29. VLife Molecular Design Suite version 3.5; VLife Sciences Technologies Pvt. Ltd., Pune, India; 2010.
30. Sharma V, Sharma P.C, Kumar V. In silico Molecular Docking Analysis of Natural Pyridoacridines as Anticancer Agents. Adv. Chem. 2016; 1-9.
31. Hansch C, Fujita T. p-σ-π Analysis. A method for the correlation of biological activity and chemical structure. J. Am. Chem. Soc. 1964; 86(8): 1616-1626.
32. Life Molecular Design Suite 3.0, VLife Sciences Technologies Pvt. Ltd; Baner Road: Pune, Maharashtra, India. www.Vlifescien ces. com. Accessed Jan 2019
33. Nandi S, Bagchi M. 3D-QSAR and Molecular Docking Studies of 4-anilinoquinazoline Derivatives: A Rational Approach to Anticancer Drug Design. Mol Divers. 2010, 14, 27.
34. Bora P, Kumar A, Kumar Singh A, Singh H, Narasimhan B, Kumar P. Molecular Docking and QSAR Studies of Indole Derivatives as Antifungal Agents. Cur. Chinese Chemistry. 2023; 3:1-12.
35. Ou-Yang S, Lu J, KongX, Liang Z, Luo C, Jiang H. Computational drug discovery. Acta Pharmacol. Sin.2012; 33(9): 1131-1140.
36. Habeeb AG, Parveen P, Knaus EE. Design and synthesis of 4, 5-diphenyl-4-isoxazolines: Novel Inhibitors of Cylooxygenase-2 with Analgesic and Anti-Inflammatory Activity. J Med. Chem. 2001; 44: 2921-7.
37. Palomer A, Perez J. J, Navea S, Llorens O, Pascual J, Garcia L. ModelingCyclooxygenase Inhibition: Implication of active site Hydration on the Selectivity of Ketoprofen Analogues. J Med. Chem. 2000; 43: 2280-4.
38. Price ML, Jorgensen WL. Analysis of Binding Affinities for Celecoxib Analogues with COX-1 and COX-2 from Combined Docking and monte carloSimulations and Insight into the COX-2/COX-1 Selectivity. J Am. Chem. Soc. 2000; 94: 55-66.
39. Price ML, Jorgensen WL. The Rationale for the Observed COX-2/COX-1 Selectivity of Celecoxib from Monte Carlo Simulation. Bioorg. Med. Chem. Lett. 2001; 11:1541-4.

HOW TO CITE THIS ARTICLE: Pawar SJ, Zope D, Kale AP. *In-silico* Studies of Heterocyclic Benzoxazole Derivatives as an Anticancer Agent: Molecular Docking, 2D and 3D QSAR. Int. J. Pharm. Sci. Drug Res. 2023;15(6):780-788. **DOI:** 10.25004/IJPSDR.2023.150612

IJCRT.ORG ISSN : 2320-2882

INTERNATIONAL JOURNAL OF CREATIVE RESEARCH THOUGHTS (IJCRT)

An International Open Access, Peer-reviewed, Refereed Journal

REVIEW ON HERBAL MOUTHWASH FOR ORAL CARE

Tonde Amrapali Shahaji [1], Solanke Pratiksha Gajanan[2], Sonawane Shubham Raju[3], Wagh Prasad Eknath [4] ,Taware Viraj Dipak[5]

Bachelor's Of Pharmacy ,PDEA' Seth Govind Raghunath Sable College of Pharmacy Saswad, Pune.

GUIDED BY:-MS. VISHAKHA JAGTAP.

Abstract

From the beginning of human civilization until the twenty-first century, people have understood the value of keeping their mouth and teeth clean. There is an abundance of mouthwash products available to patients and oral health professionals that contain various active and inactive ingredients. Medicinal plants play a predominant role because of their strong antimicrobial and antibacterial actions against microorganisms .medicinal plants are essential for the prevention and treatment of disease. The present investigation aims to create an antibacterial mouthwash, test it, and assess its efficacy against oral cavity pathogens. Those act on bacteria in the mouth and pathogens, lessen discomfort, and ceasing to have any negative side effects. The different herbs and its extracts, including those of tulsi, green tea, and nagamotha, were chosen to be transformed into mouthwash. Formulation was further studied for its physical characteristics and examined for antibacterial effectiveness against culture attributes. Mouthwash has powerful antibacterial properties whenever it's present. This remedy can be applied to decrease oral microbial growth and may also be used for other purposes, such as analgesic activity, gingivitis, and anti- inflammatory action.

Keyword:- oral health, medicinal plant, herbal mouthwash, gingivitis, tooth decay

Introduction

I was introduced to various homemade mouthwashes and tried them out. in any case, Results in the existing literature are inconsistent regarding this clinical significance[1,2,3]. Herbal mouthwash to fight plaque and aggravated gums Meta-analysis is lacking compared to fake treatment and CHX Evidence highlighting the general effectiveness of homemade mouthwash as an adjunct Cleanliness of words through daily self-execution of gingivitis patients. The most important thing is to do it regularly The dynamic fixative used in mouthwash and toothpaste is chlorhexidine, Hyaluronic acid and fluoride. Despite being mandated, chemical products can have clinical drawbacks such as tooth discoloration, taste changes, and oral problems. Dryness, supragingival tartar accumulation, oral mucosal damage[3,4,5]. Many types of microorganisms present in our mouths can cause tooth

damage attenuation. Research reveals that *S. mutans* is evolving Approximately 30% of microorganisms form cavities due to tooth decay. of *S.mutant* involvement in dental caries is of great importance for detection Implies effects on antibacterial agents. It is dangerous to use antibiotics on a daily basis. As an anti-caries agent, mouthwash is considered an essential choice [6,7,8,9].

Benefits of herbal mouthwash

- The non-irritating, non-staining, and alcohol free properties of domestic developed mouthwash have given it an advantage over chemical mouthwashes.
- They have especially unimportant or no side affect and they are less harmful.
- All domestic developed mouthwashes do not contain alcohol and/or sugar.
- Domestic developed mouthwashes are delicate for in fact the most fragile mouth.
- Domestic developed mouthwashes are inherently antibacterial.
- It contains no brutal additives.Domestic developed mouthwash doesn't cause dry mouth.
- It is significantly in demand. It keeps your mouth strong and plaque frees[10,11].

Herbal Agents

❖ **Cinnamon**

Synonyms:-Dalchini, Ceylon, Cinnamon, Cinnamon bark.

Biological source:-Cinnamon consists of dried bark, freed from the outer cork and from the underlying parenchyma, from the shoots growing on the cut stumps of *Cinnamomum zeylanicum Neel[12]*

Family:–Lauraceae

Figure 1 Cinnamon [15]

Use:-These date is utilized as aromatic stimulant, antibacterial,antifungal,antiseptic, carminative, stomachic and astringent. Commercially, it is additionally used as flavor, condiment, in sweet arrangement, dentrifices Cinnamon oil and cinnamaldehyde are irritating to skin and mucous film.

Chemical constituents:

Table 1

Part of the plant	Compound
Leaves	Cinnamaldehyde: 1.00 to 5.00% Eugenol: 70.00 to 95.00%
Bark	Cinnamaldehyde: 65.00 to 80.00% Eugenol: 5.00 to 10.00%
Root bark	Camphor: 60.00%
Fruit	rans-Cinnamyl acetate (42.00 to 54.00%) and caryophyllene (9.00 to 14.00%)
C. zeylanicum buds	Terpene hydrocarbons: 78.00% alpha-*Bergamotene*: 27.38*% alpha-Copaene*: 23.05% Oxygenated terpenoids: 9.00%
C. zeylanicum flowers	(E)-Cinnamyl acetate: 41.98% trans-alpha-Bergamotene: 7.97% Caryophyllene oxide: 7.20%

Refer[13,14]

Antioxidant property:-Cancer prevention agents have been utilized to delay or anticipate nourishment decay.Flavors and medicinal plants have gotten fast thought as sources of advantageous antioxidants against different illnesses. Cancer prevention agents have been considered themost vital drivers within the advance and presence of people, as they react to free radicals and harm in metabolic maladies and age-related disorders of humans and other creature.[16,17].

Anti-inflamatory activity:- Several studies on medicinal plants and their components have indicated the anti-inflammatory activities of cinnamon. Various studies reported the anti-inflammatory activity of cinnamon and its essential oils. To date, there are several flavonoid compounds (e.g., gossypin, gnaphalin, hesperidin, hibifolin, hypolaetin, oroxindin, and quercetin) that have been isolated and have antiinflammatory activities.

- **Clove**

Synonyms:-Caryophyllum; Clove flower ;Clove bud ; Laung.

Biological Source: Cloves consist of dried flower buds of *Eugenia caryophyllus*, **Family**:Myrtaceae. It should contain not less than 15 %

chemical Constituents: The drug contains about 15 to 20 % of volatile oil; 10 to 13 % of tannin (gallotannic acid), resin, chromone and eugenin.The volatile oil contains eugenol (about 70 to 90 %), eugenol acette, methylamylketone,caryophyllenes and small quantities of esters and alcohols.[17,18,19,20]

Figure 2 Clove [23]

Clove uses:-Clove is utilized as a dental pain relieving, carminative, stimulant, enhancing specialist, an aromatic and sterile. Depleted cloves are utilized in arrangement of cigarettes. The oil is used in perfumery additionally in fabricate of vanillin. [21]

Antibacterial property:- Clove was tried for antimicrobial exercises against a few organisms and microbes strains. Amid lab trials, clove appeared total bacteria-killing movement against all foodborne pathogens, counting E. coli, Bacillus cereus, and Staphylococcus aureus. Clove oil was found to be effective against Staphylococcus species. Aspergillus niger (parasites) was profoundly delicate to clove oil. Too, clove oil appeared germicidal impact against Klebsiella Pneumoniae, Pseudomonas aeruginosa, Clostridium perfringens, S. aureus, E. coli, and Candida albicans amid a lab consider. It was too found to slaughter Bacillus tuberculosis efficiently. The antimicrobial properties have been watched in lab considers. More trials are required to back clove against irresistible illnesses in people. Hence, don't utilize clove oil some time recently counseling your healthcare supplier.[22]

Antioxidant:-

Clove oil (eugenol) may offer assistance clear the respiratory sections and act as an expectorant for overseeing a few upper-respiratory infections like bronchitis, hack, cold, asthma, and sinus conditions. Clove contains different flavonoids like Î²-caryophyllene, kaempferol, and rhamnetin that might contribute to its antioxidant and anti-inflammatory activity.You must conversation to your healthcare supplier some time recently utilizing clove or its oil for any provocative conditions.[22]

- **Neem**

Synonyms:-margosa,nimtree,indian lilac

Biological Source :-Neem consists of almost all the part of the plant which are used as drug of Azadirachta indica. It is belong to family Meliaceae It is also known as margosa, *indian Lilac* and *Azadirachta indica*.[24]

Chemical constituents :-Various parts of the plant is used for various therapeutic and commercial purposes due to presence of different type of chemical in different parts of this plant. Some of them being Leaf :- quercetin, nimbosterol, nimbin[25]

Figure 3 Neem [26]

Bark:- nimbin, nimbidin, nimbosterol

Seeds :- Azadirachtin,Azadiradione, nimbin, vepinin

Azadirachtin :- Provide repellant, anti- hormonal and anti- feedant properties.

Nimbin:-Provide anti-inflammatory, anti-pyretic, anti-histamine, and anti- fungal properties

Nimbidin :- Provide anti- bacterial, anti- ulcer and anti- fungal properties

Nimbidol :- Provide anti tubercular, anti- protozoa and anti- pyretic properties

Sodium nimbinate :-provide Diuretic and Spermicidal properties

Gedunin :- Provide vasodilator, anti- malaria and anti-fungal properties.

Quercetin :- Provide anti protozoal, anti- oxidant and anti-inflammatory properties

Neem uses:-All parts of neem tree utilized as anthelmintic, against contagious, hostile to diabetic, hostile to bacterial, hostile to viral, prophylactic and sedative. Oil of neem utilized in cleanser, shampoo, balms and Cream as well as toothpaste. Neem gum is utilized as a bulking operator and for the planning of uncommon reason food (For diabetic).A decoction arranged from Neem roots is ingested to soothe fever in conventional Indian pharmaceutical.[24]

- **Turmeric**

Synonyms :-Saffron Indian; haldi (Hindi); Curcuma; Rhizoma cur-cumae.

Biological Source :-Turmeric is the dried rhizome of *Curcuma longa Linn.(syn.C.domestica Valeton).*, belonging to family Zingiberaceae.[27]

Chemical Constituents :-Turmeric contains yellow colouring matter called as curcuminoids (5%) and essential oil (6%).The chief constituent of the colouring matter is curcumin I (60%) in addition with small quantities of curcumin III, curcumin II and dihydrocurcumin.The volatile oil contains mono- and sesquiterpenes like zingiberene (25%), α-phellandrene,sabinene, turmerone, arturmerone, borneol, and cineole. Choleretic action of the essential oil is attributed to β-tolylmethyl carbinol.The volatile oil also contains α- and β-pinene, camphene, limonene, terpinene, terpinolene, caryophyllene, linalool, isoborneol, camphor, eugenol, curdione, curzerenone, curlone, AR-curcumenes, β-curcumene, γ-curcumene. α- and β-turmerones, and curzerenone.

Figure 4 Turmeric

Antioxidant property:-Turmeric prevents the initial stages of carcinogenesis due to its antioxidant and free radical properties. It has an impactin several biological pathways related to mutagenesis, oncogene expression, cell cycle regulation, apoptosis, tumorigenesis and metastasis. Apart from this, turmeric arrests carcinomatous cells in the G2/M phase of the cell cycle.Thus, it can be effective against various types of cancer.[28]

Uses:-Turmeric is utilized as fragrant, anti-inflammatory, stomachic, diuretic, anodyne gallstones, stimulant, tonic, carminative, blood purifier, antiperiodic,choice, taste, color administrator for medicines and joint family medication for cold and chopping. Curcuminoids have an anti-inflammatory impact, subsequently.[28]

- **Myrrh**

Synonyms :-Gum Myrrh, Commiphora, Bissabol Myrrh

Biological source:- It is gum resin obtained from the stem of the *commiphora molmol Engier***.**

Chemical Constituents :-The drug contains mixture of resin (25%), volatile oil (2.5-6.5%) and gum (60%). Along with these compounds, three free resin acids α, β and γ-Commiphoric acids, esters of resinacid, commiphorinic acid, two phenolic resins α and β-heerabomyrrhol, volatile oil consist terpene, cuminic aldehyde and eugenol etc.[29]

Anti-Inflamatory property:- Extracellular mediators and regulators such as cytokines, growth factors, and eicosanoids are inflammatory mediators that control inflammation. In most published studies,Myrrh showed anti-inflammatory properties by inhibiting pro-inflammatory mediators and enhancing anti-inflammatory mediators .The anti-inflammatory properties of Myrrh are utilized within the treatment of verbal inflammations such as periodontal infections, gingivitis and for diminishing the regrowth of plaques.[29]

Figure 5 Myrrh [30]

Uses :-It has stimulant, antiseptic property, uterine stimulant, emmenagogue. Because of its astringent property to mucous membrane it is also used for mouth wash and gargles.[29]

- **Oral Infections**

❖ **Tooth Decay:-**Tooth rot starts when microbes in your mouth make acids that assault the tooth's surface (finish). This will lead to a little gap in a tooth, called a depth. On the off chance that tooth rot isn't treated, it can cause torment disease, and indeed tooth loss**.** [31]

Causes: When decay-causing microbes come into contact with sugars and starches from foods and drinks, they shape corrosive. This corrosive can assault the tooth's finish,causing it to lose minerals.[32]

Figure 6 Tooth Decay [34]

symptoms:-In early tooth rot, there are not as a rule any symptoms.As tooth rot propels, it can cause a toothache (tooth torment) or tooth affect ability to sweets, hot, or cold.[33]

❖ **Gingivitis**

Bacterial buildup around the teeth is the foremost common cause of gingivitis.The fundamental side effect of gingivitis is red, puffy gums that will drain when a individual brushes their teeth.Gingivitis frequently settle with great verbal cleanliness, such as longer and more frequent brushing and customary flossin.In expansion, an clean mouthwash may helps.[35]

Causes: The most common cause of gingivitis is the accumulation of bacterial plaque between and around the teeth. Dental plaque may be a biofilm that collects normally on the teeth. It occurs when microscopic organisms connect to the smooth surface of a tooth.This plaque can harden into calculus, or tartar, close the gums at the base of the teeth. This features a yellow-white color. As it were dental experts can expel calculus.Buildup of plaque and tartar can trigger resistant reactions that lead to gingival or gum tissue annihilation. In the long run, it may lead to encourage complications, counting the misfortune of teeth. [35]

Figure 7 Gingivitis [36]

signs and indications of gingivitis include: gum irritation and discoloration tender gums which will be difficult to the touch bleeding from the gums when brushing or flossing halitosis, or terrible breath receding gums soft gums[35]

❖ **Enamel Erosion**

Enamel erosion often include: increased sensitivity to taste, textures, and temperature cracks and chips discoloration indentations known as cups on the surface of your teeth.[37]

Causes:- Enamel erosion can be caused by what you eat, particularly: sugary foods, such as ice cream, syrups, and caramel starchy foods, such as white breads acidic foods, such as apples, citrus fruits, berries, and rhubarb fruit drinks and juices sodas, which typically contain damaging citric acid and phosphoric acid in addition to sugar excess vitamin C, found in citrus fruits.[37]

Figure 8 Enamel erosion [38]

❖ **Dental Trauma**

Dental trauma refers to any injury or damage that occurs to the teeth, gums, or surrounding structures as a result of an external force. Oro dental trauma specifically refers to dental trauma that occurs in the oral cavity, which includes the teeth, gums, tongue, and other soft tissues Causes of oro dental trama.[39]

common causes of oro dental trauma, including Accidents: Accidents, such as motor vehicle accidents, falls, and workplace accidents, are one of the leading causes of oro dental trauma. The impact from accidents can cause teeth to be knocked out, fractured, or displaced, and can also cause injuries to the gums and other soft tissues in the oral cavity.Sports injuries: Sports-related activities, especially contact sports such as football, basketball, and hockey, can result in oro dental trauma. Impact from collisions, falls, or blows to the face during sports activities can cause tooth fractures, avulsion (complete displacement of a tooth from its socket), and other traumatic injuries to the oral cavity.Dental procedures: Although rare, dental procedures can sometimes result in oro dental trauma. For example, tooth extractions, root canal treatments, and other dental procedures can occasionally cause iatrogenic (treatment-induced) injuries, such as fractures, perforations, or injuries to the surrounding soft tissues.[39]

.**Common Symptoms of Dental Trauma Fractures**. Following an incident of some kind, a fracture may develop in a tooth or jawbone.Tooth Displacement another common symptom of dental trauma may be a loose tooth or a permanent tooth that's been knocked out of its socket. [40]

Figure 9 Dental Trauma [41]

Other mouthwash:-

Name of the herbal plant used	Use of mouthwash
Root of liquorice	Antimocrobial,anti-inflamatory
Miswak	Antibacterial
Pomegranate,mint	Antibacterial
Holy basil	Anti-cancer,antipyretics
Green tea ,guava marigold leaves	Antimicrobial activity

Table 2

Conclusion:- Increased bacterial resistance toward anti-microbials or side impacts of chemical antiplaque specialists there's substantial intrigued within the headway of other classes of antimicrobial operators for control of disease and way better verbal wellbeing. The use of an innate home grown mouthwash can move forward the verbal wellbeing status of an individual. A assortment of mouthwashes can be endorsed depending on the oral diseases. Subsequently, verbal healthcare specialists must got to be cognizant of various etiologic variables and inclining conditions of the verbal depth.

References:-

1) A. Chatterjee, M. Saluja, N. Singh, and A. Kandwal, "To evaluate the antigingivitis and antipalque effect of an Azadirachta indica (neem) mouthrinse on plaque induced gingivitis: a double-blind, randomized, controlled trial," Journal of Indian Society of Periodontology, vol. 15, no. 4, pp. 398–401,2011.
2) J. D. Lauten, L. Boyd, M. B. Hanson, D. Lillie, C. Gullion, and T. E. Madden, "A clinical study: Melaleuca, Manuka, Calendula and green tea mouth rinse," Phytotherapy Research,vol. 19, no. 11, pp. 951–957, 2005.
3) S. Mahyari, B. Mahyari, S. A. Emami et al., "Evaluation of the efficacy of a polyherbal mouthwash containing Zingiber officinale, Rosmarinus officinalis and Calendula officinalis extracts in patients with gingivitis: a randomized double-blind placebo-controlled trial," Complementary Ierapies in Clinical Practice, vol. 22, pp. 93 98, 2016.
4) World Journal of Pharmaceutical Research SJIF Impact Factor 8.084 Volume 9, Issue 10, 665-678.Research Article ISSN 2277–
5) 16 Edition of Trease and Evans Pharmacognosy Text Book (Pg. No. :- 433)
6) James, P.; Worthington, H.V.; Parnell, C.; Harding, M.; Lamont, T.; Cheung, A.; Whelton, H.; Riley, P.Chlorhexidine mouthrinse as an adjunctive treatment for gingival health. Cochrane Database Syst. Re
7) Marinho, V.C.; Chong, L.Y.; Worthington, H.V.; Walsh, T. Fluoride mouthrinses for preventing dental cariesin children and adolescents. Cochrane Database Syst. Rev. 2016,7, CD002284. [CrossRef
8) Su CY, Chen CC, Chen HY, Lin CP, Lin FH, Fang HW. Characteristics of an alternative antibacterial biomaterial for mouthwash in the absence of alcohol. J Dent Sci. 2019; 14: 192-7.
9) Rathod S, Gaddad SM, Shivannavar CT. Minimum inhibitory concentration spectrum of the S. mutans isolates in relation to dental caries. World J Sci Tech. 2012; 2: 21-5.
10) Özan F, Sümer Z, Polat ZA, Er K, Özan U, Deer O. Effect of Mouthrinse Containing Propolis on Oral Microorganisms and Human Gingival Fibroblasts. Eur J Dent 2007; 1(4):195–201.
11) G.A. van der Weijden and K. P. Hioe, "A systematic review of the effectiveness of self-performed mechanical plaque removal in adults with gingivitis using a manual toothbrush," Journal of Clinical Periodontology, vol. 32, no. Suppl 6, pp. 214–228, 2005.

12) Chang C-W, Chang W-L, Chang S-T, Cheng S-S. Antibacterial activities of plant essential oils against Legionella pneumophila . Water Research. 2008;42(1-2):278–286.
13) Senanayake UM, Lee TH, Wills RBH. Volatile constituents of cinnamon (Cinnamomum zeylanicum) oils. Journal of Agricultural and Food Chemistry. 1978;26(4):822–824.
14) Singh G, Maurya S, deLampasona MP, Catalan CAN. A comparison of chemical, antioxidant and antimicrobial studies of cinnamon leaf and bark volatile oils, oleoresins and their constituents. Food and Chemical Toxicology. 2007;45(9):1650–1661
15) Figure1refer :https://images.app.goo.gl/L5cnPwapdF4k26xW7
16) Halliwell B. Free radicals and antioxidants—quo vadis? Trends in Pharmacological Sciences. 2011;32(3):125–130.
17) Suhaj M. Spice antioxidants isolation and their antiradical activity: a review. Journal of Food Composition and Analysis. 2006;19(6-7):531–537.
18) Yunusa S, Yusuf UM, Haruna I. Comparison of Essential Oil of Clove Buds Extracted Using Soxhlet and Ultrasonic-Assisted Extraction Method (Short Communication), 2018; 7: 1.
19) Khalil AA, Rahman UU, Khan MR, Sahar A, Mehmood T, Khan M. Essential oil eugenol: Sources, extraction techniques and nutraceutical perspectives. RSC Adv, 2017; 7(52): 32669–81.
20) Overly KR. Microwave-Assisted Isolation of Eugenol from Cloves. J Chem Educ., 2019; 96(11): 2665–7.
21) Gokhale S.B, Kokate C.K, A Text Book of pharmacognosy, 21th Edition, Publication,
22) Ayala-Zavala JF, Silva-Espinoza B, Cruz-Valenzuela M, et al. Pectin-cinnamon leaf oil coatings add antioxidant and antibacterial properties to fresh-cut peach. Flavour and Fragrance Journal. 2013;28(1):39–45.
23) Figure 2 refer https://images.app.goo.gl/P7meyYGvMURRb3Cu5
24) Chaieb, K., Hajlaoui, H., Zmantar, T., Kahla-Nakbi, A. B., Rouabhia, M., Mahdouani, K. and Bakhrouf, A. The chemical composition and biological activity of clove essential oil, Eugenia caryophyllata (Syzygium aromaticum L.). Phytother. Res. 2007, 21, 501-506
25) 16 Edition of Trease and Evans Pharmacognosy Text Book (Pg. No. :- 433)
26) Figure 3 refer https://images.app.goo.gl/KE7TJ2Hhx7V6nFMh7
27) 16 Edition of Trease and Evans Pharmacognosy Text Book (Pg. No. :- 292)
28) Curcumin: An age-old anti-inflammatory and anti-neoplastic agent https://www.sciencedirect.com/science/article/pii/S2225411016302528
29) Analysis of inorganic and organic constituents of myrrh resin by GC–MS and ICP-MS: An emphasis on medicinal asset https://www.sciencedirect.com/science/article/pii/S131901641630127X 55 Edition of pharmacognosy by c.k.kokate (pg.no. 10.1-10.22)
30) Refer fig 4https://images.app.goo.gl/jUyCY334TKts89Hm8
31) Azarpazhooh A, Main PA. Pit and fissure sealants in the prevention of dental caries in children and adolescents: a systematic review. J Can Dent Assoc. 2008;74(2):171–177.
32) Hicks J, Garcia-Godoy F, Flaitz C. Biological factors in dental caries: role of remineralization and fluoride in the dynamic process of demineralization and remuneration (part 3) J Clin Pediatr Dent. 2004;28(3):203–214.
33) Prabhakar AR, Dodawad R, Os R. Evaluation of flow Rate, pH, buffering capacity, calcium, total protein and total antioxidant levels of saliva in caries free and caries active children—an in vivo study. Int J Clin Pediatr Dent. 2009;2(1):9–12.
34) Refer fig 6 https://images.app.goo.gl/xsLvXGdgTr2A4WMf9.

35) Jennifer Archibald, DDS — By Tim Newman — Updated on February 9, 2023
36) Refer fig 7https://images.app.goo.gl/yvebssCWNnnfQktA7
37) Johansson AK. Dental erosion. Modernt tandslitage och en ny folksjukdom. The Journal of the Swedish Dental Association (Tandläkartidningen) 2005;97(4):56–61.
38) Refer fig 8https://images.app.goo.gl/q6ntQ2S7icw5LVYN9.
39) Andersson L. Epidemiology of traumatic dental injuries. J Endod. 2013;39 03:S2–S5.
40) Petti S, Glendor U, Andersson L. World traumatic dental injury prevalence and incidence, a meta-analysis-one billion living people have had traumatic dental injuries. Dent Traumatol. 2018;34(02):71–86.
41) Refer fig 9 https://images.app.goo.gl/TeNaMe2AWuLbwQRg7

International Journal of Enhanced Research in Medicines & Dental Care (IJERMDC),
ISSN: 2349-1590, Vol. 11 Issue 5, May 2024, Impact Factor: 8.325

A review on Pharmaceutical cocrystal: coformer selection, method of preparation, characteristics of cocrystal and its regulatory aspects

Miss. Tanuja Rajendra Pawar*[1], Mr. Nilesh R. Bhosle[2], Dr. Rajashree S. Chavan[3], Miss. Apurva Madhav Bhuse[4], Miss. Sakshi Sukhdev Dhamal[5], Miss. Shreya D. Shinde[6]

[1,4,5,6]Student, Pune District Education Association's Seth GovindRaghunath Sable College of Pharmacy, Saswad
[2]Assistant Professor, Research Scholar, Shri JJT University, Jhunjhunu, Rajasthan
[3]Principal, Pune District Education Association's Seth GovindRaghunath Sable College of Pharmacy, Saswad

Correspondence: Tanuja Rajendra Pawar, Saswad Pune, Email id: tanujapawar308@gmail.com

ABSTRACT

Pharmaceutical co-crystals are a novel class of pharmaceutical materials with a potential for improving their polished physical characteristics to produce stable, patentable solid forms. These complex crystalline forms have an impact on relevant physicochemical factors such as the rate of dissolution, chemical stability, physical stability, and so forth that in ultimately produce materials with better qualities than the free medication. Nonetheless, coformer selection is crucial for enhancing the cocrystallization-derived API properties. Choosing the right coformers enhances the drug's physicochemical characteristics, therapeutic efficacy, and minimizes side effects. Different method can be used for the selection of coformer and the preparation of cocrystal which contain solvent evaporation, Neat grinding, Solvent grinding, antisolvent method etc. This review concluded with brief discussion of pharmaceutical consideration and regulatory guidelines for the cocrystal.

INTRODUCTION

The optimization of properties such as solubility, dissolution rate, mechanical properties, hygroscopicity, physical stability, and chemical stability is of strategic importance when determining the physical form in which active pharmaceutical ingredients (APIs) will be administered. Since crystalline APIs tend to be more stable, reproducible in their properties, and easier to isolate in high purity than amorphous drugs, most APIs are solid, crystalline, and exist in crystal form.[1]In spite of this, 40 percent of commercial compounds and drugs under development and 80% of drug substances in production have solubility issues.[2]Biopharmaceutical classification system (BCS) class II drugs have low solubility and are limited in their oral absorption. Thus, poor solubility is one of the most common issues hindering drug development [3]

The arrangement of atoms in the crystal lattice and unit cell directly affects the properties of crystalline materials. As a result, tailoring the crystal packing arrangement can modify the physicochemical properties of solid drug forms.[4, 5] It is hard to define a co-crystal exactly, but it can be defined as a crystalline compound containing two or more neutral molecules in a definite stoichiometric ratio. A co-crystal differs from a salt crystal due to the arrangement of cationic and anionic components in salt crystals. Pharmaceutical co-crystals comprise one or more secondary components known as crystal co-formers in addition to at least one API (active pharmaceutical ingredient). An organic substance, such as a carboxylic acid, an amino acid, alcohol, or sugar, is the co-former.[6]When it comes to pharmaceutical cocrystals, coformers are materials that the FDA has classified as GRAS (Generally Recognized As Safe), or safe substances to eat.[7] Cocrystals are described as "homogenous (single phase) crystalline structures made up of two or more components in a single structure" by the European Medicines Agency (EMA).specific stoichiometric ratio at which the crystal's arrangement .Unlike with salts, the lattice is not based on ionic bonds. In contrast to According to the FDA and EMA's definition, cocrystals are an effective substitute for the same API salts.[8] Stated differently, theCocrystal and API are thought to be equivalent, but cocrystal displays unique characteristics of pharmacokinetics.[9]

In this review, we will summarize the recent advances of pharmaceutical cocrystals, including selection of conformer, chemistry of cocrystal formation, preparation methods, characterization, challenges, and application of cocrystal.

2.Methods used for selection of coformer:

As was previously mentioned, coformers are crucial to the development of cocrystals. When forming cocrystals with a specific coformer, variables like the kind of functional group, pKa, their molecular size, and their physical form must be taken into account.[10] The knowledge-based approach and the experimental method are the main methods used to choose the coformers. Trial and error is the foundation of the experimental approach. A variety of factors are used to select suitable coformers, including hydrogen bonding, pKa-based models, supramolecularsynthon compatibility using the Cambridge Structure Database (CSD), lattice energy calculation, Hansen solubility parameter, thermal analysis, saturation temperature measurements, virtual cocrystal screening (using molecular electrostatic potential surfaces-MEPS), etc.[11][12]. Because of the structural characteristics of the coformer and API, the knowledge-based approaches can therefore predict the formation of cocrystals even before experiments are conducted. The structural components of supermolecules that can result from intermolecular interactions are known as supramolecular synthons.Two categories of supramolecularsynthons exist: homosynthonssupramoleculars possessing similar supramolecularheterosynthons with distinct but complementary functions and self-complementary features. Heterosynthons are usually more resilient. Generally speaking, carboxylic acid heterosynthons and amide homodimers are preferred [13, 14].

Cambridge Structural Database (CSD):

Crystallographic data about the hydrogen bonds that are formed between the drug and the coformer is contained in the CSD. There are currently more than 1.2 million crystals in the CSD repository frameworks [15, 16]

Hydrogen-Bond Rules:

The hydrogen-bond rule represents an additional method for choosing a coformer. An attractive interaction between an electronega-tive atom (X) and a hydrogen atom is known as the hydrogen bond (X-H). A molecule can form a hydrogen bond with another molecule or with itself [17]. For a particular functional group or combination of functional groups in which hydrogen bonds are formed, the hydrogen bond rule offers useful information about the favored hydrogen-bond selectivity, connectivity patterns, and stereo-electronic properties of hydrogen bonds. In general, the formation of hydrogen bonds follows three rules.Donohue proposed the first rule, which states that hydrogen bonds will be formed using all of the available acidic hydrogen in a compound's molecular crystal structure.[18]

pKa Rule:

The BCS Class II medications are categorized into three groups according to their pH-dependent solubility: Iia (acidic drugs), Iib (basic drugs), and Iic (neutral drugs). Medications categorized as weakly acidic ($pKa \leq 5$) have a greater water solubility at the intestinal pH of alkalinity. In contrast, weakly basic drugs ($pKa \geq 6$) are categorized as class basic drugs because they have a higher aqueous solubility at the acidic pH of the stomach. Neutral drugs are those that do not show apH-dependent solubility.[19][20]. A study of proton transfer can predict the formation of cocrystal and salt, and this can be found using the formula $\Delta pKa = [pKa\ (base) - pKa\ (acid)]$. Proton transfer between acid and base is indicated by a pKa value difference of more than two or three between the API and coformer. Cocrystal formation is indicated by a smaller pKa value difference (less than 0), whereas a large A variation in pKa values (≥ 2 or 3) signifies the formation of salt [21]

Method of Preparation of Cocrystal:

The cocrystallization of an API by a supersaturated solution in the presence of a coformer is the most widely used technique for the large-scale industrial production of cocrystals. Most of the time, an undersaturated mixture is slowly cooled until the dissolution limit is reached, resulting in about 40% supersaturation. In addition, the amount of the coformer (reaction cocrystallization) can be adjusted to induce solution mediated phase transitions (SMPT).[1]

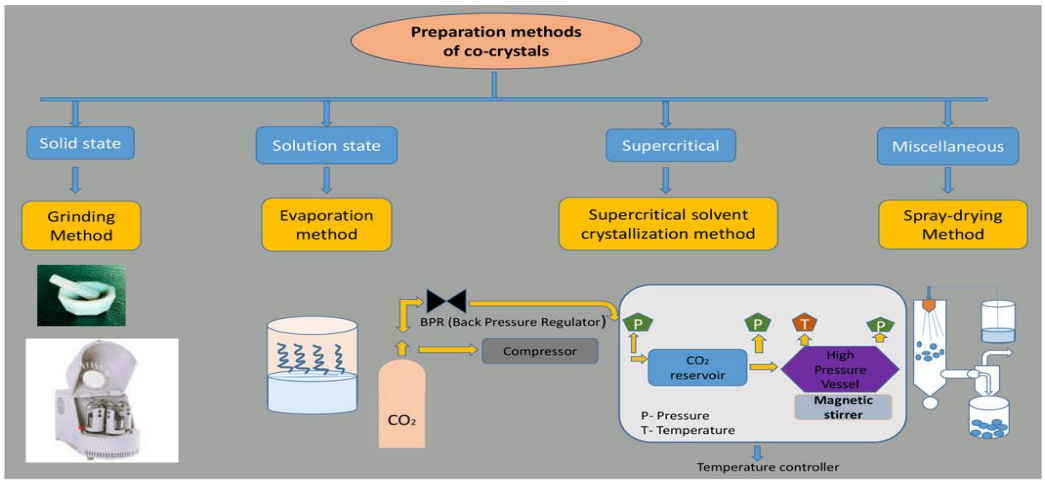

Figure 1. Different method of co crystal Preparation

Solvent Evaporation Method:
This method is the most widely applied one for producing cocrystals. In a common solvent with an appropriate stoichiometric ratio, the materials (API and coformer) are dissolved until they entirely evaporate[22]. A thermodynamically preferred product is produced during evaporation when the molecules' solution changes due to the formation of hydrogen bonds between various functional groups. The choice of solvent has a significant impact on solubility. The component with the lower solubility will precipitate if the two components have different solubilities. Solvent evaporation is a small-scale method of preparing cocrystals that produces high-quality, pure crystals without the need for complicated equipment. However, there are two drawbacks: it requires a lot of solvent, and its scalability is restricted.[1, 23]

Neat grinding method:
This process of cocrystallization doesn't use a solvent. The cocrystal is produced by admixing the appropriate stoichiometric amounts of solid materials, pressing and crushing them together using a mortar and pestle, ball mill, or vibrator mill. The typical grinding time is between thirty and sixty minutes. This technique can be used to prepare a large number of cocrystals, and any failure is usually the result of using the incorrect settings.[1]

Solvent grinding method:
This is a modification of neat grinding that has been used to improve supramolecular selectivity in crystalline systems, both polymorphic and stoichiometric, by incorporating a small amount of solvent into the grinding process[24]. A very tiny amount of solvent (~a few tenths of an equivalent amount of solvent per mole of the component) is added after the two components have been mixed. Given that the solvent's tiny quantity does not contribute to the finished product, its action can be characterized as catalytic. Its benefits include better product crystallinity, enhanced performance, and controllability over polymorph production. Moreover, a wide range of coformers can be used for cocrystallization. Liquid-assisting grinding has several drawbacks, such as being a small-scale process with high energy consumption and poor product purity performance. Pterostilbene-carbamazepine cocrystals were patented using liquid-assisted grinding .

Slurring technique:
The addition of the crystallization solvent is a straightforward procedure [25]. After the coformer is added to the solution created by the solid API dissolving in the solvent, the suspension is agitated, filtered, and dried.

Antisolventcocrystallization:
To encourage the precipitation of the solids, a solvent that is less soluble in the compound is frequently added to the solution. After filtering the resultant suspension, XRPD can be used to characterize the collected solid. This method's drawbacks include its poorer performance in comparison to solvent-based grinding and the substantial amount of solvent required.[1]

Use of supercritical fluids:
Supercritical fluid (SCF) is an excellent solvent that can replace organic solvents due to its exceptional ability to dissolve materials like a liquid and diffuse through solids like a gas (gas flow properties and dissolving liquid properties). The most popular supercritical fluid for cocrystallization is CO2; it can be used as a solvent, an anti-solvent, or an atomized anti-solvent [26]. It include cocrystallization with supercritical solvent, supercritical antisolvent, atomized antisolvent.[1]

Characterization of Cocrystals:
A variety of techniques have been used to clarify intermolecular interactions and characterize pharmaceutical cocrystals.The methods for characterizing cocrystals, particularly those that are frequently employed in drug delivery and development laboratories, are briefly covered in the final section of this review.

Single-crystal and powder X-ray diffraction (XRD): XR
The most common tool for characterizing cocrystals is a combination of methods. Since cocrystals have distinctive sharp peaks that differ from the peaks of the cocrystal components, single-crystal XRD is frequently used for the structure solution of cocrystals, whereas powder XRD (PXRD) is primarily used for identification purposes.[1]

Thermal analysis:
The term "thermal analysis" refers to a set of methods that record changes in the physical or chemical properties of a sample's thermal properties through time-controlled temperature changes (heating, cooling, alternating, or maintaining at a constant temperature) in a controlled atmosphere. The measured properties that can be recorded include mass, heat or heat flow, enthalpy, and so on. The most applicable methods for characterizing cocrystals are thermogravimetric analysis (TGA), differential scanning calorimetry (DSC), and differential scanning calorimetry (DSC), along with hot-stage microscopy (HSM). The following provides a brief overview of the methods used for cocrystal characterization.

Differential Scanning Calorimetry (DSC):
In the pharmaceutical industry, differential scanning calorimetry, or DSC, is frequently employed to characterize co-crystals. Utilizing this method, the co-crystal and pure components heat up gradually under control. The obtained thermogram is examined carefully to ensure the potential for co-crystal development. In this manner, eutectic melt produced when heating slowly Re-forms crystals melts after reaching the co-crystal form, regardless of the drug to coformer ratio. Since it enables co-crystal detection, the thermogram produced by the DSC scan is used for co-crystal screening. In contrast to the pure thermogram of drug and coformer, the thermogram of co-crystals displays an exothermic peak that is followed by an endothermic peak. Co-crystals will exhibit distinct melting points and heats of fusion when compared to their pure component counterparts. A thermogram of a physical mixture that is incapable of forming co-crystals will only show one endothermic peak connected to eutectic melting.[27]

Spectroscopy – vibrational, nuclear magnetic resonance:
The energy absorbed or scattered by the co-crystals' chemical bonds will differ from that of the pure components in vibrational spectroscopy (Raman and infrared), which helps to identify the co-crystals' structural behavior. Because of the hydrogen bonding that occurs between them, cocrystals display a different spectrum of bands in infrared spectroscopy than the pure drug and coformer. The bands of functional groups that have experienced hydrogen bonding clearly differ from one another. Because solid-state nuclear magnetic resonance can provide structural information about cocrystals, it is frequently used to characterize pharmaceutical ccrystals. Since this technique can determine the degree of proton, it is also used to differentiate between salts and cocrystals transfer. One of this method's primary drawbacks is the instrument's low sensitivity.[27]

Field emission scanning electron microscopy (FESEM):
To investigate the surface morphology of co-crystals, topography or FESEM are utilized. For the comparison, micrographs of the constituents and co-crystals from the FESEM investigations are used. Heat energy is not used in the field emission electron microscope; instead, a "cold" source is used. The electrons are released from the conductor's surface using a strong electric field. The cathode is made of a tungsten filament with a needle that is both thin and sharp (tip diameter 10-100 nm). A scanning electron microscope is attached to the field emission source in order to take co-crystal micrographs.[27]

Physical Properties modified by co crystal:
Melting Point:
A thermodynamic process where the free transition energy is zero, the melting point is a fundamental physical property that is defined as the temperature at which the solid and liquid phases are in equilibrium. While low m.p. may impede processing, drying, and stability, high m.p. is generally preferred but can also lead to low solubility (S) and hinder some molding processes. Because of their capacity to identify supplementary thermal data, differential scanning calorimetry (DSC) and the Kofler method are regarded as the preferred techniques for obtaining melting point data. A compound's purity can be determined and its classification can be made by finding its melting point**.**

Mechanical Properties:
In the production of solid dosage forms, the mechanical characteristics of crystalline materials play a crucial role in the processes of blending, milling, granulating, tableting, and coating. Elastic, plastic, viscoelastic, and fragmentation are the

mechanical deformation mechanisms for solid materials.Better plasticity qualities typically translate into superior compressibility, which is permanent and irreversible once stress is removed. For organic materials, good tableting behavior predicts greater plastic deformation and less elastic recovery. Slip plane-containing crystal structures would facilitate plastic deformation and ultimately enhance the behavior of bulk compaction.[28]

Bioavailability :
The term "bioavailability" describes the percentage of a medication that enters the bloodstream. Low bioavailability was a major reason for the preclinical failure of many drug candidates during the drug development process. Over the past ten years, cocrystallization has demonstrated its ability to enhance in vivo performance by increasing the solubility and bioavailability of drugs that are poorly soluble in water.[29]

Solubility:
A poorly soluble drug's solubility or rate of dissolution may be improved or decreased by cocrystallization[28]. Acyclovir l-tartaric acid, for instance, is more soluble than acyclovir 21's hydrate and amorphous forms. The melamine and cyanuric acid 1:1 cocrystal is a special illustration of the decreased solubility caused by cocrystallization. Because solubility and dissolution go hand in hand, if cocrystal solubility rises relative to API, intrinsic dissolution for cocrystals rises relative to pure drug, and vice versa. Co-crystal of ionized medication pH of the solution is the primary determinant of co-crystal solubility. This can be predicted using calculations based on the cocrystals' dissociation and degree of ionization equilibria[30, 31]

Pharmaceutical Considerations:
Co-crystals can enhance medications in a number of ways. These characteristics ought to be examined for every drug candidate to make sure that the advantages (much) outweigh any potential drawbacks of the novel dosage form. First off, one crucial factor is a drug's stability. It is necessary to take into account a number of stability factors, including moisture, chemical structure, air sensitivity, and the impact of acids and bases. These will affect the drug's effectiveness in the body as well as its shelf life. The drug may be exposed to a variety of environments. For example, the mouth's pH should always be higher than 5.5[32], whereas the stomach's gastric acid has a pH range of 1.5 to 3.5[32], The co-crystal frequently dissolves, and precipitation of a less soluble compound is possible. Adding surfactants to the medication could be one way to stop the medication from unintentionally re-crystallizing. Another crucial consideration in processing, packing, and storage is sensitivity to moisture. Moisture may cause the API to undergo undesired phase changes.[33]

Regulatory Guidelines for Pharmaceutical Cocrystals:
Guidelines for pharmaceutical cocrystals have been released by the European Medicines Agency (EMA) and the US Food and Drug Administration (USFDA). Pharmaceutical cocrystals are regarded by the USFDA as novel crystalline solid forms that improve the stability, bioavailability, and processability characteristics of APIs. The elements that make up the crystalline lattice of pharmaceutical cocrystals should interact nonionically, which sets them apart from salts. Cocrystals and solvates are closely related, but in pure form, at room temperature, the conformer is not a liquid.

The ΔpKa rule, which states that for the formation of a cocrystal, the difference between the pKa values of the cocrystal components should be less than 0, or any analytical evidence can be used by the applicant to demonstrate that the interaction between the API and conformer is nonionic. Additionally, the applicant must demonstrate that the API and conformer dissociate before reaching the site of action for pharmacological activity through in vitro dissolution and/or solubility studies. Regulation-wise, cocrystals of an API are viewed as distinct variations of the same API rather than as a brand-new API. Drug-drug cocrystals are regarded as fixed-dose combination products rather than as a novel single API, whether they contain an inactive conformer or not.[34]

CONCLUSION

The main causes of an active pharmaceutical ingredient's (API) failure in the current situation are poor permeability, low bioavailability, poor solubility, poor dissolution rate, and instability. The researchers' main goal is to mitigate these problems with APIs. Cocrystallization is a tried-and-true method for improving the physicochemical characteristics of APIs and resolving their associated issues. Because the final properties of the cocrystal depend on the coformer's characteristics and how it interacts with the API, coformers are essential to the cocrystallization process. Studies that show how the cocrystallization trials improved the previously listed API properties have been presented. In summary, this review offers a thorough explanation and examples of the physicochemical characteristics, preparation techniques, and range of uses for cocrystals. The cutting-edge technologies comprehensive regulatory guidance will also progress the translational research on drug cocrystal development for applications in healthcare. More medication products based on crystals are thought to be offered commercially to patients in the future.

REFERENCES

[1]. Karagianni, A., M. Malamatari, and K. Kachrimanis, *Pharmaceutical cocrystals: New solid phase modification approaches for the formulation of APIs.* Pharmaceutics, 2018. **10**(1): p. 18.

[2]. Loftsson, T. and M.E. Brewster, *Pharmaceutical applications of cyclodextrins: basic science and product development.* Journal of pharmacy and pharmacology, 2010. **62**(11): p. 1607-1621.

[3]. Lipinski, C.A., et al., *Experimental and computational approaches to estimate solubility and permeability in drug discovery and development settings.* Advanced drug delivery reviews, 1997. **23**(1-3): p. 3-25.

[4]. Schultheiss, N. and A. Newman, *Pharmaceutical cocrystals and their physicochemical properties.* Crystal growth and design, 2009. **9**(6): p. 2950-2967.

[5]. Datta, S. and D.J. Grant, *Crystal structures of drugs: advances in determination, prediction and engineering.* Nature Reviews Drug Discovery, 2004. **3**(1): p. 42-57.

[6]. Wouters, J. and L. Quéré, *Pharmaceutical salts and co-crystals*. 2011: Royal Society of Chemistry.

[7]. Roberts, A. and L.A. Haighton, *A hard look at FDA's review of GRAS notices.* Regulatory Toxicology and Pharmacology, 2016. **79**: p. S124-S128.

[8]. Agency, E.M., *Reflection paper on the use of cocrystals of active substances in medicinal products*. 2015, European Medicines Agency Amsterdam, The Netherlands.

[9]. Kavanagh, O.N., et al., *Pharmaceutical cocrystals: from serendipity to design to application.* Drug Discovery Today, 2019. **24**(3): p. 796-804.

[10]. Manin, A.N., et al., *Hydrogen bond donor/acceptor ratios of the coformers: Do they really matter for the prediction of molecular packing in cocrystals? The case of benzamide derivatives with dicarboxylic acids.* Crystal Growth & Design, 2018. **18**(9): p. 5254-5269.

[11]. Kumar, S. and A. Nanda, *Pharmaceutical Cocrystals: An Overview.* Indian Journal of Pharmaceutical Sciences, 2017. **79**(6).

[12]. Surov, A.O., et al., *Virtual Screening, Structural Analysis, and Formation Thermodynamics of Carbamazepine Cocrystals.* Pharmaceutics, 2023. **15**(3): p. 836.

[13]. Vishweshwar, P., et al., *Pharmaceutical co-crystals.* Journal of pharmaceutical sciences, 2006. **95**(3): p. 499-516.

[14]. Kuminek, G., et al., *Cocrystals to facilitate delivery of poorly soluble compounds beyond-rule-of-5.* Advanced drug delivery reviews, 2016. **101**: p. 143-166.

[15]. Singh, M., et al., *Cocrystals by Design: A Rational Coformer Selection Approach for Tackling the API Problems.* Pharmaceutics, 2023. **15**(4): p. 1161.

[16]. Thakuria, R., B. Sarma, and A. Nangia, *7.03—Hydrogen bonding in molecular crystals.* Comprehensive supramolecular chemistry II. Elsevier, Oxford, 2017: p. 25-48.

[17]. Arunan, E., et al., *Definition of the hydrogen bond (IUPAC Recommendations 2011).* Pure and applied chemistry, 2011. **83**(8): p. 1637-1641.

[18]. Etter, M.C., *Hydrogen bonds as design elements in organic chemistry.* The Journal of Physical Chemistry, 1991. **95**(12): p. 4601-4610.

[19]. Goswami, P.K., R. Thaimattam, and A. Ramanan, *Crystal engineering of multicomponent crystal forms of p-aminosalicylic acid with pyridine based coformers.* Crystal Growth & Design, 2016. **16**(3): p. 1268-1281.

[20]. Fei, T., et al., *Design and synthesis of a series of CL-20 cocrystals: six-membered symmetrical N-heterocyclic compounds as effective coformers.* Crystal Growth & Design, 2019. **19**(5): p. 2779-2784.

[21]. Childs, S.L., G.P. Stahly, and A. Park, *The salt− cocrystal continuum: the influence of crystal structure on ionization state.* Molecular pharmaceutics, 2007. **4**(3): p. 323-338.

[22]. Weyna, D.R., et al., *Synthesis and structural characterization of cocrystals and pharmaceutical cocrystals: mechanochemistry vs slow evaporation from solution.* Crystal Growth and Design, 2009. **9**(2): p. 1106-1123.

[23]. Childs, S., *Novel Cocrystallization of Hydrochloric Acid Salt of an Active Agent.* Can. Patent CA2514092 A, 2004. **1**: p. 5.

[24]. Jones, W., W.S. Motherwell, and A.V. Trask, *Pharmaceutical cocrystals: An emerging approach to physical property enhancement.* MRS bulletin, 2006. **31**(11): p. 875-879.

[25]. Takata, N., et al., *Cocrystal screening of stanolone and mestanolone using slurry crystallization.* Crystal Growth and Design, 2008. **8**(8): p. 3032-3037.

[26]. Padrela, L., et al., *Formation of indomethacin–saccharin cocrystals using supercritical fluid technology.* European Journal of Pharmaceutical Sciences, 2009. **38**(1): p. 9-17.

[27]. Thayyil, A.R., et al., *Pharmaceutical co-crystallization: Regulatory aspects, design, characterization, and applications.* Advanced Pharmaceutical Bulletin, 2020. **10**(2): p. 203.

[28]. Guo, M., et al., *Pharmaceutical cocrystals: A review of preparations, physicochemical properties and applications.* Acta Pharmaceutica Sinica B, 2021. **11**(8): p. 2537-2564.

[29]. Childs, S.L., P. Kandi, and S.R. Lingireddy, *Formulation of a danazol cocrystal with controlled supersaturation plays an essential role in improving bioavailability.* Molecular pharmaceutics, 2013. **10**(8): p. 3112-3127.
[30]. Aakeröy, C.B., S. Forbes, and J. Desper, *Using cocrystals to systematically modulate aqueous solubility and melting behavior of an anticancer drug.* Journal of the American Chemical Society, 2009. **131**(47): p. 17048-17049.
[31]. Masuda, T., et al., *Cocrystallization and amorphization induced by drug–excipient interaction improves the physical properties of acyclovir.* International journal of pharmaceutics, 2012. **422**(1-2): p. 160-169.
[32]. Rekdal, M., et al., *Applications of Co-Crystals in Pharmaceutical Drugs.* Systematic Reviews in Pharmacy, 2018. **9**(1).
[33]. Airaksinen, S., et al., *Excipient selection can significantly affect solid-state phase transformation in formulation during wet granulation.* Aaps Pharmscitech, 2005. **6**: p. E311-E322.
[34]. Kumar Bandaru, R., et al., *Recent advances in pharmaceutical cocrystals: From bench to market.* Frontiers in Pharmacology, 2021. **12**: p. 780582.

International Journal of All Research Education and Scientific Methods (IJARESM),
ISSN: 2455-6211, Volume 12, Issue 6, June-2024, Available online at: www.ijaresm.com

Formulation and Evaluation of Controlled Release Naproxen Microsphere Loaded Gel for the Treatment of Inflammation

Mr. Gaurav Anil Patil* , Mr. Nilesh R. Bhosle [1], Dr. Rajashree S. Chavan [2], Mr. Gaurav V. Tekade[3], Mr. Prasad S. Wagh[4], Mr. Aniket V. Chandankhede[5]

[*,3,4,5]Student, Pune District Education Association's Seth Govind Raghunath Sable College of Pharmacy, Saswad. Pune.
[1]Assistant Professor, Research Scholar, Shree JJT University, Jhunjhunu, Rajasthan
[2]Principal, Pune District Education Association's Seth Govind Raghunath Sable College of Pharmacy, Saswad. Pune

----------**********----------

ABSTRACT

Topical controlled release drug delivery system is getting greater attention due to its therapeutic advantages. Naproxen is a non-steroidal anti-inflammatory drug with potent analgesic and anti-arthritic properties. In the present study, a suitable particulate system of Naproxen has been developed by Solvent evaporation method for controlled release that would result in prolong drug release, reduced frequency of administration and lesser side effects. Different ratios and percentages of hydroxypropyl methyl cellulose and ethyl cellulose were used to formulate the microspheres. The effect of various formulation variables on evaluation parameters such as size, entrapment efficiency, drug content and in vitro release of naproxen were studied. Gel was formulated of Formulation No. 5 which was optimised batch.

Keywords: Controlled drug delivery, Microsphere, Gel, NSAID, Naproxen, Solvent evaporation method

INTRODUCTION

Microspheres are defined as homogenous, monolithic particles in the size range of 1-1000µm and are widely used as a drug carrier for controlled release action. The limitations of traditional dosage forms and traditional oral drug delivery systems are propelling the pharmaceutical community into a new era of drug delivery systems known as Novel Drug Delivery Systems (NDDS). The concept of targeted drug delivery, as a subset of NDDS, is currently being extensively researched[1].

The selective accumulation of cargo in organs, tissues, cells, or intracellular structures by systemic or local drug delivery is referred to as targeting. The preferential accumulation of drugs at the targeted site prevents the rest of the body's healthy tissues and increases the drug's therapeutic index, improving the entire therapeutic outcome. Targeting a drug delivery system requires the use of carriers such as nanoparticles, liposomes, micellar systems, microspheres, and so on[2].

Naproxen is a nonsteroidal anti-inflammatory drug (NSAID), mainly used in osteoarthritis, rheumatoid arthritis, and ankylosing spondylitis.

Naproxen :

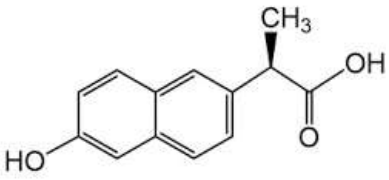

Naproxen is a non-steroidal anti-inflammatory drug (NSAID), mainly used in osteoarthritis, rheumatoid arthritis, and ankylosing spondylitis. The anti-inflammatory mechanism of naproxen is due to decreased prostaglandin synthesis by inhibiting COX-1 and COX-2. The majority of anti-inflammation that Naproxen induces is mostly due to inhibition of the COX-2 iso-enzyme; though, it should be noted that COX-1 is also expressed at distinct inflammatory sites. Further, COX-1 is also expressed in the joints of patients with rheumatoid arthritis or osteoarthritis, especially in the synovial lining. Therefore, although Naproxen targets both COX-1 and COX2, it is slightly more selective for the former.

Additionally, naproxen is most effective in the setting of pain receptor sensitivity. It appears prostaglandins, specifically prostaglandins E and F, are responsible for sensitizing these pain receptors; therefore, naproxen has an additional, indirect analgesic effect by inhibiting further prostaglandin production[3].

MATERIALS

Naproxen (Arti Pharma pvt ltd, Mumbai), Ethyl Cellulose (SGRS college of Pharmacy), Hydroxypropyl methyl cellulose (SGRS college of Pharmacy)

Table No. 1 : List of ingredients

Sr. No	Ingredients	Category
1	Naproxen (API)	API
2	HPMC	Film former
3	Ethyl Cellulose	Polymer
4	Tween 80	Solvent
5	Acetone	Surfactant

PREPARATION:

❖ **Method of preparation microsphere:**

Naproxen microspheres was prepared by solvent evaporation method. The solvent evaporation method seemed to be promising for the preparation of Naproxen microspheres as it is easy and has the advantage of avoiding solvent toxicity.

Table No. 2 : Composition of formulation batches of Naproxen microspheres

Formulation	Naproxen (mg)	Ethyl cellulose (mg)	HPMC (mg)	Acetone (ml)	Twin 80 (ml)	Water (ml)	Stirring speed (RPM)
F1	250	100	100	20	0.5	100	600
F2	250	100	250	20	0.5	100	600
F3	250	100	400	20	0.5	100	600
F4	250	250	100	20	0.5	100	600
F5	250	250	250	20	0.5	100	600
F6	250	250	400	20	0.5	100	600
F7	250	400	100	20	0.5	100	600
F8	250	400	250	20	0.5	100	600
F9	250	400	400	20	0.5	100	600

A. Procedure of Microsphere preparation :

i To prepare the internal phase, Hydroxypropyl methyl cellulose & Ethyl Cellulose is dissolved in Acetone.

ii The drug can be then added to the solution and dissolved under ultra-sonication for 5 minutes.

iii The internal phase containing drug (250mg) and solvent Acetone was gradually added into a 100 ml distilled external phase(water), containing Tween 80 as an emulsifying agent.

iv The mixture was stirred on a magnetic stirrer at 600 rpm for 3 hrs to remove Acetone.

v The formed microspheres were filtered through Whatman filter paper no. 41 (Whatman, UK).

vi Washed with n hexane, dry at 35-40 °C for 12 hrs and weigh the yield.

B. Method of Preparation of Gel :

All the ingredients were accurately weighed. Carbopol 940 was soaked overnight with distilled water to hydrate and then hydrated carbopol was again dispersed in distilled water by stirring on a magnetic stirrer for about 1 hour, then propylene glycol along with other excipients such as Butylated Hydroxy Toulene and Methyl paraben were added with continuous stirring to the carbopol 940 solution. Then the mixture was neutralized by the drop-wise addition of

triethanolamine which act as a neutralizing agent. Mixing was continued until transparent gel appeared, while the amount of base was adjusted to achieve a gel with a pH value of about 6.8.

Incorporation of Microspheres into the Gel:
The prepared Microspheres equivalent to 1% of Naproxen was weighed and dispersed into carbopol gel with continuous stirring on a magnetic stirrer for 20 minutes to get uniformly distributed microspheres into the gel base.

Table No. 3 : Formulation table for gel

Sr. no.	Components	Quantity
1	Microspheres equivalent to 100 mg of Naproxen	300 mg
2	Carbopol-940	800 mg
3	Propylene glycol	1.5 gm
4	Butylated Hydroxy Toulene	10 mg
5	Methyl paraben	10 mg
6	Triethanolamine	Qs.
7	Distilled Water	Qs.

CHARACTERIZATION & EVALUATION PARAMETERS

MIROSPHERES

1. Description: The microspheres were observed for their colour, nature.

2. Compatibility Study:
Naproxen and the polymer were subjected to drug – excipients compatibility studies. FTIR measurements of the drug, individual polymer, and drug-polymer mixtures were obtained on FTIR JascoV-630. Samples were prepared by mixing with KBr and placing it in the sample holder. The spectra were scanned over the wave number range of 4000- 400 cm^{-1} at ambient temperature.

3. Frequency Distribution Analysis:
Particle size of all the prepared batches of microspheres was determined using optical microscopy at 10X and 40X. A minute quantity of microspheres was spread on a glass slide and the average size of microspheres was determined.

4. Production Yield:
The percentage of production yield (w/w) was calculated from the weight of dried microspheres (W1) recovered from batches and the sum of the initial dry weight of starting materials (W2) as the following equation:

$$\text{Percentage yield (\%)} = \frac{\text{Practical yield}}{\text{Therotical yield}} \times 100$$

The yields of production were calculated as the percentage weight of the final product after drying, concerning the initial total amount of Naproxen and polymer used for preparation

5. Entrapment Efficiency:
100 mg of microspheres were dissolved completely in 100 ml phosphate buffer pH 7.4 to produce a clear solution to the phosphate buffer pH 7.4. Then the solution was filtered with a 0.45-micron membrane filter. By making suitable dilutions the drug content was determined spectroscopically at 331 nm by using a UV spectrophotometer.
Entrapment efficiency was calculated by using the following formula:

$$\text{Entrapment efficiency} = \frac{Actual\ \ drug\ \ loading}{Theoretical\ \ drug\ \ loading} \times 100$$

6. Theoretical Drug Content:
Theoretical drug loading was determined by calculation assuming that the entire Naproxen present in the polymer solution used was entrapped in Naproxen microspheres and no loss was observed at any stage of preparation of Naproxen microspheres.

7. Actual Drug Content:
Actual drug loading was analysed by using the following procedure, Weighed amount of naproxen microspheres equivalent to 100 mg of Naproxen was dissolved in 100 ml of phosphate buffer pH 7.4. This solution was kept overnight for the complete dissolution of Naproxen in phosphate buffer pH 7.4.this solution was filtered and diluted to make a conc. of 10 µg/ml solution. The absorbance of the solutions was measured at 331nm using double beam UV-Visible spectrophotometer against phosphate buffer pH 7.4 as blank and calculated for the percentage of drug present in the sample**.**

8. In-Vitro Drug Release Study
Dissolution Test (In Vitro Drug Release) Of Microspheres :
In the present study, the USP apparatus II was used. The microspheres equivalent to 100 mg Naproxen were placed directly in a dissolution basket. The dissolution test was performed using 900 ml of phosphate buffer pH 7.4, at 37±0.50 C and 100 rpm. A sample of 1 ml of the solution was withdrawn from the dissolution apparatus at certain intervals for 9 hrs. and the samples were replaced with fresh dissolution medium to maintain sink condition. The samples were filtered through 0.45-micron filters. The absorbance of these solutions measured at 331 nm. The cumulative percentage of drug release was calculated using an equation obtained from a standard curve.

EVALUATION OF BASIC GEL PARAMETERS

1. Physical examination:
The prepared gel formulations were inspected visually for their color, homogeneity, consistency, and appearance.
2. pH:
Weighed 10 gm of gel formulation were transferred in 10 ml of the beaker and measured it by using the digital pH meter. pH of the topical gel formulation should be between 3–9.
3. Viscosity:
Brookfield digital viscometer was used to measure the viscosity (in cps) of the prepared gel formulation. The spindle (T-D) was rotated at 10 rpm. Reading was reported 30 sec after putting the motor on. The determinations were carried out in triplicate and the average of three reading is recorded.
4. Spreadability:
Two glass slides of 20 x 20 cm were selected. The gel formulation whose spreadability had to be determined was placed over one of the slides. The other slide was placed upon the top of the gel such that the gel was sandwiched between the two slides and 100g weight was placed upon the upper slide so that the gel between the two slides was pressed uniformly to form a thin layer. The weight was removed and the fixed to a stand without slightest disturbance and in such a way that only the upper slide without slights disturbance and in such a way only the upper slide to side off freely, to the force of weight tied to it. A 20g weight was tied to the upper side carefully. The time taken for the upper slide to travel the distance of 7.5 cm and separate away from the lower slide under the certain of weight was noted. The determinations were carried out in triplicate and the average of three readings recorded.

$$S = M \times L / T$$

5. In-vitro diffusion study:
The % cumulative release of formulation was determined by using Franz (vertical) diffusion cell with area 3.14 cm^2 for 9 hrs. egg membrane was mounted on the receptor compartment with facing upwards into donor compartment. The donor compartment was filled with the 1 gm of topical gel formulation. A 30 mL aliquot of phosphate buffer pH 7.4 was used as receptor medium to maintain sink condition. The available diffusion area of cell was 3.14 cm^2 .The receptor compartment was maintained at 37 ±0.5 ^{0}c and stirred by Teflon coated magnetic bars at 100 rpm. The donor compartment was kept in contact with the receptor compartment. At predetermined time intervals for 9 hr., pipetted out 1 ml of solution from the receptor compartment and immediately replaced with the fresh 1 ml phosphate buffer. The drug concentration of the receptor fluid was measured at 331 nm by using UV spectrophotometer against appropriate blank.

RESULT AND DISCUSSION

A. PREFORMULATION STUDIES :
1. Organoleptic properties :
A sample of Naproxen was found to be white to off white crystalline powder, Odourless as per its standard.
2. Melting Point Determination
The melting point of Naproxen was found to be 153°C ± 0. 5 °C which complies standard range in I.P.
3. Solubility
Naproxen is Freely soluble in DMSO, soluble in Acetone, Ethanol and Dichloromethane, where Partially insoluble in water. As it complies with I.P.

4. UV spectroscopy :

Selection of Sampling Wavelength for Analysis:

All the dilutions showed maximum absorbance at 331 nm for Naproxen hence 331 nm was selected as the working analytical wavelength for UV calibration spectroscopy.

5. Calibration curve for Naproxen in methanol :

Concentration (µg/ml)	Absorbance
0	0
20	0.1705
40	0.2821
60	0.4225
80	0.5605
100	0.7176
120	0.8453

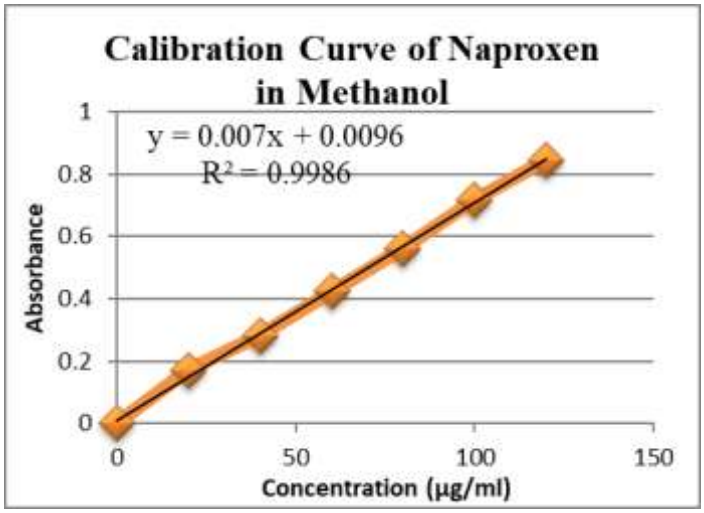

Figure No. 1 : Calibration curve of naproxen in methanol

6. FT-IR Spectroscopy :

Identification of Drug Naproxen :

The spectrum of Naproxen drug is shown in Figure 9.2 and interpretation of FTIR spectra is given in Table 9.5. These peaks are specific for specific functional groups. The functional groups shown by FTIR spectrum of drug indicate that the observed peaks of obtained drug were correctly matches with the reported peaks. From this result it was concluded that given Naproxen drug and it was pure and complied the standards.

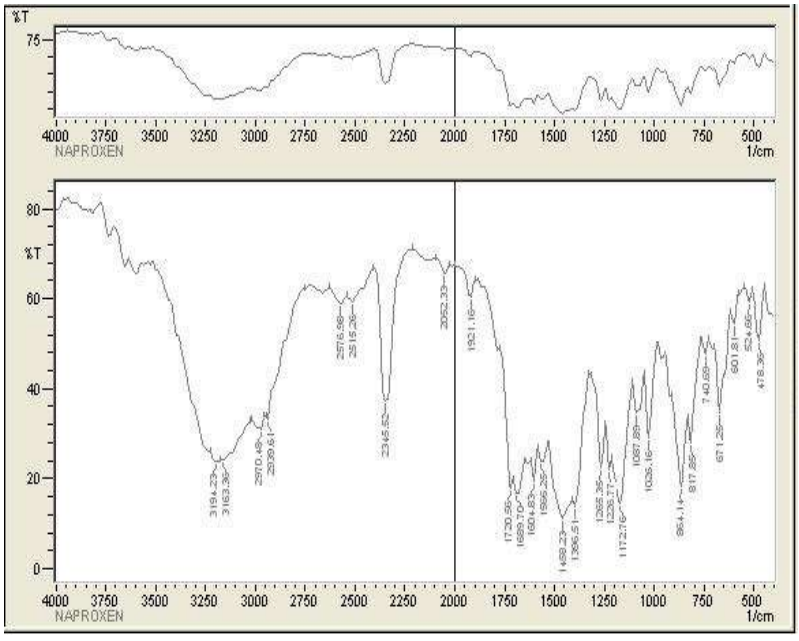

Figure No. 2 : IR Spectrum of Ethyl cellulose

7. DSC :

The DSC of Naproxen was carried out to conform its purity. Naproxen was heated in crimped aluminium pan with scanning rate of 100°C /min in atmosphere of nitrogen flow (40 ml/min).

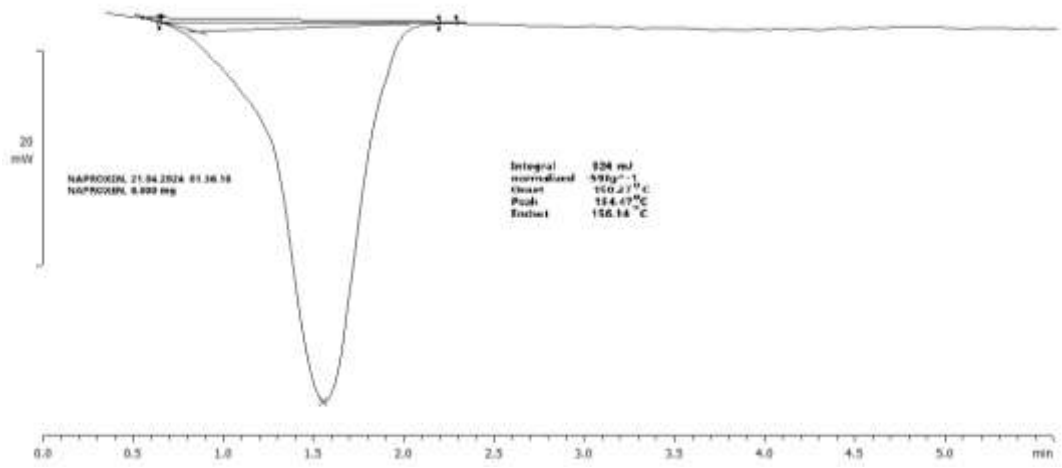

Figure No. 3 : DSC curve of Naproxen drug

B. EVALUATION OF NAPROXEN MICROSPHERES :

1. IR spectroscopy:

From the spectra of Naproxen microsphere formulation, it was observed that all characteristics peaks of Naproxen were present in the combination spectrum and in the formulation, thus indicating compatibility of the drug and polymer. The process used for the formulation is also compatible as no changes in the drug purity occur as microspheres formulation of the drug takes place.

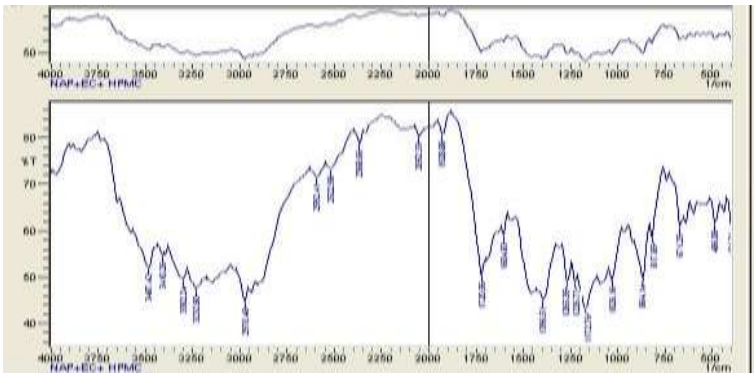

Figure No. 4 : DSC curve of Naproxen drug

2. Results of Percentage yield, Drug content, Particle size and Drug entrapment efficiency :

percentage yield, Drug content, particle size and Entrapment efficiency determination of the prepared microspheres were carried and the results are summarized in Table 9.7. Percentage yield of different formulation was determined by weighing the microspheres after drying. The range of drug content varies from 83.18% to 94.75%. Drug entrapment efficiency from 74.86% to 85.28%.

Formulation	Percentage yield	Drug content	Particle size (µm)	Drug entrapment efficiency
F 1	88.47%	86.11%	280	77.50±0.14
F 2	85.37%	90.45%	292	81.41±0.07
F 3	78.18%	87.38%	270	78.64±0.17
F 4	81.32%	83.18%	330	74.86±0.21
F 5	91.58%	94.75%	356	85.28±0.18
F 6	79.21%	88.31%	249	79.48±0.07
F7	80.33%	90.54%	351	81.48±0.13
F8	76.29%	89.41%	261	80.47±0.28
F9	82.34%	88.58%	294	79.72±0.09

International Journal of All Research Education and Scientific Methods (IJARESM),
ISSN: 2455-6211, Volume 12, Issue 6, June-2024, Available online at: www.ijaresm.com

Table No. 3 : Evaluation of Formulated Naproxen Microspheres
Percentage yield

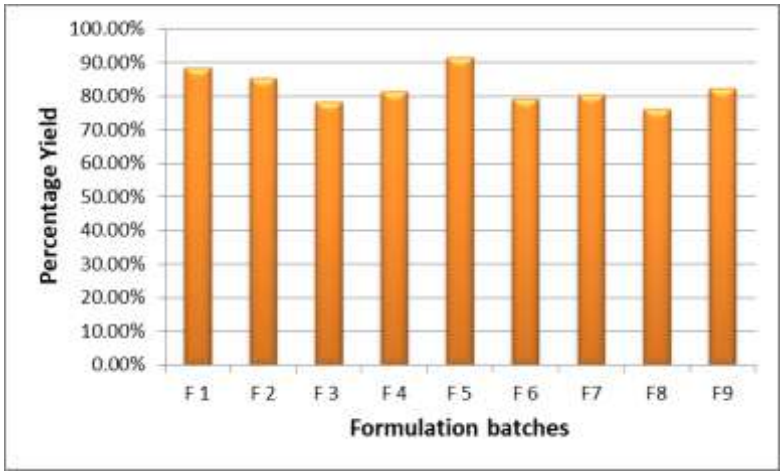

Figure No. 5 : Percentage yield of Naproxen microspheres

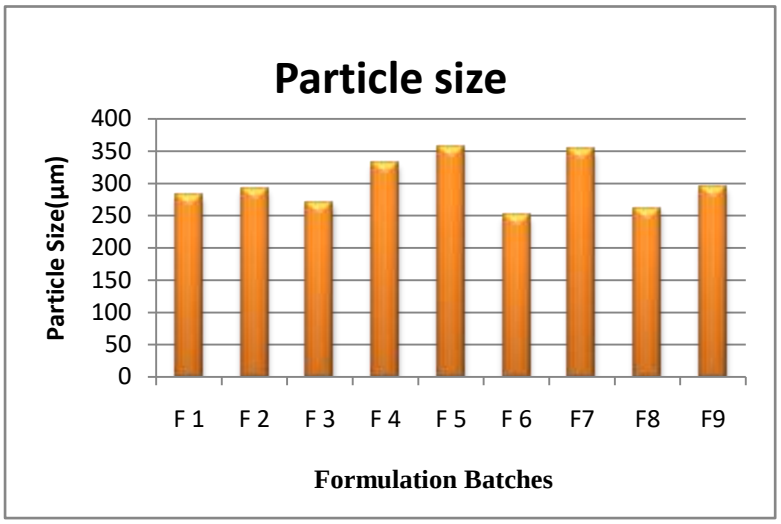

Figure No. 6 : Particle size of Naproxen microspheres

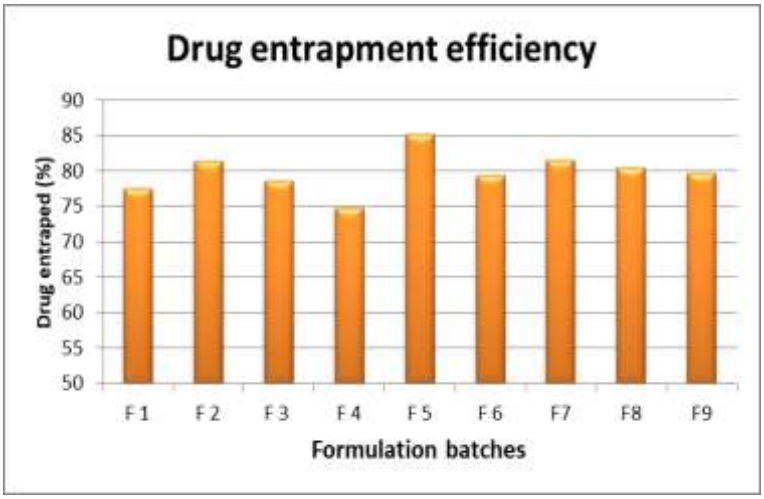

Figure No. 7 : Drug entrapment efficiency of Naproxen microspheres

3. In vitro drug release study of microspheres :

Table No. 4 : In vitro drug release study of microspheres

Time (Hrs)	F1	F2	F3	F4	F5	F6	F7	F8	F9
0	0	0	0	0	0	0	0	0	0
1	11.36%	13.23%	12.67%	15.16%	16.27%	13.45%	14.41%	12.32%	15.71%
2	19.54%	20.87%	19.75%	23.59%	24.61%	21.01%	22.68%	18.43%	23.11%
3	31.41%	32.66%	30.43%	31.23%	36.78%	29.96%	29.12%	26.47%	31.87%
4	44.54%	40.65%	41.26%	42.49%	45.84%	42.43%	35.26%	35.38%	42.35%
5	52.19%	44.98%	53.48%	50.69%	53.65%	51.56%	42.28%	46.55%	51.06%
6	60.89%	56.58%	62.79%	56.21%	64.89%	59.35%	50.94%	54.26%	62.57%
7	71.67%	62.34%	70.39%	61.38%	72.36%	69.97%	61.29%	62.58%	70.91%
8	79.56%	71.54%	79.66%	67.29%	79.93	76.79%	68.24%	68.39%	79.18%
9	86.12%	77.34%	84.17%	71.69%	87.45	84.35%	76.87%	75.39%	85.69%
10	94.67%	83.3%	93.3%	78.3%	97.9%	90.8%	84.1%	82.1%	94.5%

At the end of 10 hrs. the percentage cumulative release of Naproxen from Microspheres was found in the range of 78.3% to 97.9 %.

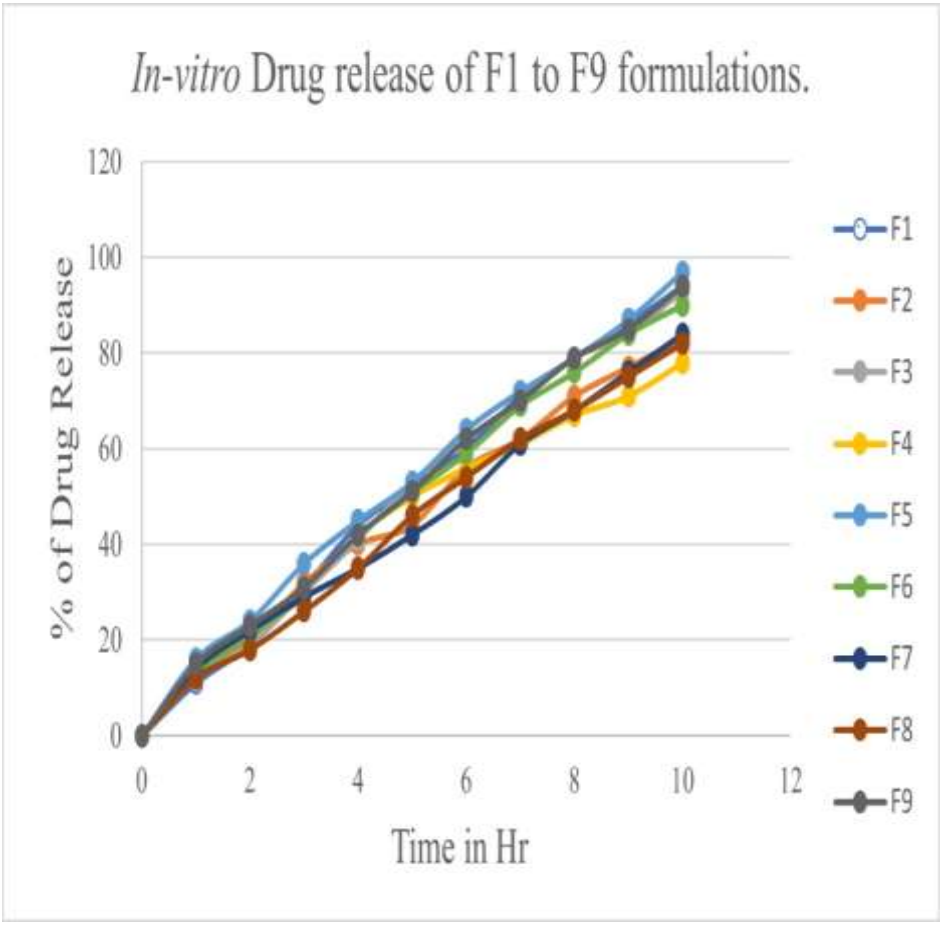

Figure No. 7 : In vitro drug release study of Naproxen microspheres

4. Morphology:

Morphology of microspheres was examined by using scanning electron microscopy. The Fig. 8 shows the top view of chitosan microspheres. The top view of the microspheres showed a spherical structure

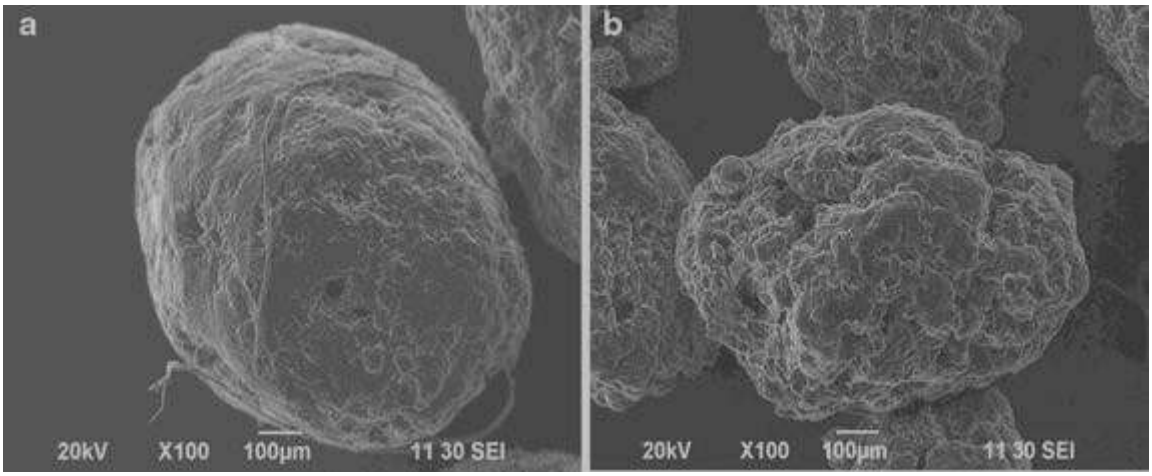

Figure No. 8 : Scanning electron microscopy of naproxen microsphere

- On the basis of various evaluation parameters of naproxen microspheres it's concluded that **Formulation batch No. 5 is our optimised batch**. Then, Gel of Naproxen microsphere batch no. 5 was formulated

C. EVALUATION OF NAPROXEN MICROSPHERE GEL :

Appearance was found to be Opaque, elegance, homogeneous, and consistent in nature. pH was 6.4± 0.36. Viscosity was3140 cps and Spreadibility was17.14 ±0.12 gm.cm/sec

Table No. 5 : Evaluation of Naproxen microsphere gel

Test	Observation
Appearance	Opaque, elegance, homogeneous, and consistent in nature
pH	6.4± 0.36
Viscosity	3140 cps
Spreadibility	17.14 ±0.12 gm.cm/sec

In-vitro diffusion study :

In vitro drug diffusion study was done with the help of franz diffusion cell apparatus.

Table No. 6 : In-vitro diffusion study

Time (hr.)	% Drug permeated of batch F5
1	11.73
2	24.47
3	31.69
4	47.21
5	59.18
6	67.24
7	73.16
8	82.91
9	88.64
10	90.48
11	92.37
12	94.04

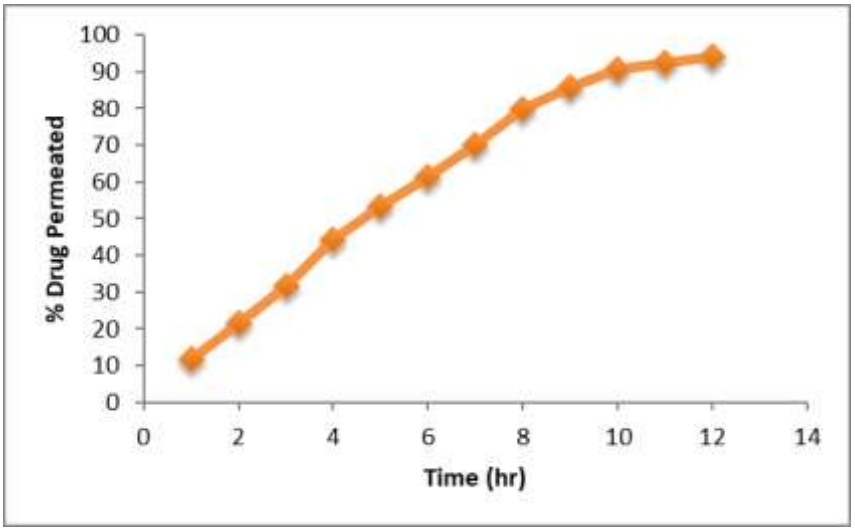

Figure No. 8: In-vitro diffusion study

SUMMARY & CONCLUSION

Nowadays topical gels are more popular because they are more stable and also provide controlled release of drug than other semisolid preparations.

- Naproxen is an NSAID drug that exhibits anti-inflammatory activity. It is potent, highly selective. It inhibits COX 1 & 2 synthesis to show anti-inflammatory effect. It was necessary to increase solubility of drug hence the topical drug delivery in the form of microsphere gel was prepared.
- The aim of the study was to optimize the process of formulation of Naproxen microsphere by altering the process parameters like polymer concentration i.e. Hydroxypropyl methyl cellulose and Ethyl Cellulose. Microsphere was formulated by solvent evaporation method and evaluate by various parameters like entrapment efficiency, particle size, percent yield and in vitro dissolution study.
- Naproxen microsphere gel was formulated by incorporating naproxen microsphere in gel base and on various parameters like spreadability, appearance, viscosity and drug diffusion study.
- It was concluded that it is possible to optimize the release of Naproxen for better therapeutic efficacy. Naproxen microspheres prepared using Hydroxypropyl methyl cellulose & Ethyl Cellulose polymer was found to be suitable to for the controlled release formulation and also Naproxen microsphere containing gel showed the controlled release action.
- It was concluded that drug release time depend on concentration of polymers in gel. Microspheres gel shows drug release of 94.04% in 12 hours.

REFERENCES

[1]. Venkateshan P, Manavalan R and Villiappan K. Microencapsulation :a vital technique in novel drug delivery system. Journal of pharmaceutical Sciences and research :2009;1(4):26-35.
[2]. Ganja c, Prakash B. Saha R.N.Microspheres technology its applications. (PDF).http://docstoc.com/docs/38166355/review-on microspheres, Nov 2010.
[3]. Riendeau D, Charleson S, Cromlish W et al. Comparison of the cyclooxygenase-1 inhibitory properties of nonsteroidal anti-inflammatory drugs (NSAIDs) and selective COX-2 inhibitors, using sensitive microsomal and platelet assays. *Can J Physiol Pharmacol*.1997;75:108895.http://www.ncbi.nlm.nih.gov/pubmed/9365818?dopt=AbstractPlus.
[4]. Vyas SP, Khar RK. Targeted and Controlled drug delivery; 7th Edition; Vallabh Prakashan, New Delhi India, 420-445.
[5]. Sree Giri Prasad B., Gupta V. R. M., Devanna N., Jayasurya K., Microspheres as drug delivery system, JGTPS. 2014; 5(3): 1961 -72.
[6]. Prasad BSG, Gupta VRM, Devanna N, Jayasurya K. Microspheres as Drug Delivery System. 2014 5(3): 1961-1972.
[7]. Patel JK, Patel RP, Amin AF, Patel MM,Formulation and Evaluation of Bioadhesive Microspheres Of Ketoprofen: 4(6).

[8]. Mukherjee S., Bandyopadhyay P. Magnetic microspheres: A latest approach in novel drug delivery system, JPSI. 2012; 1(5): 21-25.
[9]. Batra D., Kakar S., Singh R., Nautiyal U. Magnetic microsphere as a targeted drug delivery system. Jddr. 2012; 1(3): 1-17.
[10]. Najmuddin M, Ahmed A, Shelar S, Patel V, Khan T. 2010. Floating Microspheres Of Ketoprofen: Formulation and Evaluation, International Journal Of Pharmacy and Pharmaceutical sciences. 2(2):83-87.
[11]. Najmuddin M, Ahmed A, Shelar S, Patel V, Khan T. 2010. Floating Microspheres Of Ketoprofen: Formulation and Evaluation, International Journal Of Pharmacy and Pharmaceutical sciences. 2(2):83-87.
[12]. Deshmukh V, Warad S,Solunke R, Walunj S,Palve S. Jagdale G.Microspheres:As New Drug Delivery system. 2013;2(6):4504-4519
[13]. Sahil K, Akanksha M. Premjeet S. Bilandi A and Kapoor B.Microsphere: A Review.Int J ofResin Pharmacy and Chemistry.2011;1(4):2231-2781.
[14]. Ramteke K.H., Jadhav V.B., Dhole S.N., Microspheres: As carrieres used for novel drug delivery system, IOSRPHR. 2012; 2(4):44-48.
[15]. Patel B., Modi V., Patel K., Patel M., Preparation and evaluation of ethyl cellulose microspheres prepared by emulsification emulsification - solvent evaporation method, International Journal For Research In Management And Pharmacy. 2012; 1(1):83-91.
[16]. Patel N. R., Patel D. A., Bharadia P.D., Pandya V., Modi D. Microsphere as a novel drug delivery. Int J Pharm. Life Sci. 201; 2(8): 992-7.
[17]. Ming Li, Olivier Rouaud, Denis Poncelet, Microencapsulation by solvent evaporation: State of the art for process engineering approaches , International Journal of Pharmaceutics Volume 363, Issues 1–2, 3 November 2008, Pages 26-39

IJCRT.ORG ISSN : 2320-2882

INTERNATIONAL JOURNAL OF CREATIVE RESEARCH THOUGHTS (IJCRT)

An International Open Access, Peer-reviewed, Refereed Journal

"Unveiling The Healing Power: Dragon Fruit Herbal Cough Syrup Review"

Chanchal S.Nawale[1], Namrata R.Nevse[2], Prashant K.Newase[3], Nikita R.Raskar[4], Aniket K.Pathare[5], P.S.khatate.

Bachelor of Pharmacy,Department of Pharmacognosy,

PDEA'S SGRS college of pharmacy,saswad.412301.maharashtra,india.

Abstract: Dragon fruit, known for its vibrant appearance and potential health benefits, is increasingly recognized for its medicinal properties. This review article provides an in-depth analysis of the development of dragon fruit-based cough syrup, emphasizing its emergence as a natural and efficacious remedy for respiratory health. Dragon fruit (Hylocereus costariscensis) has been recognized for its abundant vitamin C content, potent antioxidants, and anti-inflammatory properties, all of which make it a promising candidate for cough syrup formulation. This study not only offers an innovative approach to herbal cough syrup development but also emphasizes the importance of utilizing natural ingredients for respiratory health. The dragon fruit herbal cough syrup with a honey base provides an alternative, plant-based option for individuals seeking relief from common respiratory complaints while aligning with the increasing demand for natural remedies[24]. Preliminary findings indicate that the dragon fruit herbal cough syrup exhibits notable litre antioxidant and anti-inflammatory properties, making it a promising candidate for alleviating cough symptoms. [30,31]

Keywords: Dragon fruit*(H.costariscensis),* Herbal Cough Syrup, Anti-oxidant, Anti-inflammatory

Introduction:

A herbal cough syrup is a liquid medication formulated with natural, plant-based ingredients such as herbs, honey, and other botanical extracts. It is used to provide relief from coughs, sore throats, and related symptoms. Herbal cough syrups are often considered an alternative to synthetic cough medicines and are believed to have soothing and expectorant properties.These syrups are often used as a more natural and holistic approach to managing respiratory symptoms. They are believed to offer relief from coughing, soothe irritated throats, and may have expectorant or antimicrobial properties.[15]

Herbal medicine is a holistic approach to healing that relies on the vast knowledge of traditional and indigenous practices from various cultures around the world. The use of plants, herbs, and natural substances in herbalism is deeply rooted in the wisdom passed down through generations. As our understanding of the properties and effects of these natural remedies continues to evolve, so does the integration of herbal medicine into modern healthcare. Many people today seek the benefits of herbal remedies, not only for their potential effectiveness in addressing health issues but also for their perceived gentleness on the body and the belief that they can complement conventional medical treatments. However, it's essential to remember that, just like pharmaceuticals, herbal treatments should be used with care and guidance from qualified practitioners to ensure safety and efficacy.[29]

Cough:

Coughing is a reflex action that helps clear the airways of mucus, irritants, or foreign particles. It can be a symptom of various conditions, such as respiratory infections, allergies, or even a common cold.[20] If you have a persistent or severe cough, it's advisable to consult a healthcare professional for a proper diagnosis and appropriate treatment. They can help determine the underlying cause and recommend the best approach to manage and relieve your cough.[18]

Causes of Cough:

Coughing can be caused by a variety of factors and underlying conditions, including:

- Respiratory Infections: The most common cause of cough is respiratory infections, such as the common cold, flu, bronchitis, or pneumonia.
- Allergies: Allergic reactions to pollen, dust, pet dander, or other allergens can lead to a persistent cough.
- Asthma: People with asthma may experience coughing as a symptom, often triggered by allergens or irritants.
- Gastroesophageal Reflux Disease (GERD): Acid reflux can lead to a chronic cough when stomach acid flows back into the esophagus and irritates the throat.[19]
- Environmental Irritants: Exposure to pollutants, smoke, or chemicals can cause coughing.
- Medications: Certain medications, especially those like ACE inhibitors, can cause a persistent cough as a side effect.
- Chronic Obstructive Pulmonary Disease (COPD): COPD, including chronic bronchitis and emphysema, can result in a chronic cough.
- Postnasal Drip: Excess mucus running down the back of the throat due to allergies or sinus issues can trigger coughing.
- Lung Conditions: Other lung conditions like interstitial lung disease or lung cancer can cause persistent coughing.
- Psychological Factors: Coughing can sometimes be related to psychological factors, such as stress or anxiety. [18,19]

Classification of cough :

[5]

Sr.no.	Types of cough	Properties
I.	Acute cough	Not more than three week's duration.
II.	Chronic cough	More than three week's.
III.	Dry cough	No mucous or secretion.
IV.	Wet cough	With mucous and secretion.
V.	Cough from chest and throat	Productive or non- productive.
VI.	Paroxysmal cough	Spasmodic and recurrent.
VII.	Bovine cough	Soundless cough due to paralysis or larynx

Mechanism of action:

The mechanism of action of a cough involves the detection of irritants in the airway, which stimulates sensory nerves. These nerves transmit signals to the brainstem's cough reflex center. In response, muscles in the respiratory system rapidly contract, creating a quick inhalation followed by the closure and subsequent reopening of the glottis to forcefully expel air, expelling irritants or mucus and clearing the airway. This reflex helps protect the respiratory system from harmful substances.[6,29]

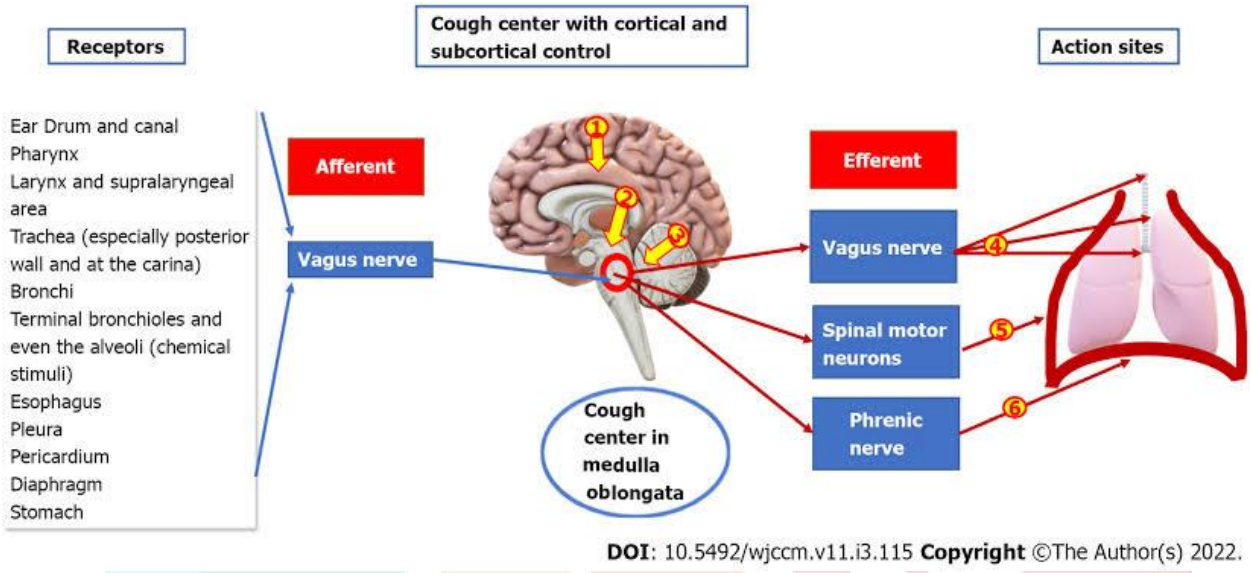

Figure .1. Mechanism of action of Cough

Dragon fruit:

Pink-fleshed dragon fruit, also known *as* *Hylocereus costaricensis* or the red dragon fruit, is a tropical fruit with distinctive characteristics.

Different species of dragon fruit

1. Hylocereus Undatus(white flesh pitaya)
2. Hylocereus Costaricensis(Pink flesh pitaya)
3. Hylocereus Megalanthus(Yellow skin ,white flesh pitaya)

Figure 2.Pink Dragon fruit (*H. Costariscensis*)

- **Origin and distribution**

The dragon fruit's(H.Costariscensis) scientific name is deduced from the Greek word hyle(woody), the Latin word cereus(waxen) and Latin word undatus, which refers to the crimpy edges of fruit's stems. The origin of the dragon fruit is yet unknown, but it's presumably native to Central America. It's also known as pitahaya in Mexico, and pitaya roja in Central America and northern South America. The Spanish name pitahaya may also relate to several other species of altitudinous cacti with flowering fruit

- **Variant names:**

Common names: dragon fruit, dragon pearl fruit,pitaya,strawberry pear, night-blooming cereus, Belle of the Night, and Cinderella plant.

Scientific name: *Hylocereus Costarscensis*

Malay/Indonesian: buah naga or buah mata naga

Mandarin: long guo

Vietnamese: thanh long

Pink dragon Fruit:

- **Biological Source** – Pink dragon is obtained from climbing plants of genus *Hylocereus* ,species *costariscensis,* belonging to family *Cactaceae.*
- **Chemical constituent:** Dragon fruit, also known as pitaya, contains several chemical constituents, including:

1. Vitamins: Dragon fruit is rich in vitamins such as vitamin C, which is an antioxidant that supports the immune system, and B vitamins like B1 (thiamine), B2 (riboflavin), and B3 (niacin), which are essential for various bodily functions.
2. Minerals: It contains minerals like iron, which is important for blood health, and calcium, which is vital for bone and teeth health.

3. Dietary Fiber: Dragon fruit is a good source of dietary fiber, which aids in digestion and can help manage blood sugar levels.
4. Phytonutrients: It contains various phytonutrients, including betalains, which are responsible for the fruit's vibrant colours and have antioxidant properties.
5. Antioxidants: Dragon fruit contains antioxidants that can help protect cells from damage caused by free radicals.
6. Carbohydrates: It is primarily composed of carbohydrates, particularly natural sugars like fructose.
7. Protein: While it's not a significant source of protein, it does contain a small amount.
8. Fats: Dragon fruit is low in fat, and the fat it contains is mostly healthy unsaturated fats.
9. Water: The fruit has a high water content, which helps keep you hydrated.
10. Phosphorus and Magnesium: These minerals are also found in smaller amounts in dragon fruit

Characteristics of dragon fruit:-

- Appearance: Pink-fleshed dragon fruit has bright pink to red flesh with tiny, black, edible seeds, contrasting with its vibrant green or red exterior. The skin is covered in small, leaf-like scales.
- Taste: The flavour of pink dragon fruit is often described as sweet and mildly tangy. It's likened to a combination of kiwi and pear.
- Nutritional Value: Pink dragon fruit is a nutritious fruit rich in vitamins, minerals, and antioxidants. It's a good source of vitamin C, fibres, and several essential minerals like iron and magnesium.[13]
- Health Benefits: The fruit's high vitamin C content supports the immune system, while its fibre can aid digestion. Antioxidants in dragon fruit may help protect cells from damage.
- Culinary Uses: Pink dragon fruit can be eaten fresh by cutting it in half and scooping out the flesh. It's also used in fruit salads, desserts, and as a garnish for various dishes.
- Growing Conditions: This variety of dragon fruit is typically grown in tropical and subtropical regions. It requires well-drained soil and prefers a warm climate with ample sunlight.
- Cultivation: Pink dragon fruit is usually grown on climbing cacti. The plant produces large, white, fragrant flowers, followed by the fruit. It's known for its ability to grow in arid conditions.
- Varieties: There are different cultivars of pink-fleshed dragon fruit, each with slight variations in flavour, skin colour, and size.[12]
- **Materials and method used:**

Materials –

1. **Dragon fruit**
2. **Honey**
3. **Fennel**
4. **Tulsi**
5. **Adulsa**

Scientific Classification of materials:-

I) Dragon fruit:

1. **Kingdom –** Plantae
2. **Clade –** Tracheophytes
3. **Order –** Caryophyllales
4. **Family-** *Cactaceae*
5. **Genus –** *Selenicereus*
6. **Species – *H. Costariscensis***

II) Tulsi:

1. **Kingdom** – Plantae
2. **Clade –** Tracheophytes
3. **Order –**Lamiales
4. **Family-** *Lamiaceae*
5. **Genus –***Ocimum*
6. **Species – *O.Sanctum Linn.***[9]

III) Fennel:

1. **Kingdom –** Plantae
2. **Clade** – Tracheophytes
3. **Order –**Apiales
4. **Family-** *Apiaceae*
5. **Genus –** *Foeniculum*
6. **Species – *F.Vulgare.***[7]

IV) Adulsa :

1. **Kingdom –** Plantae
2. **Clade –** Tracheophytes
3. **Order -** Lamiales
4. **Family-** Acanthaceae
5. **Genus –**justicia
6. **Species – *J.Adhatoda***[8]

Tulsi

Fennel

Adulsa

Dragon fruit

Honey

Figure 3. Material of herbal formulation.

Extraction methods of dragon fruit peel :

Extracting dragon fruit peel can be done by following these steps:

1. Wash the Fruit: Start by washing the dragon fruit to remove any dirt or pollutants from the skin.
2. Cut the Fruit :Use a sharp cutter to cut the dragon fruit in half. You can cut it vertically or horizontally.
3. Peel the Skin: Gently peel the skin down from the meat. The skin should come off fairly fluently.
4. Use a ladle You can also lade out the meat with a ladle if the peel isn't coming off fluently.
5. Rinse and Store: wash the peel to remove any remaining fruit bits and stroke it dry. You can also use the peel in colorful ways, similar as in smoothies, teas, or as a nature[13]

Formulation of Dragon fruit cough syrup (100 ml) :

Sr.no.	Ingredients	Uses
1)	Dragon fruit extract *(H.Costariscensis)*	Antioxidant, Anti-inflammatory, Anti-microbial
2)	Honey	Expectorant
3)	Adulsa extract *(Justica Adhatoda)*	Anti-tussive Anti-inflammatory[16]
4)	Tulsi extract *(Ocimum Sanctum)*	Anti-tussive Antioxidant Anti-inflammatory[16]
5)	Fennel extarct *(Foeniculum Vulgare)*	Aromatic flaour[16]
6)	Methyl paraben ,Propyl paraben	Preservatives
7)	Sucrose	Base Sweetening agent

Fennel:

Figure 3. Foeniculum Vulgare

- **Synonyms**:- Large Fennel, Sweet Fennel, Fennel fruit, Saunf (Hindi); *Fructus Foeniculi.*

- **Biological source: -**

Fennel is the dried ripe fruits of plant known as *Foeniculum vulgare Mill*,Family:*Umbelliferae,* obtained by cultivation. It should contain not less than 0.6% of anethol calculated on dried basis.

- **Cultivation and Collection:**

Fennel is cultivated by dibbling method. Quality fruits of good germination rate are sown just before the spring. Free branching of herb and specific arrangements of leaves on the stems required plenty of space in between two plants and rows. 4-5 seeds are put at a time, in holes at a distance of 25cm in between them. Well drained and calcareous soil sunny situation is found to be favourable for cultivation of fennel. In India nearly 90% of the fennel production comes from Gujarat only.

- **Geographical source:-**

Fennel is indigenous to Mediterranean region of Asia and Europe. It is widely cultivated in Russia, India, Japan, southern Europe, China and Egypt.

- **Chemical constituents:-**

Fennel contains volatile oil (2-6.5%) and fixed oil (12%). The main constituent of the volatile oil Are phenolic ether, anethole (50-60%) and ketone, fenchone (18-20 %) which give the fruits its Distinct odour and taste; the other constituents of volatile oil are anisic aldehyde, anisic acid, dipentene and phellandrene,Etc.[28]

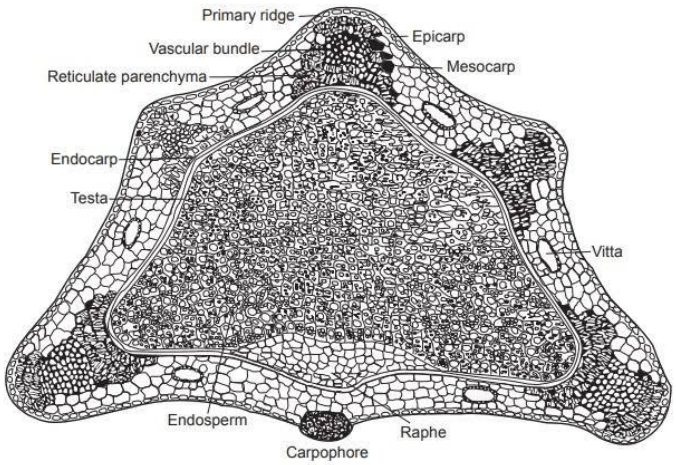

Figure 4: T.S. of fennel.

- **Uses**:-

Fennel is used as stimulant, aromatic, stomachic, carminative, and expectorant. Anethole is used in oral and dental preparations. Fennel is used in diseases of the chest, spleen and kidney. Pharmaceutically it is used as flavouring agent.

Tulsi :

Figure 5. *Ocimum sanctum Linn.*

- **Synonyms:-**

Sacred basil, Holy basil,
Merr.Lumnitzera tenuiflora (L.) Spreng.
Moschosma tenuiflorum (L.) Heynh[9]
Ocimum anisodorum F.Muell.
Ocimum caryophyllinum F.Muell.

- **Biological Source:-**

Tulsi consists of fresh and dried leaves of *Ocimum sanctum Linn*. (Syn. *Ocimum tenuiflorum*) Family -*Lamiaceae*. and It contains not less than(0.40 %) Eugenol on dried basis. [1,9]

- **Geographical Source: -**

It is herbaceous, multi branched annual plant found throughout India. It is considered as sacred by Hindus. The plant is commonly cultivated in garden and also grown near temples. It is Propagated by seeds, Currently Tulsi is cultivated commercially for its volatile oil.[1,9]

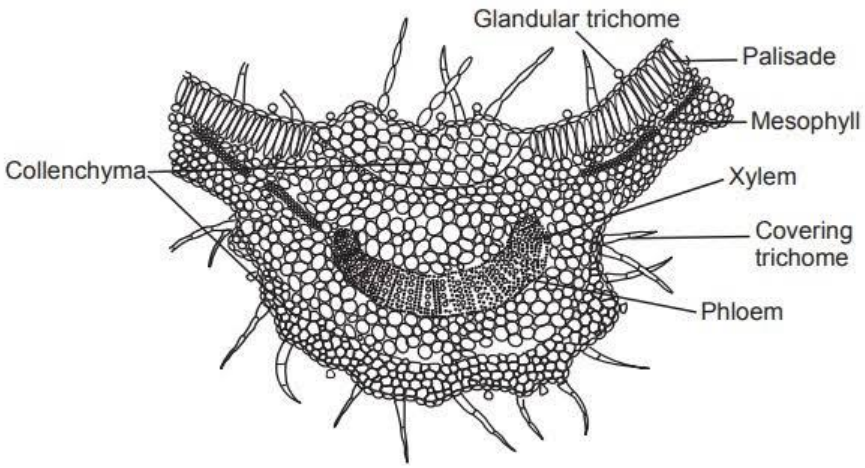

Figure 6: T.S. Tulsi leaf.

- **Chemical constituents:-**

It contains approximately 70 per cent eugenol, carvacrol (3%) and eugenol-methyl-ether (20%). It Also contains caryophyllin. Seeds contain fixed oil with good drying properties. Also contains alkaloids,glycosides,saponin, tannins,and Vitamin C. [1]

- **Standards of quality:-**

Foreign organic matters : Not more than 2.0%
Ash value: Not more than 15.0%
Acid insoluble ash: Not more than 5.0%
Loss on drying: Not more than 12.0%
Aci soluble extract: Not less than 3.0%
Water soluble extract: Not less than 10.0%

- **Uses**:-

The oil is antibacterial and insecticidal. The leaves are used as stimulant, aromatic, anti-catarrhal, Spasmolytic, and diaphoretic. The juice is used as an antiperiodic .Tulsi has expectorant and anti-Inflammatory properties.[1,9]

Adulsa:

Figure 7. J. *Adhatoda* .

- **Synonyms**: -Malabar nut, *Adhatoda* , *Justica adhatoda,* vasaka.[1]

- **Biological sources**: -

The biological source of Adhatoda is dried and fresh leaves of this plant. It belongs to family *Acanthaceae.* and contains not less than 0.6 % of vasicine on dried basis[1].

- **Chemical constituents**:-

The chemical constituent of Adhatoda are alkalis tannins flavonoids Serpent sugar and glucoside.
The leaves of Vasaka contain Vitamin C in large amount. The roots of this plant contain Vasicinolone, basil and peganine.[24] It contains quinazoline derivatives such as vasicine 2.0 to 2.5 %,vasicinone and 6-Hydroxy vasicine. Biochemically vasicine is oxidised to its ketonic derivatives vasicinone and the latter exerts main activity as bronchodilator.The drug also contains volatile oil betain and vasakin. It is also reported as vasaka contains Adhatodic acid.[1]

- **Standards of Quality:-**

Foreign oraganic matter: not less than 2.0%
Total ash value: Not more than 21.0%
Acid insoluble ash: Not more than 2.0%
Loss on drying: Not more than 12.0%
Water soluble extract: Not less than 22.0%
Alcohol soluble extract: Not less than 3.0%

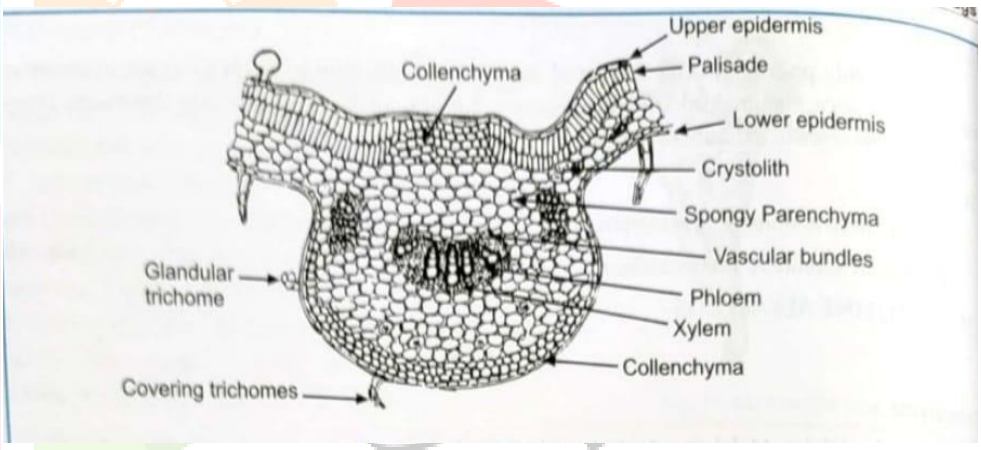

Figure 8: T.S of adhatoda leaf

- **Uses**:-

Used as expectorant. It is used to treat leprosy blood disorder thirst and vomiting. It is used to treat Infertility it also have anti-ulcer activity.[1,24]
The pharmacological investigation have shown that vasicine also shows oxytocic property similar to oxytocin and methyl ergometrin.

Honey:

Figure 9:. Honey.

- **Synonyms:-** Madhu, Mel [1] ,Nectar Sweet nectar,Ambrosia (in a poetic context)[10]

- **Biological sources:-**

Honey is produced by honeybees primarily from the nectar of flowering plants. Honey is a sugar secretion deposited in Honey comb by the bees , *Apis mellifera* ,*Apis dorsata* , and other species of *Apis* ,belonging to Family – *Apidae*.[1]

- **Chemical constituents**:-

Honey has a content of 80–85% carbohydrates, 15–17% water, 0.3% proteins, 0.2% ashes and minor quantities of amino-acids, phenols, pigments[10] and vitamins, Glucose 35% ,Fructose 45%,sucrose 2%.[1]

- **Uses**:

Raw honey is rich in antioxidants,Using honey to replace table sugar helps improve diabetes.
The antioxidants in honey help lower blood pressure.[11]
Honey helps improve cholesterol,Honey helps reduce triglyceride levels.[11,27]

Evaluation test for Herbal cough syrup:-

1) **Colour Examination**.
2) **Odour examination.**
3) **Taste Examination .**
4) **pH Determination.**
5) **Viscocity Determination.**[3]
   The viscocity of each formulation was determined by using Ostwald's Viscometer.
6) **Determination of Density.**
   1. The symbol "p" is used to denote density.
   2. Formula of density:[15]

Density of liquid under test (syrup) = weight of syrup under test(W_3) /
volume of final syrup under test(V).

7) **Determination of anti-microbial activity.**
8) **Stability testing.**[2]
9) **Determination of ethanol extractive value.**[26]

Conclusion:

Herbal cough syrup is an Ayurveda medicine which is useful in many chronic health problem such as cough, cold, fever, respiratory infection and disorders among human. As a combination of herbs, it is safe. Herbal syrup including natural herbs, like tulsi, Honey, fennel ,Dragon fruit, and adulsa which have various action and effect on reducing acute or chronic cough and cold and act as cough suppressant having expectorant and anti-tussive property.

(H.clostarscensis) known as Pink Dragon fruit is the fruit in family *Cataceae.* Reach in Vitamin C, Anti-microbial ,Anti-inflammatory and Tulsi , Adulsa reach in Anti –tussive properties used in herbal cough syrup. In this review, I conclude about herbal cough syrup that, herbal cough syrups is a safest herbal medicine which is use for treatment of cough and cold.

Aknowledgement:

The authors are thankful to Principal Dr. R. S. Chavan and college PDEA's Seth Govind Raghunath Sable College of Pharmacy, Saswad necessary facilities.

REFERENCE:

[1]C.k.kokate,A.R.Purohit,S.B.Gokhale, PHARMACOGNOSY BOOK, 55 Edition.2014

[2] Choudhary N and Sekhon BS. An overview of advances in the standardization of herbal drugs. J Pharm Educ Res. 2011;2(2):55-70.

[3] Anu Kaushik Vivek, Chauhan and Dr. Sudha, Formulation and Evaluation Of Herbal Cough Syrup. European Journal of Pharmaceutical & Medical Research, 2016; 3(5): 517-522.

[4] Farhat pirjade mujawar, manojkumar patil, jyotiram sawale. "Formulation And Evaluation of Herbal Cough Syrup of echinops echinatus roxb Roots", International Journal of Pharmacy & Technology.

[5] Ankush Patil , Kaivalya Mirajakar, Pranav Savekar, Chetana Bugadikattikar, Somesh Shintre "Formulation and Evaluation of Ginger Macerated Honey Base Herbal Cough Syrup", International Journal of Innovative Science and Research Technology ISSN No:-June 2020.(5), 2456-2165

[6] Meenakshi parihar, Ankit Chouhan, M. S. Harsoliya, J. K. Pathan, S. Banerjee, N. Khan, V. M. Patel, " A Review- Cough & Treatments", International Journal of Natural Products Research, May 2011, 1(1): 9-18.

[7] "Classification for Kingdom Plantae Down to Genus Foeniculum Mill.". US Department of Agriculture, Natural Resources Conservation Service. 2015. Archived from the original on 4 April 2021. Retrieved 24 March 2015.

[8] Common name for Malabar Nut, *(J.Adhatoda)* Encyclopedia of Life. Retrieved 3 January 2013.

[9] *"Ocimun tenuiflorum"* Integrated Taxonomic Information System. 26 June 2023. Retrieved 26 June 2023.

[10] White JW. Composition of honey. In: Crane E, editor. *Honey: A Comprehensive Survey.* London: Heinemann; 1979. pp. 157–192

[11] Alvarez-Suarez JM, Tulipani S, Romandini S, Bertoli E, Battino M. Contribution of honey in nutrition and human health: a review. *Mediterr J Nutr Metab.* 2010;3:15–23

[12] Choo W S and Young W K 2011 Antioxidant properties of two species of Hylocereus fruits *Advances in Applied Science Research* **2** 418-425.

[13] *Hammel, B. (2013).* "Hylocereus costariscensis. IUCN Red ListOf Threatended Specie.2013

[14] Dr.JaveshK.Patil ,DipaliR.Mali, KomalR.More ,Shraddha M.Jain."Formulation and evaluationof herbal syrup".World journal of pharmaceutical research volume 8,1061-1067.

[15] Miss. Telange-Patil P.V, Miss. Gorad S.U., Miss. Mane P.K.,Miss. Thavare S.B. "Formulation and evaluation of herbal cough syrup of clove by using jaggery base" issn: 2320-2882.

[16] Miss.Priya D.Khode, Rupali R. Singanjude, Urwashi D. Lanjewar. Formulation and evaluation of herbal cough syrup issn- 2394-5125.

[17] Vikash Sharma, Saurabh Singh, Arushi Dixit and Alka Saxena. formulation and evaluation of herbal cough syrup from seeds extract of hedge mustardissn: 2231-2781.

[18] Chung KF, Mazzone SB. Cough. In: Broaddus VC, King TE, Ernst JD, et al, eds. Murray and Nadel's Textbook of Respiratory Medicine. 7th ed. Philadelphia, PA: Elsevier; 2022:chap 37.

[19] Kraft M. Approach to the patient with respiratory disease. In: Goldman L, Schafer AI, eds. Goldman-Cecil Medicine. 26th ed. Philadelphia, PA: Elsevier; 2020:chap 77.

[20] Bouros D, Siafakas N, Green M. second edition. New York: Marcel Dekker Inc; 1995. Cough. Physiological and Pathophysiological Considerations. In: C. Roussos (Ed). The Thorax, NY Marcel Dekker 1995. Part B: Applied Physiology; pp. 1346–54.

[21] Extraction of Fennel Oil Using Different Methods and Effect of Solvent and Time to Maximize Yield www.ijppr.humanjournals.com

[22] Tongnuanchan, P.; Benjakul, S. Essential Oils: Extraction, Bioactivities,and Their Uses for Food Preservation. J. Food Sci., 2014,79, 1231–1249).

[23] Bruneton, J. Pharmacognosy, phytochemistry, medicinal plants. Lavoisier publishing, 1995.

[24] Whole extract optimization of Adhatoda vasica, Nees leaf by using Response Surface Methodology (RSM) Md Zakir Ansari*, Ghulamuddin Sofi, Hamiduddin, Haqeeq Ahmad, Imran Khan, Rabia Ba. ISSN 2320-480X JPHYTO 2020; 9(1): 24-29

[25] B.Susilo, S.M Sutan, Y.Hendrawan and R, Damayanti .Improving quality of Dragon fruit *"Hylocereus costaricensis"* syrup processing with double jacket vaccum evaporator. Doi.10.1088/1755-1315/924/1/0120121.

[26] Ojas patel, Mona patel. Development and Evaluation of Poly- Herbal cough syrup from natural ingredients having expectorant and anti- pyretic activity. ISSN: 2229-3566.

[27] Naveed Ahemed ,Alastair G.Sutcliffe, Claire Tipper. Feasibility Study: Honey for Treatment of cough in children.(Pedriartic Reports 2013;5:e8).

[28] Shamkant B. Badgujar, Vainav V. Patel, Atmaram H. Bandivdekar .Foeniculum vulgareMill: A review of its Botany ,Phytochemistry, Pharmacology ,Contemporary Application ,and Toxicology .doi:10.1155/2014/842674.

[29] Kubra F.Naqui, Stuart B.Mazzone, and Michael U. Shiloh. Infectious and Inflammatory pathways to cough. Vol. 85:71-91 . https://doi.org/10.1146/annurev-physical-031422-092315.

[30] Dawesh Tewari and Manoj Kumar. Formulation and comparative evaluation of different Sitopaladi herbal syrups.Der Pharmacia Lettre,2014,6(2):178-183.

[31] Dr. KN Sunil Kumar.Herbal Pharmacopoeias-an overviews of international and Indian representation. Journal of Ayurvedic and Herbal Medicine .2015;1(3):59-60.

International Journal of Scientific Research in Engineering and Management (IJSREM)
Volume: 08 Issue: 05 | May - 2024 SJIF Rating: 8.448 ISSN: 2582-3930

Preparation and Formulation of Herbal Hard Lozenges

Ms. S. S. PHADTARE[1], Mr. D N. SHEVATE[2], Mr. A. V. SALUNKE[3], Ms. S. G. SHINDE[4]

[1]Assistant Prof. Department of Pharmaceutical Chemistry PDEA's SGRS College of Pharmacy Saswad (Purandar) 412301

[2,3,4]Students of PDEA's SGRS College of Pharmacy Saswad (Purandar) 412301

Abstract

The herbal based lozenges were formulated properly to provide proper relief from the cough symptoms by using natural herbal ingredients with potential and therapeutic properties. Our research involved with the proper and appropriate preparation of the lozenges we followed by evaluation, identification and analysis of their physical characteristics, organoleptic properties and antimicrobial testing.

● Keyword: Lozenges, Troches, Guduchi, Liquorice

Introduction

Oral dosage forms are different and have advantages over other dosage forms. They are economical and safe for the patient. They are the most natural and easiest way to administer the medicine. Their toxicity is delayed due to the effect, which allows easier recovery than with other formulations. They are suitable for all patients their toxicity is slowed due to an effect that allows easier recovery than with other forms of medication. They are suitable for all patients regardless of age. Oral dosage forms also have disadvantages. If the patient suffers from chronic vomiting, it is not the first choice of medicine. They are not a good choice for uncooperative patients such as children and infants. They are not suitable for emergency or unconscious patients. They are not suitable for patients with gastrointestinal disorders such as diarrhoea, constipation, ulcers and hyperacidity of the stomach. Oral formulations are not suitable for drugs that are susceptible to GIT inactivation or destruction.[1]

"Dissolvable tablets are a solid dosage form containing flavors and sweeteners designed to slowly dissolve or disintegrate in the mouth or oral cavity. Most often, they are used for a local effect in the oral cavity, and they can also have a systemic effect if they are well absorbed by the oral mucosa and pharynx." [2] Troms are solid preparations containing one or more substances in a usually salty, sweet base designed to slowly dissolve or disintegrate in the mouth.[3] They can be made by moulding or compressing sugar-based tablets. The development of troches dates back to the 20th century and is still in commercial production. Most lozenges are available over the counter. Lozenges provide a palatable way of administering dosage forms and enjoy their position in the pharmaceutical market due to certain advantages.[4],[5] Many experts say that if there is any benefit from taking zinc or a zinc tablet, it is very minimal. [6], [7]

Advantages of natural ingredients: Herbal lozenges are made with natural ingredients, which mean they do not contain synthetic chemicals or artificial additives. Potentially effective: Some herbs used in herbal lozenges have been shown to have medicinal properties that can help soothe sore throats, reduce coughing, and promote overall

wellness. Fewer facet outcomes: Because they may be made with herbal ingredients, natural lozenges may also have fewer facet outcomes in comparison to conventional medicines. Easy to use: Herbal lozenges are clean to use, as they may be taken orally and do now no longer require any unique system or preparation. Available over-the-counter: Many herbal lozenges are available over-the-counter, which makes them easily accessible.

Some of the common purposes of herbal lozenges can be:

1. Relief of symptoms of cough and sore throat.

2. Promote respiratory health.

3. Strengthen the immune system.

4. Supporting digestion and intestinal health.

5. Relaxation and tension.

6. Alleviation of allergy symptoms.

7. Maintaining oral health and hygiene.

Materials and method

INGREDIENTS:

Liquorice: It can be made by extracting the liquorice's root. In regions of Asia, including Southern Europe and India, liquorice naturally grows as *herbaceous perennial legume*. It is commonly utilized in the Indian market and is also known as Jestamadu and Muretti. Ayurvedic medical system for treating a range of respiratory conditions. It is employed as a mucous agent and expectorant. This Glycyrrhizin acid is responsible for certain characteristics.[25]

Guduchi: A member of the Heart-leaved Moonseaceae family, Guduchi is made from mature, dry stems of *Tinospora cordifolia*. Giroy is the name of a very common herb in Ayurveda that is frequently used to treat fever, respiratory issues, diabetes, anaemia, heart damage, etc more.[26]

Turmeric: These are the dried rhizomes of the ginger family member turmeric. Due to its bright yellow hue, turmeric is one of the spices that is most frequently used in Indian cooking. It is used to treat bronchitis and coughs because of its antiseptic characteristics. and other issues with the upper respiratory system. It contains curcuminoids, the primary component of many curcumin-based products.

Ginger: Ginger is *Zingiber officinale*. It is well-known for its antioxidant, analgesic, and anti-inflammatory effects, which make it a popular component in herbal medicines for a variety of illnesses, including respiratory conditions like colds and coughs. It's critical to remember that ginger have effects that thin the blood, therefore anyone taking blood-thinning medications should use them with caution. Bleed problems or taking blood-thinning drugs[28]

Jaggery: Made from *the juice or sap of Palmyra*, date, or coconut palms (Phoenix dactylifera, Borassus flabellifer, or Cocos nucifera L., Jaggery is a sweet substance that is high in sugar. goods and medications. It functions as a preservative as well as a sweetener.[29] Through the use of molds and melting, soft lozenges were created. Jaggery was combined with the powder and other components (which had been melted over a water bath) to create a homogeneous mixture. Subsequently, The stainless steel mould was filled with the mixture.[30]

Honey: *Bees Apissmallifera, Apisdorsata*, and other species deposit a sweet solution derived from flower nectar onto themselves. Apis (bee). The viscosity of honey has made it renowned as a natural treatment for dry and phlegmy coughs. It has ' an ability to calm the throat, thereby easing any discomfort or irritation. [31]

Tulsi: Also known as *holy basil*, Tulsi has long been employed in Ayurvedic medicine for its range of therapeutic advantages.[32]It is a common component in herbal cough medicines due to its anti-inflammatory, anti-bacterial, and anti-viral effects. colds as well as other respiratory conditions.

Cumin: A blooming plant of the *Apiaceae* family that is indigenous to the Irano-Turanian Region is called *cuminumcyminum*.[33] Its seeds, which are each encased within a dried fruit, are utilized in many different civilizations' cuisines both whole and crushed. Although cumin is a common ingredient in traditional medicine, there isn't any solid proof to support its efficacy or safety.[34]

Extraction of raw materials –

Tulsi -The extraction was conducted in a Clevenger apparatus, coupled to a bottom flask of 500 ml. It was added 30 g of crushed leaves of Tulsi or basil and 300 ml of water into the flask. The extracted time was fixed at four hours. The extracted oil was diluted in hexane & filtered after separation.

Guduchi - Stems of *Tinospora cordifolia* were dried under shade for 7–10 days and pulverized using an electric grinder. Firstly, dried sample was extracted with solvent of methanol and acetone in the ratio of 70 : 30 (4000 mL × 4 cycles) at 40°C for 16 hours in soxhlet apparatus

Liquorice - In this study, a simple and convenient method for the extraction of glycyrrhizic acid and glabridin from liquorice is developed and validated. Mixture of ethanol/water (30:70, v/v) and extraction time 60 min under 50°C is the optimum condition to extract GA and glabridin from liquorice.

Turmeric - In order to extract turmeric oil, researchers have used steam distillation, hydro-distillation, and extraction using hexane. Hexane was combined with the oils after curcumin extraction and heated to 60 °C three times for one hour. The solvent was removed, which resulted in successful turmeric oil extraction.

Ginger – The dried steamed ginger is baked for 3 hours to 5 hours at a temperature of 20ºC. to 150ºC. in an ocher kiln installed to radiate far infrared rays, and the ginger obtained in the above process is pulverized using a grinder to remove 80 to 150 mesh nets.

Formulation Table -

Sr. No	Ingredients	Quantity
1	Jaggery	50gm
2	Liquorice	500mg
3	Turmeric	200mg
4	Guduchi	500mg
5	Honey	q.s.

6	Cumine	250mg
7	Tulsi	500mg

Evaluation parameters for herbal lozenges

1. Physicochemical properties: Physicochemical properties such as physical stability, colour, odour, taste etc.[35]

Sr. No	Parameter	Observation
1	Colour	Golden brown
2	Odour	Pleasant
3	Taste	Sweet
4	Texture	Smooth
5	Shape	Coffee bean shape

2. Weight variation test: 10 lozenges were taken and individual weights were noted, then average weight of lozenges was calculated by total weight divided by ten.[36]

Weight of lozenges = 1.78+1.74+1.80+1.56+1.76+1.74+1.84+1.63+1.59+1.639(gm)

10

=1.707gm

3.Moisture content: By Gravimetric method, one gram sample is weighed and placed in a desiccator at for 24 h. Find the initial weight of the sample before drying. Set parameter and dry sample. Weigh sample after drying and compare to the initial weight to calculate the Loss on Drying.[37]

Moisture content = Initial weight - Weight after the test

Sr. No	Moisture Content
1	1.92
2	1.88
3	1.88
4	1.83
5	1.74

4. Thickness test- The thickness of the lozenges was determined by using vernier caliper. Five lozenges were used. The average values were calculated.[38] Formula

Sr. No	**Average thickness**
1	0.90mm
2	0.93mm
3	0.98mm
4	0.95mm
5	0.96mm

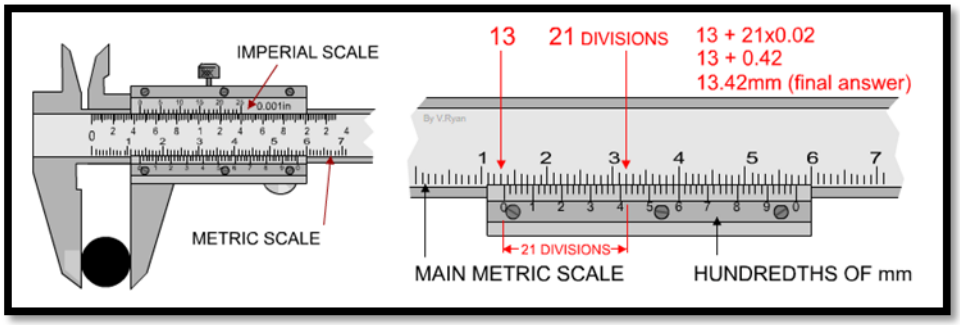

5. Measurement of pH- The acidity or alkalinity of lozenges was indicated by using lab pH meter, a scale from 1.0 to 14.0. 1% W/Solution was prepared by dissolving 1 g candy in 100 ml distilled water and its pH was recorded.[39]

Acidic in nature ph is given 3.2- 4.1

6. Friability- The friability of tablets was determined using Roche Friabilator. It is expressed in percentage (%). Ten tablets were initially weighed and transferred into friabilator. The friabilator was operated at 25 rpm for 4 minutes. The tablets were weighed again after taking out tables and brushing the dust away. If tablets are found broken or cracked and the final value exceed the limit test is consider failed. The value should be no more than 1% (0.5- 1.0%). If exceed repeat three time for overall estimation. The % friability was then calculated with help of following formula. Friability= (Initial Weight -Final Weight) X 100/Initial Weight.[40]

Friability= (17.32gm-17.20gm)×100/17.32gm

Friability= 0.6%

7. Determination of antimicrobial activity-

The agar plate method was used to examine the antimicrobial activity of the lozenges. The test compound (50µL) was introduced in the well. The plate was incubated over night at room temperature. The antimicrobial spectrum of the extract was determine for the bacterial species in terms of zone sizes around the well.[41]

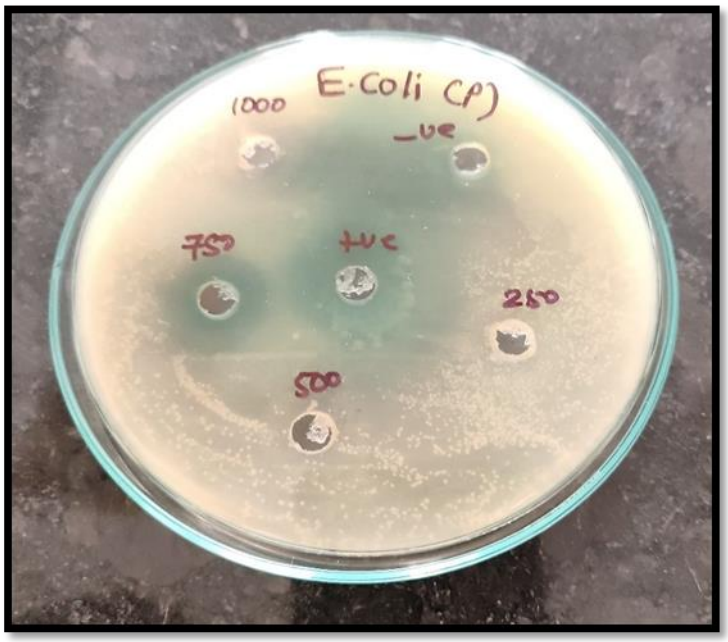

Fig: MIC against E.Coli

The result obtained in this study suggest that herbal formulation prepare and possess anti-microbial activity, the component of herbal lozenges was selected due to their reported action that plays preventive and curative role in prevention of cough.

Result

The lozenges were prepared with the combination of all powders using jaggery as a base. Physicochemical evaluation was done. Weight variation test were completed and calculate the average weight of lozenges are given **1.707gm**. The quality control parameter such as Moisture content of lozenges was determine and calculate the loss on drying of 5 lozenges that is **0.04%,0.12%,0.13%,0.08%,0.07%.** Thickness test of lozenges are done by using vernier caliper and calculated value is **0.90mm,0.93m, 0.98mm,0.95mm,0.96mm**. PH of lozenges are given is **5-6**. Friability of lozenges is determine it given **0.6%.** Antimicrobial evaluation was done.

Conclusion

Purpose behind lozenges was to achieve throat relief. To intention behind formulating herbal lozenges was to prevent the adverse reaction caused by synthetic lozenges.The studied formulation proved to be satisfactory from the perceptive as well. After consuming this lozenges there was no irritation in throat and throat relief was observed.

References

1. Peters, D. (2005): Medical lozenges. In: Lieberman HA, Lachman L, Schwartz JB, editors. Pharmaceutical dosage forms: tablets. 2nd edition New York: Marcel Dekker, Inc.; s. 419-577.
2. Mendes, RW, Bhargava H. (2006): Lozenge. In: Swarbick J, editor. Encyclopaedia of Pharmaceutical Technology. 3rd ed Pohjois California, USA: Informa Healthcare Inc.; s. 2231-2235.
3. Firriolo, JF. (1994): Oral cavity review. Oral Surg Med Oral Pathol. 78(2): 189–93.
4. Batheja, P, Thakur, R, Michniak, B. (2006): Basic Biopharmaceutics of Buccal Cavity Sublingual Absorption, Enhancing Drug Delivery. London, New York: edited by Touitou E, Barry BW. CRC Press, Taylor & Francis Group. 1: 189.
5. Sastry, SV, Nyshdham JR. (2000): Review of the oral formulation. Pharm Sci and Technol today. (3): 138–145.
6. Stephen o. Majekodunmi: a lozenge review American Journal of Medicine and Medicine p-issn: 2165-901x e-issn: 2165-9036 2015; 5 (2): 99–104.
7. Allen, LV. (200): Troches and lozenges. According to Artem Up-to-date and practical aggregate information for pharmaceutical employees. 4 (2).
8. .Tanaya A. Peshave1, Smita J. Kad2, Rahul R. Rathod3, Shubham D. Raskar4, Amruta B. Pandit51B Pharm, 12. December 2022
9. .Parul Vyas1 *, Harshita Jain2 , Shipra Singh3 , Nitin Nama4Career Point International Journal of Research (CPIJR) ©2022 CPIJR | Osa 1 | Numero 2 | ISSN:

10. Peters, D. Medicated lozenges. In Pharmaceutical Dosage Forms: Tablets, 2nd Ed.; Lieberman, H.A., Lachman, L.,Schwartz, J.B., Eds.; Marcel Dekker, Inc.: New York, 1989; I, 419–463.
11. Technical bulletin. In Machines, Production Lines and Process Technologies for the Confectionery Industry; Robert Bosch Corp.: Bridgman, MI; 1998.
12. Beahm, J.S. Dextromethorphan Continuous Lozenge Manufacturing Process. US Patent 5,302,394, April 12, 1994.
13. Duchow, R.W. Lozenge Cutter Apparatus. US Patent 5,676,982. Oct 14, 1997.
14. Spatafora, M.; Gamberini, A. Distributing Device for Feeding Flat Products to a User Machine. US Patent5,199,546, April 6, 1993.
15. Bandelin, F.J. Compressed tablets by wet granulation. In Pharmaceutical Dosage Forms: Tablets; Lieberman, H.A.,Lachman, L., Schwartz, J.B.,, Eds.; Marcel Dekker, Inc.: New York, 1989; I, 160–164.
16. Özakar RS, Medya KA, Maman A. Preparation, characterization, and radiation absorption study of bentonite clay included soft chewable lozenge formulations. Journal of Pharmaceutical Technology.;1(3):54-9.
17. https://www.femina.in/wellness/home-remedies/3-natural-cures-to-rid-you-of-your-dry-cough-25103.html
18. https://organicindiausa.com/blog/ayurvedic-herbs-the-immortal-guduchi/
19. https://www.healthline.com/nutrition/top-10-evidence-based-health-benefits-of-turmeric
20. Kathiresan K, Vijin P, Moorthi C, Manavalan R. (2010) Formulation and evaluation of loratadine chewable tablets. Res J Pharm Biological Chem Sci. 2010; 1(4): 763-774
21. Abdelbary G, Eouani C, Prinderre P, Joachim J, Reynier JP, et al. (2004) Determination of the in vitro disintegration profile of rapidly disintegrating tablets and correlation with oral disinte-gration. Int J Pharm. 2004; 292(1-2): 29-41.
22. https://gpatindia.com/black-pepper-biological-source-morphology-chemical-constituents-uses/[23] https://www.healthifyme.com/blog/jaggery-benefits-nutrition-sugar/
23. Özakar RS, Medya KA, Maman A. Preparation, characterization, and radiation absorption study of bentonite clay included soft chewable lozenge formulations. Journal of Pharmaceutical Technology.;1(3):54-9.

24. https://www.femina.in/wellness/home-remedies/3-natural-cures-to-rid-you-of-your-dry-cou gh-25103.html
25. .https://organicindiausa.com/blog/ayurvedic-herbs-the-immortal-guduchi/
26. .https://www.healthline.com/nutrition/top-10-evidence-based-health-benefits-of-turmeric
27. Bhowmik D, Pankaj C, Tripathi KK, Chandira MR, Kumar KPS. Zingiberoffcinale the herbal and traditional medicine and it's therapeutically importance. Res J Pharmacognosy Phytochemical. 2010; 2(2):102-10.
28. .https://www.healthifyme.com/blog/jaggery-benefits-nutrition-sugar/
29. http://www.chem.ualberta.ca/~orglabtutorials/Techniques%20Extra%20Info/TLC.html
30. Abdelbary G, Eouani C, Prinderre P, Joachim J, Reynier JP, et al. (2004) Determination of the in vitro disintegration profile of rapidly disintegrating tablets and correlation with oral disinte-gration. Int J Pharm. 2004; 292(1-2): 29-41. 32.Sastry SV, Nyshadham JR, Fix J
31. Sastry SV, Nyshadham JR, Fix JA. Recent technological advances in oral drug deliverya review. Pharm Sci Tech Today, 2000; 3: 138 45.
32. a b Kislev, Mordechai E.; Hartmann, Anat; Galili, Ehud (1 September 2004). "Archaeobotanical and archaeoentomological evidence from a well at Atlit- Yam indicates colder, more humid climate on the Israeli coast during the PPNC period". Journal of Archaeological Science. 31 (9): 1301-1310
33. ."Cumin" . Drugs.com. 2018. Retrieved 24 February 2018.
34. .https://www.soilmanagementindia.com/soil-mineralogy-2/infrared-spectroscopy-principle-and-types-soil-mineralogy/13268
35. .https://www.yourarticlelibrary.com/medicine/ayurvedic/determination-of-ash-values/49966

36. .https://www.google.com/url?sa=i&url=https%3A%2F%2Fstudy.com%2Facademy%2Flesson%2Fdesiccator-in-chemistry-lab-definition-lesson-quiz.html&psig=AOvVaw1VOOVWroNgemAiN-6K7jLD&ust=1654447793171000&source=images&cd=vfe&ved=0CA0QjhxqFwoTCNCVk8GglPgCFQAAAAAdAAAAABAI
37. Behnam Davani, Ph.D., MBA, Senior Scientist, Expert Committee: (MDAA05) Monograph Development - Antivirals and Antimicrobials USP29-NF24 Page 569
38. .https://www.sciencedirect.com/topics/chemistry/uv-vis-spectroscopy
39. Giridhar V. Quality control of herbal drugs through UV-Vis spectrophotometric analysis. International Journal of Ayurvedic Medicine. 2015;6(1):102-9.
40. .Vikash Sharma, Saurabh Singh , Arushi Dixit and Alka Saxena FORMULATION AND EVALUATION OF HERBAL COUGH SYRUP FROM SEEDS EXTRACT OF HEDGE MUSTARD , INTERNATIONAL JOURNAL OF RESEARCH IN PHARMACY AND CHEMISTRY 2020, 10(1), 1-10

IJCRT.ORG ISSN : 2320-2882

INTERNATIONAL JOURNAL OF CREATIVE RESEARCH THOUGHTS (IJCRT)

An International Open Access, Peer-reviewed, Refereed Journal

FORMULATION AND EVALUATION OF HERBAL COUGH SYRUP BY USING POMEGRANATE PEELS

[1]POOJA PISAL*, [2]PRANALI A. ZENDE, [3]PRANOTI S. JADHAV, [4]POOJA PETKAR

[1]Assistant professor, [2]Student, [3]Student, [4]Assistant professor

Abstract :

The most common problem suffered by individuals everywhere over many centuries is cough. Coughing is the protective mechanism of the body. Coughs are classified further accordingly which are depending upon factors such as signs and symptoms, duration, type, character, etc. The most commonly used, prepared and popular dosage form to cure cough and cold is syrup. Syrup is a very popular dosage form of cough and cold medications, which eases patient compliance. By adding the decoction of herbal drugs with a base of honey is helpful to the formulation thick and preserve the formulation. The quality of the final herbal cough syrup was evaluated with parameters such as physical appearance colour, odour, taste, pH, and viscosity. It was found that antitussive activity produced by the herbal formulation in the minimum dose was much better than the standard drug.

Keywords : Herbal treatment, Cough, Antimicrobial activity, Honey base.

I. INTRODUCTION -

Health and nutrition are the most important factors in the human resources development of the country. Pomegranate (*Punica granatum*) is one of the oldest fruits and originates from Iran north to the Himalayas in India and is cultivated throughout the Mediterranean region in Asia, Africa and Europe. Early fall is the best time for pomegranates in October and November in the northern hemisphere, but they are usually available in early winter. Pomegranate is also a good source of many essential substances Vitamin B complexes such as pantothenic acid (vitamin B-5), folates, pyridoxine and vitamin K and minerals such as calcium, copper, potassium and manganese[1].

The peels of this fruit make up 26-30% of the total weight of the fruits and they cover the internal membranes. The astringent effect is due to the skin (pericarp). Despite the large number of polyphenolic compounds and beneficial biological effects of pomegranate peel (PP), unfortunately, it is often treated as waste and thrown away. Phenolic compounds such as anthocyanins, ellagic acid glycosides, free ellagic acidification, ellagitannins, punicalagin, punicalin and gallotannins are found deep in the PP. Pomegranate Peel Extract (PPE) is rich in phenols, flavonoids and tannins, which is why it has found an important place in providing by-product pomegranate juice-related preparations to the food industry[2]. They also contain many antioxidants, antivirals, anti-cancer and anti-tumor properties and these antioxidants are equally high, able to protect low-density lipoproteins LDL cholesterol against oxidation and reduces the risk of cancer and heart

disease. It attracts attention because of its obvious wound healing properties and immunomodulatory effects[1].

fig 1 : bioactive components present in the pomegranate peel[2] -

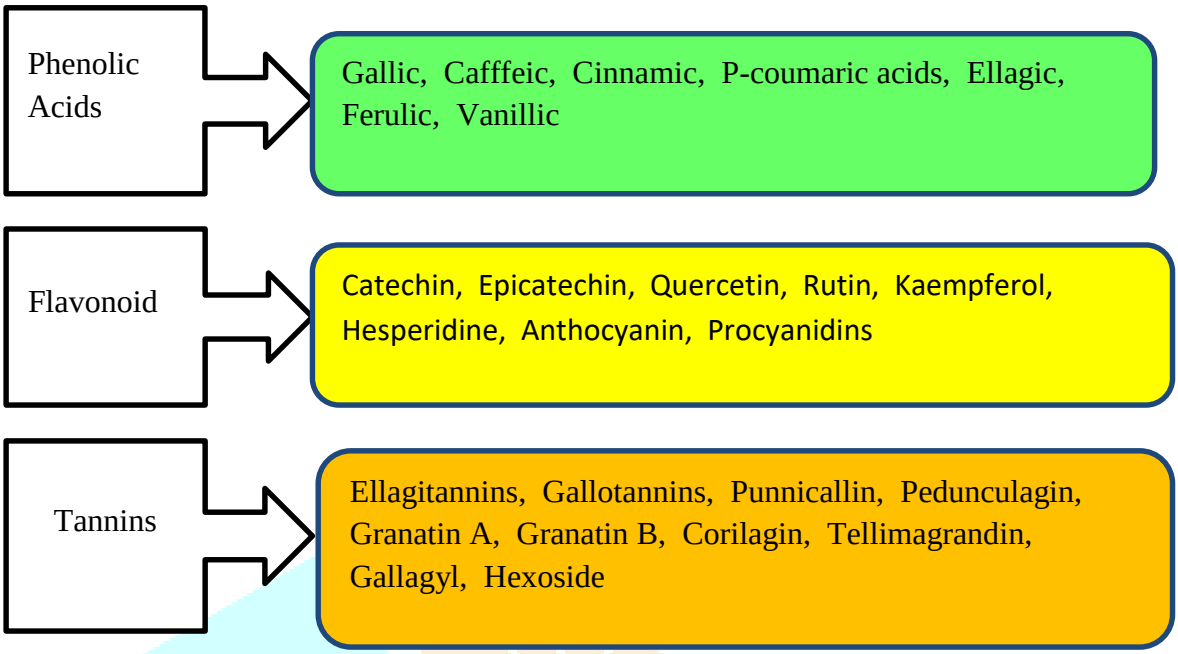

table 1 : classification of cough[3] -

Sr. No.	Types of cough	Properties
1.	Acute cough	Not more than three weeks duration
2.	Chronic cough	More than three weeks
3.	Dry cough	No mucous or secretion
4.	Wet cough	With mucous or secretion
5.	Cough from chest and throat	Productive or non – productive
6.	Paroxysmal	Spasmodic and recurrent
7.	Bovine cough	Soundless cough due to paralysis or larynx
8.	Psychogenic cough	Self – conscious activity of the patient to draw attention

Herbal treatment for cough :

The most popular antitussive is a medicinal plant treatment. Herbal preparations play an important role in improving the health sector. Herbal remedies used for mild to severe health disorders include asthma, tuberculosis, cough, pneumonia, kidney diseases, cancer, diabetes, allergies, lung cancer and viral infections. WHO estimates 80 per cent of the population even use herbal medicines in primary health care standards Medicinal plants have always been used, e.g. with traditional primary providers and especially in Asian countries. The main use of herbal medicines is prescribed chronic health promotion and therapy, for differently conditions that are life-threatening. Most of the synthetic drug treatments used cause a lot of side effects such as vomiting, nausea, sedation, allergies, respiratory infections, change in appetite, irritability,

drowsiness, addiction and overload can damage organs or parts of organs. In recent years, researchers have done focusing mainly on herbal medicines and herbal medicines with less or no side effects during and after treatment[4].

Fig 2.

Fig 3.

Table 2: methods and materials[5] -

Sr. No.	Material	Uses
1	Pomegranate peel	Antitussive
2	Clove	Expectorant
3	Tulsi	Antitussive
4	Fennel	Flavouring agent
5	Black pepper	Preservative
6	Honey	Base

Extraction of pomegranate peels[6] :

The soxhlet extraction meth**o**d is commonly used to extract compound from solid materials, such as pomegranate peel. Here's a basic overview of the process -

- Grind the pomegranate peel into small particles to increase the surface area for extraction.
- Weigh the ground pomegranate peel to accurately determine the amount used in the extraction.
- Place the ground peel into a thimble, which is a small cylindrical container typically made of filter.
- Set up the soxhlet apparatus, consisting of a round bottom flask, a condenser, and a soxhlet extractor. The thimble with the packed peel was placed in the soxhlet extractor.
- Use a suitable solvent (e.g. ethanol, distilled water) in the round bottom flask. The solvent will continuously cycle through the extractor, extracting compounds from the pomegranate peel. Add a mixture of ethanol and water as a solvent in a ratio 1:1.

- Apply heat to the round bottom flask for 12 hours, causing the solvent to evaporate and rise into the soxhlet extractor. The solvent extracts compounds from the pomegranate peel and then drips back into the round bottom flask.
- The process continues in a cyclical manner, with the solvent cyclic through the extraction thimble until a concentrated extract is obtained.
- Collect the extracted solution in a round bottom flask.
- Remove the solvent from the collected solution using techniques like rotary evaporation to obtain the concentrated extract.
- Store the extract in a proper container.

Extraction of Tulsi :

Leaves of *Ocimum sanctum L*. tulsi were collected from different sites and washed with sterile water, 50g of tulsi was placed in the thimble of soxhlet apparatus with 50ml of water and 50 ml of ethanol over 24 hours[7].

Extraction Process of Decoction of Fennel, Clove :

Take 5-7 gm of each herbal ingredient. Herbs were mixed using 500ml of water. Attach reflux condenser and material was boiled carefully by using a water bath for 3 hrs. Boil until the total volume becomes one-fourth part of the previous. Then the liquid was cooled and filtered[7].

Extraction of Black pepper :

The pepper was dried and ground to a fine powder and approximately 10 g was placed in a soxhlet thimble and then extracted using 100 ml of ethanol for 240 minutes[8].

Table 3 : formulation for 15 ml -

Sr. no.	Ingredient	Quantity
1	Pomegranate peel	5ml
2	Clove	1.5 ml
3	Tulsi	3 ml
4	Fennel	1.5 ml
5	Black pepper	1 ml
6	Honey	3 ml

Evaluation parameters :

a) Colour examination [9]:

2ml of prepared syrup was taken on watch glass and it was placed under white tube light. Then colour was observed.

b) Odour examination :
2ml of prepared syrup was taken and smelled by an individual.

c) Taste examination[9]:
Pinch of final syrup was taken and examined the taste buds of the tongue.

d) pH examination[9] :
Steps -
1) The glass electrode is washed with distilled water and cleaned.
2) Place the electrode in the pH 7 buffer solution and set the pH meter to 7 by turning the calibration knob on the meter .
3) The electrode was removed, washed with distilled water and cleaned.
4) The inserted electrode was in a buffer solution of pH 4. Adjust the value.
5) The electrode was then placed in the final syrup and the pH was monitored .

e) Density examination[9] :
Steps –
1) Cleaned the specific gravity bottle.
2) The bottle was cleaned at least two times with distilled water.
3) Measured the weight of empty dry bottle syrup with stopper (w1).
4) The bottle was filled with final syrup and the stopper, wipe out excess syrup from outside the tube.
5) Measure the weight in grams of syrup(w2).
6) Calculate weight in grams of syrup(w3).
7) Formula of density :

$$\text{density of liquid under test (syrup)} = \frac{\text{weight of syrup under test}}{\text{volume of final syrup under test}}$$

f) Viscosity examination[10] :

Steps-

1) An organic solvent such as acetone.
2) Mount the viscometer in a vertical position on a suitable stand.
3) Fill water in a dry viscometer up to mark G.
4) Count time required, in seconds for water to flow from mark A to mark B.
5) Repeat step 3 at least 3 times to obtain accurate reading.
6) Rinse the viscometer with test liquid and then fill it up to mark A, and find out the time required for liquid to flow to mark B.
7) Determination of densities of liquid as mentioned in the density determination experiment

Formula:

$$\text{viscosity} = \frac{\text{density of test liquid} \times \text{time required to flow test liquid}}{\text{density of water} \times \text{time required to flow water}} \times \text{viscosity of water}$$

g) Determination of antimicrobial activity[11] :

The agar plate method was used to examine the antimicrobial activity of the herbal cough syrup. The test compound (50µL) was introduce in the well. The plate was incubated over night at room temperature. The antimicrobial spectrum of the extract was determine for the bacterial species in terms of zone sizes around the well.

Fig 4 : MIC against E.Coli

Result :

The results obtained in this study suggest that herbal formulations prepare and possess anti-microbial activity, the component of herbal cough formulation was selected due to their reported action that plays preventive and curative role in the prevention of cough. The syrup prepared passes all physical parameters and shows significant anti-microbial activity.

Table 4 : Result of Physicochemical parameters of developed herbal syrup -

Sr.no.	Parameter	Observation value
1.	Color	Reddish brown
2.	Odour	Sweet aromatic
3.	Taste	Sweet
4.	pH	5.9
5.	Viscosity	0.029 P
6.	Density	0.77 g/cm^3

Table 5: The antimicrobial activity and MIC of the prepared extract

Test bacteria	Zone of inhibition (mm)	
	50µL	Positive
E-coli	3	13

Conclusion :

In conclusion, our study showed that Pumica granatum showed antitussive activity and a satisfactory result was found. Pumica granatum has no adverse effects comparable to chemical drugs. Hence, it has the potential to be used as a cheap, non-toxic formulation for standard antitussive activity. This is an in-vitro study, the data of which can be useful for further studies on animals and then eventually on human beings. Pumica granatum has no adverse effects comparable to chemical drugs. Hence, it has the potential to be used as a cheap, non-toxic formulation for standard antitussive activity. This study will help us understand cough and measures to prevent cough. This study helps us understand the effectiveness of herbal cough syrups compared to chemical-based syrups This is an in-vitro study, the data of which can be useful for further studies on animals and then eventually on human beings.

Acknowledgement :

The authors express gratitude to the Principal, Dr. R.S . Chavan, Seth Govind Raghunath Sable College of Pharmacy, Saswad, Department of Chemistry for providing facilities required for the article, also thankful to Ms. Pooja Pisal for providing consistent support and timely guidance.

Reference

1 Sayeeda Fathima, Yamuna Devi Puraikalan, 2015, Developement of food products using pomegranate skin, International Journal of Science and Research (IJSR), Page no- 1756-1757.

2 Yaxian Mo, Jiagi Ma, Wentao Gao, leizhang Jiangui Li, Jingaming and Jiachen zang, 09 June 2022 Volume – 09, Pomegranate peel as a source of bioactive compounds: a mini review on their physiological function.

3 Ankush Ganpat patil, Kaivalya Gajanan, Mirajkar, Prnav Laxamn Savekar, Chetana V. Bugadikattikar, Somesh S. Shintre, 2020, Formulation and evaluation of ginger macerated honey base herbal cough syrup, Internantional journal of innovative science and research technology page no. 582-588, Classification of cough.

4 Pratikeshwar Panda, Arpita Sahu 2023, Formulation and evaluation of cough syrup, Asian Journal of herbal pharmaceutical research and development, page no 28-32 (herbal treatment for cough).

5 S.C Kushwaha, M.B.Bira and Pradyuman Kumar, Nov-Dec 2013, Nutritional composition of detanninated and fresh pomegranate peel powder (material and methods) Page no- 38-41.

6 Jing chen chuhling Liao, Xiaolu Ouyang, Ibrahim Kahramanoglu, Yudi Gan, and 4 Nov 2020, Antimicrobial activity of pomegranate peel and its application on food preservation (the extract process of pomegranate peel).

7 Miss. Priya D. Khode, Rupali R. Singanjude, Urwashi D. Lanjewar, Formulation and Evaluation of herbal Cough Syrup, Journal of Critical Reviews, Vol 06, Issue 03, 2019.

8 H. G., Matena, Z.N., Kariuki and B.C., Ongarora OPTIMIZATION OF PIPERINE EXTRACTION FROM BLACK PEPPER (PIPER NIGRUM) USING DIFFERENT SOLVENTS FOR CONTROL OF BEDBUGS.

9 Dr. Javesh K. Patil, Dipali R. Mali*, Komal R. More and Shraddha M. Jain. FORMULATION AND EVALUATION OF HERBAL SYRUP, World Journal of Pharmaceutical Research Volume 8, Issue 6, 1061-1067.

10 Krishna Suresh Gupta, Yatin Nitin Gorhekar , Pratiksha Subhash Gharat , Maheshwari Ashok Gawari , Saroj Changdev Firke Formulation and Evaluation of Herbal Syrup , International Journal of Research Publication and Reviews Vol 4, no 6, pp 3300-3304 June 2023

11 Vikash Sharma, Saurabh Singh , Arushi Dixit and Alka Saxena FORMULATION AND EVALUATION OF HERBAL COUGH SYRUP FROM SEEDS EXTRACT OF HEDGE MUSTARD , INTERNATIONAL JOURNAL OF RESEARCH IN PHARMACY AND CHEMISTRY 2020, 10(1), 1-10

IJCRT.ORG ISSN : 2320-2882

INTERNATIONAL JOURNAL OF CREATIVE RESEARCH THOUGHTS (IJCRT)

An International Open Access, Peer-reviewed, Refereed Journal

REVIEW ON ANALYSIS OF KIWI FRUIT AND KIWI PEEL EXTRACT

Gaikwad Sudarshan macchindra[1] , Bhoite Adarsh Jalindar[2] , Botre Rutuja Sanjay[3] ,

Budhe Rupali Prakash[4] , Ghatole Pooja Sunil[5]

Bachelor's Of Pharmacy , PDEA's Seth Govind Raghunath Sable College of Pharmacy Saswad, Pune.

Guided by : Ms. Shweta.L.Phadtare

Abstract: The current study evaluated four different solvent compositions for their proportional ability to extract total phenolic, total flavonoid, and total tannin (TF and TT) components from the peels of kiwis (Actinidia Deliciosa Planch), as well as to profile the composition of these plant by-products and to measure their antioxidant, antimicrobial, and anticancer activities. Chemical studies revealed that the content of moisture, protein, crude fat, total carbs, and ash was 85.27% of fresh weight, 12.62, 3.70, 76.92, and 6.50% of dry weight, respectively. Kiwifruit is widely known for its ability to combat digestive difficulties, cardiovascular illnesses, skin health, diabetes, inflammation, and microbial activity, among other things, making it ideally suited for therapeutic interventions.

Key words: Kiwifruit, Nutritional composition, therapeutic uses, Kiwi extract, Kiwi Peel

1. INTRODUCTION

The edible fruits produced by plants in the genus actinidia are known as kiwifruit. Kiwi plants originated in China, where they grow wild, and were transferred to New Zealand by missionaries in the early twentieth century, when they were finally tamed and grown. Kiwifruit are nutrient-dense fruits that are high in Phytonutrients, minerals, and vitamins that improve one's health (Stonehouse et al., 2013). It is exceptionally high in sugars (glucose and fructose), vitamin C (420mg/100g), vitamin A, E, K, fiber, flavonoids, antioxidants (beta-carotene, xanthin, and lutein), and minerals (potassium as 312 mg/100g, zinc, selenium, magnesium, iron, copper), all of which provide functional and metabolic benefits. Kiwifruits also have laxative action, digestive characteristics, cardiovascular protective qualities, anti-diabetic properties, anti-inflammatory properties, and antibacterial properties (Ma et al., 2019). Kiwi fruit is used to make dried kiwifruit, jams, jellies, nectars, and many more products. As a result, this study focuses on the therapeutic profile and significant health advantages of Kiwifruit (Actinidia deliciosa). Actinidia fruits are botanically berries with many black seeds encased in a delicious pericarp. The most popular commercial cultivar with exceptional flavor is Actinidia deliciosa (A. Chev.) 'Hayward' ('green' kiwifruit). It's an oval berry the size of a hen's egg, with a light brown hairy exterior and emerald-green flesh containing numerous small black seeds trapped in a luscious pericarp. Fruits of Actinidia deliciosa feature long, stiff, bristlelike hairs that are partially removed during grading and packing.

2.Nutritional Composition

Fresh A. deliciosa and A. chinensis fruit's nutritional profile per 100 g is shown in Table 1 (US Department of Agriculture, 2011). Kiwifruit are rich in vitamin C, dietary fiber, and various phytochemicals that are good for your health. Magnesium and potassium levels are also high. A. deliciosa that is ripe contains carotenoids such b-carotene, lutein, violaxanthin, and neoxanthin as well as chlorophylls a and b. The cyclic sugar alcohol myoinositol, which is present in many meals, is also extremely abundant in kiwifruit. Early fruit growth had a high myoinositol level, which decreased to 1-2% as the fruit ripened. The kiwifruit does not contain a lot of energy.

A. Fibers

About 2-3% (fresh wt) of kiwifruit's weight is made up of nonstarch polysaccharide. According to recent studies, the dietary fiber in green and gold kiwifruit is made up of roughly one-third soluble fiber and two-thirds insoluble fiber. Gold kiwifruit, however, have less nutritional fiber than green varieties. Pectic polysaccharides make up the soluble portion of fibers, whereas cellulose, hemicellulose, and minor amounts of pectin make up the insoluble portion. 10% of the daily required dietary fiber intake can be met by kiwis.

B. Sugars

The three main sugars found in Actinidia are glucose, fructose, and sucrose. With different kiwifruit varieties and maturation phases, sugar content and ratios change. In A. deliciosa Hayward, a total sugar content of 8.4 g 100 g^{-1} fresh wt was recorded. According to the New Zealand Institute for Plant & Food Research, fresh weight samples had total sugar contents ranging from 7.7 to 10.8 g 100 g^{-1}. Kiwifruits have a low glycemic index, and the sugar they contain helps to regulate blood sugar levels.

C. Protein

The protein content of kiwis is not very high. Actinidin, a cysteine protease found in kiwifruit, is well known for its capacity to hydrolyze proteins. Actinidin makes up 40% of the soluble protein in green kiwifruit, making it the most prevalent soluble protein. Kiwellin and a protein that resembles thaumatin are among the other proteins found. There are studies that detail how actinidin helps with digestion and digestive motility.

D. Vitamin E

Vitamin E levels in kiwis are fairly high, and the major a-tocopherol form of the vitamin is found in the flesh, where it may be more accessible. D-tocomonoenol, a novel type of vitamin E, has been discovered in kiwifruit. The seeds of kiwifruit are the only parts of the fruit that contain any lipids. From the raw pulp extracts of Hayward, three vitamin E forms—b-sitosterol, stigmasterol, and its D isomer—were discovered.

E. Carotenoids

The carotenoid molecules b-carotene, lutein, violaxanthin, and neoxanthin are among those found in kiwifruit. The most prevalent carotenoids are lutein and beta-carotene. Kiwifruit has the greatest concentration of lutein among the numerous regularly consumed fruits, ranging from 0.09 to 1.080.17 mg 100 g^{-1} fresh weight. The highest concentrations of lutein are found in A. arguta and A. rufa, followed by A. deliciosa and A. chinensis. Similar levels of b-carotene can be found in A. chinensis and A. deliciosa (0.070.01 to 0.150.04 mg 100 g^{-1} fresh wt), with A. arguta having the highest level (0.290.04 mg 100 g^{-1} fresh wt). The overall carotenoid concentration of green variants is typically higher than that of gold/yellow kinds.

F. Organic Acids

The main acids in kiwifruit are citric, malic, and quinic acids, along with considerably lower levels of glucuronic and galacturonic acids. In kiwifruit, quinic acid is present in very high proportion. Other fruits often contain tiny levels of quinic acid. Kiwifruit acidity is also influenced by ascorbic acid.

G. Phytochemicals

The identification of two caffeic acid glucosy derivatives, two coumarin glucosides, campesterol, chlorogenic acid, and a few flavone and flavanol substances came from phytochemical study of crude extracts of kiwifruit pulp from "Hayward." In kiwifruit juice, phenolic components were distinguished and identified. Juice had a low concentration of phenolic chemicals. The most prevalent 3,4-dihydroxybenzoic acid derivatives, coumaric and caffeic acid derivatives, protocatechuic acid, and chlorogenic acid are among the strongly acidic phenolic acid compounds that have been found. The weekly acidic phenolic acid in clarified juice is composed of catechin, epicatechin, procyanidin dimers, and oligomers. The flavanols that are present are the glucoside, rhamnoside, and rutinoside glycosides of quercetin and the rhamnoside and rutinoside glycosides of kaempferol. Kiwifruit's anthocyanin level overall is smaller than that of many other berries, hence it makes little difference in the fruit's antioxidant capability. Anthocyanins are located in a ring around the fruit's center in A. deliciosa. Cyanidin-3-O-xylo-galactoside, with lower levels of cyanidin-3-O-galactoside, was the main anthocyanin found in A. chinensis. The two main anthocyanins found in A. deliciosa are cyanidin 3-O-galactoside and cyanidin 3-O-glucoside; no cyanidin-3-Oxylo-galactoside was found.

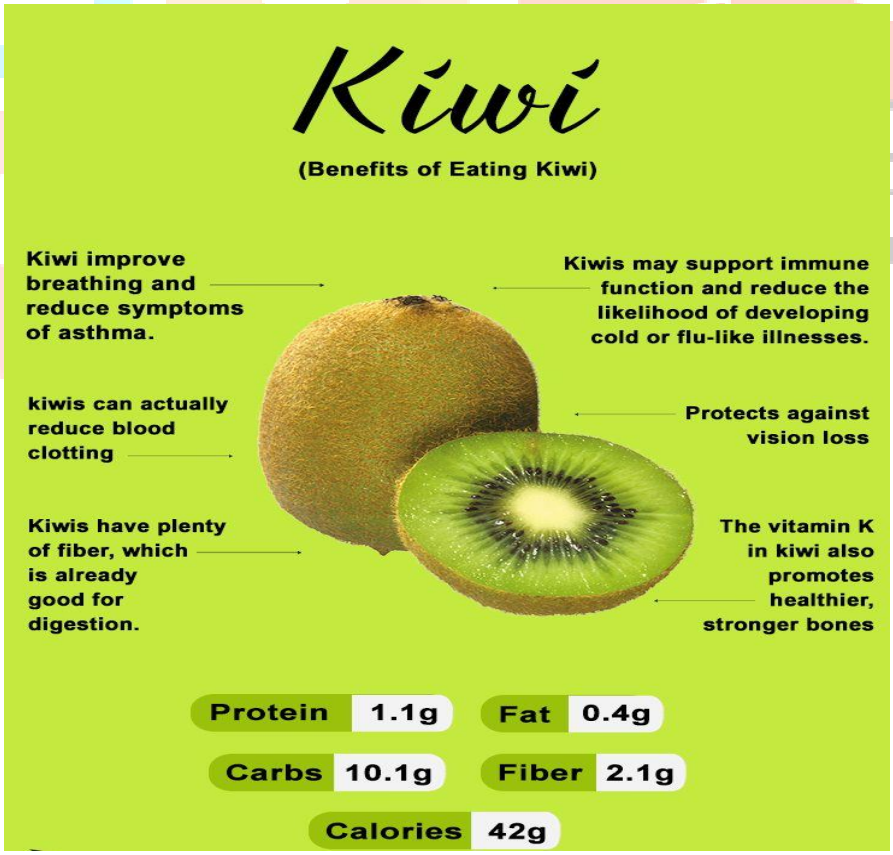

Table 1 Nutritional composition of kiwifruit in 100 g edible portion[a]

Nutrient	*Unit*	Actinidia chinensis *Yellow kiwifruit (Hort16A)*	Actinidia deliciosa *Green kiwifruit*
Proximates			
Water	g	83.22	83.07
Energy	kcal	60	61
Protein	g	1.23	1.14
Total lipid	g	0.56	0.52
Carbohydrate	g	14.23	14.66
Total fiber	g	2.0	3.0
Total sugars	g	10.98	8.99
Minerals			
Calcium, Ca	mg	20	34
Iron, Fe	mg	0.29	0.31
Magnesium, Mg	mg	14	17
Phosphorus, P	mg	29	34
Potassium, K	mg	316	312
Sodium, Na	mg	3	3
Zinc, Zn	mg	0.10	0.14
Vitamins			
Vitamin C	mg	105.4	92.7
Thiamin	mg	0.024	0.027
Riboflavin	mg	0.046	0.025
Niacin	mg	0.280	0.341
Vitamin B6	mg	0.057	0.063
Folate, DFE	µg	34	25
Vitamin A, RAE	µg	4	4
Vitamin A, IU	IU	72	87
Vitamin E	mg	1.49	1.46
Vitamin K	µg	5.5	40.3
Choline	mg	5.0	7.8
Lipids			
Total saturated fatty acids	g	0.149	0.029
Total monounsaturated fatty acids	g	0.036	0.047
Total polyunsaturated fatty acids	g	0.207	0.287
Cholesterol	g	0	0

[a]Source: The USDA National Nutrient Database for Standard Reference.

3.Material and Methods :

A. Plant material

Actinidia deliciosa kiwi fruits were purchased from the local Giza, Egypt, market. Chemicals and reagents: The analytical grade chemicals used in this investigation were all manufactured by Sigma (US), Aldrich, and Biodiagnostic Company.

B. Preparation of sample

A sharp knife was used to wash and separate the kiwi fruit from the peels. Kiwi peels were peeled, powdered, and then kept in the refrigerator at -4 °C until extraction by air-drying for ten days, followed by three days of drying in an oven at 40 °C.

C. Preparation of kiwi peels extracts

The dried kiwi peel samples (10 g) were dispersed separately in 100 ml of distilled water, 80% ethanol, 80% methanol, and 80% acetone for 24 hours at room temperature with shaking. Following three extraction steps, the mixture was filtered through Whatmann No. 1 filter paper. The filtrate was then concentrated in a rotary evaporator to dryness at 40 °C. Before analysis, the raw extracts were kept in a refrigerator.

D. Proximate analysis

According to AOAC[3], the amounts of moisture, ash, crude protein, total fat, total carbs, and macro-microelements were measured.

Table : 2

Proximate analysis of kiwi peels

Proximate analysis*	Composition (%)
Moisture	85.27± 0.18
Carbohydrate	76.92+0.76
Crude fat	3.70±0. 55
Crude protein	12.62± 0.56
Ash content	6.50± 0.40

* The other compounds than water were expressed to dry weigh bases.

E. Total phenolic content

According to Singleton and Rossi[4], the total phenolic content (TP) of kiwi peel extracts was spectrophotometrically assessed using the Folin Ciocalteu reagent assay and gallic acid as the reference. At 750 nm, the absorbance was measured using a spectrophotometer (Unicum UV 300). Gallic acid equivalents (GAE)/g dry weight sample was used to measure the total phenolic content in the samples. Each sample was examined three times.

F. Total flavonoid content

Using quercetin as a reference substance, the aluminum chloride method was used to spectrophotometrically measure the total flavonoid concentration (TF) of kiwi peel extracts. At 510 nm, the absorbance was measured using a spectrophotometer (Unicum UV 300). The sample's total flavonoids were calculated as mg quercetin equivalents (QE)/g dry weight. Each sample was examined three times.

G. Total tannins content

According to Polshettiwar et al[5], the total tannin content (TT) of kiwi peel extracts was determined using the Folin-Ciocalteu reagent. A spectrophotometer (Unicom UV 300) was used to detect absorbance at 775 nm in comparison to a produced reagent blank. The sample's total tannins were calculated as mg tannic acid equivalent (TE)/g of dry weight. Each sample was examined three times.

H. Identification of phenolic compounds by HPLC

Ben-Hammouda et al[6] report that phenolic components in kiwi peel acetone extract were detected using HPLC. Agilent's 1100 series HPLC system is attached to a UV-Vis detector (G1315B) and a degasser (G1322A). Chromatographic separations were carried out on a ZORBAX-Eclipse XDB-C18 column (4.6250 mm, particle size 5 m) using sample injections of 5 l from an Agilent 1100 series auto-sampler. Two mobile phases—(A) 0.5% acetic acid in distilled water at pH 2.65 and solvent (B) 0.5% acetic acid in 99.5% acetonitrile—were utilized with a constant flow rate of 1 ml/min. Using a UV detector set at a wavelength of 280 nm, the elution gradient was linear, beginning with A and ending with B over a period of 50 minutes. By comparing the relative retention durations of the kiwi peel extract's phenolic components to those of the standard mixture chromatogram, these compounds' identities were determined. Based on peak area measurements, the concentration of a certain component was estimated and then translated to mg/100g dry weight.

4. Results and Discussion

A. Chemical studies

Chemical Composition

Tables 2 and 3 contain the results of an analysis of the kiwi peels' moisture, ash, crude protein, crude lipid, total carbohydrate, and macro- and microelement contents. The contents of moisture, ash, and protein were respectively 85.27% of FW, 6.50, and 12.62% of DW. These results exceeded those of Anhwange et al. [7] and Shyamala and Jamuna [8] in terms of value.

Minerals content of kiwi peels

Macronutrients	Concentration (ppm)	Micronutrients	Concentration (ppm)
K	2300 ± 1.74	Fe	82.26± 18.77
Ca	2300± 0.08	Cu	6.64 ± 1.14
Na	900 ± 0.02	Zn	9.26 ± 3.31
P	600 ± 0.01	Mn	14.83 ± 4.25
Mg	8200 ± 0.05	----------	-------

Table 3

Total carbs made up 76.92% and fat 3.70% of the dry weight, respectively. The amount of fat was comparable to what Mahmoudi et al[9]. had previously discovered. Additionally, the total carbohydrate was higher than that found in two different types of kiwi fruits by Parameswaran and Murthi[10], but it was lower than that found by the same authors[9], who recorded 71 g/Kg FW.

B. Biological Studies

Antimicrobial activity of kiwi peels

Table 4 lists the ethanol and acetone extracts of Kiwi peels' antibacterial and antifungal properties. At concentrations of 400 and 600 ppm, both extracts exhibit a zone of inhibition against gram-positive and gram-negative bacteria (Bacillus subtilis and Staphylococcus aureus), yeasts (Saccharomyces cerevisiae and Candida albicans), and fungi (Aspergillus flavus). 80% acetone-prepared extract has more antibacterial activity than 80% ethanol-prepared extract. With an inhibition zone of 19.82 mm for B. subtilis at 600 ppm acetone extract and 17.65 mm for St. aureus at 600 ppm ethanolic extract, kiwi peels displayed superior antibacterial activity against gram-positive bacteria.

Table : 4

Antimicrobial activity of kiwi peels extract.

Extracts	Conc. µg/ml (ppm)	Zone Inhibition (mm)						
		Bacteria				Fungus	Yeast	
		B. subtilis (+)	*St. aureus* (+)	*E. coli* (-)	*P. aeruginosa* (-)	*A. fluves*	*S. cerevisiae*	*C. albicans*
Ethanol 80%	200	00.00	00.00	00.00	00.00	00.00	00.00	00.00
	400	13.20	11.30	10.23	10.23	11.70	12.40	11.67
	600	18.16	17.65	18.15	18.15	16.56	17.66	15.25
Acetone 80%	200	00.00	00.00	00.00	00.00	00.00	00.00	00.00
	400	14.16	11.73	13.12	12.56	10.10	11.62	10.87
	600	19.82	15.50	19.52	19.50	17.85	16.81	16.52

Additionally, kiwi peel acetone (80%) extract demonstrated the highest antimicrobial activity against gram-negative bacteria, with an inhibition zone of 19.52 and 19.50 mm for E. Coli and P aueginosa, respectively, and a fungus of 17.85 mm for A. flavus at a concentration of 600 ppm, higher than that found by Chou et al[11]. For kiwi fruit at a concentration of 200 g/ml, they also reported a zone of inhibition of 7 to 14 mm against gram-positive, 9 to 13 mm against gram-negative, and 7 to 13 mm against fungus. Human and plant pathogenic bacteria, fungi, and viruses can be defeated by plant ingredients without causing hazardous side effects or environmental hazards[12].

C. Health Effects

I. Antioxidant Capacity

The cells are shielded by dietary antioxidants from the oxidative reactive oxygen species produced by various biological activities. Studies have shown that eating a diet high in fruits and vegetables can lower your risk of developing degenerative diseases like cancer and cardiovascular disease. Fruits' antioxidant potential is aided by vitamins C and E, carotenoids, and phenolic substances. In general, the antioxidant capacity of kiwifruit is considerable, and it appears that vitamin C and polyphenol content play a significant role in this. The species and cultivars of Actinidia have a significant impact on their antioxidant capacity. Numerous antioxidants, including vitamin C, vitamin E, lutein, zeaxanthin, and other phytochemicals, can be found in kiwifruit.

II. Immune Functions

A good source of several phytonutrients and other compounds linked to a strong immune system is kiwifruit. A few studies using human and animal cells have looked into the immunomodulatory effects of kiwifruit ingestion. Human blood cells' ex vivo innate and adaptive immune cell functions were markedly improved by gold kiwifruit extract. Studies on elderly adults and young children looked at how frequently consuming gold kiwifruit affected the frequency and signs of upper respiratory tract infections. These investigations showed that eating gold kiwis decreased the intensity of cold and flu symptoms in the research groups. The older persons who ate gold kiwifruit also showed increases in plasma vitamin C, tocopherol, lutein/zeaxanthin, and erythrocyte folate content.

III. Cardiovascular Diseases

When compared to a healthy control diet, eating two green kiwis per day for four weeks improved the plasma HDL-C, TC/HDL-C ratio, and apolipoprotein B/apolipoprotein A1 ratio in a hypercholesterolemic male. According to some additional research, eating 1-3 green or gold kiwis per day for four to eight weeks improved HDL-C, decreased the TC/HDL-C ratio, and lowered triglycerides in comparison to baseline levels. When compared to the control treatment, eating three green kiwis per day for eight weeks dramatically lowered the diastolic and systolic blood pressure among male smokers. A decrease in the activity of the angiotensin-converting enzyme was also noted.

IV. Anticarcinogenic Activity

Two of the 12 phenolic compounds discovered in the roots of A. chinensis shown exceptional cytotoxic action against the leukemia-causing P-388 and cancer-causing A-549 cell lines. A polysaccharide component derived from the root of A. chinensis also showed antitumorous activity in mice in a different investigation. Different gold kiwifruit extracts demonstrated targeted cytotoxicity against human oral carcinoma cell lines. Additionally, human adenocarcinoma and human liver cancer cell lines were sensitive to two triterpenoids derived from A. chinensis roots. HepG2 and HT-29 cell growth was significantly reduced by extracts from A. arguta. Kiwifruit juice or extracts demonstrated an antimutagenic activity against chemical carcinogens, such as heterocyclic amines like 2-amino-1-methyl-6-phenylimidazo [4,5-b] pyridine (PhIP), in in vitro systems.

V. Kiwifruit Allergy

Additionally, kiwis contain allergens that, in those who are sensitive, might cause allergic reactions. A 53-year-old woman who got urticaria, wheezing, and laryngeal edema after handling kiwifruit was the first to report having an allergy to it in 1981. As kiwifruit use has expanded globally since then, there have been an increasing number of reports of allergy to this fruit. A kiwifruit allergy may manifest itself in a number of ways. Oral allergy syndrome and urticaria are frequent manifestations of kiwifruit allergy symptoms. The symptoms of oral allergy syndrome include mouth, lip, and throat itching, throat and lip swelling, and the development of tiny blisters on the oral mucosa. Indigestion, nausea, vomiting, Kiwifruit 493 wheezing, skin rashes, and other serious allergic responses like anaphylaxis have also been recorded as symptoms. Kiwifruit consumption can cause allergy in some people, but pollen and latex allergies are more common in others. This is because the allergens in kiwifruit and natural rubber latex, a condition known as the latex-fruit syndrome, are comparable to one another.[13]

5. Conclusion

1. Kiwi peels in acetone have antioxidant and antibacterial properties; hence, acetone would be a good solvent for kiwi peel extraction.

2. Kiwi fruit peels make excellent antioxidant and antibacterial sources for food goods, according to research. For the isolation of bioactive components and biological assay techniques for therapeutic formulations, more research is advised.[14]

References :

1. Nutritional composition and potential health benefits of Kiwifruit (Actinidia deliciosa): A review © 2022 IJCRT | Volume 10, Issue 1 January 2022 | ISSN: 2320-2882

2. Brevik A, Gaivao I, Medin T, et al. (2012) Supplementation of a western diet with golden kiwifruits (actinidia chinensis var. 'hort 16A') effects on biomarkers of oxidation damage and antioxidant protection. Nutrition Journal 10: 54.

3. AOAC, Official Methods of Analysis of the Association of Official Analytical Chemist International, AOAC, Virginia, USA, 2457 (2005)

4. Singleton V.L. and Rossi J.A., Colorimetry of total phenolics with phosphomolybdic-phosphotungstic acid reagents, Amer. J. Enol. Viticult., 16(3), 144-158 (1965)

5. Polshettiwar S.A., Ganjiwale R.O., Wadher S.J. and Yeole P.G., Spectrophotometric estimation of total tannins in some ayurvedic eye drops, Indian J. Pharm. Sci., 69, 574-576 (2007)

6. Ben-Hammouda M., Kremer R.J., Minor H.C. and Sarwar M.A., Chemical basis for the differential allelopathic potential of sorghum hybrids on wheat, J. Chem. Ecol., 21, 775–786 (1995)

7. Anhwange B.A., Ugye T.J. and Nyiaatagher T.D., Chemical composition of Musa Sapientum (banana) peels, Elec. J. Env. Agricult. Food Chem., 8(6), 437-442 (2009)

8. Shyamala B.N. and Jamuna P., Chemical composition and antioxidant potential of peels from three varieties of banana, As. J. Food Ag-Ind., 4(1), 31-46 (2011)

9. Mahmoudi M., Aryaee P. and Mokhtari S., Evaluation of compositions and Nutritional facts in some varieties of kiwi fruit, 2 nd International Conference on Environmental Science and Technology, IACSIT Press, Singapore, 6, 344–350 (2011)

10. Parameswaran I. and Murthi V.K., Comparative study on physical and phytochemical analysis of Persea Americana & Actinidia deliciosa, International Journal of Scientific and Research Publication, 4(5), 1-5 (2014)

11. Chou H.N., Nee C.C., Ou A.S.M., Chou T.H. and Chien C.C., Characterization of the physicochemical and antioxidant properties of Taiwanese kiwifruit (Actinidia Setosa), Botanical Studies, 49, 215–224 (2008)

12. Lu Y., Zhao Y. and Fu C., Biological activities of extracts from a naturally wild kiwifruit, Actinidia macrosperma, Afr. J. Agric. Res., 6(10), 2231–2234 (2011)

13. P Padmanabhan and G Paliyath, University of Guelph, Guelph, ON, Canada ã 2016 Elsevier Ltd. All rights reserved

14. Research Journal of Chemistry and Environment Vol. 22 (9) September (2018) Res. J. Chem. Environment. Active Constituents of Kiwi (Actinidia Deliciosa Planch) Peels and Their Biological Activities as Antioxidant, Antimicrobial and Anticancer Salama Zeinab A.[1*], Aboul-Enein Ahmed M.[2] , Gaafar Alaa A.[1] , Abou-Elella Faten [2] , Aly Hanan F. [3] , Asker Mohsen S.[4] and Ahmed Habiba A.[1]

ISSN 2063-5346

DEVELOPMENT AND VALIDATION OF RP-HPLC METHOD FOR ASSAY OF FLUTICASONE FUROATE FROM NASAL SPRAY FORMULATION

Vitthal Chopade[1*], Vishnu Neharkar[2], Padmanabh Deshpande[3], Makarand Puri[4], Priti Khanapure[1], Vaishnavi Chopade[5], Minal Ghante[6], Jayshree Jagtap[7], Shital Godse[6], Vidhya Bhusari[6], Vasundhara Sawant[6], Sonali Labhade[8], Rajendra Kawade[9], Deepali Kadam[10], Nilesh Jadhav[11], Gaffar Sayyad[12], Dipti Phadtare[13], Shital Godse[6], Pandurang Vijapure[14], Kunal Survade[13], Rahul Mohan[9], Arvind Hatkar[9], Atul Baravkar[15]

Article History: Received: 01.02.2023 Revised: 07.03.2023 Accepted: 10.04.2023

Abstract

The literature search reveals that, several HPLC methods for the determination of Fluticasone furoate in combination with other drugs are reported with long run time, high solvent consumption or with less available instrument as compared with HPLC. There is no any reported HPLC method for individual assay of Fluticasone furoate from nasal spray formulation. So the purpose of present experimental work is to develop a rapid, simple, precise, accurate, specific, and sensitive high performance liquid chromatographic method for assay of Fluticasone furoate from nasal spray formulation. The desired chromatographic separation was achieved on the Inertsil ODS-3V 250 x 4.6 mm, 5µ column, using isocratic elution at 240 nm wavelength. The optimized mobile phase constituted of purified water and acetonitrile in the ratio of 20:80 % v/v delivered at the flow rate 1 ml/min with isocratic elution. The retention time of fluticasone furoate was 5 min. The method was validated according to International conference of harmonization guidelines in terms of accuracy, precision, specificity, robustness, linearity and other aspects of analytical validation. Linearity was established in the concentration range of 27.5 to 82.5 ppm (r^2=1.000). The recoveries obtained were 99.4 -100.5 %. Similarly the % RSD value for precision was also found to be within the acceptable limit. Developed method was simple and convenient which could be successfully applied for the routine analysis.

KEYWORD: Fluticasone furoate, Corticosteroid, Asthma, Allergic Rhinitis, RP-HPLC, Validation, ICH guidelines.

[1]Modern College of Pharmacy, Pune, India. 411044

[2]Rasiklal M. Dhariwal Institute of Pharmaceutical Education and Research, Pune, India. 411019

[3]AISSMS College of Pharmacy, Pune, India. 411001

[4]School of Pharmacy, Vishwakarma University, Pune, India. 411048

[5]PRES College of Pharmacy for Women, Chincholi, Sinnar, Nashik, India. 422102

[6]SMT Kashibai Navale College of Pharmacy, Kondhwa, Pune, India. 411048

[7]SGRS's College of Pharmacy, Saswad, Pune, India. 412301

[8]Dr. D Y Patil Institute of Pharmaceutical Sciences & Research, Pimpri, Pune, India. 411018

[9]Nandkumar Shinde College of Pharmacy, Vaijapur, Aurangabad, India. 413701

[10]K. K. Wagh College of Pharmacy, Nashik, India. 422006

[11]Dr. N. J. Paulbudhe College of Pharmacy, Ahmednagar, India. 414003

[12]SAJVPM's College of Pharmaceutical Science and Research Center, Beed, India. 431122

[13]KCT's R G Sapkal Institute of Pharmacy, Nashik, India. 422213

[14]Sarsam College of Pharmacy, Palashiwadi, Pune, India. 413110

[15]Shardabai Pawar Institute of Pharmaceutical Sciences and Research, Baramati, Pune, India. 413115

Corresponding author atul20068@gmail.com

DOI:10.31838/ecb/2023.12.s1-B.256

INTRODUCTION

HPLC is an analytical technique used to separate, identify and quantify the component. It finds its use for research, manufacturing, medical, legal purposes. The development of an analytical method for the identification and quantification of drugs by HPLC has received considerable attention in recent years because of their importance in quality control of drugs and drug products. In the present study attempt is made to develop and validate a simple HPLC method for Fluticasone furoate (FF).

Fluticasone furoate is a synthetic fluorinated corticosteroid having the chemical name [(6S,8S,9R,10S,11S,13S,14S,16R,17R)-6,9-difluoro-17-(fluoromethylsulfanylcarbonyl)-11-hydroxy-10,13,16-trimethyl-3-oxo-6,7,8,11,12,14,15,16-octahydrocyclopenta[a]phenanthren-17-yl] furan-2-carboxylateand the empirical formula is $C_{27}H_{29}F_3O_6S$. Chemical structure of Fluticasone furoate is presented in figure 1.

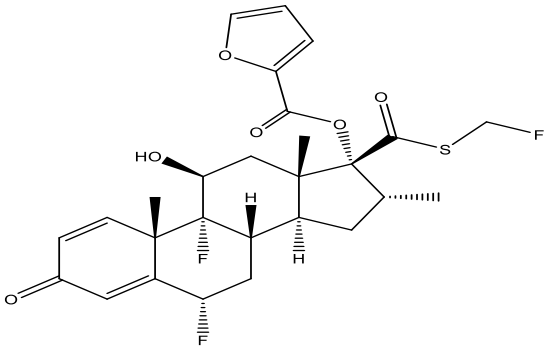

Figure 1: Chemical structure of fluticasone furoate

Fluticasone furoate is a white powder with a molecular weight of 538.58. It is practically insoluble in water. Fluticasone furoate nasal spray is a new topical corticosteroid, with enhanced-affinity and a unique side-actuated delivery device. As it has high topical potency and low potential for systemic effects, it is a good candidate for rhinitis treatment [1]. Fluticasone furoate has demonstrated treatment efficacy for asthma between 100µg and 200µg alone[2-3]. The advantages of the therapeutic profile of Fluticasone furoate have led to increasing use in the clinical practice, which encourages the development of new analytical method to provide driving force in today's pharmaceutical industry [4].

A detailed Literature survey of Fluticasone revealed that Fluticasone furoate and Fluticasone propionate (FP) though have same steroidal backbone but are completely different drugs with Fluticasone furoate showing distinct and superior properties [5]. There are many analytical method are available as spectrophotometry [6], LC [7], LC-MS [8-9], HPLC [10-17], UPLC [18], UPLC-MS [19-20], MEKC [21], RS-RD and MCR [22], others [23-24] for the determination of Fluticasone propionate as single or in combination with another drugs from pharmaceutical formulation and biological fluids. Literature survey also reveals that there are few analytical methods spectrofluorimetry [25], spectrophotometry [26], HPLC [25, 27-28], UPLC [29] methods for determination of fluticasone furoate in combination with another drugs. There is no any reported RP-HPLC method for individual assay of Fluticasone furoate from nasal spray formulation. Therefore there is need to develop a simple assay method for the Fluticasone furoate.

MATERIALS AND METHODS

Materials:

High purity water was generated by using Milli-Q Plus water purification system (Millipore® Elix 100). HPLC grade Acetonitrile and analytical reagent grade Hydrochloric acid were procured from Rankem Chemicals India-Lab chemicals, Mumbai. Analytical grade reagents Sodium Hydroxide, Hydrogen Peroxide were obtained from Merck Chemicals Limited, Mumbai. Reference standard of Fluticasone furoate, drug product, placebo

solution were provided by Sava Healthcare Ltd, MIDC, Chinchwad, Pune.

Chromatographic System:

The HPLC system (model: LC-2010C_{HT}, Make-Shimadzu corporation, Kyoto, Japan.) composed of Lab solutions software certified for QA/QC was used. It consists of vacuum degasser, automatic front panel control, PDA detector, thermostat column compartment with C18 column [4.6mm x 250mm, pore size 5µm], high performance auto sampler, thermostat for high performance auto sampler. Its integrated solvent and sample management capabilities provide the flexibility and ruggedness needed to accommodate an enormous range of HPLC separation challenges.

Chromatographic condition:

The chromatographic condition was optimized using Inertsil ODS-3V 250 x 4.6 mm, 5µ column (G. L. Sciences, Japan). Mixture of HPLC grade milli-Q water and acetonitrile in the ratio of 20:80 % v/v was used as mobile phase. Mobile phase was used as a diluent. The finally selected and optimized conditions were as follows: injection volume 10µL, isocratic elution, at a flow rate of 1 mL/min at 30°C (column oven) temperature, detection wavelength 240 nm. The stress degraded samples and the solution stability samples were analysed using a PDA detector covering the range of 200-400 nm.

Standard solution preparation:

Accurately weighed quantity of about 27.5 mg of Fluticasone Furoate working standard transferred to a 50 mL volumetric flask. Then added 20 ml of diluent and sonicated in an ultrasonic bath for 5 min to dissolve. This solution was then diluted up to the mark with diluent and mixed well. 5ml of this solution is then diluted to 50 ml with diluent to prepare standard stock solution of 55 ppm of Fluticasone furoate.

Sample solution preparation:

An accurately weighed 5 gm of sample (equivalent to 2.75 mg of Fluticasone furoate) solution was taken to into the 50 ml volumetric flask. About 20 ml of diluent was added and sonicated in an ultrasonic bath for 5 min. This solution was then diluted up to the mark with diluent and Sample solution of 55 ppm was prepared. It was then filtered through 0.45 µm nylon syringe filter and the filtrate was collected after discarding first few milliliters.

Placebo (other substance without Fluticasone furoate) solution preparation:

An accurately weighed 5 gm of sample solution was taken to into the 50 ml volumetric flask. About 20 ml of diluent was added and sonicated in an ultrasonic bath for 5 min. This solution was then diluted up to the mark with diluent and mixed well. It was then filtered through 0.45 µm nylon syringe filter and the filtrate was collected after discarding first few milliliters.

Method validation

Validation of the optimized HPLC method was carried out with the following parameters.

System suitability parameters:

System suitability tests are an integral part of chromatographic method validation [30]. The tests were used to verify that the reproducibility of the chromatographic system is adequate for analysis. To ascertain its effectiveness system suitability tests were carried out on freshly prepared standard solution. 10 µL of solution was injected into the optimized chromatographic system. For system suitability six replicates of working standard samples were injected and the parameters like retention time (RT), theoretical plate (N), peak area, tailing

factor and resolution of sample were calculated.

Linearity:

The linearity of an analytical procedure is its ability (within a given range) to obtain test results which are directly proportional to the concentration (amount) of analyte in the sample [30]. The linearity of a method demonstrated by preparing solutions over the concentration levels ranging from 50 % to 150 % of working concentration. These solutions injected in triplicate into the system and the peak area of analyte peak recorded. Linearity graph of concentration Vs average peak area of analyte plotted separately. The correlation co-efficient, slope and y intercept evaluated.

Accuracy:

The accuracy of an analytical procedure expresses the closeness of agreement between the value which is accepted either as a conventional true value or an accepted reference value and

the found value [30]. The accuracy of the method was determined by analysing the sample solution at three different concentration levels 50 %, 100 % and 150 % of the usual sample preparation concentration, and injected for the accuracy studies. The area under curve obtained was checked and analysed for the recovery percentage.

Precision:

The precision of an analytical procedure expresses the closeness of agreement (degree of scatter) between a series of measurements obtained from multiple sampling of the same homogeneous sample under the prescribed conditions [30]. The precision of the method was checked and verified by system precision, method precision and intermediate precision (Ruggedness) variation studies. In system precision studies six injections of standard solution prepared as per the usual analytical method and injected into the system. In method precision six replicates of sample solution of the same batch were prepared and injected into the system. In intermediate precision (ruggedness) six replicates of a single batch samples were prepared and analysed by different analyst, on different day and on different instrument.

Robustness of the method:

The robustness of an analytical procedure is a measure of its capacity to remain unaffected by small, but deliberate variations in method parameters and provides an indication of its reliability during normal usage [30]. The effect of change in flow rate (±0.1mL/min), column oven temperature (±5°C), wavelength (±3 nm), mobile phase composition (±5%) on the retention time, theoretical plates and tailing factor were studied. During study other chromatographic conditions were kept same as per the experimental section.

Specificity:

Specificity is the ability to assess unequivocally the analyte in the presence of components which may be expected to be present. Typically these might include impurities, degradants, matrix, etc [30]. To determine the peak purity selectivity studies was performed by injecting diluents, standard solution and sample solution. Forced degradation study was carried out to prove the specificity of the method.Sample and placebo was exposed under relevant stress conditions: Thermal, photolytic, humidity, acid & base hydrolysis and oxidation (table 1). Peak of Fluticasone furoate was investigated for spectral purity in the chromatogram.

Table 1: Forced Degradation study conditions and % degradation

S.N.	Condition	Degrading agents/ conditions	Exposure period	% Degradation
1	Acid degradation	1N HCl	for 2 Hrs. at R.T.	6.2
2	Base degradation	1N NaOH	for 2 Hrs. at R.T.	0.4
3	Peroxide degradation	30% H_2O_2	for 24 Hrs. at R.T.	0.4
4	Thermal degradation	60°C	for 2 Days	0.6
5	Photolytic degradation	1.2 million lux hours and 200 watt hrs./m^2	-------	2.1
6	Humidity degradation	40°C/75% RH	For 7 days	4.3

Filter validation:

Sample solution was prepared according to the method. The solution was filtered through 0.45 µm filter and vials were filled by discarding 0 mL, 2 mL and 5 mL of solution and these solutions were injected as sample solutionand percentage assay was determined and absolute % difference between centrifuged and filtered sample was calculated.

Solution stability:

The system suitability solution and sample solutions were prepared on day 0 of experiment, stored these solutions at room temperature for every time interval up to 3 days and analyzed these solutions on subsequent days. The standard solution was prepared freshly at the time of analysis and calculated the % assay of analyte in the standard solution and in the sample solution.

RESULTS AND DISCUSSION

Method development and optimization:

The initial literature search indicated that very few HPLC methods are available for the drug as individual or in combination with different drugs which uses the buffer in mobile phase. Based on literature search, attempts were made to develop a simple method which requires less solvent, short runtime and high selectivity. Top priority was given elute the peak with water and acetonitrile only instead of buffer solution or only with organic solvents. In preliminary experiment the water and acetonitrile were used as mobile phase in different ratio with BDS C-18 (150mm X 4.6 mm X 5µm) column with flow rate 1ml/min and detection wavelength 240 nm. The column temperature was maintained ambient. Injection volume is 10µL and runtime is for 20 min. The expected peak with short retention time was obtained with the water and acetonitrile (20:80) ratio but peak shape was broad. The effect of column was checked. It improved peak shape. Finally the method was developed with Inertsil ODS -3V 250 x 4.6 mm, 5µ column. The chromatogram obtained was better than the previous one in all aspects with good peak shape, tailing factor, resolution and theoretical plate as per USP requirement. The retention time of fluticasone peak was about 5.0±1 minute. The Representative chromatogram of standard solution and sample solution is shown in the figure 2 and figure 3 respectively.

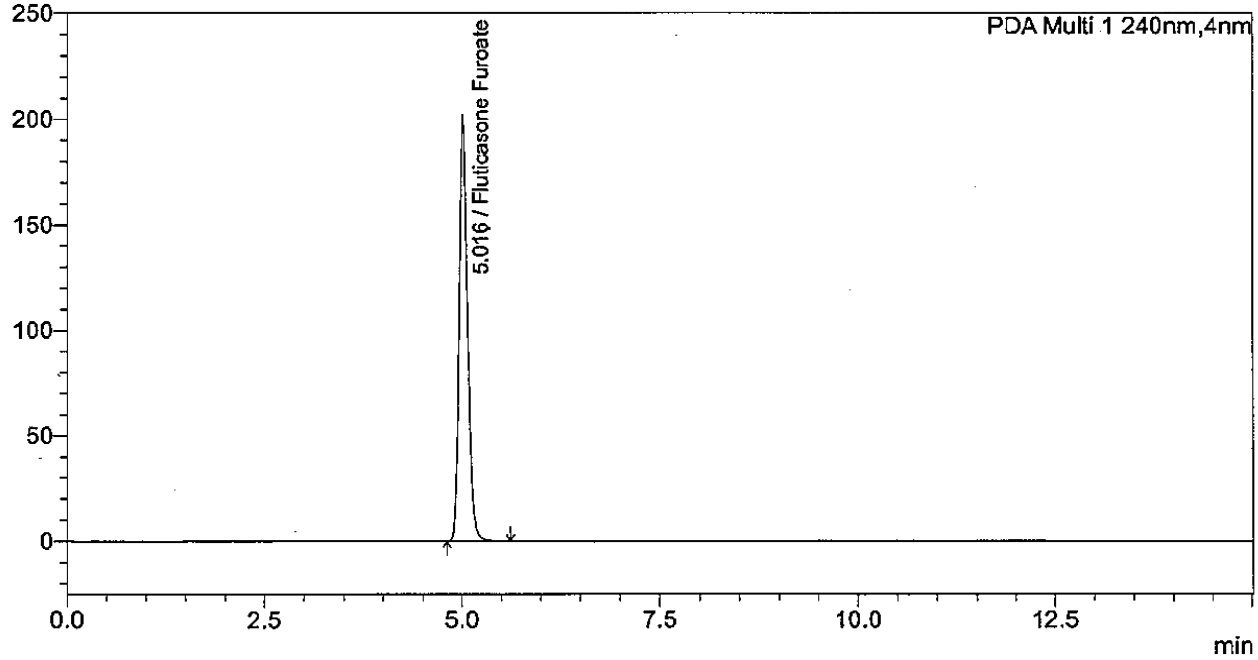

Figure 2: Representative chromatogram of standard solution

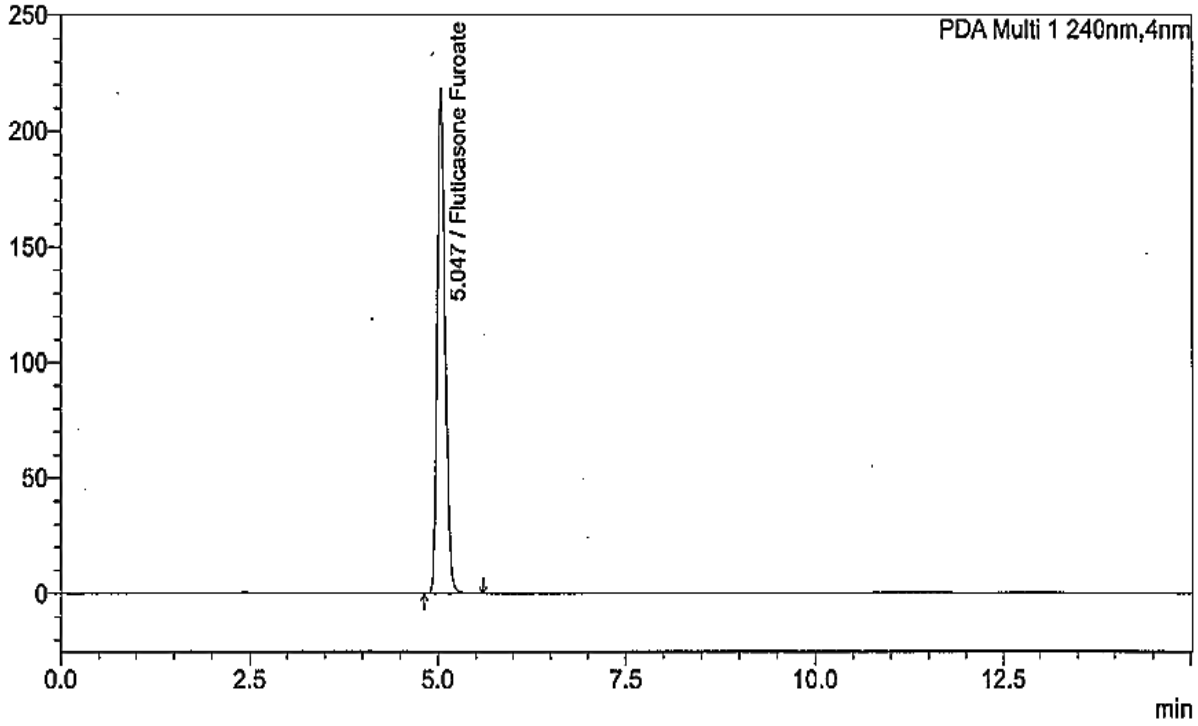

Figure 3: Representative chromatogram of sample solution

Method validation results:

The system suitability testing is used to verify that the reproducibility of the system are adequate for the analysis performed [30]. The system suitability parameters such as runtime, theoretical plates, peak purity, tailing factor were associated with confined values. The plot of peak area response against concentration is linear as shown in figure 4 over the concentration range of 27.5ppm-82.7ppm. The results of linearity are shown in table 2.

Table 2: Linearity results

Linearity Level	Conc. (%)	Conc. (ppm)	Area
1	50	27.58	813243
2	80	44.13	1302729
3	100	55.16	1630071
4	120	66.19	1950490
5	150	82.74	2444963
		Slope	29551.5238
		Intercept	-1762.8544
		Correlation Coefficient [R]	1.000
		R^2	1.000

It was found that correlation coefficient (r^2=1.00) and regression analysis were within the limits (table 4). To ensure the reliability and accuracy of the method recovery studies were carried out at 3 different levels (50 %, 100 %, and 150 %). The results of recovery studies are presented in table 3.

Table 3: Accuracy Results

Level	Amount added(ppm)	Amount recovered(ppm)	%Recovery*	%RSD
50%	27.60	27.72	100.5	0.64
100%	55.20	54.86	99.4	0.26
150%	82.80	82.70	99.9	0.12

* mean of three determinations

From results it is revealed that there is good correlation between amount added and drug found in overall concentration range. The system precision, method precision and intermediate precision (ruggedness) are calculated. The % RSD values (table 4) were below 2.0 % indicating a good precision [30].

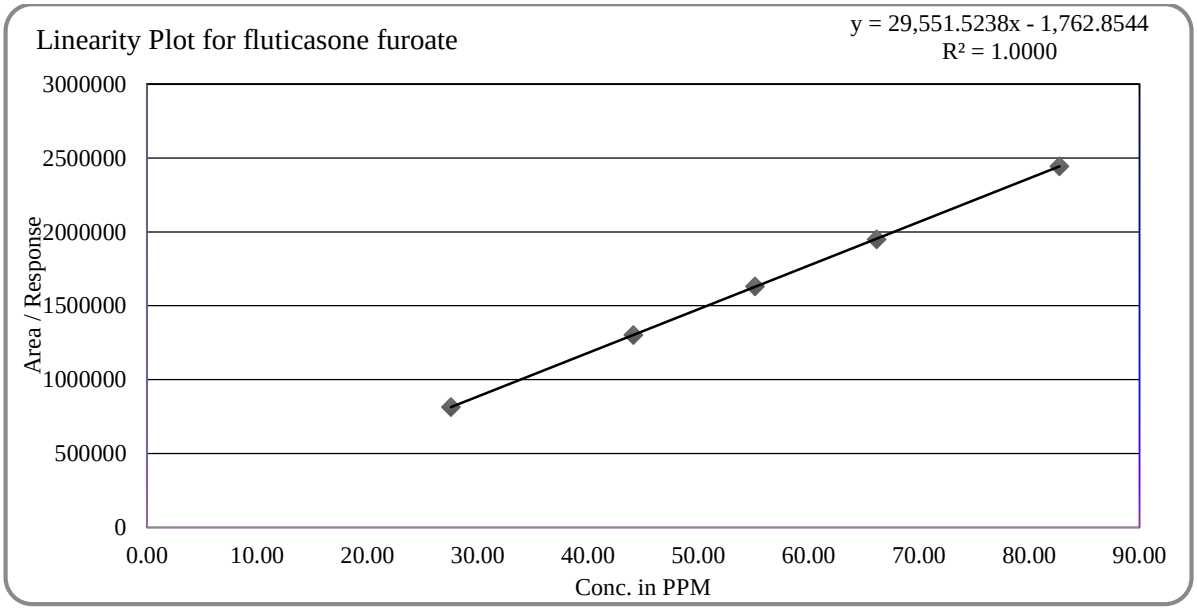

Figure 4: Linearity graph for assay of fluticasone furoate

Robustness of the method was determined by small deliberate changes in method parameters and the content of the drug was not adversely affected by these changes as evident from the low value of % RSD (table 4) that the method was robust. During assay study, there was no change in the content of the drug due to presence of excipient which reveals that the method is specific [30]. Forced degradation studies were performed to demonstrate selectivity and stability indicating capability of the proposed HPLC method. Analyte peaks were investigated for spectral purity in the chromatogram of all exposed sample and found spectrally pure (table 4).

Table 4: Overall results of parameters used in validation

S.N.	Parameter	Results
1	Linearity	27.5 (ppm)- 82.7 (ppm) linearity Equation y=29551.5238x-1762.8544 r2= 1.000
2	Accuracy	Mean % Recovery=99.93 %
3	Precision	
	system precision	% RSD=0.18
	method precision	% RSD=0.90
	intermediate precision	% RSD=0.90
	Overall results of analyst 1&2	% RSD=0.82
3	Specificity	
	Selectivity	No interference of diluent and placebo at the retention time of analyte peak and the analyte peak passes peak purity.

	Forced Degradation	Degradants peaks are well separated from the analyte peak and peak purity passes for analyte peak.	
4	Robustness	low (-)	high(+)
	Change in flow rate	0.9(ml/min) % RSD=0.05	1.1(ml/min) % RSD=0.07
	change in column oven temperature	25°C % RSD=0.03	35°C % RSD=0.13
	change in wavelength	237(nm) % RSD= 0.79	243(nm) % RSD=0.80
	change in mobile phase organic composition	(24:76 %v/v) (16:84 %v/v) % RSD=0.25	% RSD=0.37
5	Filter validation	% difference in result with centrifuged sample	
		0ml discarded=0.27 2ml discarded=0.05 2ml discarded=0.07	
6	Solution stability	stable for 3 days % RSD of standard solution=0.62 % RSD of sample solution=0.75	

The % RSD between results for the analyte obtained for stored standard and sample solution (table 4) is within limit up to the 3 days at room temperature then it can be concluded that solution is stable up to 3 days at room temperature. During filter validation % absolute difference between filtered and centrifuged test solution are less than 2.0 % (table 4) hence nylon membrane filter can be used by discarding first 5 ml.

CONCLUSION

An isocratic RP-HPLC method was successfully developed for the assay of Fluticasone furoate in liquid pharmaceutical formulation. The developed method is selective, precise, accurate, linear, and robust. Forced degradation data proved that the method is specific for the Fluticasone furoate. It can be utilized for assay determination of bulk

and finished product of Fluticasone furoate.

REFERENCES

1. Binachi P.G., Agondi R., Stelmach R., Cukier A., Kalil J. Fluticasone furoate nasal spray in the treatment of allergic rhinitis. Therap. Clinic. Risk. Manag., 2008;4(2):465-472

2. Liburn P. A., Ainge A. H., Thomas P. S. Fluticasone furoate once daily preparation in patient with persistant asthma. J. Lung. Health. Dis.,2019;3(2):3-10.

3. Lotvall J.et. al. Efficacy and safety of fluticasone furoate 100µg once-daily in patients with persistent asthma: A 24-week placebo and active-controlled randomized trial.Respi. Medic.,2014;108:41-49.

4. Bernal J.L., Del Nozal M. J., Martin M. T., Diez-Masa J. C., Cifuentes A. Quantitation of active ingredients and excipients in nasal sprays by high performance liquid chromatography, capillary electrophoresis and UV spectroscopy. J. Chroma.A.,1998;823:423-431.

5.Biggadike K. Fluticasone furoate/fluticasone propionate-different drugs with different properties. Clin. Respir J., 2011;5(3):183-184

6. El-Abasawy N. A., Attia K. A., Abouserie A. A., El-Olemy A, Elsayed A. O. Different spectrophotometric methods applied for simultaneous analysis of binary mixture of formoterol and fluticasone: a comparative study J. Anal. Pharm. Res.,2018;7(2):160–165.

7. Sangoi M. S., Nogueira D. R., Silva L. M., Leal D. P., Dalmora S. L.Validation of a Stability Indicating Reversed Phase LC Method for the Determination of Fluticasone Propionate in Pharmaceutical Formulations. J of Liq. Chroma. & Related Techno., 2008;31: 2113–2127.

8. Krishnaswami S., Mo¨llmann H., Derendorf H., Hochhaus G. A. sensitive LC–MS:MS method for the quantification of fluticasone propionate in human plasma. J. of Pharm. Biomed., Anal., 2000;(22):123-129.

9. Laugher L., Noctor T. G., Barrow A, Oxford J.M., Phillips T. An improved method for the determination of fluticasone propionate in human plasma. J. of Pharm. Biomed. Anal., 1999;(21):749-758.

10. Prathap B., Jegannath S., Swathikrishna K.V., Priyanka V., Rajeshwari G., Gobalakrishnan P. Method development and validation for simultaneous estimation of azelastine and fluticasone in pharmaceutical dosage form by RP-HPLC. Asia. J. Pharm. Anal. Medi. Chem.,2016;4(2):79-87.

11. Narsimha Rao L. K. et al. simultaneous estimation of fluticasone propionate, azelastine hydrochloride polyethyleneglycol & benzalkonium chloride by RP-HPLC method in nasal spray preparation Int J. Res.Pharm.Sci., 2012 ;1(4):473-480.

12. Purvis T. simultaneous highperformance liquid chromatography assay of pentoxifylline, mupirocin, itraconazole, and fluticasone propionate in Humco™ Lavare Wound Base Chroma. 2015;*2*: 642-654.

13. Paczkowska E., Smukowska D., Tratkiewicz E., Bialasiewicz P., HPLC method for simultaneous determination of salmeterol xinafoate and fluticasone propionate for the quality control of dry powder inhalation products. Acta

Chromatographica 2015;27(2):309–320.

14. Nian Y. B. Li, Tattam B. N., Brown K. F., Seale J. P. A sensitive method for the quantification of fluticasone propionate in human plasma by high-performance liquid chromatography: atmospheric pressure chemical ionisation mass spectrometry. J. Pharm. Biomed. Anal., 1997;(16):447–452.
15. Couto A. Sá., Cardoso D. E., Cabral-Marques H.M. Validation of an HPLC analytical method for quantitative/qualitative determination of fluticasone propionate in inhalation particles on several matrixesSci Pharm., 2014; 82(4): 787–797.
16. Shahanaz M., Vageesh N.M., Nizamuddin N.D., Hazra B. B. Development and validation of RP-HPLC-PDA method for simultaneous determination of fluticasone and salmeterol in bulk and pharmaceutical dosage form. Innov. Inter. J. Medi. Pharma. Sci., 2018;3(1):25-28.
17. Murnane D., Martin G.P., Marriott C. Validation of a reverse-phase high performance liquid chromatographic method for concurrent assay of a weak base (salmeterol xinafoate) and a pharmacologically active steroid (fluticasone propionate) J. of Pharm. Biomed. Anal., 2006;(40):1149–1154.
18. Chengalva P, Kuchana M. Development and validation of ultra-performance liquid chromatographic method for the analysis of pulmonary drug product containing formoterol fumarate and fluticasone propionate. Int. Res. J. Pharm., 2018;9(9):152-157.
19. Naira S. G., Patel D. P., Sanyal M., Singhal P., Shrivastava P. S. Simultaneous analysis of glucocorticosteroid fluticasone propionate and its metabolite fluticasone propionate 17-carboxylic acid inhuman plasma by UPLC–MS/MS at sub pg/mL level. J. of Pharm. Biomed. Anal.2017 ;(135): 1–7.
20. Patel C. J., Bambhroliya V., Development of highly-sensitive method and its validation for the determination of fluticasone in human plasma by UPLC-MS/MS. IJRAR., 2019;6(1):399-411.
21. Sangoi M. S., Silva L. M., Avila F. B., Dalmora S. L. Determination of fluticasone propionate in nasal sprays by a validated stability-indicating MEKC method J. Chroma. Sci., 2010;(48): 641-646.
22. Merey H. A., El-Mosallamy S. S., Hassan N. Y., El-Zeany B. A.Simultaneous determination of fluticasone propionate and azelastine hydrochloride in the presence of pharmaceutical dosage form additives. 2016;(16):1386-1425.
23. M.S. Sangoi et al. A high-throughput liquid chromatography tandem mass spectrometry method for the comparative determination of fluticasone propionate by reversed-phase liquid chromatography and capillary electrophoresis methods in pharmaceutical nasal sprays. Eur. J. Mass Spectrom., 2009;(15):723–730.
25. El-Masrya A. A., Hammouda E. A., El-WasseefD. R., El-Ashrya S. M., Eco-friendly green liquid chromatographic separations of a novel combination of azelastine and fluticasone in the presence of their pharmaceutical dosage form additives. Current Anal. Chem., 2018;(14):1-10.
26. Patel D.et al. HPLC-UV and spectrofluorimetric methods for simultaneous estimation of fluticasone furoate and vilanterol in rabbit plasma: A pharmacokinetic study. J. Chroma. B, Anal. Techno. Biomed. Life Sci. 2019;(1132):121842.

27. Masimukku S. K., Chintala R. Development and validation of spectrophotometric methods for simultaneous estimation of vilanterol and fluticasone furoate in pharmaceutical formulations. Asian J. Pharm. Clini. Res., 2017;10(4):302-305.

28. Masimukku S. K., Chintala R. Development and validation of stability indicating RP-HPLC method for fluticasone furoate and vilanterol in pharmaceutical formulations. Asian J. Pharm. Clini. Res., 2018;55(3):27-31.

29. Gampa V. K. et al. Analytical Method Development and Validation for the Simultaneous Estimation ofFluticasone and Vilanterol by RP-HPLC Method in its Pharmaceutical Dosage Forms.IJMPR., 2016;4(6): 336-343.

30. Trivedi R. K., Challa S., Patel M. C., Trivedi D. R. Chatrabhuji P. M. A Rapid, Stability-Indicating RP-UPLC Method for the Simultaneous Determination of Fluticasone Furoate and

Benzalkonium Chloride in a Pulmonary Drug Product**,** Chem. Sci. Trans., 2013;2(4):1184-1191.

31. ICH Harmonised-Tripartite Guideline (2005) validation of analytical procedures: text and methodology Q2 (R1).

Current Indian Science

Content list available at: https://currentindianscience.com

RESEARCH ARTICLE

Design, Synthesis and Antimicrobial Activity of 1,3-Diazine Derivatives

Pranali A. Jadhav[1,2], Jayashree R. Jagtap[2,*], Meenakshi N. Deodhar[3], Rajashri S. Chavan[2] and Smita J. Pawar[2]

[1]*Department of Pharmaceutical Chemistry, D. Y. Patil Unitech Society's, D. Y. Patil Institute of Pharmaceutical Sciences and Research, Pimpari, Pune, Maharashtra 411018, India*

[2]*Department of Pharmaceutical Chemistry, Pune District Education Association's Seth Govind Raghunath Sable College of Pharmacy, Saswad, Pune, Maharashtra 411018, India*

[3]*Lokmanya Tilak Institute of Pharmaceutical Sciences, Pune, Maharashtra 411018, India*

Abstract:

Background:

Pyrimidines have been shown to possess numerous biological activities, such as antimicrobial, anticancer, anticonvulsant, antiviral, and anti-inflammatory.

Objective:

Encouraged by these data, the synthesis of 2-((1*H*-benzo[*d*]imidazol-2-yl)methylthio)-4- amino-6-phenylpyrimidine-5-carbonitrile (3a-g) was performed.

Methods:

4-amino-2-mercapto-6-phenylpyrimidine-5-carbonitrile was dissolved in an aqueous sodium hydroxide solution, and to this clear solution, 2-chloromethyl-1*H*-benzimidazole in methanol was added, and the reaction mixture was stirred under reflux to get the desired product. The structures of the newly synthesized compounds were confirmed by their physical, chemical, and spectral data. The synthesized derivatives were screened for their *in vitro* antibacterial activity against Gram-positive bacteria, *Staphylococcus aureus* and *Bacillus subtilis*, and Gram-negative bacteria, *Escherichia coli* and *Pseudomonas aeruginosa*, by using ciprofloxacin as a reference standard. While, their antifungal activity was evaluated against *Aspergillus niger* and *Candida albicans* using fluconazole as a reference drug. The docking study was performed to check the interactions of target compounds (3a-g) with homo sapiens DHFR (PDB: 1S3V), bacterial (*S. aureus*) DHFR (PDB: 2W9T), and DHPS (PDB: 1AD4) protein. The dock score and binding interactions were recorded.

Results:

The antimicrobial activity study indicated compounds with chloro (3b), fluoro (3f), and bromo (3g) substituents to show good antibacterial as well as antifungal activity. The docking study revealed that the same compounds, *i.e.*, 3b, 3f, and 3g, showed good dock score and comparable interactions compared to the reference ligand (trimethoprim/sulfadiazine), which confirmed their selectivity.

Conclusion:

It can be presumed that the synthesized compounds have the capability for further promotion as novel antimicrobial agents.

Keywords: Antimicrobial, Pyrimidine, Antibacterial, Docking, DHFR, DHPS.

Article History	Received: October 22, 2022	Revised: March 21, 2023	Accepted: April 10, 2023

1. INTRODUCTION

According to the World Health Organization (WHO), the emergence and spread of resistance to existing antimicrobial agents have been recognized as one of the biggest threats to global public health. This increased resistance has limited the selection of antimicrobials to treat the disease. Therefore, there is a need to develop new and improved antibacterial drugs with novel targets and that are not liable to the existing resistance mechanisms [1].

Currently, pyrimidine ring-containing compounds have attracted the major interest for antibacterial drug discovery. In view of their good activities and varied mechanisms of action, plentiful pyrimidine-containing heterocyclic compounds have directed the focus of many scientists towards them [2]. Therefore, a large number of pyrimidine derivatives have become of considerable biological and chemical interest. In the

* Address correspondence to this author at the Department of Pharmaceutical Chemistry, Pune District Education Association's Seth Govind Raghunath Sable College of Pharmacy, Saswad, Pune, Maharashtra 411018, India;
E-mail: jayarjagtap@gmail.com

last several decades, there has been a significant increase in the preparation of pyrimidine derivatives and the evaluation of their biological activity [3]. Variation of substituents on the pyrimidine nuclei could potentially affect the interaction of the molecules with biological targets. Many substituted pyrimidines have been reported to display a large panel of biochemical properties, including anticonvulsant [4, 5], antibacterial, antifungal [6], antitumor [7, 8], antiviral [9], and antibiotic activities [10].

Pyrimidine-containing molecules carry out essential functions in human metabolism as ribonucleotide bases in RNA (uracil and cytosine) and as deoxyribonucleotide bases in DNA (cytosine and thymine). Various drugs that act as antimicrobial agents via inhibition of nucleic acid biosynthesis contain a pyrimidine ring in their structure. Pyrimidine derivatives also act as antifolates by inhibiting the folic acid biosynthesis pathway by inhibiting dihydrofolate reductase (DHFR) and dihydropteroate synthase (DHPS) enzymes [11].

Abd El-Aleam *et al.* synthesized a series of 1,2,4-triazolo[1,5-a]pyrimidine derivatives and screened them for their antibacterial and antifungal activities, as well as their safety profile. Furthermore, compounds displaying significant growth inhibition percentage (80–100%) at 32 μg/mL against any of the tested bacterial or fungal species were screened for their minimum inhibitory concentrations (MIC). Among the synthesized compounds, pyrimidine-containing benzohydrazide derivatives exerted high activity against the tested bacterial strains with MIC values of 0.25–1 μg/mL, respectively [12]. T Panneerselvam and J R Mandhadi synthesized new series of antimicrobial thiosemicarbazide substituted pyrimidine derivatives. In accordance with the data obtained from antimicrobial activity, all the synthesized derivatives have shown good activity against the tested microbes. Among them, compounds bearing 2-hydroxy and 3-chloro derivatives of thiosemicarbazide substituted pyrimidine have shown good activity against all the tested organisms [13]. Al- Juboori and Mahmood have reported the synthesis, antimicrobial evaluation, density functional theory, and docking studies of some new 2-mercapto pyrimidine Schiff bases displaying antimicrobial and antifungal activities. Results obtained from molecular docking discovered compounds with bulky phenyl groups to be important for blocking the active centres of glucose-6-phosphate synthase in bacteria and fungi [14]. Khatri and Shah reported the effective microwave synthesis of bioactive thieno [2,3-d] pyrimidines. The compounds were found to exhibit significant antimicrobial activity [15]. Shehab *et al.* synthesized a series of pyrimidines and condensed pyrimidine derivatives. The oxazolopyrimidine derivative showed the highest antibacterial activity [16]. Besides these synthetic derivatives, marketed antimicrobial drugs containing pyrimidine nucleus are available, such as trimethoprim, piromidic acid, flucytosine, broxuridine, *etc.*

The intensifying rate of microorganisms exhibiting resistance to known chemotherapeutic agents has led to continued interest in the advancement and research on potent, broad-spectrum antibacterial agents [17]. Among the various strategies, the targeting of proteins is the most promising strategy for the development of new antibacterial therapeutics; DHFR is generally a significant target for the treatment of a variety of microbial infections [18, 19]. The noticeable variances between the eukaryotic and prokaryotic DHFRs have motivated the discovery of the antibacterial agent trimethoprim (TMP). TMP binds bacterial DHFRs 10^5 times firmer than it does vertebrate DHFRs. The clinical success of trimethoprim reveals that this enzyme is a beneficial target for the invention of novel antibacterial agents [20].

2. MATERIALS AND METHODS

2.1. Chemistry

All chemicals used in the synthesis were of laboratory grade. Melting points were determined in an open capillary with Veego (model: VMP-D) electronic apparatus, and are uncorrected. Thin layer chromatography (TLC) was performed on precoated aluminium sheets (silica gel 60F254, 6 x 2.5 cm) using appropriate solvent systems. The spots were visualized under ultraviolet light. The IR spectra of the synthesized compounds were recorded on a Shimadzu 8400-S FT-IR spectrophotometer using potassium bromide. The ^{1}H NMR spectra were recorded in $CDCl_3$ and DMSO using NMR BRUKER 500 MHz, and chemical shift values are given in units as parts per million, downfield from tetramethyl silane (TMS) as an internal standard. The mass spectra were recorded using the Bruker Impact mass analyser. Molecular docking was carried out using Vlife MDS 4.6 software. The synthetic scheme adopted for the synthesis of the intermediate as well as final compounds is depicted in Fig. (**1**). The key intermediates were synthesized in our lab as explained below.

2.1.1. Synthesis of 4-amino-2-mercapto-6-phenylpyrimidine-5-carbonitrile (1a-g)

Sodium ethoxide was prepared by dissolving 0.23gm (0.01 mol) sodium metal in 15ml of absolute ethanol; to this, 0.55gm (0.01 mol) malononitrile was added, the solution was stirred well, and then 1.01ml (0.01 mol) benzaldehyde and 0.76gm (0.015 mol) thiourea were added. The reaction mixture was heated at reflux in a water bath till the completion of the reaction. The reaction progress was monitored using TLC. The reaction mixture was poured on crushed ice and 3-4 drops of glacial acetic acid were added. The separated solid was filtered, dried, and the crude product was recrystallized using aqueous ethanol [21].

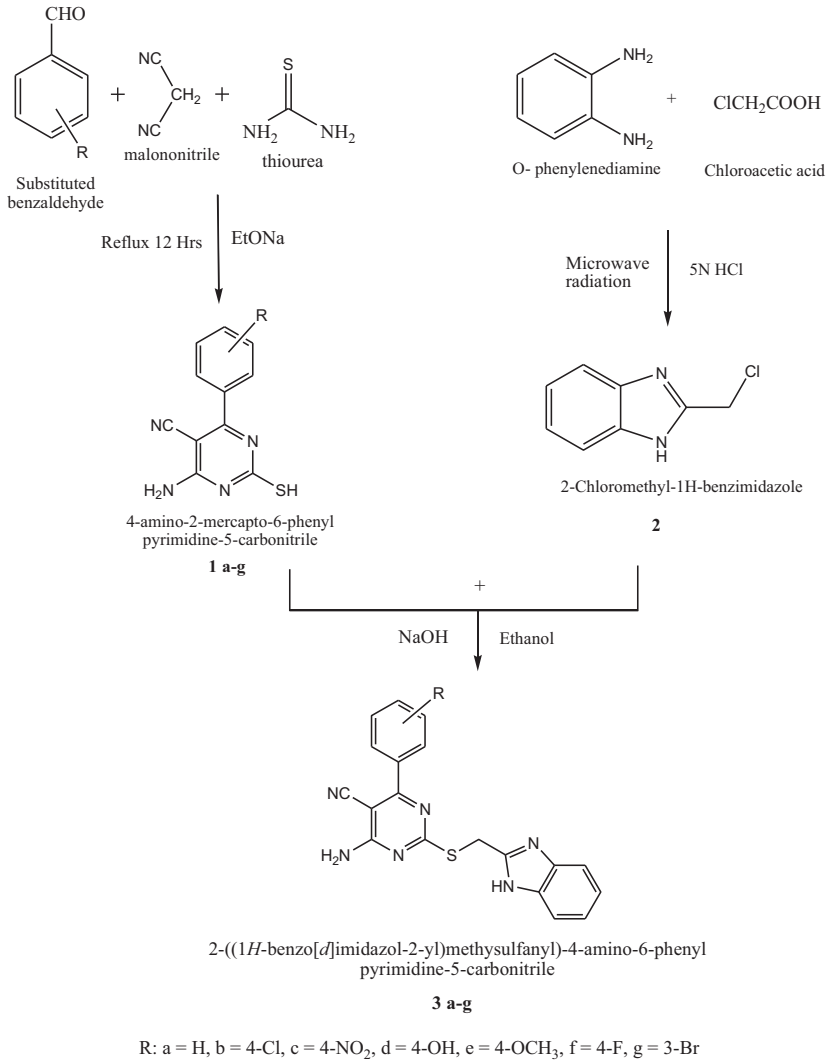

Fig. (1). Scheme for the synthesis of target compounds.

2.1.1.1. 4-amino-2-mercapto-6-phenylpyrimidine-5-carbonitrile (1a)

Yellow powder, yield: 73%, M.P. 188-190 °C, IR (cm^{-1}): 3427.98 (N-H), 3039.91 (aromatic C-H), 2585.45 (S-H), 2191.21 (C≡N), 1658.84 (C=N), 1519.95 (C=C), 1172.76 (C-N), 601.21 (C-S).

2.1.1.2. 4-amino-6-(4-chlorophenyl)-2-mercaptopyrimidine-5-carbonitrile (1b)

Faint yellow powder, yield: 64%, M.P. 124-126°C, IR (cm^{-1}): 3448.84 (N-H), 3448.84 (aromatic C-H), 2515.26 (S-H), 2229.79 (C≡N), 1712.85 (C=N), 1581.68 (C=C), 1095.60 (C-N), 825.56 (C-Cl), 709.83 (C-S).

2.1.1.3. 4-amino-2-mercapto-6-(4-nitrophenyl) pyrimidine-5-carbonitrile (1c)

Dark brown powder, yield: 78%, M.P. 194-196°C, IR (cm^{-1}): 3363.97 (N-H), 3109.35 (aromatic C-H), 2613.57 (S-H), 2241.35 (C≡N), 1604.83 (C=N), 1527.67 (C=C), 1350.22 (N=O), 1111.03 (C-N), 709.83 (C-S).

2.1.1.4. 4-amino-6-(4-hydroxyphenyl)-2-mercaptopyrimidine-5-carbonitrile (1d)

Cream coloured powder, yield: 59%, M.P. 282-284°C, IR (cm^{-1}): 3564.57 (O-H), 3387.11 (N-H), 3132.50 (aromatic C-H), 2589.25 (S-H), 2353.23 (C≡N), 1627.97 (C=N), 1512.24 (C=C), 1265.35 (C-N), 671.25 (C-S).

2.1.1.5. 4-amino-2-mercapto-6-(4-methoxyphenyl) pyrimidine-5-carbonitrile (1e)

Reddish brown powder, yield: 76%, M.P. 164-166°C, IR (cm^{-1}): 3248.23 (N-H), 3055.35 (aromatic C-H), 2592.41 (S-H), 2214.35 (C≡N), 1697.41 (C=N), 1519.96 (C=C), 1257.63 (C-O), 1180.47 (C-N), 524.66 (C-S).

2.1.1.6. 4-amino-6-(3-bromophenyl)-2-mercaptopyrimidine-5-carbonitrile (1f)

Yellowish powder, yield: 81%, M.P. 180-182°C, IR (cm^{-1}): 3363.97 (N-H), 3178.79 (aromatic C-H), 2691.21 (S-H), 2191.21 (C≡N), 1651.12 (C=N), 1481.38 (C=C), 1172.76 (C-N), 694.40 (C-S), 509.22 (C-Br).

2.1.1.7. 4-amino-6-(4-fluorophenyl)-2-mercaptopyrimidine-5-carbonitrile (1g)

Cream coloured powder, yield: 68%, M.P. 246-248°C, IR (cm^{-1}): 3317.67 (N-H), 3035.35 (aromatic C-H), 2685.00 (S-H), 2222.07 (C≡N), 1620.26 (C=N), 1558.54 (C=C), 1234.48 (C-F), 1157.33 (C-N), 709.11 (C-S).

2.1.2. Synthesis of 2-chloromethyl-1H-benzimidazole (2)

In a 250 ml three-necked flask, a solution containing 7.5 gm (0.08 mol) of chloroacetic acid and 7.5 gm (0.07 mol) of *o*-phenylenediamine was dissolved in 60 ml of 5N HCl. The mixture was irradiated in a microwave at 750 W for 30 min. The reaction progress was monitored by TLC. The reaction mixture was cooled to about 5°C. It was neutralized with aq. ammonium hydroxide. The product was filtered and washed with water, dried, and crude product was recrystallized from methanol [22]; creamy white crystals, yield: 72%, M.P. 152-154°C, IR (cm^{-1}): 3333.10 (N-H), 3109.35 (aromatic C-H), 3109.35 (aliphatic C-H), 1597.11 (C=N), 1442.80 (C=C), 1072.46 (C-N), 879.57 (C-Cl).

2.1.2.1. Synthesis of 2-((1H-benzo[d]imidazol-2-yl)methylthio)-4-amino phenyl pyrimidine-5-carbonitrile (3a-g)

0.57 gm (0.0025 mol) 4-amino-2-mercapto-6-phenylpyrimidine-5-carbonitrile (1a-g) was dissolved in 5ml of aqueous sodium hydroxide solution (0.2 gm: 0.005 mol) by stirring at room temperature. To this well stirred solution, another clear solution of 0.41 gm (0.0025 mol) of 2-chloromethyl-1*H*-benzimidazole (2) in 5 ml methanol was added portion-wise with stirring for about 30 minutes. After addition, the reaction mixture was further stirred under reflux. The reaction progress was monitored using TLC. The reaction mixture was cooled at 5-10°C for half an hour and 3-4 drops of glacial acetic acid were added. Then, the separated solid was filtered, washed with cold water, and dried. The crude product was recrystallized from aqueous ethanol.

2.1.2.2. 2-((1H-benzo[d]imidazol-2-yl)methylthio)-4-amino-6-phenylpyrimidine-5-carbonitrile (3a)

Cream coloured powder, yield: 78%, M.P. 202-204°C, IR (cm^{-1}): 3456.55 (N-H), 3147.93 (aromatic C-H), 2924.18 (aliphatic C-H), 2322.37 (C≡N), 1620.26 (C=N), 1450.51 (C=C), 1026.16 (C-N), 740.69 (C-S). ^{1}H NMR (500 MHz, DMSO-d_6) (δ ppm): 3.32 (s, 2H, NH_2), 4.61 (s, 2H, CH_2), 7.32-7.35 (t, 2H, benzimidazole), 7.54-7.57 (t, 3H, pyrimidine), 7.89-7.90 (d, 2H, benzimidazole), 8.53-8.52 (d, 2H, pyrimidine). MS (EI) m/z (%): 358 [M^+], 359 [M^+ +1], anal. calc. for ($C_{19}H_{14}N_6S$) 358.

2.1.2.3. 2-((1H-benzo[d]imidazol-2-yl)methylsulfonyl)-4-amino-6-(4-chlorophenyl)pyrimidine-5-carbonitrile (3b)

Yellow powder, yield: 57%, M.P. 108-110°C, IR (cm^{-1}): 3356.25 (N-H), 3039.91 (aromatic C-H), 2924.18 (aliphatic C-H), 2337.80 (C≡N), 1620.26 (C=N), 1450.52 (C=C), 1064.74 (C-N), 748.41 (C-Cl), 694.40 (C-S). ^{1}H NMR (500 MHz, DMSO-d_6) (δ ppm): 3.36 (s, 2H, NH_2), 4.91 (s, 2H, CH_2), 7.13-7.64 (m, 8H, aromatic), 9.65 (s, 1H, NH). MS (EI) m/z (%): 392 [M^+], 393 [M^+ +1], anal. calc. for ($C_{19}H_{13}N_6SCl$) 392.

2.1.2.4. 2-((1H-benzo[d]imidazol-2-yl)methylsulfonyl)-4-amino-6-(4-nitrophenyl)pyrimidine-5-carbonitrile (3c)

Brown powder, yield: 63%, M.P. 186-188°C, IR (cm^{-1}): 3425.69 (N-H), 3194.53 (aromatic C-H), 2924.18 (aliphatic C-H), 2214.35 (C≡N), 1643.41 (C=N), 1519.96 (C=C), 1350.22 (N=O), 1111.08 (C-N), 694.40 (C-S). ^{1}H NMR (500 MHz, DMSO-d_6) (δ ppm): 3.41 (s, 2H, NH_2), 4.61 (s, 2H, CH_2), 7.48-7.51 (d, 2H, benzimidazole), 7.91-7.96 (d, 2H, benzimidazole), 8.16-8.25 (m, 4H, pyrimidine). MS (EI) m/z (%): 403 [M^+], 404 [M^+ +1], anal. calc. for ($C_{19}H_{13}N_7SO_2$) 403.

2.1.2.5. 2-((1H-benzo[d]imidazol-2-yl)methylsulfonyl)-4-amino-6-(4-hydroxyphenyl)pyrimidine-5-carbonitrile (3d)

Yellowish powder, yield: 58%, M.P. 250-252°C, IR (cm^{-1}): 3572.29 (O-H), 3456.55 (N-H), 3055.35 (aromatic C-H), 2924.18 (aliphatic C-H), 2260.65 (C≡N), 1620.26 (C=N), 1512.24 (C=C), 925.86 (C-N), 717.54 (C-S). ^{1}H NMR (500 MHz, DMSO-d_6) (δ ppm): 3.34 (s, 1H, -OH), 3.41 (s, 2H, NH_2), 4.61 (s, 2H, CH_2), 7.48-7.51 (d, 2H, benzimidazole), 7.91-7.96 (d, 2H, benzimidazole), 8.16-8.25 (m, 4H, pyrimidine). MS (EI) m/z (%): 374 [M^+], 375 [M^+ +1], anal. calc. for ($C_{19}H_{14}N_6OS$) 374.

2.1.2.6. 2-((1H-benzo[d]imidazol-2-yl)methylsulfonyl)-4-amino-6-(4-methoxyphenyl)pyrimidine-5-carbonitrile (3e)

Yellowish brown powder, yield: 67%, M.P. 190-192°C, IR (cm-1): 3471.98 (N-H), 3171.08 (aromatic C-H), 2970.48 (aliphatic C-H), 2214.35 (C≡N), 1604.83 (C=N), 1519.96 (C=C), 1257.63 (C-O), 1026.16 (C-N), 648.10 (C-S). 1H NMR (500 MHz, DMSO-d6) (δ ppm): 3.36 (s, 2H, NH2), 3.99 (s, 3H, -OCH3), 4.91 (s, 2H, CH_2), 7.13-7.64 (m, 8H, aromatic), 9.65 (s, 1H, NH). MS (EI) m/z (%): 388 [M^+], 389 [M^+ +1], anal. calc. for ($C_{20}H_{16}N_6SO$) 389.

2.1.2.7. 2-((1H-benzo[d]imidazol-2-yl)methylsulfonyl)-4-amino-6-(3-bromophenyl)pyrimidine-5-carbonitrile (3f)

Cream colored powder, yield: 71%, M.P. 166-168°C, IR (cm^{-1}): 3394.83 (N-H), 3024.48 (aromatic C-H), 2916.47 (aliphatic C-H), 2214.35 (C≡N), 1643.41 (C=N), 1450.52 (C=C), 1180.47 (C-N), 709.83 (C-S), 516.94 (C-Br). ^{1}H NMR (500 MHz, DMSO-d_6) (δ ppm): 3.34 (s, 2H, NH_2), 4.93 (s, 2H, CH_2), 7.13-7.66 (m, 8H, aromatic), 9.72 (s, 1H, NH). MS (EI) m/z (%): 436 [M^+], 437 [M^+ +1], anal. calc. for ($C_{19}H_{13}N_6SBr$) 436.

2.1.2.8. 2-((1H-benzo[d]imidazol-2-yl)methylsulfonyl)-4-amino-6-(4-fluorophenyl)pyrimidine-5-carbonitrile (3g)

Faint yellow powder, yield: 69%, M.P. 212-214°C, IR (cm^{-1}): 3387.11 (N-H), 3086.21 (aromatic C-H), 2955.04 (aliphatic C-H), 2214.35 (C≡N), 1643.41 (C=N), 1512.24 (C=C), 1234.48 (C-F), 1157.33 (C-N), 748.21 (C-S). ^{1}H NMR (500 MHz, DMSO-d_6) (δ ppm): 3.32 (s, 2H, NH_2), 4.92 (s, 2H, CH_2), 7.23-7.62 (m, 8H, aromatic), 9.72 (s, 1H, NH). MS (EI) m/z (%): 394 [M^+], 395 [M^+ +1], anal. calc. for ($C_{19}H_{13}N_6SF$) 394.

2.2. Biological Evaluation

All target compounds, 3**a-g**, were screened for their antibacterial and antifungal activity. The synthesized compounds were evaluated for their antibacterial activity against two-gram positive bacteria (*Staphylococcus aureus* and *Bacillus subtilis*) and two-gram negative bacteria (*E. coli* and *Pseudomonas aeruginosa*) by using ciprofloxacin as a reference antibacterial agent. Antifungal activity was evaluated against *Candida albicans* and *Aspergillus niger*. Fluconazole was used as a reference drug. The synthesized compounds were evaluated for their antimicrobial activity against gram-positive and gram-negative bacteria, and fungi by determining the zone of inhibition and minimum inhibitory concentration (MIC).

2.2.1. Measurement of the Zone of Inhibition using the Cup Plate Method

The compounds were evaluated for antibacterial activity by the cup plate method. The results were recorded for each tested compound as the average diameter of the inhibition zone of bacterial and fungal growth around the cup in mm. The bacteria were subcultured in the nutrient agar medium containing peptone (0.6%), yeast extract (0.3%), beef extract (0.13%), sodium chloride (0.2%), and agar (2.1%) in distilled water. The solution was sterilized for 20 min in an autoclave at 15 psi pressure at 121°C. The basal medium of 15-20 ml was poured into the sterile petri dishes. After solidification of the medium, the microorganisms were sub-cultured, and then holes of 6 mm diameter were bored. To these cups, the test compounds at concentrations of 50, 100, and 150 µg/ml were added by micropipette. Petri dishes were kept in a refrigerator to facilitate the diffusion for about 2 h. These plates were then incubated at 37°C for 48 h. The extent of inhibition was determined by measuring the diameter of the inhibition zone in mm. For antibacterial and antifungal studies, 150 µg/ml of ciprofloxacin and 150 µg/ml of fluconazole were used as reference drugs, respectively.

2.2.2. Measurement of Minimal Inhibitory Concentration using the Two-fold Dilution Method (MIC)

The broth dilution was performed by using microtiter plates. The nutrient broth was prepared using peptone (1%), beef extract (0.5%), and sodium chloride (0.8%). The nutrient broth was prepared and added to microtiter plates, except for the first well. The first well of the microtiter plate was used to check the sterility of the medium as a negative control in which inoculum was not added. The stock solution of test compounds was prepared in DMSO (200µg/ml), followed by twofold dilution at concentrations of 100, 50, 25, ….3.125 µg/ml, respectively. The inoculums were added to the other wells containing test compounds ranging from 100, 50, 25, ….3.125 µg/ml, respectively. The microtiter plates were then incubated at 37°C for 24 h for bacteria and 48 h for fungi, and minimal inhibitory concentrations were measured for growth in the form of turbidity. Ciprofloxacin (150µg/ml) was used as a reference drug for antibacterial activity study, while fluconazole (150µg/ml) was used for the antifungal activity study [23].

2.3. Molecular Docking Study

To check the type of interactions existing between the enzyme and the ligand, a docking study is an important tool. The finding of major binding modes of a ligand to a protein of known three-dimensional structure is one of the important goals of ligand-protein docking. Docking studies of the target compounds were carried out using the Vlife MDS 4.6 software.

2.3.1. Computer Hardware and Software

The molecular modelling study was performed on the Windows 10 operating system using Vlife MDS 4.6 software. The crystal structure of the dihydrofolate reductase (DHFR) and dihydropteroate synthase (DHPS) was obtained from the Protein Data Bank (PDB) with PDB ID: 2W9T (homo sapiens DHFR), 1S3V (*S. aureus* DHFR) and 1AD4 (DHPS).

2.3.2. Conformer Generation

Structures of the target molecules were drawn using ChemDraw Ultra 8.0 and saved in mol file, and each structure was minimized using the MMFF force field. Conformers were generated utilizing a systemic conformational search method.

2.3.3. Docking Study

The molecular docking tool, Vlife MDS 4.6, was used for docking. Protein preparation was performed using homology modelling. After chemical correctness was ensured, hydrogen was added, where it was missing. Water molecules present in the PDB were deleted. The generated conformers were docked into the generated grid by the batch docking method. The final assessment was done by considering the dock score.

3. RESULTS AND DISCUSSION

3.1. Chemistry

The procedure adopted for synthesis to obtain the target compounds is illustrated in Fig. (**1**). Both key intermediates **1 a-g** and **2** were prepared according to a previously reported procedure. The synthesis of derivatives of 4-amino-2-mercapto-6-phenylpyrimidine-5-carbonitrile (**1a-g**) was done by refluxing benzaldehyde, malononitrile, and urea, which were further recrystallised by aqueous ethanol [21]. 2-chloromethyl-1*H*-benzimidazole (**2**) was synthesized by irradiating chloroacetic acid and *o*-phenylenediamine in 5N HCl and neutralizing with aq. ammonium hydroxide [22]. The compounds (**3a-g**) were synthesized by the condensation of 4-amino-2-mercapto-6-phenylpyrimidine-5-carbonitrile (**1a-g**) with 2-(chloromethyl)-1*H*-benzo[*d*]imidazole (**2**) in the presence of aqueous sodium hydroxide. The reaction involved nucleophilic substitution. Lone pair of the electrons from the sulphur of pyrimidine derivatives attacked the electron-deficient carbon of 2-(chloromethyl)-1*H*-benzoimidazole derivatives. Removal of HCl resulted in the formation of the target compounds.

The structural confirmation of the synthesized compounds was done by performing spectral characterization, such as FT-IR, ^{1}H NMR, and mass spectroscopy. The IR (KBr, cm^{-1}) spectra of these compounds revealed characteristic aromatic C-H, aliphatic CH, C=N, C-N, C=C, C-S, N-H, C≡N, and S-H

peaks. ^{1}H NMR of synthesized compounds was taken in DMSO, which showed sharp solvent peaks between 2.3 and 2.5 δ ppm, respectively. The compounds displayed aromatic protons of pyrimidine as doublets at 8.53-8.52 δ ppm and triplets at 7.54-7.57 δ ppm. The NH_2 proton was depicted at 3.32 δ ppm as a singlet. While the aromatic protons of benzimidazole displayed a doublet at 7.89-7.90 δ ppm and triplets at 7.32-7.35 δ ppm. The CH_2 protons were observed at 4.61 δ ppm as a singlet. The absence of an S-H proton peak confirmed the formation of target compounds.

3.2. Biological Evaluation

All synthesized compounds (**3a-g**) were evaluated for their antibacterial and antifungal activity. The synthesized compounds were evaluated for their antimicrobial activity by determining the zone of inhibition using the cup plate method. The minimum inhibitory concentration of these compounds was determined using a two-fold dilution method [23]. All of the synthesized compounds were evaluated for their antibacterial activity against two gram-positive bacteria, *Staphylococcus aureus* and *Bacillus subtilis,* and two gram-negative bacteria, *E. coli* and *Pseudomonas aeruginosa*, by using ciprofloxacin as a reference antibacterial agent. Zones of inhibition of the synthesized compounds (**3a-g**) were measured against two species of fungi, *Candida albicans* and *Aspergillus niger*. Fluconazole was used as a reference drug. Fig. (**2**) represents the diameters of the inhibition zones, which are attributed to the examined original concentration (150 µg/mL). In addition, the zone of inhibition (nm) and minimum inhibitory concentration (µg/mL) values are shown in Tables **1** and **2**, respectively.

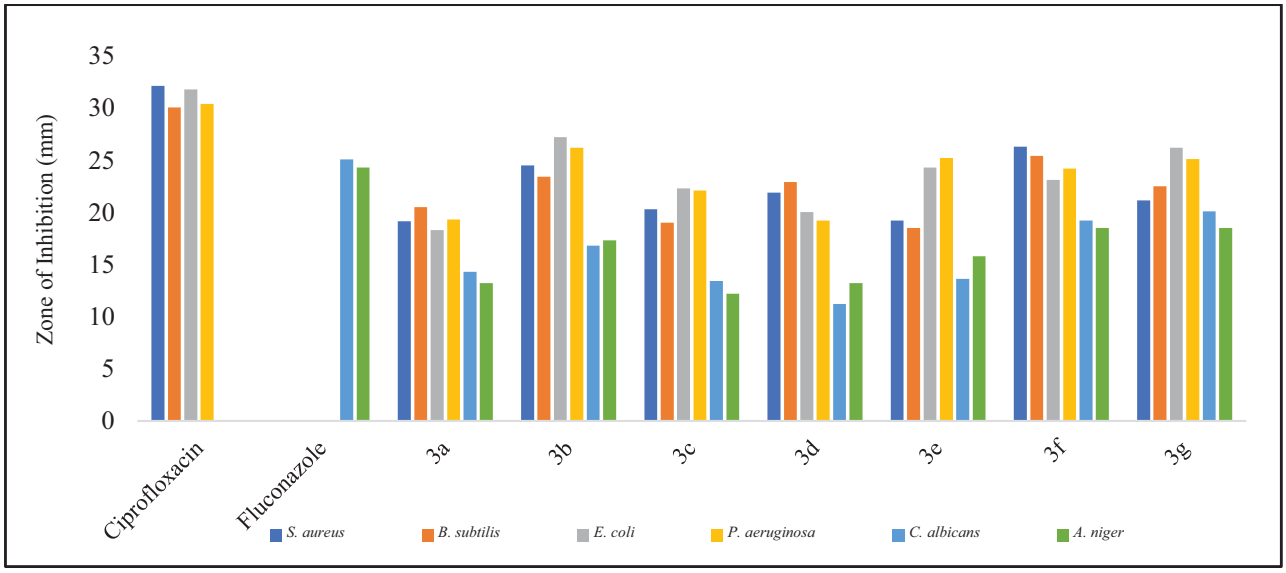

Fig. (2). Graph of the zone of inhibition of the synthesized compounds (3**a-g**).

Table 1. Zone of inhibition of synthesized compounds (3a-g).

Sr. No.	Compound	MIC (µg/ml)					
		Gram-positive Bacteria		Gram-negative Bacteria		Fungi	
		S. aureus	*B. subtilis*	*E. coli*	*P. aeruginosa*	*C. albicans*	*A. niger*
1	Ciprofloxacin	6.25	12.5	3.125	3.125	-	-
2	Fluconazole	-	-	-	-	12.5	6.25
3	3a	100	50	50	100	50	100
4	3b	6.25	12.5	3.125	6.25	12.5	12.5
5	3c	50	25	50	50	100	50
6	3d	50	50	25	12.5	25	50
7	3e	50	50	25	50	25	25
8	3f	6.25	12.5	12.5	6.25	12.5	6.25
9	3g	12.5	25	6.25	3.125	6.25	6.25

Table 2. Observation table for minimum inhibitory concentration in µg/ml.

Compound	Conc. (µg/ml)	Zone of Inhibition (mm)					
		Gram-positive Bacteria		Gram-negative Bacteria		Fungi	
		S. aureus	*B. subtilis*	*E. coli*	*P. aeruginosa*	*C. albicans*	*A. niger*
Ciprofloxacin	150	32.12±0.08	30.05±0.08	31.8±0.31	30.4±0.2	-	-
Fluconazole	150	-	-	-	-	25.06±0.06	24.3±0.08
3a	50	12.25±0.3	10.9±0.09	10.3±0.08	11.2±0.3	9.1±0.50	8.3±0.05
	100	16.01±0.07	15.4±0.5	15.8±0.15	16±0.22	11.2±0.20	9.8±0.10
	150	19.14±0.03	20.5±0.14	18.3±0.10	19.3±0.06	14.3±0.05	13.2±0.11
3b	50	14.5±0.11	13.8±0.03	14.9±0.12	15.2±0.03	10±0.20	12.1±0.08
	100	20.09±0.08	19.3±0.23	19.3±0.03	18.1±0.5	13.4±0.12	15.1±0.02
	150	24.5±0.14	23.4±0.06	27.2±0.06	26.2±0.11	16.8±0.08	17.3±0.17
3c	50	9.8±0.25	9.5±0.17	15±0.02	14.8±0.05	9.08±0.50	8.4±0.10
	100	13.5±0.06	14.2±0.25	18.1±0.06	19.3±0.06	10.2±0.06	9.8±0.02
	150	20.3±0.03	19±0.06	22.3±0.15	22.1±0.17	13.4±0.20	12.2±0.14
3d	50	13.2±0.06	15.2±0.07	11.8±0.11	12.8±0.17	7.3±0.08	8.4±0.08
	100	18±0.02	19.2±0.06	16±0.08	15.6±0.05	9.2±0.20	10.2±0.14
	150	21.9±0.03	22.9±0.03	20.02±0.6	19.2±0.11	11.2±0.10	13.2±0.02
3e	50	10.4±0.14	11.3±0.08	13±0.04	14.8±0.06	8.2±0.08	9.2±0.10
	100	14.2±0.07	15.5±0.14	18.2±0.2	19.3±0.17	11.3±0.10	12.4±0.23
	150	19.2±0.06	18.5±0.03	24.3±0.06	25.2±0.11	13.6±0.05	15.8±0.06
3f	50	13.5±0.02	14±0.12	15.2±0.6	16.2±0.01	12±0.20	13.3±0.17
	100	19.03±0.7	20±0.05	19.4±0.5	18.1±0.06	16.4±0.50	15.2±0.20
	150	26.3±0.03	25.4±0.14	23.1±0.03	24.2±0.05	19.2±0.12	18.5±0.14
3g	50	15.2±0.07	16±0.06	14.2±0.17	16±0.08	13±0.06	12.5±0.06
	100	18.1±0.06	19.2±0.07	19.3±0.11	20.5±0.02	15.3±0.12	14.2±0.50
	150	21.16±0.15	22.5±0.3	26.2±0.02	25.1±0.05	20.10.20	18.5±0.02

The compounds, **3b** and **3f**, have shown significant zones of inhibition against gram-positive bacteria amongst the synthesized compounds. Compound **3f** was found to have comparable antibacterial activity with ciprofloxacin at 150µg/ml against both gram-positive bacteria. The compound **3e** was found to possess minimum antibacterial activity against gram-positive bacteria among the synthesized compounds. Zone of inhibition study for gram-negative bacteria has shown compound **3b** to possess a better zone of inhibition in comparison to the reference drug ciprofloxacin among the synthesized compounds. Compounds **3e** and **3g** showed a significant zone of inhibition, and compound **3a** possessed the least activity against gram-negative bacteria compared to the reference drug. Antibacterial activity data revealed that all tested compounds showed moderate to good antibacterial potential. Compound **3g** was found to be more active as an antifungal agent among all the synthesized compounds compared to fluconazole as a reference drug. Compound **3c** showed the least antifungal activity compared to other synthesized compounds.

The minimum inhibitory concentration (MIC) against the selected microorganisms was determined by using a microtiter plate. All compounds were dissolved in DMSO to give a concentration of 200µg/ml. Two-fold dilutions of the test and standard compounds were prepared in nutrient broth. The stock solution was serially diluted to give a concentration of 200-3.12 µg/ml in nutrient broth. The compounds with chloro **(3b),** fluoro **(3f),** and bromo **(3g)** substitution showed good antimicrobial activity. The compounds **3b** and **3f** showed good antibacterial activity against gram-positive bacteria *S. aureus* at an MIC value of 6.25 µg/ml and moderate activity against *B. subtilis* at 12.5 µg/ml. For gram-negative bacteria, compound **3b** has shown good activity against *E. coli* at an MIC value of 3.125 µg/ml and moderate activity against *P. aeruginosa* at an MIC value of 6.25 µg/ml. The compound **3g** has shown good activity against *P. aeruginosa* at an MIC value of 3.125 µg/ml and moderate activity against *E. coli* at an MIC value of 6.25 µg/ml. The compound **3g** showed good antifungal activity against *C. albicans* and *A. niger* at an MIC value of 6.25 µg/ml and compound **3f** showed good activity against *A. niger* at an MIC value of 6.25 µg/ml and moderate activity against *C. albicans* at an MIC value of 6.25 µg/ml.

It was observed that compounds possessing 4-chloro (3b), fluoro **(3f)**, and bromo **(3g)** substitutions were found to hold better antibacterial activity against gram-positive and gram-negative bacteria among the synthesized compounds, whereas most of the compounds showed moderate antifungal activity against *C. albicans* and *A. niger* species compared to fluconazole.

3.3. Molecular Docking Study

The binding of ligands to a large protein target is essential for several biological processes. The correct estimation of the binding approaches between the ligand and protein is required in modern structure-based drug design. The docking study was carried out to check the interactions of target compounds with

protein molecules [24, 25]. Dihydrofolate reductase is a highly reviewed enzyme in the folate pathway due to its significance in the maintenance of the folate cycle. DHFR catalyzes the reduction of dihydrofolate to tetrahydrofolate, and also, at a much slower rate, the conversion of folate to tetrahydrofolate. The reduction of dihydrofolate (DHF) confirms an intracellular pool of different THF derivatives that are used in numerous one-carbon transference reactions and biosynthetic processes. The variance in the primary structure of human DHFR and DHFRs from other species permits the selective inhibition of pathogen growth with satisfactory inhibitors devoid of unfavorable effects on human cells [26]. Dihydropteroate synthase (DHPS) is an enzyme of the folate biosynthesis pathway, which catalyzes the formation of 7,8- dihydropteroate from 6-hydroxymethyl-7,8-dihydropterin pyrophosphate and para-aminobenzoic acid [27].

All synthesized compounds (3a-g) were docked with homo sapiens DHFR (PDB: 1S3V), bacterial (*S. aureus*) DHFR (PDB: 2W9T), and DHPS (PDB: 1AD4) protein [28]. Docking studies of the target compounds were done by using the Vlife MDS 4.6 software. Trimethoprim was used as a reference compound for comparing the binding of synthesized compounds with DHFR, and sulfadiazine was used as a reference molecule for comparing the binding of synthesized compounds with DHPS. Comparative studies of docking of the synthesized compounds and dihydrofolic acid (DHF) with homo sapiens DHFR and bacterial (*S. aureus*) DHFR were performed to check the selectivity for the pathogenic species. The dock score and binding interactions were recorded. Hydrogen bond interaction (HB), hydrophobic interaction (HP), ionic interaction (charge), and van der Waals interaction (VDW) were checked. Dock score and binding energy of the synthesized compounds are shown in Table **3**.

Table 3. Dock score and binding energy of target compounds with selected proteins.

Sr. No.	Compound	PDB					
		Homo Sapiens DHFR: 1S3V		Bacterial DHFR: 2W9T		DHPS: 1AD4	
		Dock Score	Binding Energy (kcal/mol)	Dock Score	Binding Energy (kcal/mol)	Dock Score	Binding Energy (kcal/mol)
1	Trimethoprim	-4.307	148.59	-3.493	-221.76	-	-
2	Sulfadiazine	-	-	-	-	-5.085	-119.13
3	DHF	-3.018	-384.13	-2.290	-966.93	-	-
4	3a	-4.745	55.49	-3.765	-551.76	-3.940	-180.93
5	3b	-4.853	-244.34	-3.986	-362.5	-4.557	-388.42
6	3c	-4.642	-58.21	-3.888	-496.87	-4.025	-400.07
7	3d	-4.662	-63.92	-3.567	-567.56	-4.234	-15.97
8	3e	-4.543	-311.9	-3.917	-553.37	-3.731	-299.62
9	3f	-4.884	-251.62	-4.047	-373.37	-4.526	0.54
10	3g	-4.576	-21.66	-4.157	-435.11	-3.732	-275.22

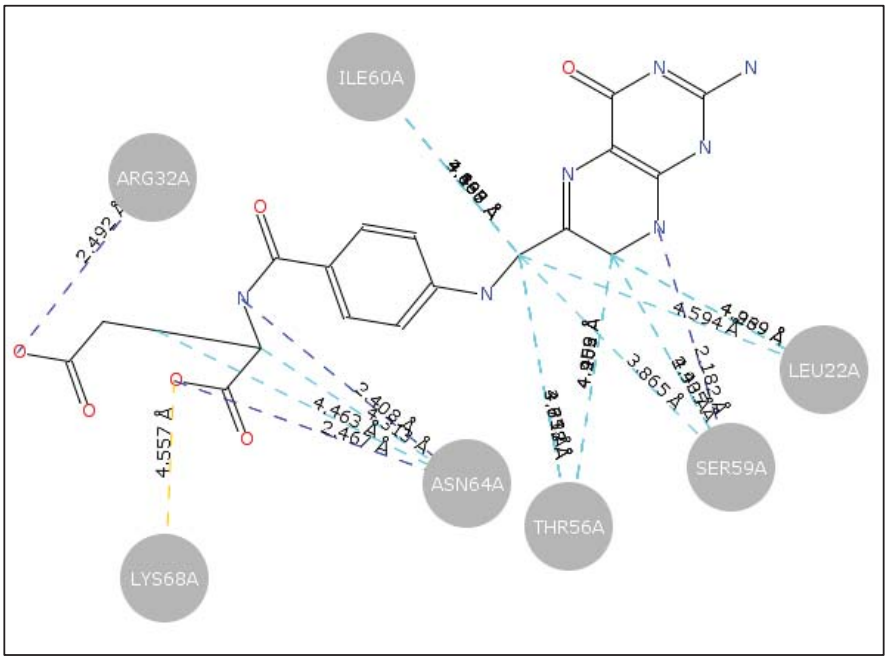

Fig. (3). Interactions of dihydrofolic acid with homo sapiens DHFR.

3.3.1. Docking Studies with Homo Sapiens DHFR

Docking of dihydrofolic acid (DHF) to homo sapiens DHFR revealed that interactions between the ligands and ARG32A, SER59A, ASN64A (HB), LEU22A, THR56A, SER59A, ILE60A, ASN64A (HP) and LYS68A (charge) are important for increased affinity for human DHFR (Fig. **3**). Avoidance of these interactions should guide selectivity for pathogenic species. The docking study revealed compound **3f** to possess -4.8845 Kcal/mol as the highest dock score with homo sapiens DHFR (Fig. **4**). The observed dock score of trimethoprim was -4.3071 Kcal/mol (Fig. **5**). All compounds showed good dock score and interaction as compared to the reference ligand, trimethoprim (Table **4**).

A comparative study of docking of synthesized compound (3f) and dihydrofolic acid with homo sapiens DHFR revealed a conformational change in the ligand that enhanced the hydrophobic interactions with residues ILE60A and LEU67A (LEU22A, THR56A, SER59A, ILE60A, and ASN64A in DHF), charge interaction with ARG70A (LYS68A in DHF), and aromatic interactions with TRP24A (ARG32A, SER59A, and ASN64A in DHF), thus yielding selectivity. Docking of the synthesized compounds with homo sapiens DHFR revealed that the binding interactions shown by the target compounds were different than dihydrofolic acid (DHF), which indicates that the synthesized compounds had less affinity for homo sapiens DHFR, thus reducing the potential side effects.

Table 4. Dock score and different binding interactions of target compounds with homo sapiens DHFR (HB- hydrogen bond interaction, HP- hydrophobic interaction, Charge- charge (ionic) interaction, VDW- van der Waals interaction).

Compound	Dock Score	Binding Energy (kcal/mol)	Interactions
DHF	-3.0182	-384.13	**HB-** ARG32A, SER59A, ASN64A **HP**- LEU22A, THR56A, SER59A, ILE60A, ASN 64A **CHARGE**- LYS68A **VDW**- ALA9A, ILE16A, GLY17A, LEU22A, PRO23A, TRP24A, PHE31A, ARG32A, THR56A, SER59A, ILE60A, ASN64A, LEU67A, LYS68A, ARG70A
Trimethoprim	-4.3071	148.59	**HB**- ILE16A **HP**- ALA9A, PHE31A, THR56A, ILE60A, LEU67A **VDW**-ILE16A, GLY17A, GLU30A, PHE31A, PHE34A, THR56A, SER59A, ILE60A, LEU67A
3a	-4.7452	55.49	**HP**- ILE60A, LEU67A **AROMATIC**-PHE34A **VDW**- VAL8A, ALA9A, ILE16A, GLY17A, LEU22A, TRP24A, PHE34A, GLN35A, SER59A, ILE60A, LEU67A, TYR121A
3b	-4.8535	-244.34	**HP**- ILE60A, LEU67A **AROMATIC**- PHE31A, PHE34A **VDW**- VAL8A, ALA9A, ILE16A, GLY17A, LEU22A, PHE34A, GLN35A, SER59A, ILE60A, ASN64A, LEU67A, ARG70A, TYR121A
3c	-4.6420	-58.21	**HP**- ILE60A, LEU67A **AROMATIC**-PHE34A **VDW**- VAL8A, ILE16A, LEU22A, PHE31A, PHE34A, GLN35A, THR38A, THR56A, SER59A, ILE60A, LEU67A, GLY117A, TYR121A
3d	-4.6623	-63.92	**HP**- ILE60A, LEU67A, **CHARGE**- ARG70A **AROMATIC**- PHE34A **VDW**- VAL8A, ILE16A, LEU22A, PHE34A, GLN35A, THR38A, THR56A, SER59A, ILE60A, LEU67A, ARG70A, VAL115A, GLY116A, GLY117A
3e	-4.5430	-311.9	**HP**- VAL8A, ILE16A, ILE60A, GLY117A, PHE148A **AROMATIC**- PHE31A **VDW**- VAL8A, ILE16A, GLY17A, LEU22A, PHE31A, THR56A, ILE60A, ASN64A, TYR121A, PHE148A
3f	-4.8845	-251.62	**HP**- ILE60A, LEU67A **CHARGE**- ARG70A, **AROMATIC**-TRP24A **VDW**- VAL8A, ALA9A, ILE16A, LEU22A, PRO23A, TRP24A, PHE31A, PHE34A, ILE60A, LEU67A, ARG70A, TYR121A
3g	-4.5761	-21.66	**HP**- ILE60A, LEU67A **AROMATIC**-PHE31A **VDW**- VAL8A, ALA9A, ILE16A, GLY17A, ASP21A, LEU22A, GLN35A, SER59A, ILE60A, ASN64A, TYR121A

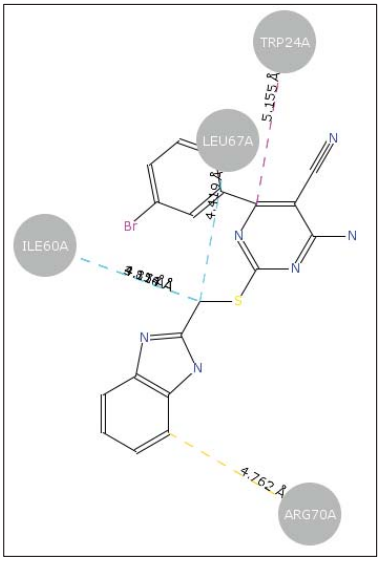

Fig. (4). Interactions of compound 3f with homo sapiens DHFR.

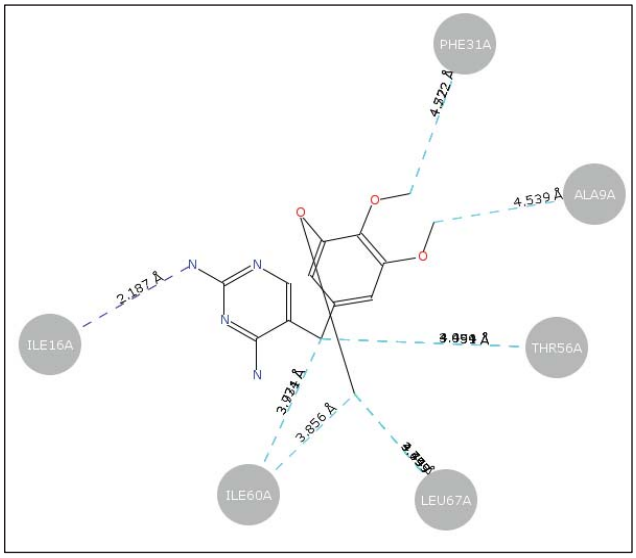

Fig. (5). Interactions of trimethoprim with homo sapiens DHFR.

3.3.2. Docking study with bacterial (S. aureus) DHFR

Docking of dihydrofolic acid (DHF) with bacterial (*S. aureus*) DHFR revealed that the ligand showed hydrogen bond interactions with THR35B, LYS52B, and ARG57B, hydrophobic interactions with ILE31B, LYS32B, THR35B, LEU40B, LYS52B, LEU54B, and ARG57B, ionic interactions with LYS32B and ARG57B, and van der Waals interactions with ILE5B, LEU20B, ILE31B, LYS32B, THR35B, LEU40B, LYS52B, LEU54B, PRO55B, ARG57B, and PHE92B. These interactions have been found to be important for the increased affinity for bacterial DHFR (Fig. **6**).

Among the synthesized compounds, **3g** exhibited -4.1578 Kcal/mol as the highest dock score against bacterial (*S. aureus*) DHFR (Fig. **7**), which was comparable with the dock score of trimethoprim (-3.4931 Kcal/mol) (Fig. **8**). All compounds showed good dock score and similar interactions compared to the reference ligand, trimethoprim (Table **5**). A comparison of the docking study of synthesized compounds and dihydrofolic acid (DHF) with bacterial DHFR showed nearly similar binding interactions, confirming the selectivity. The synthesized compounds showed different binding interactions with homo sapiens DHFR, but similar interactions with bacterial DHFR, indicating the selectivity of the synthesized compounds towards bacterial DHFR.

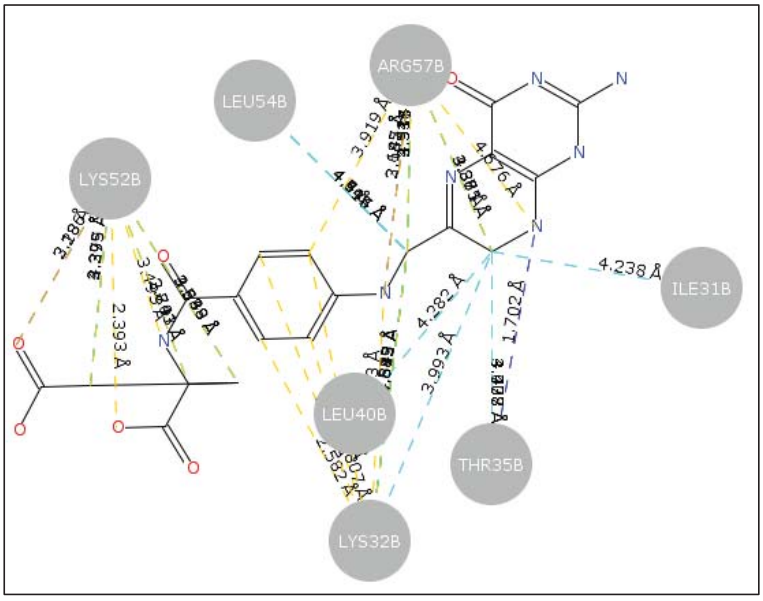

Fig. (6). Interactions of dihydrofolic acid with bacterial DHFR.

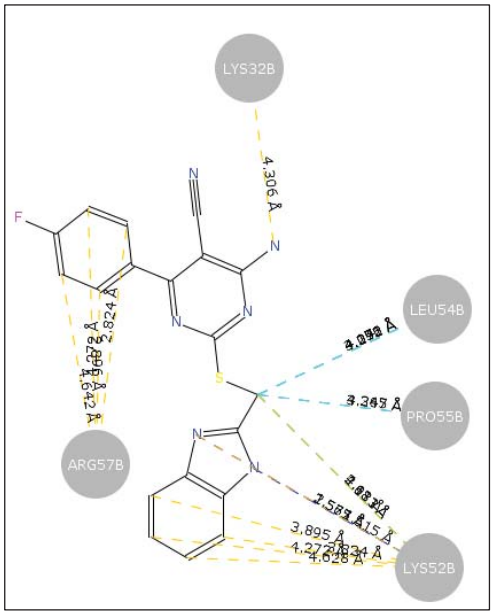

Fig. (7). Interactions of compound 3g with bacterial (*S. aureus*) DHFR.

Table 5. Dock score and different binding interactions of target compounds with bacterial (*S. aureus*) DHFR (HB- hydrogen bond interaction, HP- hydrophobic interaction, Charge- charge (ionic) interaction, VDW- van der Waals interaction).

Compound	Dock Score	Binding Energy (kcal/mol)	Interactions
DHF	-2.2900	-966.93	**HB-** THR35B, LYS52B, ARG57B **HP-** ILE31B, LYS32B, THR35B, LEU40B, LYS52B, LEU54B, ARG57B **CHARGE-** LYS32B, ARG57B **VDW-** ILE5B, LEU20B, ILE31B, LYS32B, THR35B, LEU40B, LYS52B, LEU54B, PRO55B, ARG57B, PHE92B
Trimethoprim	-3.4931	-221.76	**HP-**LEU20B, LEU28B, ILE31B, LYS32B, THR35B LEU54B, PRO55B, ASN56B **CHARGE-** LYS32B, LYS52B **VDW-** LEU20B, LEU28B, ILE31B, LYS32B, THR35B, LYS52B, LEU54B, PRO55B, ASN56B, ARG57B

(Table 5) contd.....

Compound	Dock Score	Binding Energy (kcal/mol)	Interactions
3a	-3.7653	-551.76	**HB-** LYS32B **HP-** LYS32B **CHARGE-** LYS32B, LYS52B, ARG57B **VDW**-LEU20B, PRO21B, LEU28B, ILE31B, LYS32B, THR35B, LEU40B, LYS52B, LEU54B, PRO55B, ARG57B, PHE92B
3b	-3.9864	-362.5	**HB-** LYS32B, ARG57B **HP-** LEU54B, PRO55B **CHARGE-** LYS32B, LYS52B, ARG57B **VDW**- LEU20B, ILE31B, LYS32B, THR35B, THR36B, LEU40B, LYS52B, LEU54B, PRO55B, ARG57B
3c	-3.8883	-496.87	**HB-** LYS32B, ASN56B **HP-** LEU20B, ILE50B, LYS52B, LEU54B **CHARGE-** LYS32B, LYS52B **AROMATIC**- TRP22B **VDW**- GLN19B, LEU20B, LYS32B, SER49B, ILE50B, LYS52B, LEU54B, PRO55B, ASN56B
3d	-3.5672	-567.56	**HB-** LYS52B **HP-** LYS32B, LEU54B **CHARGE-** LYS32B, LYS52B, ARG57B **VDW**- LEU20B, LEU28B, ILE31B, LYS32B, THR35B, LEU40B, LYS52B, PRO53B, LEU54B, PRO55B, ARG57B, PHE92B
3e	-3.9179	-553.37	**HB-** ASN59B **HP-** LYS32B, ILE50B, LEU54B **CHARGE-** LYS32B, LYS52B **VDW**-LEU20B, LYS32B, LEU40B, MET42B, THR46B, ILE50B, LYS52B, LEU54B, ASN59B, PHE92B
3f	-4.0470	-373.37	**HB-** LYS52B **HP-** ILE50B, LYS52B, PRO53B, LEU54B **CHARGE-** LYS32B, LYS52B **VDW**- LEU28B, LYS32B, MET42B, PHE47B, ILE50B, GLY51B, LYS52B, PRO53B, LEU54B, PRO55B, ARG57B, ASN59B
3g	-4.1578	-435.11	**HB-** LYS52B **HP-** LYS52B, LEU54B, PRO55B **CHARGE-** LYS32B, LYS52B, ARG57B **VDW**- LEU20B, ILE31B, LYS32B, THR35B, THR36B, LEU40B, LYS52B, LEU54B, PRO55B, ASN56B, ARG57B, PHE92B

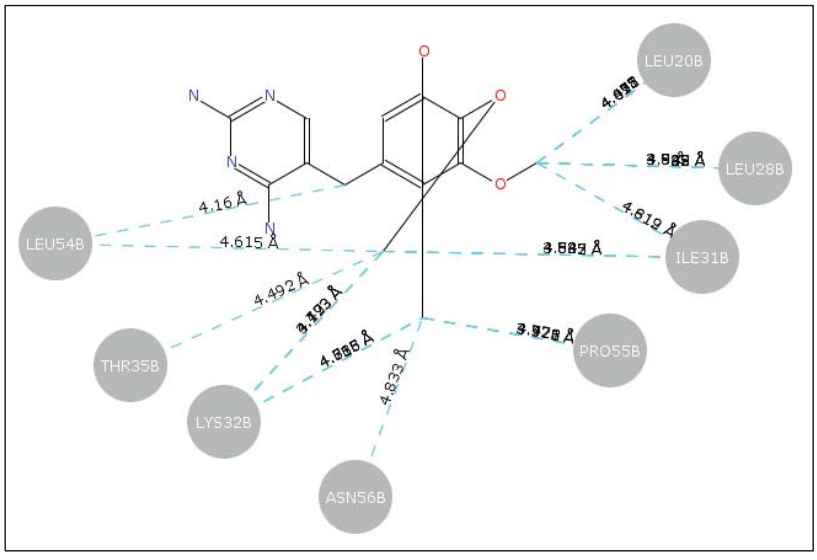

Fig. (8). Interactions of trimethoprim with bacterial (*S. aureus*) DHFR.

3.3.3. Docking study with DHPS

Among the synthesized compounds, **3b** possessed -4.5570 Kcal/mol as the highest dock score with DHPS, which was comparable to the dock score of sulfadiazine (-5.0855Kcal/mol). All compounds showed comparable dock scores and similar interactions compared to the reference

ligand, sulfadiazine (Table **6**).

Docking of sulfadiazine with DHPS (Fig. **9**) showed hydrogen bond interaction with ASN11A, ionic interactions with ARG202A, and van der Waals interaction with LEU10A, ASN11A, VAL12A, THR13A, PRO14A, SER16A, PHE17A, ARG32A, ARG202A, and HIS241A, respectively. Docking studies of compound 3b with DHPS (Fig. **10**) showed hydrogen bond interaction with ASN11A, hydrophobic interaction withASN11A, VAL12A, THR13A, PRO14A, ASP15A, SER16A, and PHE17A, and van der Waals interaction with ILE9A, ASN11A, VAL12A, THR13A, PRO14A, SER16A, PHE17A, SER18A, ASN24A, ASN25A, ARG32A, MET36A, and HIS241A, respectively. The comparative study of docking of sulfadiazine and synthesized compounds revealed the presence of similar interactions, which indicated the affinity of newly synthesized compounds for DHPS.

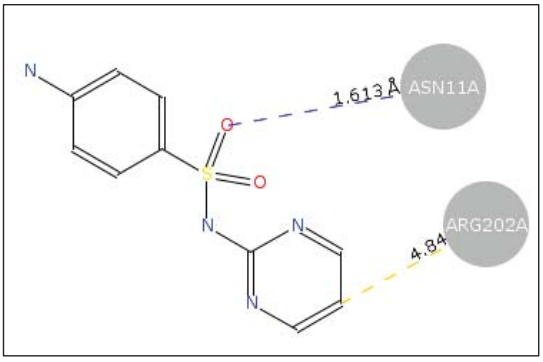

Fig. (9). Interactions of sulfadiazine with DHPS.

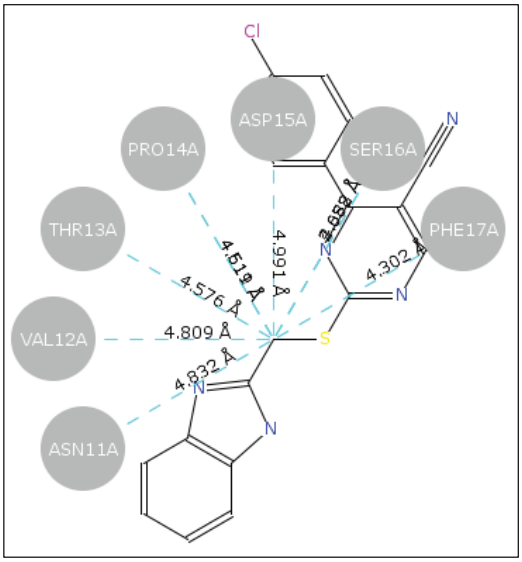

Fig. (10). Interactions of compound 3b with DHPS.

Table 6. Dock score and different binding interactions of target compounds with DHPS (HB- hydrogen bond interaction, HP- hydrophobic interaction, Charge- charge (ionic) interaction, VDW- van der Waals interaction).

Compound	Dock Score	Binding Energy (kcal/mol)	Interactions
Sulfadiazine	-5.0855	-119.13	**HB**- ASN11A **CHARGE**- ARG202A **VDW**- LEU10A, ASN11A, VAL12A, THR13A, PRO14A, SER16A, PHE17A, ARG32A, ARG202A, HIS241A
3a	-3.9401	-180.93	**HB**- ASN11A, SER16A **HP**-LEU10A, ASN11A, VAL12A, SER16A **VDW**- LEU10A, ASN11A, VAL12A, SER16A, ASN25A, VAL26A, SER28A, ALA29A, ARG32A, ARG202A, HIS241A

(Table 6) contd.....

Compound	Dock Score	Binding Energy (kcal/mol)	Interactions
3b	-4.5570	-388.42	**HB-** ASN11A **HP**- ASN11A, VAL12A, THR13A, PRO14A, ASP15A, SER16A, PHE17A **VDW**- ILE9A, ASN11A, VAL12A, THR13A, PRO14A, SER16A, PHE17A, SER18A, ASN24A, ASN25A, ARG32A, MET36A, HIS241A
3c	-4.0256	-400.07	**HB**- ASN11A, SER16A, HIS241A **HP**-LEU10A, ASN11A, VAL12A, SER16A, PHE17A **CHARGE**- ARG32A **VDW**- ILE9A, LEU10A, ASN11A, VAL12A, PRO14A, SER16A, PHE17A, ASN24A, ASN25A, ALA29A, ARG32A, HIS241A
3d	-4.2341	-15.97	**HB**- ASN11A **HP**- ASN11A, SER16A, PHE17A **CHARGE**- ARG32A **VDW**- ILE9A, ASN11A, VAL12A, THR13A, PRO14A, SER16A, PHE17A, SER18A, ASN24A, ASN25A, ARG32A, MET36A, GLU39A, HIS241A
3e	-3.7310	-299.62	**HB**- SER16A **HP**-LEU10A, ASN11A, VAL12A, SER16A, ALA29A, ARG202A, PRO216A, HIS241A **CHARGE**- ARG32A, ARG202A **VDW**- ASN11A, VAL12A, PRO14A, SER16A, PHE17A, ASN25A, VAL26A, ALA29A, ARG32A, VAL70A, ARG202A, PRO216A, HIS241A
3f	-4.5269	0.54	**HP**-LEU10A, VAL12A, ALA29A **VDW**- LEU10A, ASN11A, VAL12A, THR13A, SER16A, PHE17A, ASN25A, VAL26A, ALA29A, ARG32A, VAL70A, HIS241A
3g	-3.7320	-275.22	**HB**- SER16A **HP**-LEU10A, ASN11A, VAL12A, SER16A **CHARGE**- ARG202A **VDW**- LEU10A, ASN11A, VAL12A, SER16A, VAL26A, SER28A, ALA29A, ARG32A, VAL70A, PRO216A, HIS241A

CONCLUSION

The compounds with chloro **(3b),** fluoro **(3f),** and bromo **(3g)** substitution showed good activity. Compounds possessing chloro **(3b)** substitution were found to hold better antibacterial activity against gram-positive and gram-negative bacteria among the synthesized compounds, whereas most of the compounds showed moderate antifungal activity against *C. albicans* and *A. niger* species compared to fluconazole. The docking study revealed compound **3f** to possess -4.8845 Kcal/mol as the highest dock score with homo sapiens DHFR. Compound **3g** was observed to possess -4.1578 Kcal/mol as the highest dock score with bacterial DHFR, and compound **3b** possessed -4.5570 Kcal/mol as the highest dock score with DHPS protein. All compounds showed a good dock score compared to the reference ligand (trimethoprim/sulfadiazine). Docking of dihydrofolic acid with homo sapiens DHFR revealed that interactions between the ligands and ARG32A, SER59A, ASN64A (HB), LEU22A, THR56A, SER59A, ILE60A, ASN64A (HP) and LYS68A (charge) are important for increased affinity for human DHFR. Avoidance of these interactions should guide selectivity for pathogenic species. A comparative study of the docking of synthesized compound (3f) and dihydrofolic acid with homo sapiens DHFR revealed that the conformational change in the ligand enhanced interactions with residues ILE60A, LEU67A (LEU22A, THR56A, SER59A, ILE60A, and ASN64A in DHF), ARG70A (LYS68A in DHF), and TRP24A (ARG32A, SER59A, and ASN64A in DHF), yielding selectivity. Docking of the synthesized compounds showed interactions comparable to the standard drugs, which confirms their selectivity. Thus, we can conclude that the synthesized compounds have the potential for further development as novel antimicrobial agents.

LIST OF ABBREVIATIONS

WHO	=	World Health Organization
MIC	=	Minimum Inhibitory Concentration
TLC	=	Thin Layer Chromatography
DHFR	=	Dihydrofolate Reductase
DHPS	=	Dihydropteroate Synthase
PDB	=	Protein Data Bank

ETHICS APPROVAL AND CONSENT TO PARTICIPATE

Not applicable.

HUMAN AND ANIMAL RIGHTS

No animals/humans were used in this research.

CONSENT FOR PUBLICATION

Not applicable.

AVAILABILITY OF DATA AND MATERIALS

The data and supportive information are available within the article.

FUNDING

Pune District Education Association's Seth Govind Raghunath Sable College of Pharmacy, Saswad (Maharashtra) 412301, provided financial support for this study.

CONFLICT OF INTEREST

The authors declare no conflict of interest, financial or otherwise.

ACKNOWLEDGEMENTS

The authors acknowledge the financial support from Pune District Education Association's Seth Govind Raghunath Sable College of Pharmacy, Saswad (Maharashtra) 412301.

REFERENCES

[1] MacGowan, A.; Macnaughton, E. Antibiotic resistance. *Medicine (Abingdon),* **2017**, *45*(10), 622-628. [http://dx.doi.org/10.1016/j.mpmed.2017.07.006]

[2] Verma, V.; Joshi, C.P.; Agarwal, A.; Soni, S.; Kataria, U. A Review on pharmacological aspects of pyrimidine derivatives. *J. Drug Deliv. Ther.,* **2020**, *10*(5), 358-361. [http://dx.doi.org/10.22270/jddt.v10i5.4295]

[3] Natarajan, R.; Anthoni Samy, H.N.; Sivaperuman, A.; Subramani, A.; Subramani, A. Structure-activity relationships of pyrimidine derivatives and their biological activity - a review. *Med. Chem.,* **2022**, *19*(1), 10-30. [PMID: 35579151]

[4] Song, M.; Zhao, W.; Zhu, Y.; Liu, W.; Deng, X.; Huang, Y. Design, synthesis, and evaluation of anticonvulsant activities of new triazolopyrimidine derivatives. *Front Chem.,* **2022**, *10*925281 [http://dx.doi.org/10.3389/fchem.2022.925281] [PMID: 35815216]

[5] Severina, H.; Skupa, O.O.; Voloshchuk, N.I.; Suleiman, M.M.; Georgiyants, V.A. Synthesis and anticonvulsant activity of 6-methyl-2-((2-oxo-2-arylethyl)thio)pyrimidin-4(3 H)-one derivatives and products of their cyclization. *Pharmacia,* **2019**, *66*(3), 141-146. [http://dx.doi.org/10.3897/pharmacia.66.e38137]

[6] Provenzani, R.; San-Martin-Galindo, P.; Hassan, G.; Legehar, A.; Kallio, A.; Xhaard, H.; Fallarero, A.; Yli-Kauhaluoma, J. Multisubstituted pyrimidines effectively inhibit bacterial growth and biofilm formation of *Staphylococcus aureus. Sci. Rep.,* **2021**, *11*(1), 7931. [http://dx.doi.org/10.1038/s41598-021-86852-5] [PMID: 33846401]

[7] Mahapatra, A.; Prasad, T.; Sharma, T. Pyrimidine: A review on anticancer activity with key emphasis on SAR. *Future J Pharma Sci,* **2021**, *7*(1), 123. [http://dx.doi.org/10.1186/s43094-021-00274-8]

[8] Tylińska, B.; Wiatrak, B.; Czyżnikowska, Ż.; Cieśla-Niechwiadowicz, A.; Gębarowska, E.; Janicka-Kłos, A. Novel pyrimidine derivatives as potential anticancer agents: Synthesis, biological evaluation and molecular docking study. *Int. J. Mol. Sci.,* **2021**, *22*(8), 3825. [http://dx.doi.org/10.3390/ijms22083825] [PMID: 33917090]

[9] Jadhav, P.A.; Baravkar, A. Recent advances in antimicrobial activity of pyrimidines: A review. *Asian J. Pharm. Clin. Res.,* **2021**, *15*(2), 4-10. [http://dx.doi.org/10.22159/ajpcr.2022.v15i2.43686]

[10] Tolba, M.S.; El-Dean, A.M.K.; Ahmed, M.; Hassanien, R.; Sayed, M.; Zaki, R.M.; Mohamed, S.K.; Zawam, S.A.; Abdel-Raheem, S.A.A. Synthesis, reactions, and applications of pyrimidine derivatives. *Curr Chem Lett,* **2022**, *11*(1), 121-138. [http://dx.doi.org/10.5267/j.ccl.2021.8.002]

[11] Raimondi, M.; Randazzo, O.; La Franca, M.; Barone, G.; Vignoni, E.; Rossi, D.; Collina, S. DHFR inhibitors: Reading the past for discovering novel anticancer agents. *Molecules,* **2019**, *24*(6), 1140. [http://dx.doi.org/10.3390/molecules24061140] [PMID: 30909399]

[12] Abd El-Aleam, R.H.; George, R.F.; Hassan, G.S.; Abdel-Rahman, H.M. Synthesis of 1,2,4-triazolo[1,5-a]pyrimidine derivatives: Antimicrobial activity, DNA Gyrase inhibition and molecular docking. *Bioorg. Chem.,* **2020**, *94*103411 [http://dx.doi.org/10.1016/j.bioorg.2019.103411] [PMID: 31711767]

[13] Panneerselvam, T.; Mandhadi, J.R. Microwave assisted synthesis and antimicrobial evaluation of novel substituted thiosemicarbazide derivatives of pyrimidine. *J. Heterocycl. Chem.,* **2020**, *57*(8), 3082-3088. [http://dx.doi.org/10.1002/jhet.4013]

[14] Al-Juboori, S.B.; Mahmood, A.A.R. Synthesis, antimicrobial evaluation, density functional theory, and docking studies of some new 2-mercapto pyrimidine schiff bases. *Asian J. Pharm. Clin. Res.,* **2019**, *12*(2), 496-502. [http://dx.doi.org/10.22159/ajpcr.2019.v12i2.30858]

[15] Khatri, T.T.; Shah, V.H. Effective microwave synthesis of bioactive thieno[2,3-d]pyrtmidines. *J. Chil. Chem. Soc.,* **2017**, *62*(1), 3354-3358. [http://dx.doi.org/10.4067/S0717-97072017000100010]

[16] Shehab, W.S.; Assy, M.G.; Moustafa, H.Y.; Abdellattif, M.H.; Rahman, H.M.A. Pyrimidines as block units in heterocycles: novel synthesis of pyrimidines and condensed pyrimidine derivatives. *J. Indian Chem. Soc.,* **2019**, *16*, 2451-2461.

[17] Fernández-Villa, D.; Aguilar, M.R.; Rojo, L. Folic acid antagonists: Antimicrobial and immunomodulating mechanisms and applications. *Int. J. Mol. Sci.,* **2019**, *20*(20), 4996. [http://dx.doi.org/10.3390/ijms20204996] [PMID: 31601031]

[18] Shamshad, H.; Bakri, R.; Mirza, A.Z. Dihydrofolate reductase, thymidylate synthase, and serine hydroxy methyltransferase: Successful targets against some infectious diseases. *Mol. Biol. Rep.,* **2022**, *49*(7), 6659-6691. [http://dx.doi.org/10.1007/s11033-022-07266-8] [PMID: 35253073]

[19] He, J.; Qiao, W.; An, Q.; Yang, T.; Luo, Y. Dihydrofolate reductase inhibitors for use as antimicrobial agents. *Eur. J. Med. Chem.,* **2020**, *195*112268 [http://dx.doi.org/10.1016/j.ejmech.2020.112268] [PMID: 32298876]

[20] Hitchings, G.H.; Burchall, J.J. Inhibition of folate biosynthesis and function as a basis for chemotherapy. *Adv. Enzymol. Relat. Areas Mol. Biol.,* **2006**, *27*, 417-468. [http://dx.doi.org/10.1002/9780470122723.ch9] [PMID: 4387360]

[21] Patil, DR; Salunkhe, SM; Deshmukh, MB; Anbhule, PV One step synthesis of 6-amino-5-cyano-4-phenyl-2-Mercapto pyrimidine using phosphorous pentoxide. *Catal J,* **2010**, *3*, 83-86.

[22] Petkar, K.; Parekh, P.; Mehta, P.; Kumari, A.; Baro, A. Synthesis and evaluation of 2-chloromethyl-1H-benzimidazole derivatives as antifungal agents. *Int. J. Pharm. Pharm. Sci.,* **2013**, *5*(2), 115-119.

[23] Kokare, C. *Pharmaceutical Microbiology Principles and Applications,* 9th ed; Nirali Publication, **2013**.

[24] Vilar, S.; Cozza, G.; Moro, S. Medicinal chemistry and the molecular operating environment (MOE): Application of QSAR and molecular docking to drug discovery. *Curr. Top. Med. Chem.,* **2008**, *8*(18), 1555-1572. [http://dx.doi.org/10.2174/156802608786786624] [PMID: 19075767]

[25] Dar, A.M.; Mir, S. Molecular docking: Approaches, types, applications and basic challenges. *J. Anal. Bioanal. Tech.,* **2017**, *8*(2), 1-3. [http://dx.doi.org/10.4172/2155-9872.1000356]

[26] Hawser, S.; Lociuro, S.; Islam, K. Dihydrofolate reductase inhibitors as antibacterial agents. *Biochem. Pharmacol.,* **2006**, *71*(7), 941-948. [http://dx.doi.org/10.1016/j.bcp.2005.10.052] [PMID: 16359642]

[27] Capasso, C.; Supuran, C.T. Sulfa and trimethoprim-like drugs – antimetabolites acting as carbonic anhydrase, dihydropteroate synthase and dihydrofolate reductase inhibitors. *J. Enzyme Inhib. Med. Chem.,* **2014**, *29*(3), 379-387. [http://dx.doi.org/10.3109/14756366.2013.787422] [PMID: 23627736]

[28] Available From: www.rcsb.org

https://doi.org/10.48047/AFJBS.6.2.2024.1556-1579

African Journal of Biological Sciences

Journal homepage: http://www.afjbs.com

Research Paper Open Access

Analytical Method Development and Validation of RP-HPLC Method for Estimation of Metformin HCL, Vildagliptin, and Remogliflozin Etabonate in Bulk Drug and its Tablet Dosage Form

Shifa A. Shikalgar[1], Dr. Rajashree S. Chavan[2]

[1]Research Scholar, Pharmaceutical Chemistry, Pune District Education Associations Pune District Education Associtions Seth Govind Raghunath Sable College of Pharmacy, Saswad Ta: Purandar Dist: Pune, Maharashtra, India.

[2]Principal, Pharmaceutical Chemistry, Pune District Education Associations Pune District Education Associtions Seth Govind Raghunath Sable College of Pharmacy, Saswad Ta: Purandar Dist: Pune, Maharashtra, India.

Article History

Volume 6, Issue 2, 2024
Received: 16 May 2024
Accepted : 20 June 2024
Published : 9 July 2024
Doi:
10.48047/AFJBS.6.2.2024.1556-1579

ABSTRACT:

This study reports the Method Development and Validation For Anti Diabetic Drugs By Rp-Hplc. The drug analysis is playing an vital position within the improvement of medicine, their manufacture and therapeutic use For the simultaneous estimation of medicine present in dosage forms, lot, of suitable techniques are adopted like uv – spectrophotometer HPLC. Those techniques are powerful rugged technique .they're additionally extraordinarily specific, specific, correct, linear and speedy. A pharmaceutical industry depends upon quantitative chemical analysis to make sure that the raw material used and the final product obtained meets the required specification. The drugs will occur as a unmarried factor or multi issue dosage paperwork. The later proves to be effective because of its mixed mode of movement at the body.

Keywords: RP-HPLC, Metformin (MET), Vildagliptin (VDG) and Remogliflozin (RMG), Diabetes Mellitus.

INTRODUCTION:

In pharmaceutical industry, there is a need for the invention of suitable novel analytical methods from time to time for testing the quality of bulk drugs, excipients and formulations. Method development and validation is an integral part of drug discovery and drug development. UV-visible spectroscopy and HPLC are the most popular techniques used for the identification and estimation of drugs with good accuracy and precision. Simultaneous method development is useful for analysis of combination of drugs.

DRUG PROFILE:

Metformin hydrochloride

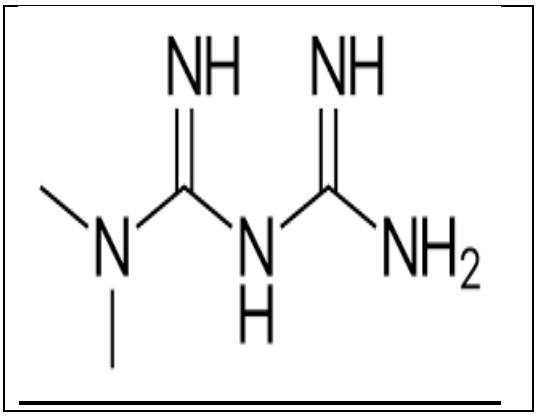

Molecular formula: C4H11N5
Molecular Weight: 129.16
Synonyms: Metfromin.
IUPAC Name: 3-(diaminomethylidiene)-1,1-dimethylguanidine;hydrochloride.
Solubility: Water,Methanol.
Category: Anti-diabetic agent.

Mechanism of action:

Metformin is an antihyperglycemic agent, which improves glucose tolerance in patients with type 2 diabetes, lowering both basal and postprandial plasma glucose. Its pharmacological mechanisms of action are different from other classes of oral antihyperglycemic agents. Metformin decreases hepatic glucose production, decreases intestinal absorption of glucose, and improve insulin sensitivity by increasing peripheral glucose uptake and utilization. Unlike sulfonylureas, metformin does not produce hypoglycemia in either patients with type 2 diabetes or normal subjects and does not cause hyperinsulinemia. With metformin therapy, insulin secretion remains unchanged while fasting insulin levels and daylong plasma insulin response may actually decrease.

Vildagliptin

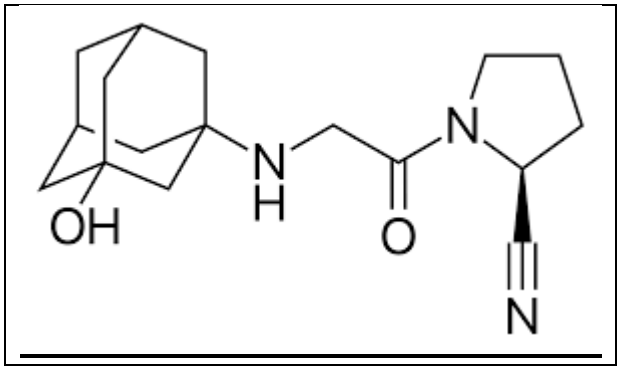

Molecular formula: C17H25N3O2
Molecular Weight: 303.399g/mol
IUPAC Name:(S)-1-[2-(3-Hydroxyadamantan-1-ylamino) acetyl]pyrrolidine-2-carbonitrile
Solubility: Water, Methanol.
Category: Type-2 diabetes mellitus.

Mechanism of action:

Inhibition of dipeptidyl peptidase-4 (DPP-4) by vildagliptin prevents degradation of glucagon-like peptide-1 (GLP-1) and reduces glycaemia in patients with type 2 diabetes mellitus, with low risk for hypoglycaemia and no weight gain. Vildagliptin binds covalently to the catalytic site of DPP-4, eliciting prolonged enzyme inhibition. This raises intact GLP-1 levels, both after meal ingestion and in the fasting state. Vildagliptin has been shown to stimulate insulin secretion and inhibit glucagon secretion in a glucose- dependent manner. At hypoglycaemic levels, the counterregulatory glucagon response is enhanced relative to baseline by vildagliptin. Vildagliptin also inhibits hepatic glucose production, mainly through changes in islet hormone secretion, and improves insulin sensitivity, as determined with a variety of methods. These effects underlie the improved glycaemia with low risk for hypoglycaemia. Vildagliptin also suppresses postprandial triglyceride (TG)-rich lipoprotein levels after ingestion of a fat-rich meal and reduces fasting lipolysis, suggesting inhibition of fat absorption and reduced TG stores in non-fat tissues. The large body of knowledge on vildagliptin regarding enzyme binding, incretin and islet hormone secretion and glucose and lipid metabolism is summarized, with discussion of the integrated mechanisms and comparison with other DPP-4 inhibitors and GLP-1 receptor activators, where appropriate..

Remogliflozin Etabonate

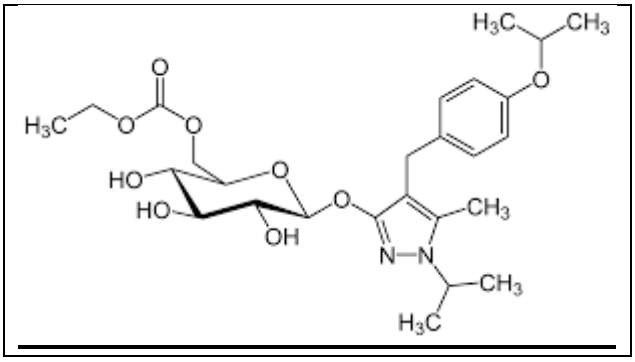

Molecular formula: C26H38N2O9 Molecular
Weight: 522.6
IUPAC Name: 5-Methyl-4-[4-(1-methylethoxy)benzyl]-1-(1-methylethyl)-1H-pyrazol-3-yl 6- O-(ethoxycarbonyl)-β-D-glucopyranoside
Solubility: Methanol
Category: Oral hypoglycemic agent used to treat type-2 diabetes mellitus.

Mechanism of action:

Remogliflozin etabonate is a pro-drug of remogliflozin. Remogliflozin inhibits the sodium-glucose transport proteins (SGLT), which are responsible for glucose reabsorption in the kidney. Blocking this transporter causes blood glucose to be eliminated through the urine.[8] Remogliflozin is selective for SGLT2.

MATERIALS AND INSTRUMENTS:

Procurement of Drug Sample

Sr. No.	Drug sample	Supplier (Gift Sample)
1	**Vildagliptin**	Glenmark Pharmaceuticals, Nashik
2	**Remogliflozin**	Glenmark Pharmaceuticals, Nashik
3	**Metformin HCl**	Glenmark Pharmaceuticals, Nashik

Marketed formulation details:

Remo-Zen MV 500 Tablet (Glenmark Pharmaceuticals)

Label claim:

Each Film coated tablet Contains
Vildagliptin – 50 mg
Remogliflozin – 100 mg
Metformin HCl–500 mg

Reagents and chemicals:

- Methanol (HPLC Grade),
- Potassium dihydrogen Phosphate (AR Grade)
- Ortho phosphoric acid (AR Grade)
- HPLC grade water.
- All chemicals and reagents that is Methanol, Potassium dihydrogen Phosphate,Ortho phosphoric acid were purchased from Merck Ltd., Mumbai.

- **Instruments:**
  1. HPLC:
     - Borwin chromatography software (version 1.50)
     - Model PU 2080 Plus Intelligent HPLC pump
     - Rheodyne sample injection port with 10µl loop
     - Nucleosil C_8 column(250 x 4.6 mm, 5µm)
     - JASCO UV-2075 UV-VIS detector
  2. Double Beam UV-Vis Spectrophotometer (Shimadzu UV-1780)
  3. Shimadzu (model AY-120) Electronic weighing balance
  4. Sonicator: PRAMA solutions for laboratory
  5. Extrapure lab link water purification system
  6. Electronic pH meter
  7. Calibrated Glassware's.

Experimental, Results and Discussion

Table 1 : Trials of mobile phase

Sr.No.	**Mobile phase**	**Observation**	**Densitogram**
1.	10 mM KH_2PO_4 (pH 4 adjusted with OPA): Methanol [40: 60 v/v]	Remogliflozin – 2.320 min Vildagliptin – 14.733 min Metformin HCl – 8.053 min High Retention Times. Broad Peaks. Peak Tailing	Remogliflozin 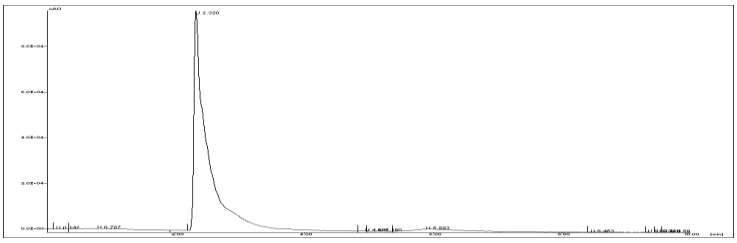 Vildagliptin 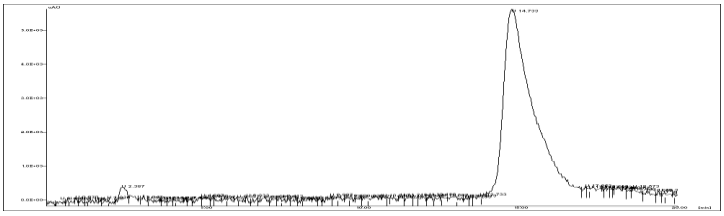 Metformin HCl 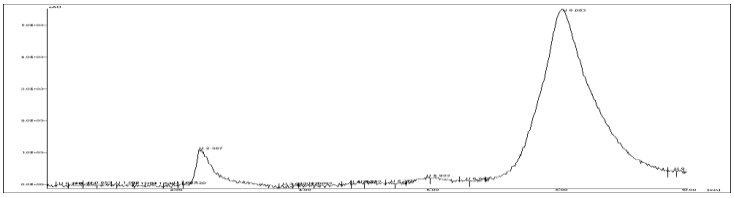
2.	10 mM KH_2PO_4 (pH 4 adjusted with OPA): Methanol [55: 45 v/v]	Remogliflozin – 2.700 min Vildagliptin – 15.808 min Metformin HCl – 6.950 min High Retention Times. Broad Peaks	Remogliflozin 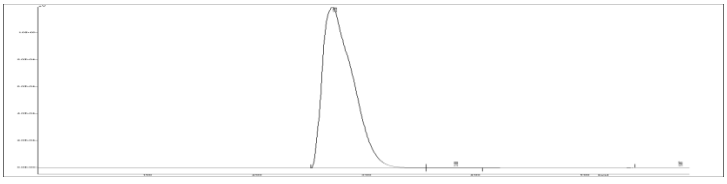 Vildagliptin

			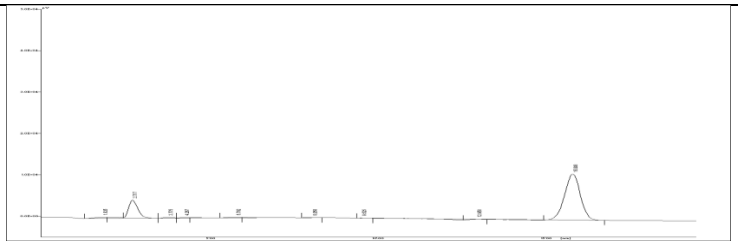 Metformin HCl 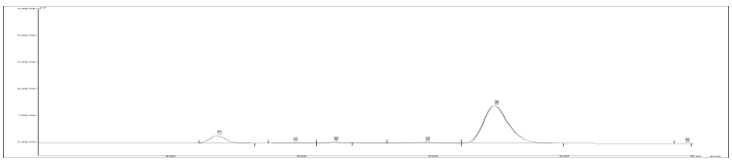
3.	10 mM KH_2PO_4 (pH 4 adjusted with OPA): Methanol [20: 80 v/v]	Remogliflozin – 2.750 min Broad Peak Vildagliptin – 3.942 min Metformin HCl – 6.183 min Good Peak Shapes, Well Resolved Peaks which pass system suitability parameters	Remogliflozin 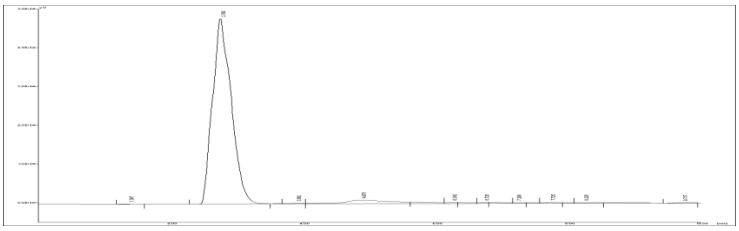 Vildagliptin 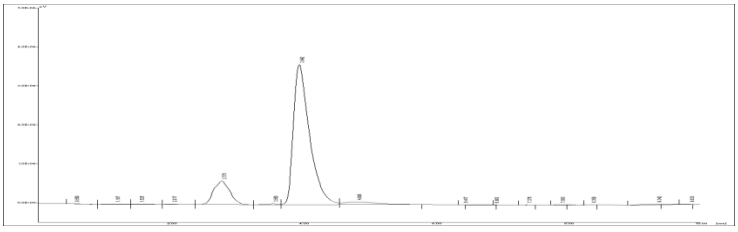 Metformin HCl 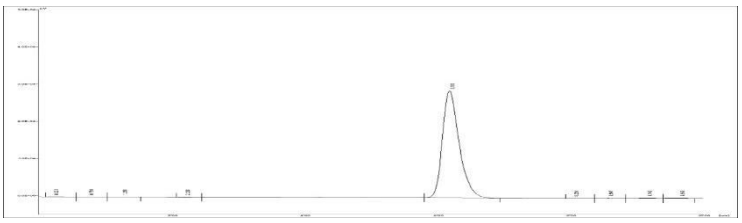

- **Preparation of Standard stock solutions:**

Standard stock solution of Vildagliptin,Remogliflozinand Metformin HClwere prepared separately by dissolving 10 mg of each drug in 10 ml of methanol separately to get concentration of 1000 µg/ml. From the respective standard stock solution, working standard solution was prepared containing 100 µg/ml of Vildagliptin, RemogliflozinandMetformin HCl, separately in methanol. These solutions were appropriately diluted with methanol to obtain desired solutions.

- **Selection of Detection Wavelength:**

From the standard stock solution further dilutions were done using methanol and scanned over the range of 200 - 400 nm and the spectra was obtained. It was observed that all drugs showed considerable absorbance at 210 nm (Fig.1)

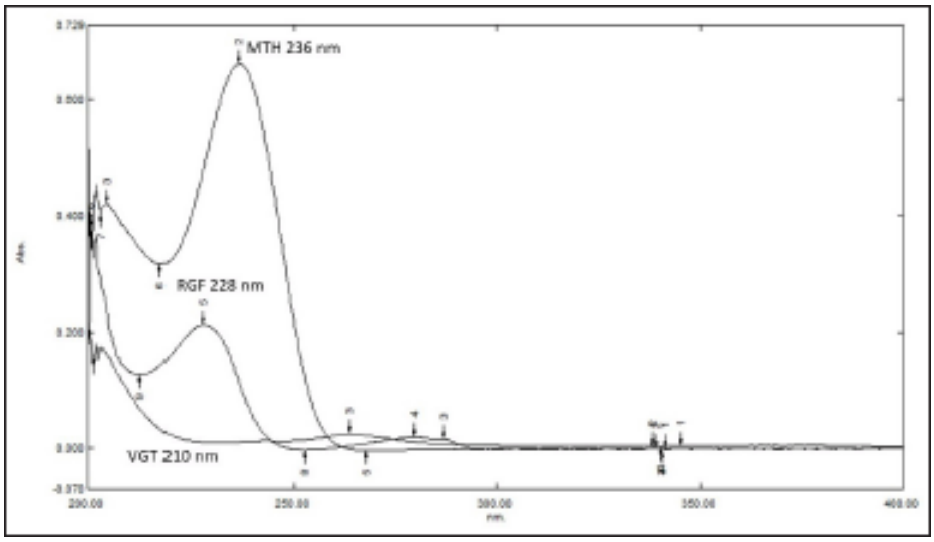

Fig.1: Overlain UV-VIS Spectra of Vildagliptin (10 µg/ml), Remogliflozin (10 µg/ml) and Metformin HCl (10 µg/ml)

- **Selection of mobile phase and chromatographic conditions:**

Chromatographic separation studies were carried out on the working standard solution of Vildagliptin (4 µg/ml) and Remogliflozin (8 µg/ml) and Metformin HCl (40 µg/ml). Initially, trials were carried out using various solvents in different proportions to obtain the desired system suitability parameters. After few trials, 10 mM KH_2PO_4 (pH 4 adjusted with OPA): Methanol [20: 80 v/v], was chosen as the mobile phase, which gave good resolution and acceptable peak parameters.

- **Chromatographs of the drug:**

Solution of 4 µg/ml of Vildagliptin, 8 µg/ml of Remogliflozinand 40 µg/ml of Metformin HClwas prepared. Individual Solutions as well as standard mixture were injected on stabilized HPLC system and chromatograph was obtained. Chromatographs were checked for system suitability parameters like number of theoretical plates (N), Asymmetry factor (AF) and resolution between the drugs

The retention time± % RSD were found to be:

Remogliflozin = 2.771 ± 0.313

Vildagliptin = 4.103 ± 0.209

Metformin HCl = 6.224 ± 0.052

A)

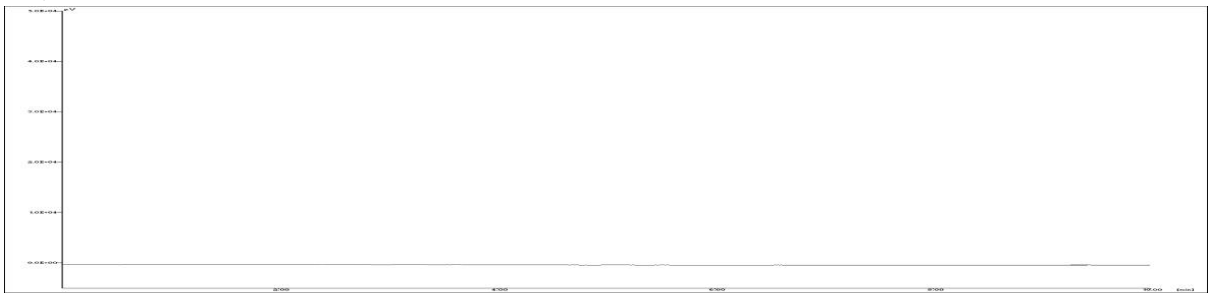

B)

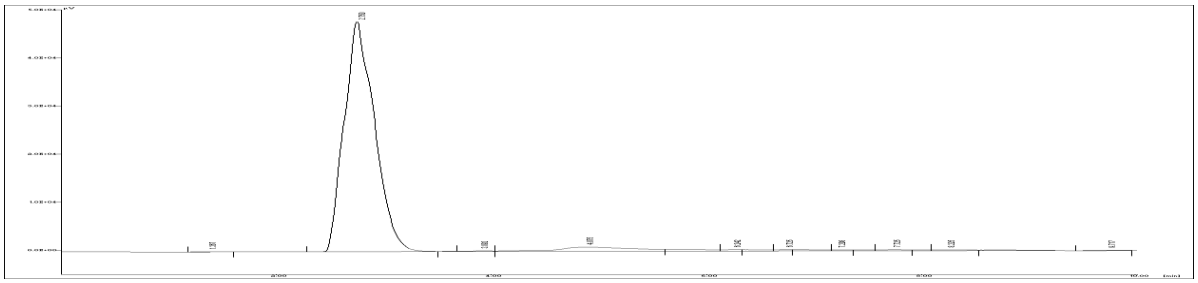

C)

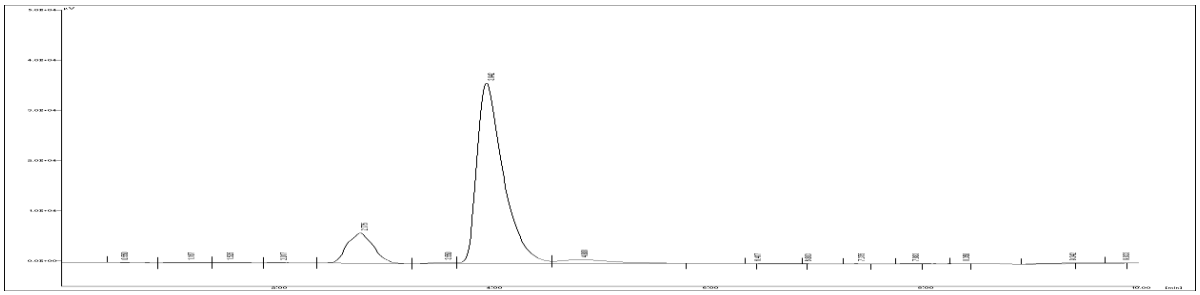

D)

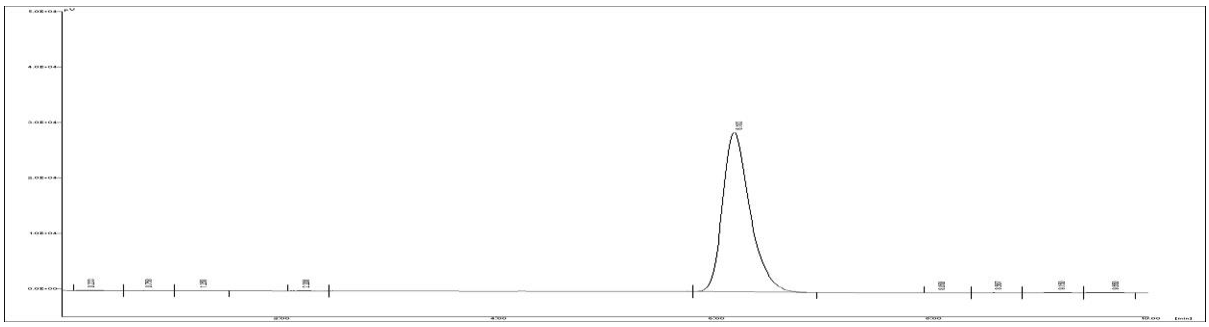

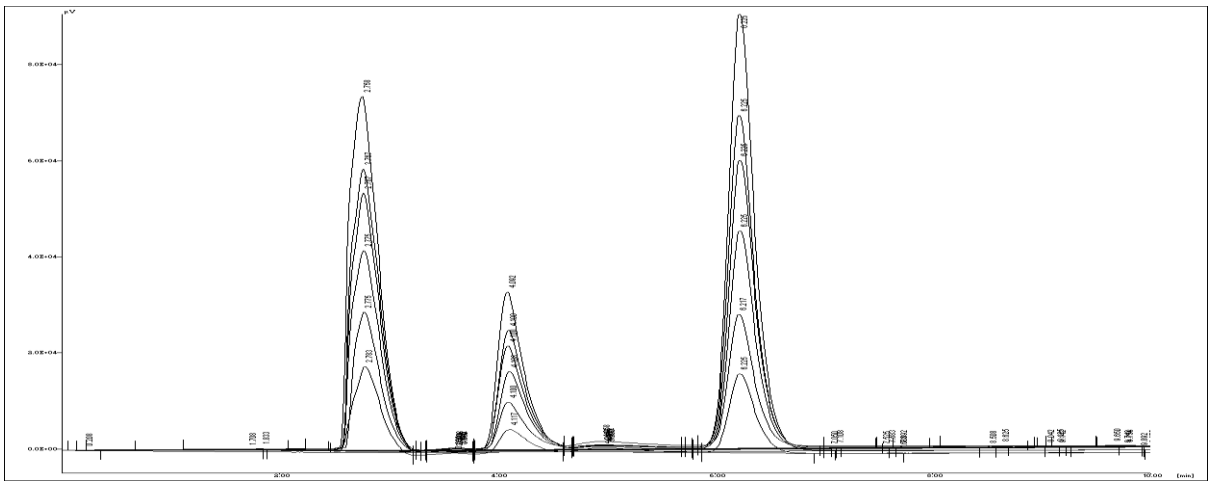

Fig.2 :Chromatograph of A) Blank B) Remogliflozin (8 µg/ml), C) Vildagliptin (4 µg/ml) D) Metformin HCl(40 µg/ml)individuals and E) mixed standard solution of all three drugs

Summary of chromatographic parameters selected:

Chromatographic parameters are summarized in Table 2 ____

Table2: Chromatographic parameters

Sr. No.	Parameter	Conditions used for Analysis
1	Stationary phase(Column)	Nucleosil C_8 column (250 x 4.6 mm, 5µm)
2.	Mobile phase	10 mM KH_2PO_4 (pH 4 adjusted with OPA): Methanol [20: 80 v/v]
3.	Detection Wavelength	210 nm
4.	Injection Volume	10 µl
5.	Temperature	Ambient

Table3: System suitability parameters for Drugs

Drug	Concentration (µg/ml)	RT ± RSD (Min)	Area	Plates	Asymmetry	Rs*
Remogliflozin	8	2.771 ± 0.313	142838.85	2342.71	1.07	-
Vildagliptin	4	4.103 ± 0.209	242698.08	2764.46	1.21	1.69
Metformin HCl	40	6.224 ± 0.052	657594.34	4138.24	1.13	3.15

*** Resolution with respect to previous peak**

- **Preparation of sample solution(Formulation Analysis):**

Ten tablets each containing 50 mg of Vildagliptin, 100 mg of Remogliflozin and 500 mg of Metformin HClwas weighed and powdered. Powder equivalent to 10 mg of Vildagliptin (20 mg of Remogliflozinand 100 mg of Metformin HCl) was transferred to 10 ml volumetric flask and was diluted with methanol, sonicated for 10 min and volume made to 10 ml with methanol. Solution was filtered and further dilutions were made to get the final concentration of 4 µg/ml of Vildagliptin, 8 µg/ml of Remogliflozin and 40 µg/ml of Metformin HCl.

Validation of Analytical Method

Linearity

From the standard stock solution (1000 µg/ml) of Vildagliptin, Remogliflozin and Metformin HCl, further dilutionswere was prepared separately by appropriate dilution with methanol. The linearity (relationship between peak area and concentration)was determined by analyzing six solutions over the concentration range 2 - 12 µg/ml for Vildagliptin, 4 - 24 µg/ml for Remogliflozin and 20 - 120 µg/ml for Metformin HCl.The results obtained are shown in Table_4 for Vildagliptin, Table_5 for Remogliflozin and in Table _6_ for Metformin HCl. Overlain chromatographs of Linearity are shown in Fig.3, 4, 5 and calibration curve shown in Fig. 6,7,8.

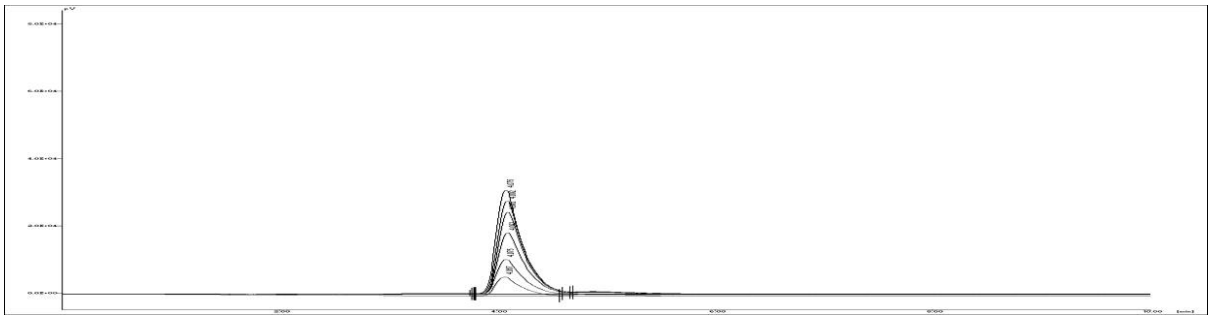

Fig _3__: Overlain chromatographs of Linearity for Vildagliptin (2-12 µg/ml)

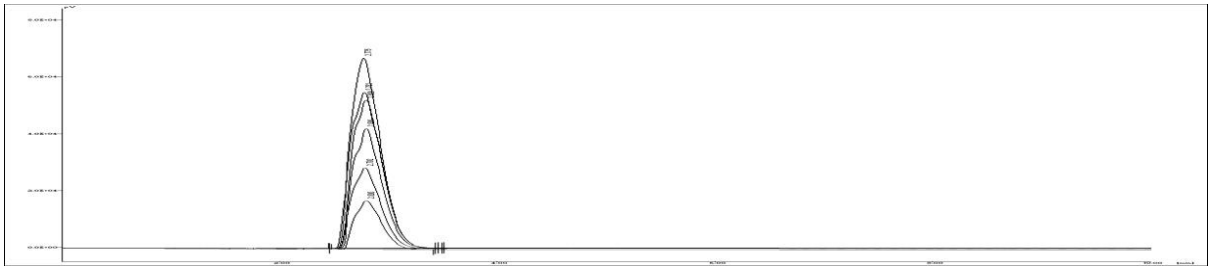

Fig _4___: Overlain chromatographs of Linearity for Remogliflozin (4-24 µg/ml)

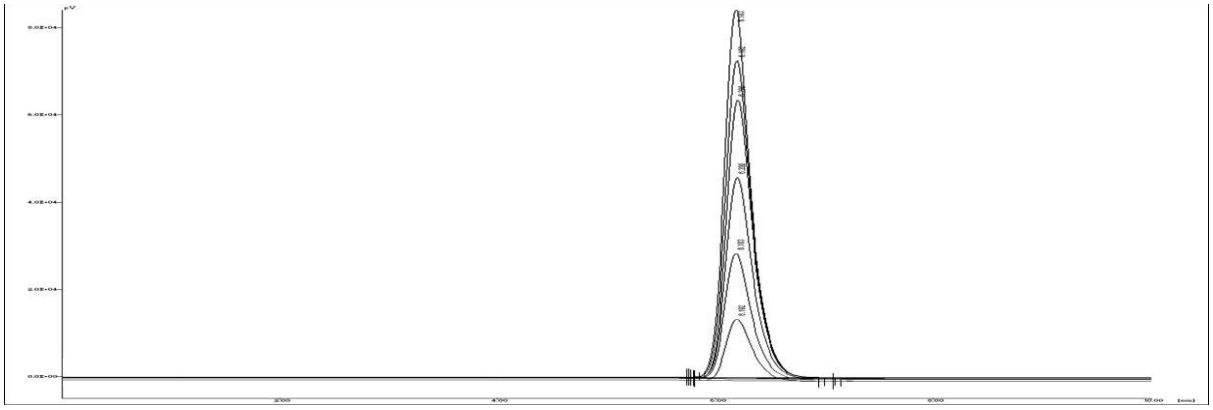

Fig _5___: Overlain chromatographs of Linearity for Metformin HCl (20 - 120 µg/ml)

Table 4___: Linearity study of Vildagliptin

Replicates						
	Concentrations of Vildagliptin(µg/ml)					
	2	**4**	**6**	**8**	**10**	**12**
	Peak Area					
1	72762.69	142233.91	214139.63	302056.76	381370.99	449293.85
2	70699.23	142838.85	208258.05	291566.28	370435.07	434569.14
3	70990.92	144299.05	214994.78	303838.54	390645.26	455535.08
4	69630.56	144632.81	217332.12	304299.00	377902.53	446636.19
5	71475.06	140987.53	214429.22	305219.92	382642.26	455424.35
6	69164.10	139704.64	214078.87	304874.57	377837.46	451155.71
Mean	70787.093	142449.463	213872.109	301975.841	380138.926	448769.050

Std.dev.	1295.935	1900.390	3005.807	5218.408	6672.792	7774.707
%RSD	1.831	1.334	1.405	1.728	1.755	1.732

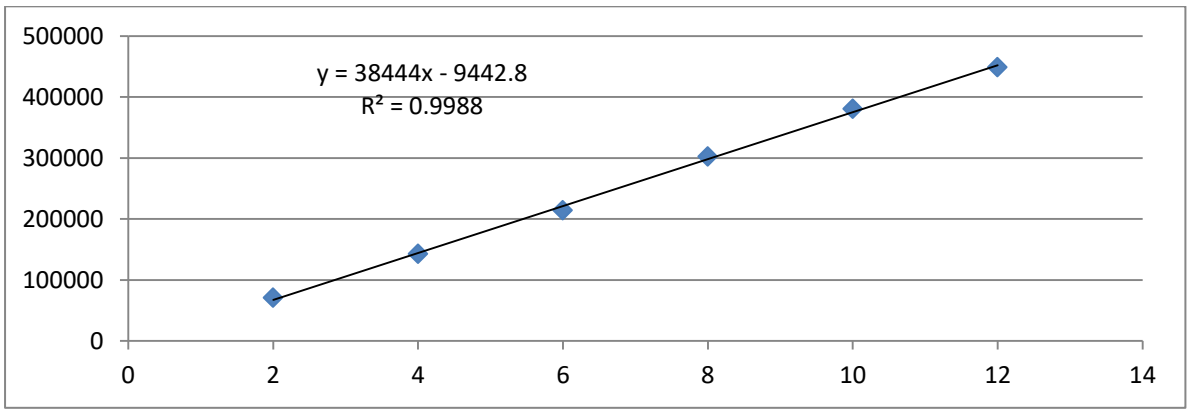

Fig.6: Calibration curve for Vildagliptin

Table 5: Linearity study of Remogliflozin

Replicates	**Concentrations of Remogliflozin(µg/ml)**					
	4	**8**	**12**	**16**	**20**	**24**
	Peak Area					
1	141261.62	239575.48	342987.58	461226.04	571742.66	696297.77
2	143135.18	242698.08	348851.31	461250.66	572852.98	691211.53
3	145262.37	247573.03	347850.69	476367.05	586189.89	693155.60
4	145290.98	249675.89	353039.68	458986.17	578101.35	703683.92
5	141423.76	243754.96	353151.37	465327.45	577560.90	703425.70
6	144882.64	246323.57	352437.80	459412.53	577861.15	674349.49
Mean	143542.756	244933.501	349719.737	463761.647	577384.821	693687.333
Std.dev.	1879.813	3646.480	3993.881	6569.661	5112.185	10788.386
%RSD	1.310	1.489	1.142	1.417	0.885	1.555

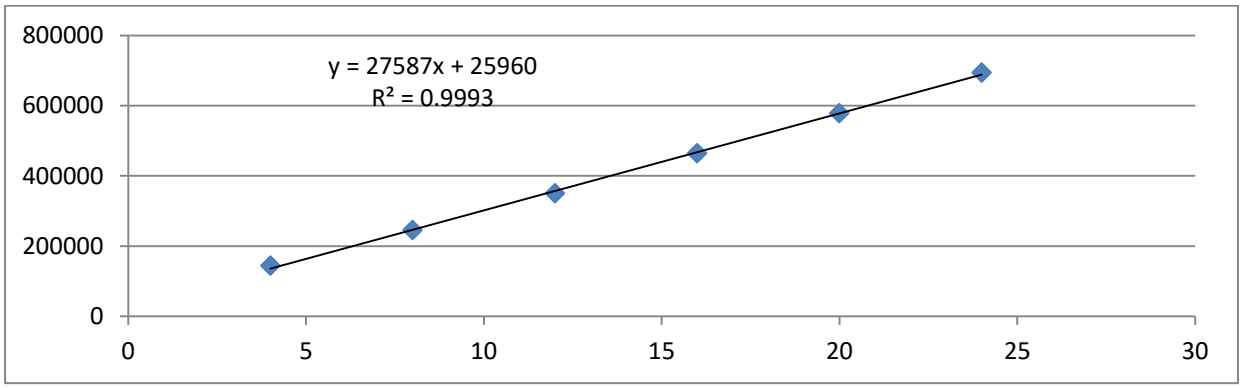

Fig.7: Calibration curve for Remogliflozin

Table 6: Linearity study of Metformin HCl

Replicates	Concentrations of Metformin HCl(µg/ml)					
	20	**40**	**60**	**80**	**100**	**120**
	Peak Area					
1	319759.92	662165.50	1041515.63	1316849.13	1736073.91	2100965.11
2	308450.91	645290.08	1006184.93	1316291.93	1701244.89	2064039.62
3	317799.74	657594.34	1039655.51	1308758.78	1767189.29	2054389.22
4	314703.57	663284.06	1033101.83	1340414.27	1719379.60	2033359.39
5	320755.17	670079.55	1044219.68	1320941.78	1699757.12	2010399.48
6	315749.03	671949.31	1035403.42	1352130.26	1756573.85	2037400.49
Mean	316203.054	661727.138	1033346.833	1325897.689	1730036.443	2050092.215
Std.dev.	4437.855	9634.610	13905.437	16681.302	28214.813	31040.705
%RSD	1.403	1.456	1.346	1.258	1.631	1.514

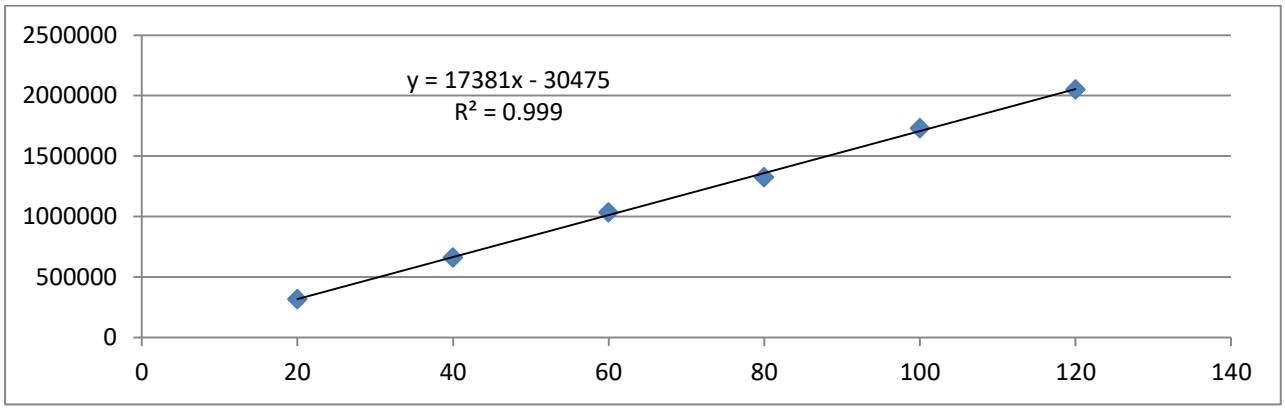

Fig.8: Calibration curve for Metformin HCl

Range

VILDAGLIPTIN = 2 – 12µg/ml

REMOGLIFLOZIN = 4- 24 µg/ml

METFORMIN HCL = 20- 120 µg/ml

Precision

The precision of the method was demonstrated by intra-day and inter-day variation studies. In the Intra-day studies, 3 replicates of 3different concentrations were analyzed in a day and percentage RSD was calculated. For the inter day variation studies, 3 different concentrations were analyzed on 3 consecutive days and percentage RSD were calculated.The results obtain for intra-day and inter day variations are shown in Table 7, 8, 9 10, 11 and 12_.

Table 7 : Intra-day precision study of Vildagliptin

Concentration (µg/ml)	Area	Practical Concentration (µg/ml)	% Recovery	Mean % Recovery ± RSD
4	144747.65	4.011	100.269	99.838 ± 0.385
	143612.82	3.981	99.531	
	143894.70	3.989	99.714	

6	220806.20	5.989	99.820	100.334 ± 0.488
	222114.66	6.023	100.387	
	223055.35	6.048	100.795	
8	298722.65	8.016	100.199	100.792 ± 0.553
	300795.39	8.070	100.873	
	302121.30	8.104	101.304	

Table 8: Inter-day precision of Vildagliptin

Concentration (µg/ml)	**Area**	**Practical Concentration (µg/ml)**	**% Recovery**	**Mean % Recovery ± RSD**
4	144626.95	4.008	100.191	99.577 ± 0.540
	143080.47	3.967	99.185	
	143344.25	3.974	99.356	
6	223174.65	6.051	100.847	99.989 ± 0.909
	221417.25	6.005	100.085	
	219001.17	5.942	99.037	
8	299858.52	8.045	100.569	100.230 ± 0.322
	298711.23	8.016	100.195	
	297878.70	7.994	99.925	

Table 9 : Intra-day precision study of Remogliflozin

Concentration (µg/ml)	**Area**	**Practical Concentration (µg/ml)**	**% Recovery**	**Mean % Recovery ± RSD**
8	247880.60	8.044	100.555	100.168 ± 0.354
	246854.10	8.007	100.090	
	246345.06	7.989	99.859	
12	356643.12	11.987	99.891	100.344 ± 0.994
	355855.66	11.958	99.653	
	361927.44	12.178	101.487	
16	467110.86	15.991	99.945	99.850 ± 0.132
	466934.75	15.985	99.905	
	466026.12	15.952	99.700	

Table 10: Inter-day precision of Remogliflozin

Concentration (µg/ml)	**Area**	**Practical Concentration (µg/ml)**	**% Recovery**	**Mean % Recovery ± RSD**
8	246019.02	7.977	99.711	100.332 ± 0.537
	248001.60	8.049	100.610	
	248146.15	8.054	100.675	
12	356540.10	11.983	99.860	99.907 ± 0.757

	359276.55	12.082	100.686	
	354273.66	11.901	99.175	
16	468101.67	16.027	100.170	100.380 ± 0.580
	467053.72	15.989	99.932	
	471934.19	16.166	101.038	

Table 11 : Intra-day precision study of Metformin HCl

Concentration (µg/ml)	**Area**	**Practical Concentration (µg/ml)**	**% Recovery**	**Mean % Recovery ± RSD**
40	659590.75	39.702	99.256	99.527 ± 0.433
	659906.75	39.720	99.301	
	664929.85	40.009	100.024	
60	1008198.00	59.759	99.599	99.763 ± 0.359
	1014202.00	60.105	100.174	
	1007348.75	59.710	99.517	
80	1355083.80	79.717	99.646	100.203 ± 0.872
	1356560.10	79.802	99.752	
	1376829.45	80.968	101.210	

Table 12: Inter-day precision of Metformin HCl

Concentration (µg/ml)	**Area**	**Practical Concentration (µg/ml)**	**% Recovery**	**Mean % Recovery ± RSD**
40	664295.10	39.973	99.932	100.364 ± 1.483
	658781.00	39.656	99.139	
	678813.20	40.808	102.021	
60	1008928.75	59.801	99.669	99.715 ± 0.237
	1007230.25	59.703	99.506	
	1012088.75	59.983	99.972	
80	1354385.55	79.677	99.596	99.727 ± 0.406
	1351732.20	79.524	99.405	
	1362525.15	80.145	100.181	

Assay (Formulation Analysis)

Tablet formulation analysis was carried out as mentioned under section preparation of sample solution. Procedure was repeated for six times. Sample solution was applied and area was recorded. Percentage recovery was determined from linearity equation. Assay results obtained are shown in Table 13, 14, 15 and representative chromatograph in Fig. 9_.

Table 13 : Assay of Marketed Formulation (Vildagliptin)

Sr. No.	Peak area	Amount Recovered (µg/ml)	% Recovery
1	145000.65	4.017	100.434
2	143700.28	3.984	99.588
3	143876.46	3.988	99.702
4	143829.05	3.987	99.672
5	144924.90	4.015	100.384
6	142667.55	3.957	98.916
Mean	143999.814	3.991	99.783
SD	867.927	0.023	0.564
%RSD	0.603	0.566	0.566

Table 14 : Assay of Marketed Formulation (Remogliflozin)

Sr. No.	Peak area	Amount Recovered (µg/ml)	% Recovery
1	248659.98	8.073	100.908
2	244516.80	7.922	99.031
3	247037.04	8.014	100.173
4	247414.75	8.028	100.344
5	246219.88	7.984	99.802
6	247523.65	8.031	100.393
Mean	246895.349	8.009	100.108
SD	1407.999	0.051	0.638
%RSD	0.570	0.637	0.637

Table 15 : Assay of Marketed Formulation (Metformin HCl)

Sr. No.	Peak area	Amount Recovered (µg/ml)	% Recovery
1	660373.67	39.747	99.368
2	659211.07	39.680	99.201
3	658600.22	39.645	99.113
4	657989.36	39.610	99.025
5	662816.60	39.888	99.720
6	666586.61	40.105	100.262
Mean	660929.585	39.779	99.448
SD	3252.565	0.187	0.468
%RSD	0.492	0.470	0.470

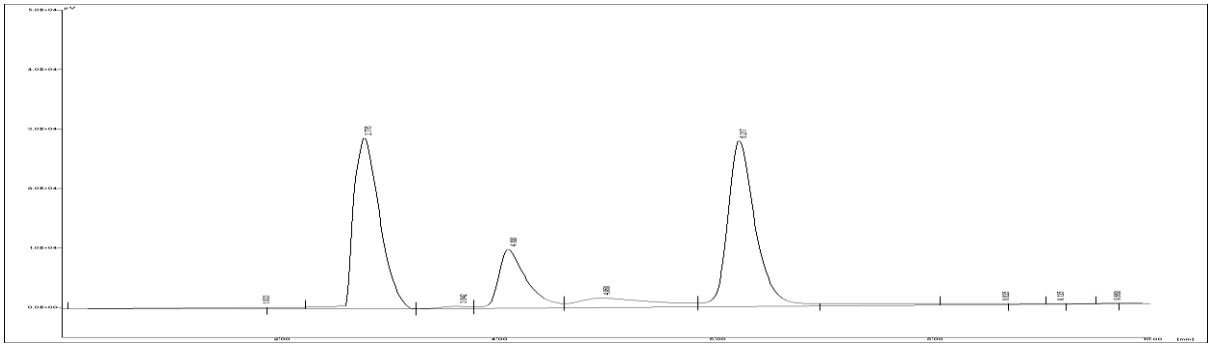

Fig. 9 : Chromatograph of Vildagliptin (4µg/ml), Remogliflozin (8µg/ml) and Metformin HCl (40 µg/ml)

Accuracy

To check accuracy of the method, recovery studies were carried out by adding standard drug to sample at three different levels 50, 100 and 150 %. Basic concentrations of sample chosen were 4 µg/mlof Vildagliptin, 8µg/mlof Remogliflozinand 40 µg/mlof Metformin HClsample solution. These solutions were injected on the system in triplicate to obtain the chromatograph. The drug concentrations of Vildagliptin,Remogliflozinand Metformin HClwere calculated by using linearity equations of each drug. The results obtained are shown in Table _16,17,18_.

Table 16: Recovery studies of Vildagliptin

Level	Conc. (µg/ml)		Area	Concentration (X)	% Recovery	Mean % Recovery ± RSD
	Sample	Std.				
50 %	4	2	220099.20	5.971	99.513	99.963 ± 0.428
			222060.93	6.022	100.364	
			221250.60	6.001	100.012	
100 %	4	4	297854.05	7.993	99.917	100.323 ± 0.357
			299522.85	8.037	100.459	
			299933.87	8.047	100.593	
150 %	4	6	376386.27	10.036	100.361	100.537 ± 0.469
			375684.87	10.018	100.179	
			379113.60	10.107	101.071	

Table 17: Recovery studies of Remogliflozin

Level	Conc. (µg/ml)		Area	Concentration (X)	% Recovery	Mean % Recovery ± RSD
	Sample	Std.				
50 %	8	4	357633.65	12.023	100.190	100.116 ± 0.075
			357394.56	12.014	100.118	
			357133.98	12.005	100.039	
100 %	8	8	469972.40	16.095	100.594	99.993 ± 0.522
			465820.29	15.944	99.653	
			466171.56	15.957	99.733	

150 %	8	12	577197.63	19.982	99.909	99.897 ± 0.164
			576196.73	19.946	99.728	
			577998.26	20.011	100.054	

Table 18: Recovery studies of Metformin HCl

Level	Conc. (µg/ml)		Area	Concentration (X)	% Recovery	Mean % Recovery ± RSD
	Sample	Std.				
50 %	40	20	1012588.20	60.012	100.019	100.162 ± 0.131
			1014374.70	60.114	100.191	
			1015268.50	60.166	100.276	
100 %	40	40	1357457.00	79.853	99.817	99.725 ± 0.106
			1356520.20	79.800	99.749	
			1354585.05	79.688	99.610	
150 %	40	60	1707759.90	100.008	100.008	99.851 ± 0.150
			1704767.40	99.836	99.836	
			1702565.80	99.709	99.709	

Limit of Detection (LOD)

LOD is calculated from the formula: -

$$LOD = \frac{3.3\ \sigma}{S}$$

Where,

σ = standard deviation of response for the lowest conc. in the range

S = slope of the calibration curve.

LOD of Vildagliptin =0.242 µg/ml

LOD of Remogliflozin =0.606µg/ml

LOD of Metformin HCl = 3.315 µg/ml

Limit of Quantification (LOQ)

The Quantitation limit is expressed as:

$$LOQ = \frac{10\ \sigma}{S}$$

LOQ of Vildagliptin=0.732 µg/ml

LOQ of Remogliflozin=1.835µg/ml

LOQ of Metformin HCl =10.046 µg/ml

Specificity:

No peaks were found in blank at retention time of drugs indicating the non interference of any other peak of degradation product or impurity or excipients.

Robustness:

Robustness of the method was determined by carrying out the analysis under conditions during which mobile phase ratio,flow rate, pH and detection wavelength were altered and the effect on the area was noted. The results obtained are shown in Table _19 A, B, C.

Table 19A:Robustness Samples - Vildagliptin			
	MP Composition		
	(18:82)	(20:80)	(22:78)
	142646.50	139199.35	140713.45
	144570.80	141419.90	139586.50
	143324.50	141594.10	141254.20
AVG	143513.933	140737.783	140518.050
STD DEV	976.036	1335.166	850.848
% RSD	0.680	0.949	0.606
RSD AVG	0.745		
	Flow Rate		
	0.95	1	1.05
	139266.30	143690.15	140826.75
	137807.05	140862.80	140950.35
	138215.70	141120.30	140620.75
AVG	138429.683	141891.083	140799.283
STD DEV	752.791	1563.348	166.508
% RSD	0.544	1.102	0.118
RSD AVG	0.588		
	pH		
	3.9	4	4.1
	142598.35	143350.25	140826.75
	142242.12	141577.75	139950.35
	141650.75	142835.25	140620.75
AVG	142163.740	142587.750	140465.950
STD DEV	478.638	911.801	458.248
% RSD	0.337	0.639	0.326
RSD AVG	0.434		
	Wavelength (nm)		
	209	210	211
	142588.05	139292.05	137850.05
	141655.49	140837.05	140595.00
	143582.00	141867.05	139631.95
AVG	142608.513	140665.383	139359.000
STD DEV	963.418	1296.055	1392.682
% RSD	0.676	0.921	0.999
RSD AVG	0.865		

Table 19B:Robustness Samples - Remogliflozin			
	MP Composition		
	(18:82)	(20:80)	(22:78)
	249923.75	250450.18	248183.17
	241891.12	249967.85	249981.72
	248261.75	250845.22	248019.75
AVG	246692.207	250421.083	248728.213
STD DEV	4240.093	439.408	1088.639
% RSD	1.719	0.175	0.438
RSD AVG	0.777		
	Flow Rate		
	0.95	1	1.05
	255019.62	251419.85	247794.15
	249189.45	248750.05	248031.85
	253398.21	251655.82	245400.16
AVG	252535.760	250608.573	247075.387
STD DEV	3009.250	1613.847	1455.649
% RSD	1.192	0.644	0.589
RSD AVG	0.808		
	pH		
	3.9	4	4.1
	251456.15	247154.61	247553.92
	252412.05	252269.42	244740.65
	250604.85	244438.15	246216.85
AVG	251491.017	247954.060	246170.473
STD DEV	904.104	3976.372	1407.208
% RSD	0.359	1.604	0.572
RSD AVG	0.845		
	Wavelength (nm)		
	209	210	211
	251208.12	250202.05	248591.47
	247783.86	248219.44	242786.51
	246952.45	248534.36	248352.59
AVG	248648.143	248985.283	246576.857
STD DEV	2255.642	1065.450	3284.709
% RSD	0.907	0.428	1.332
RSD AVG	0.889		

Table 19C :Robustness Samples - Metformin HCl			
	MP Composition		
	(18:82)	(20:80)	(22:78)
	639018.45	650245.25	641955.91

	651841.25	649352.55	652365.54
	654459.75	638380.05	658569.45
AVG	648439.817	645992.617	650963.633
STD DEV	8263.519	6607.769	8395.024
% RSD	1.274	1.023	1.290
RSD AVG	1.196		
	Flow Rate		
	0.95	1	1.05
	656474.72	641053.35	669043.24
	663975.91	651322.55	658838.84
	648135.64	652085.72	657292.65
AVG	656195.423	648153.873	661724.910
STD DEV	7923.828	6161.062	6384.837
% RSD	1.208	0.951	0.965
RSD AVG	1.041		
	pH		
	3.9	4	4.1
	641053.35	653542.05	662873.62
	641322.55	660798.82	652265.25
	652085.7	649711.65	658190.41
AVG	644820.533	654684.173	657776.427
STD DEV	6293.258	5631.134	5316.288
% RSD	0.976	0.860	0.808
RSD AVG	0.881		
	Wavelength (nm)		
	209	210	211
	663746.45	658115.55	655008.37
	651407.42	653402.41	658205.35
	661342.45	654160.53	646160.55
AVG	658832.107	655226.163	653124.757
STD DEV	6541.352	2530.830	6239.415
% RSD	0.993	0.386	0.955
RSD AVG	0.778		

Summary of validation study

The summary of validation parameters aresummarized in Table

Table 20: Summary of validation study

Sr. No.	**Validation Parameter**	**Results**		
		Vildagliptin	**Remogliflozin**	**Metformin HCl**
1.	Linearity	y = 38444x - 9442.8 R^2 = 0.9988	y = 27587x + 25960 R^2 = 0.9993	y = 17381x - 30475 R^2 = 0.9990
2.	Range (µg/ml)	2 – 12	4- 24	20- 120

3.	Precision	%RSD	%RSD	% RSD
	A) Intraday precision	0.385 – 0.553	0.132 – 0.994	0.359 – 0.872
	B) Interday precision	0.322 – 0.909	0.537 – 0.757	0.237 – 1.483
4.	Assay (Mean ± RSD)	99.783±0.566	100.108±0.637	99.448 ±0.470
5.	Accuracy (% Recovery)	**Mean % Recovery ± RSD**		
	50%	99.963 ± 0.428	100.116 ± 0.075	100.162 ± 0.131
	100%	100.323 ± 0.357	99.993 ± 0.522	99.725 ± 0.106
	150%	100.537 ± 0.469	99.897 ± 0.164	99.851 ± 0.150
6.	LOD(µg/ml)	0.242	0.606	3.315
7.	LOQ(µg/ml)	0.732	1.835	10.046
8.	Specificity	Specific	Specific	Specific
9.	Robustness	Robust	Robust	Robust

Conclusion:

The developed method was found to be simple, sensitive, accurate, precise and repeatable for analysis of Vildagliptin, RemogliflozinandMetformin HClinmixture. The method was successfully used for determination of drugs in a pharmaceutical formulationwithout any interference from the excipients.

References:

1. Mandal S, Vishvakarma P. Nanoemulgel: A Smarter Topical Lipidic Emulsion-based Nanocarrier. Indian J of Pharmaceutical Education and Research. 2023;57(3s):s481-s498.

2. Mandal S, Jaiswal DV, Shiva K. A review on marketed Carica papaya leaf extract (CPLE) supplements for the treatment of dengue fever with thrombocytopenia and its drawback. International Journal of Pharmaceutical Research. 2020 Jul;12(3).

3. Bhandari S, Chauhan B, Gupta N, et al. Translational Implications of Neuronal Dopamine D3 Receptors for Preclinical Research and Cns Disorders. African J Biol Sci (South Africa). 2024;6(8):128-140. doi:10.33472/AFJBS.6.8.2024.128-140

4. Tripathi A, Gupta N, Chauhan B, et al. Investigation of the structural and functional properties of starch-g-poly (acrylic acid) hydrogels reinforced with cellulose nanofibers for cu2+ ion adsorption. African J Biol Sci (South Africa). 2024;6(8): 144-153, doi:10.33472/AFJBS.6.8.2024.141-153

5. Sharma R, Kar NR, Ahmad M, et al. Exploring the molecular dynamics of ethyl alcohol: Development of a comprehensive model for understanding its behavior in various environments. Community Pract. 2024;21(05):1812-1826. doi:10.5281/zenodo.11399708

6. Mandal S, Kar NR, Jain AV, Yadav P. Natural Products As Sources of Drug Discovery: Exploration, Optimisation, and Translation Into Clinical Practice. African J Biol Sci (South Africa). 2024;6(9):2486-2504. doi:10.33472/AFJBS.6.9.2024.2486-2504

7. Kumar S, Mandal S, Priya N, et al. Modeling the synthesis and kinetics of Ferrous Sulfate production: Towards Sustainable Manufacturing Processes. African J Biol Sci (South Africa). 2024;6(9):2444-2458. doi:10.33472/AFJBS.6.9.2024.

8. Revadigar RV, Keshamma E, Ahmad M, et al. Antioxidant Potential of Pyrazolines Synthesized Via Green Chemistry Methods. African J Biol Sci (South Africa). 2024;6(10):112-125. doi:10.33472/AFJBS.6.10.2024.112-125
9. Sahoo S, Gupta S, Chakraborty S, et al. Designing, Synthesizing, and Assessing the Biological Activity of Innovative Thiazolidinedione Derivatives With Dual Functionality. African J Biol Sci (South Africa). 2024;6(10):97-111. doi:10.33472/AFJBS.6.10.2024.97-111
10. Mandal S, Bhumika K, Kumar M, Hak J, Vishvakarma P, Sharma UK. A Novel Approach on Micro Sponges Drug Delivery System: Method of Preparations, Application, and its Future Prospective. Indian J of Pharmaceutical Education and Research. 2024;58(1):45-63.
11. Mishra, N., Alagusundaram, M., Sinha, A., Jain, A. V., Kenia, H., Mandal, S., & Sharma, M. (2024). Analytical Method, Development and Validation for Evaluating Repaglinide Efficacy in Type Ii Diabetes Mellitus Management: a Pharmaceutical Perspective. Community Practitioner, 21(2), 29–37. https://doi.org/10.5281/zenodo.10642768
12. Singh, M., Aparna, T. N., Vasanthi, S., Mandal, S., Nemade, L. S., Bali, S., & Kar, N. R. (2024). Enhancement and Evaluation of Soursop (Annona Muricata L.) Leaf Extract in Nanoemulgel: a Comprehensive Study Investigating Its Optimized Formulation and Anti-Acne Potential Against Propionibacterium Acnes, Staphylococcus Aureus, and Staphylococcus Epidermidis Bacteria. Community Practitioner, 21(1), 102–115. https://doi.org/10.5281/zenodo.10570746
13. Khalilullah, H., Balan, P., Jain, A. V., & Mandal, S. (n.d.). Eupatorium Rebaudianum Bertoni (Stevia): Investigating Its Anti-Inflammatory Potential Via Cyclooxygenase and Lipooxygenase Enzyme Inhibition - A Comprehensive Molecular Docking And ADMET. Community Practitioner, 21(03), 118–128. https://doi.org/10.5281/zenodo.10811642
14. Mandal, S. Vishvakarma, P. Pande M.S., Gentamicin Sulphate Based Ophthalmic Nanoemulgel: Formulation and Evaluation, Unravelling A Paradigm Shift in Novel Pharmaceutical Delivery Systems. Community Practitioner, 21(03), 173-211. https://doi.org/10.5281/zenodo.10811540
15. Mishra, N., Alagusundaram, M., Sinha, A., Jain, A. V., Kenia, H., Mandal, S., & Sharma, M. (2024). Analytical Method, Development and Validation for Evaluating Repaglinide Efficacy in Type Ii Diabetes Mellitus Management: A Pharmaceutical Perspective. Community Practitioner, 21(2), 29–37. https://doi.org/10.5281/zenodo.10642768
16. Singh, M., Aparna, T. N., Vasanthi, S., Mandal, S., Nemade, L. S., Bali, S., & Kar, N. R. (2024). Enhancement and Evaluation of Soursop (Annona Muricata L.) Leaf Extract in Nanoemulgel: a Comprehensive Study Investigating Its Optimized Formulation and Anti-Acne Potential Against Propionibacterium Acnes, Staphylococcus Aureus, and Staphylococcus Epidermidis Bacteria. Community Practitioner, 21(1), 102–115. https://doi.org/10.5281/zenodo.10570746
17. Gupta, N., Negi, P., Joshi, N., Gadipelli, P., Bhumika, K., Aijaz, M., Singhal, P. K., Shami, M., Gupta, A., & Mandal, S. (2024). Assessment of Immunomodulatory Activity in Swiss Albino Rats Utilizing a Poly-Herbal Formulation: A Comprehensive Study on Immunological Response Modulation. Community Practitioner, 21(3), 553–571. https://doi.org/10.5281/zenodo.10963801

18. Mandal S, Vishvakarma P, Bhumika K. Developments in Emerging Topical Drug Delivery Systems for Ocular Disorders. Curr Drug Res Rev. 2023 Dec 29. doi: 10.2174/0125899775266634231213044704. Epub ahead of print. PMID: 38158868.
19. Abdul Rasheed. A. R, K. Sowmiya, S. N., & Suraj Mandal, Surya Pratap Singh, Habibullah Khallullah, N. P. and D. K. E. (2024). In Silico Docking Analysis of Phytochemical Constituents from Traditional Medicinal Plants: Unveiling Potential Anxiolytic Activity Against Gaba, Community Practitioner, 21(04), 1322–1337. https://doi.org/10.5281/zenodo.11076471
20. Pal N, Mandal S, Shiva K, Kumar B. Pharmacognostical, Phytochemical and Pharmacological Evaluation of Mallotus philippensis. Journal of Drug Delivery and Therapeutics. 2022 Sep 20;12(5):175-81.
21. Singh A, Mandal S. Ajwain (Trachyspermum ammi Linn): A review on Tremendous Herbal Plant with Various Pharmacological Activity. International Journal of Recent Advances in Multidisciplinary Topics. 2021 Jun 9;2(6):36-8.
22. Mandal S, Jaiswal V, Sagar MK, Kumar S. Formulation and evaluation of carica papaya nanoemulsion for treatment of dengue and thrombocytopenia. Plant Arch. 2021;21:1345-54.
23. Mandal S, Shiva K, Kumar KP, Goel S, Patel RK, Sharma S, Chaudhary R, Bhati A, Pal N, Dixit AK. Ocular drug delivery system (ODDS): Exploration the challenges and approaches to improve ODDS. Journal of Pharmaceutical and Biological Sciences. 2021 Jul 1;9(2):88-94.
24. Shiva K, Mandal S, Kumar S. Formulation and evaluation of topical antifungal gel of fluconazole using aloe vera gel. Int J Sci Res Develop. 2021;1:187-93.
25. Ali S, Farooqui NA, Ahmad S, Salman M, Mandal S. Catharanthus roseus (sadabahar): a brief study on medicinal plant having different pharmacological activities. Plant Archives. 2021;21(2):556-9.
26. Mandal S, Vishvakarma P, Verma M, Alam MS, Agrawal A, Mishra A. Solanum Nigrum Linn: An Analysis Of The Medicinal Properties Of The Plant. Journal of Pharmaceutical Negative Results. 2023 Jan 1:1595-600.
27. Vishvakarma P, Mandal S, Pandey J, Bhatt AK, Banerjee VB, Gupta JK. An Analysis Of The Most Recent Trends In Flavoring Herbal Medicines In Today's Market. Journal of Pharmaceutical Negative Results. 2022 Dec 31:9189-98.
28. Mandal S, Vishvakarma P, Mandal S. Future Aspects And Applications Of Nanoemulgel Formulation For Topical Lipophilic Drug Delivery. European Journal of Molecular & Clinical Medicine.;10(01):2023.
29. Chawla A, Mandal S, Vishvakarma P, Nile NP, Lokhande VN, Kakad VK, Chawla A. Ultra-Performance Liquid Chromatography (Uplc).
30. Mandal S, Raju D, Namdeo P, Patel A, Bhatt AK, Gupta JK, Haneef M, Vishvakarma P, Sharma UK. Development, characterization, and evaluation of rosa alba l extract-loaded phytosomes.
31. Mandal S, Goel S, Saxena M, Gupta P, Kumari J, Kumar P, Kumar M, Kumar R, Shiva K. Screening of catharanthus roseus stem extract for anti-ulcer potential in wistar rat.
32. Shiva K, Kaushik A, Irshad M, Sharma G, Mandal S. Evaluation and preparation: herbal gel containing thuja occidentalis and curcuma longa extracts.

33. Vishvakarma P, Kumari R, Vanmathi SM, Korni RD, Bhattacharya V, Jesudasan RE, Mandal S. Oral Delivery of Peptide and Protein Therapeutics: Challenges And Strategies. Journal of Experimental Zoology India. 2023 Jul 1;26(2).
34. Mandal, S., Tyagi, P., Jain, A. V., & Yadav, P. (n.d.). Advanced Formulation and Comprehensive Pharmacological Evaluation of a Novel Topical Drug Delivery System for the Management and Therapeutic Intervention of Tinea Cruris (Jock Itch). Journal of Nursing, 71(03). https://doi.org/10.5281/zenodo.10811676
35. Bonlawar, J., Setia, A., Challa, R.R., Vallamkonda, B., Mehata, A.K., Vaishali, , Viswanadh, M.K., Muthu, M.S. (2024). Targeted Nanotheransotics: Integration of Preclinical MRI and CT in the Molecular Imaging and Therapy of Advanced Diseases. Nanotheranostics, 8(3), 401-426. https://doi.org/10.7150/ntno.95791.
36. Pasala, P. K., Rudrapal, M., Challa, R. R., Ahmad, S. F., Vallamkonda, B., & R., R. B. (2024). Anti-Parkinson potential of hesperetin nanoparticles: in vivo and in silico investigations. Natural Product Research, 1–10. https://doi.org/10.1080/14786419.2024.2344740
37. Suseela, M. N. L., Mehata, A. K., Vallamkonda, B., Gokul, P., Pradhan, A., Pandey, J., ... & Muthu, M. S. (2024). Comparative Evaluation of Liquid-Liquid Extraction and Nanosorbent Extraction for HPLC-PDA Analysis of Cabazitaxel from Rat Plasma. Journal of Pharmaceutical and Biomedical Analysis, 116149. https://doi.org/10.1016/j.jpba.2024.116149
38. Chakravarthy, P.S.A., Popli, P., Challa, R.R. et al. Bile salts: unlocking the potential as bio-surfactant for enhanced drug absorption. J Nanopart Res **26**, 76 (2024). https://doi.org/10.1007/s11051-024-05985-6
39. Setia, A., Vallamkonda, B., Challa, R.R., Mehata, A.K., Badgujar, P., Muthu, M.S. (2024). Herbal Theranostics: Controlled, Targeted Delivery and Imaging of Herbal Molecules. Nanotheranostics, 8(3), 344-379. https://doi.org/10.7150/ntno.94987.
40. Dhamija P, Mehata AK, Tamang R, Bonlawar J, Vaishali, Malik AK, Setia A, Kumar S, Challa RR, Koch B, Muthu MS. Redox-Sensitive Poly(lactic-co-glycolic acid) Nanoparticles of Palbociclib: Development, Ultrasound/Photoacoustic Imaging, and Smart Breast Cancer Therapy. Mol Pharm. 2024 May 5. doi: 10.1021/acs.molpharmaceut.3c01086. Epub ahead of print. PMID: 38706253.
41. Eranti, Bhargav and Mohammed, Nawaz and Singh, Udit Narayan and Peraman, Ramalingam and Challa, Ranadheer Reddy and Vallamkonda, Bhaskar and Ahmad, Sheikh F. and DSNBK, Prasanth and Pasala, Praveen Kumar and Rudrapal, Mithun, A Central Composite Design-Based Targeted Quercetin Nanoliposomal Formulation: Optimization and Cytotoxic Studies on MCF-7 Breast Cancer Cell Lines. Available at SSRN: https://ssrn.com/abstract=4840349 or http://dx.doi.org/10.2139/ssrn.4840349
42. Setia A, Challa RR, Vallamkonda B, Satti P, Mehata AK, Priya V, Kumar S, Muthu MS. Nanomedicine And Nanotheranostics: Special Focus on Imaging of Anticancer Drugs Induced Cardiac Toxicity. Nanotheranostics 2024; 8(4):473-496. doi:10.7150/ntno.96846. https://www.ntno.org/v08p0473.htm
43. Pasala, P. K., Rcaghupati, N. K., Yaraguppi, D. A., Challa, R. R., Vallamkond, B., Ahmad, S. F., ... & DSNBK, P. (2024). Potential preventative impact of aloe-emodin nanoparticles on cerebral stroke-associated myocardial injury by targeting myeloperoxidase: In Supporting with In silico and In vivo studies. Heliyon.

International Journal of Pharmaceutics and Drug Research
ISSN: 2347-6346
Available online at http://ijpdr.com

Review Article

CHROMATOGRAPHY AND SPECTROSCOPY TECHNIQUES USED IN THE AUTHENTICATION AND ANALYSIS OF *CANNABIS SATIVA* A MEDICINAL PLANT

Rajashree Chavan*, Ganesh Nigade, Suneja Mane, Prajakta Mane, Neha Gambhire, Aditi Patil

PDEA's SGRS College of Pharmacy, Saswad, Pune (M.H)

***Correspondence Info:**
Dr. Rajashree Chavan
PDEA's SGRS College of Pharmacy, Saswad, Pune (M.H)
Email: rajchavan18@gmail.com

***Article History:**

Received: 20/10/2023
Revised: 15/11/2023
Accepted: 05/12/2023

ABSTRACT

Ayurveda uses a variety of bioactive compounds, which are abundant in plants, to cure a variety of diseases. Since ancient times, people have used medicinal herbs, and it's possible to say that this practice is where modern medicine got its start. There is an urgent need for herbal remedies to be assured of both their safety and effectiveness as medicinal plants keep increasing in popularity across the world. With this increasing need, it is very essential that the quality of the herbal medicinal plant must be controlled. In particular, the analysis of medicinal herbs has been around for decades to determine a plant's quality. There are many spectroscopic and chromatographic methods available for analysis, including ultraviolet (UV), Fourier-transform infrared spectrum, NMR spectroscopy or magnetic resonance spectroscopy (MRS), vapor-phase chromatography (VPC), high-pressure liquid chromatography (HPLC) along with mass spectrometry (MS), as well as hyphenated methods like vapor-phase chromatography (VPC)-mass spectrometry, liquid chromatography-hyphenated methods, and liquid chromatography-hyphenated methods. *Cannabis sativa* is a medical plant that is attracting more attention as a result of its strong pharmacological potential and recent changes to the law that permit diverse applications. For phytocannabinoid profiling, it is essential to create analytical techniques that are both time and money effective. The study intends to demonstrate the applicability of methodology for phytocannabinoid profiling of cannabis in addition to explore new analytical approaches in cannabis quality control, including classical spectroscopic as well as chromatographic methods.

Keywords: Medicinal plant, Chromatography, Spectroscopy, *Cannabis sativa*

INTRODUCTION

Since ancient times, most of the aromatic and medicinal plants that can be found across the world today have been used for flavouring food and medication formulations, as well as for their therapeutic and preservation characteristics. For the creation of substitute food additives, there has been a significant increase in interest in recent years for crude extracts as well as the vital oils of culinary and medicinal plants (Al Hashmi *et al.,* 2013).

In Ethiopia and other emerging nations in Asia and Africa, medicinal plants continue to play a significant part in peoples' everyday lives. In addition to enhancing the health as well as security of the local population, medicinal plants supplement or replace contemporary medical therapies, which are frequently insufficiently available (Kuldip *et al.,* 2015). Drugs made from plants are an essential component of Ayurvedic treatment. Both conventional and contemporary medical systems rely on medicinal plants as a supply of basic materials. Herbal remedies and other plant-based products have grown in use and popularity over the past few decades, significantly impacting the healthcare industry (Gavali *et al.,* 2016). Since ancient times, plants have been utilized in folk medicine. The active compounds (alkaloids, flavonoids, glycosides, vitamins, tannins, as well as coumarin compounds) found in plant organs are what give them their medicinal properties. These substances affect the physiological functioning of human as well as animal bodies or operate biologically to combat infections that are responsible for several disorders (Kamkin *et al.,* 2022). Complex plant extracts provide a difficult challenge in terms of separating components, identification plus their quantification. However, a wide range of various separation methods, particular stationary phases, and detectors are now readily available, making it possible to solve practically any separation problem with the necessary selectivity, sensitivity, and speed (Ganzera and Sturm, 2018). Since the beginning of time, tribal people all over the world have routinely used plants and plant-related products as ethnomedicine to cure a variety of illnesses (Agidew, 2022). Traditional medicine was defined by a World Health Organization (WHO) Experts Group as "the complete set of every principle and belief, whether or not, used for the diagnosis, prevention, as well as elimination of physical, mental, and also social imbalances along with depending entirely on firsthand experience and knowledge went verbally or through writing from one generation to the next" (WHO, 1976) (Sofowora *et al.,* 2013). A variety of analytical methods like capillary electrophoresis, gas chromatography or vapor-phase chromatography (VPC), high-pressure liquid chromatography (HPLC), TLC that is thin layer chromatography, and their hyphenated processes to mass spectroscopy (MS), have been used to investigate complex compounds in herbal products. Since LC MS can significantly increase the analytical selectivity as well as sensitivity, it has grown in significance in recent years for the chemical study of Hydroxymethanesulfonate (HMs) (Zhou *et al.,* 2009). The effectiveness of the analytical methodologies affects the plants' performance and safety. Every time we use the analytical procedures, they should be repeatable, accurate, and consistent. In addition to distinct methodologies, drug analysis is listed in many pharmacopeia. For the analysis of plant drugs, Central Council for Research in Ayurvedic Sciences (CCRAS) in India has devised a procedure (Gavali *et al.,* 2016).

I. *Cannabis sativa*:

Cannabis sativa (F. Cannabinaceae) is the scientific name for the annual plant known as cannabis, hashish, or hemp (Kulkarni *et al.,* 2018). Cannabis is included as one of the five sanctified plants in the Atharvana Veda and is described as an origin of joy, happiness,

and even redemption. This is where the first information on cannabis' therapeutic status in India is first documented (Ram *et al.,* 2018). It is likely one of the cultivated plants and has been utilized by humans for many years. It is extensively used and has been around for over 2500 years, according to archaeological findings (Schmidt *et al.,* 2020). Cannabis sativa, generally known as hemp, which is an annual plant with considerable pharmacological relevance that generates secondary cannabis chemicals and other metabolites with therapeutic potential for a number of human health issue (Bowen *et al.,* 2021). Cannabis has been used for medicinal purposes for many years to alleviate a broad range of ailments, including pain, spasms, breathing issues, insomnia, depressed symptoms, and even appetite loss (Mirzamohammad *et al.,* 2021).

The Cannabis genus now contains more than 500 chemicals that are divided into 18 chemical classes. Cannabinoids, also known as terpenophenolics, stand out among these compounds since they are linked to the pharmacological effects of this plant. The most well-known cannabinoids were delta-9-tetrahydrocannabinol (9-THC), a psychoactive cannabinoid, plus cannabidiol (CBD), a psychologically inactive cannabinoid that has recently been widely advocated for medical usage. 9-THC is a key component of the cannabinoids present in *Cannabis sativa* due to its considerable psychoactive effect (Mano-Sousa *et al.,* 2021). Cannabis is being used more and more, thus it's important to have a variety of effective ways for identifying its constituent parts and, in particular, for characterizing the "narcotic compound" (Galand *et al.,* 2004). Over the last ten years, numerous chromatographic procedures with various spectroscopic detection techniques have been used to identify, isolate, and characterize the chemicals in cannabis (Odieka *et al.,* 2022).

Table 1: *Cannabis sativa* L. systematic taxonomy

Division	Angiosperms
Class	Dicotyledons
Subclass	Archichlamydeae
Order	Urticales
Family	Cannabaceae
Genus	*Cannabis*
Species	*sativa* L.

Cannabis analysis is currently an important part of the quality control of plant-based goods used for health and food, as well as for scientific along with legal purposes (Ibrahim *et al.,* 2018; Zampachova *et al.,* 2021). Following are some of the spectroscopic, chromatographic and hyphenated technique analysis for *cannabis sativa* L.

II. Spectroscopic Analysis

Youbin Zheng *et al.,* (2021) discovered that cannabis inflorescence yield along with cannanoid amount i.e concentration did not rise through short-wavelength UV-b radiation, this study found that using UV light as a production technique did not increase cannabis output or the composition of secondary metabolites in inflorescence in any economically significant way.

Michael W. Jenkins *et al.,* (2021) unmasked that during the last phase of blooming at the leaf level *Cannabis sativa L.* responds readily to ultraviolet light with a narrow band, along with blue and red light combined.

In order to determine if combining narrow-bandwidth ultraviolet light with blue and red light over a couple of weeks during blossoming could change the amount of cannabinoids and terpenes without changing the crop's dry weight, gas-exchange parameters, secondary metabolite production, and yield were tested.

Jose Dorado *et al.,* (2001) studied infrared spectroscopic measurement technique for hemp (Cannabis sativa. L) subsequently after specific delignification via Bjerkandera sp. at varying nitrogen levels. In this study, alterations in C/N-modified lignocellulosic substrates of Cannabis sativa L. were discovered using Fourier-transform infrared spectroscopy (FT-IR) during a 7-week solid-state fermenting environment with the white-rot fungus Bjer-kandera spp. strain BOS55.

C.Sanchez Carnerero Callado *et al.,* (2018) reported a comparative study to examine the ability of NIR spectrometer to evaluate THC concentration in Cannabis sativa L. An technique for quantitatively detecting cannabinoids in cannabis raw materials was developed in this work employing near-infrared spectroscopy (NIR) as well as Fourier transform near infrared (FT-NIR) spectroscopy.

Wieland Peschel *et al.,* (2015) reported ^{1}H NMRas well as HPLC with diode array detect (DAD) was used for Cannabis sativa L. chemotype discrimination, extracts profiling, as well as specification. To investigate the applicability of ^{1}H NMRkey signals, four distinct chemotypes were investigated in deuterated dimethyl sulfoxide.

Ada C. Gallo-Molina *et al.,* (2019) reported Tetrahydrocannabinol was extracted, isolated, and isolated from the Cannabis sativa L. plant via supercritical fluid extraction and the solid-phase extraction, the FF can be analyzed using ^{1}H NMRand^{13}C-NMR studies.

Marco Cirrincione *et al.,* (2021) reported and describeda novel high-throughput approach using Fourier transform infrared spectroscopy– attenuated total reflectance (FTIR–ATR) which is a technology developed for determining the kind of fiber in the drug Cannabis sativa L. inflorescences. It is an evidence of concepts for the several chemotypes of the cannabis sativa L.

Francine Gloerfelt-Tarp *et al.,* (2023) developed a chemometric method for cannabinoid measurement based on a global diversity panel for Cannabis sativa L. in which NIRS was able to differentiate between C3-alkyl and C5-alkyl cannabinoids as well as between cannabinoids neutral and acidic form. When paired with chemometrics, the findings show that NIRS has the ability to accurately evaluate cannabis in raw materials.

Luis Ramos-Guerrero *et al.,* (2022) reported Raman microscopy and chemometrics were used to categorize various marijuana strains. The Raman spectrum of five marijuana strains was compared to the conventional cannabinoids THC, CBD, and CBN. Four Cannabis sativa strains (Amnesia Haze, Am-nesiaHy-Pro, Original Amnesia, plus Y Griega) and one Indica strain (Black Domina) were studied.

Stefania Porcu *et al.,* (2022) reported Rapid unchanged Identification of CBD and THC in Cannabis sativa L. employing 1064 nm Raman spectra in which all of the primary Raman modes have been assigned according to the Raman spectroscopy of two distinct cannabis families THC- as well as CBD-rich, 42 naturally obtained samples were analyzed

to get the spectra, as well as a 1064 cm^{-1} excitation wavelength was utilized.

Pedro Henrique P. M. da Silveira *et al.,* (2022) reported the effect of alkaline treatment and graphene oxide coating on the thermal as well as chemical properties of hemp (Cannabis Sativa L.) fibers. In which Hemp fibre (*Cannabis sativa L.*) was subjected to an alkaline treatment before being functionalized with graphene oxide. Chemical, thermal, as well as microstructural characterisation techniques that include Fourier transform infrared and differential scanning calorimetry, TGA which is Thermogravimetric analysis, RAMAN, X-ray diffraction as well as scanning electron microscope were used to investigate this process.

Marcus Daniel Brandbjerg *et al.,* (2023) reported Desorption Electrospray Ionization and MALDI mass spectroscopy imaging were used to look for cannabinoids along with flavonoids within extract of hemp leaves as well as trichomes, in which the cannabinoid CBGA as well as capitate-stalked trichomes have been linked through indirect DESI-MSI tests. In addition to the tiny glandular trichomes, capitate-stalked trichomes also included other cannabinoids, That includes tetrahydrocannabinolic acid (THCA) along with cannabidiolic acid (CBDA) (isomers that do not resolve in Mass spectrometry imaging (MSI) experiment).

Matrix-assisted laser desorption/ionization Imaging mass spectrometry (IMS, also termed mass spectrometry imaging (MSI)(MALDI-MSI) examines on the cross-sections of glucose leaves indicated that the cannabinoids did not originate in the leaf tissue itself, rather they came through the trichomes on the leaf's surface.

III. Chromatographic analysis

Brayan Jonas Mano-Sousa MS *et al.,* (2021) studied Color analysis technique as well as assessment of cannabis detection using thin-layer chromatography (TLC).The TLC techniques examined in this study have benefits over other analytical techniques because they are quick, easy, and effective in isolating and detecting cannabinoids. In this investigation, using FBBS or even FBRR in an acidic ethanol-based environment results in a colorimetric response for cannabis.

Si Huang, Ruiying Qiu *et al.,* (2022) reported Semiquantitative THC Analogue Screening using TLC Silica gel G with anRetention Zone Ag(I) along with Chromogenic Smartphone Detection. Whereas the Ag(I)-TLC smartphone approach suggested in this study provides for an accurate semiquantitative evaluation of total Tetrahydrocannabinolic acid, Tetrahydrocannabinol, and Cannabinol and may be used in the field as a quick screening tool over cannabis variety categorization.

N. Galand *et al.,* (2004) reported the Cannabis component separation and identification using several planar chromatography methods (TLC, AMD, Optimum performance laminar chromatography). Cannabis resins (0.1 grams) was extracted in this investigation by swirling at ambient temperature for 20 minutes with 10 mL of hexane. The mobile phase for the separation of 8-THC, 9-THC, CBN, as well as CBD was hexane and diethyl ether in the proportion of 80:20, v/v. THC, CBD, along with CBN were extracted by traditional way from cannabis resin and the Cannabis sativa plant.

As a result of AMD's excellent resolution and lack of spot stretching, it is possible to measure dose using scanning densitometry. By using OPLC in the semipreparative mode, CBN and 9-THC were separated from cannabinoids resin.

Justin T. Fischedick *et al.,* (2009) developed a Quantitative as well as Qualitative HPTLC Densitometry Method for Cannabinoids Analysis in Cannabis Sativa L. The plant material was extracted with ethanol and shaken for 15 min the whole extraction procedure was repeated twice. Chloroform was used as the mobile phase plus showed Rf values of 0.52 for Cannabidiol, 0.47 for Delta-9-tetrahydrocannabinol, 0.49 for Delta-8 tetrahydrocannabinol, 0.47 for Cannabinol, 0.47 for Tetrahydrocannabivarin, 0.47 for Cannabigerol, and 0.33 for cannabichromene. Separation of Cannabinoids is done by using C18 Waters Bondapakguard column. The mobile phase was a gradient of methanol and water with a 25 mM formic acid concentration; Methanol plus Water ratios ranged from 65: 35 to 100: 0 over 25 minutes, and isocratic to 28 minutes. The flow rate was 1.5 mL/min, with the total run time was thirty-two minutes. This method may also be used to screen the principal neutral cannabinoids found in cannabis variety.

UK Kulkarni *et al.,* (2018) developed the high-performance thin layer chromatographic technique for detecting cannabis in forensic interest, in which the cannabis standard was evaluated using HPTLC in multiple solvent systems. The three most important cannabis components for cannabis detection are THC, CBN, and CBD. Using a 9:1:1 solvent solution consisting of toluene, ethyl acetate and acetone, cannabinoids were separated using HPTLC.

Yifan Liu *et al.,* (2020) reported Cannabinoids data from ten mobile phase solutions for high-performance thin-layer chromatography (HPTLC),stationary phase used was 60 F 254 (2010cm) silica gel plates then mobile phase used was Hexane plus acetone in the proportion of 87:13, in volume by volume for cannabis biomarkers with detection wavelength: 254nm, where the supplemental material comprises the HPTLC reports (S2), RF data, and resolution data (S3, S4) of all ten systems' triplicate analyses.

Wieland Peschel *et al.,* (2015) reported In this work, that proton nuclear magnetic resonance (proton NMR, hydrogen-1 NMR) along with High-Performance Liquid Chromatography together with Diode-Array Detection were utilized for chemotype differentiation, extract profiling, as well specification of Cannabis sativa L. tetrahydrocannabinol (THC), cannabidiol (CBD), cannabigerol (CBG), their acidic counterparts (THCA, CBDA, CBGA),Cannabinol (CBN) and cannflavin A as well as B are quantified and used in two newly validated HPLC/DAD procedures for cannabis extract profiling along with identification using cannabinoids and other phenolics. To study the repercussion on the cell viability some tests were done (MTT test, Henrietta Lacks).

Virginia Brighenti et al (2017) developed a new extraction approach and HPLC method for the analysis of non-psychoactive cannabinoids in hemp. To analyze the target analytes in hemp extracts, a novel reversed-phase high-pressure liquid chromatography, technology was put forward and used in

conjunction with an ion trap mass analyzer, diode array (UV/DAD), and electrospray ionization-mass spectrometry (ESI-MS).

Sanja Zivovinovic, (2018) reported Cannabinoids within Cannabis sativa L. samples were determined using reversed-phase liquid chromatography and UV detection for recreational, medicinal, as well as forensic applications. The *Humuluslupulus L.* sample was extracted in an ultrasonic bath with ACN/H2O 1:1 for 15 minutes before being repeated three times. Eight cannabinoids were separated using a Kinetex XB-C18 HPLC column using 0.1% Formic Acid in Water as well as Acetonitrile with 0.1% Formic Acid (v/v) as solvent flow rates set to 0.8mL/min and temperatures 50 °C, appropriately. The detection wavelength of the detector was 220nm.

Ada C. Gallo-Molina *et al.,* (2019) reported THC extraction, separation, and purification from the hemp plant utilizing Supercritical fluid extraction (SCFE) plus solid-phase extraction (SPE). A sequential supercritical fluid extraction-Solid-phase extraction (SPE)method has been developed to extract tetrahydrocannabinol via high purity through Canna-bisSativa L plant matter. THC purity was determined by GC-FID to be 90.1%. To determine the concentration as well as purity of THC, 31 fractions were collected and evaluated using thin-layer chromatography (TLC) and RP-HPLC.

Mara Mandrioli *et al.,* (2019) developed RP-HPLC-UV Method for Rapid Identification of 10 Cannabinoids in Cannabis sativa L. In this case, the RP-HPLC-UV is employed for separation and detection.This study found that the 10 most significant cannabinoids may be quantitatively measured in 8 minutes with just single wavelength (220 nm). Even with the difficult elution sequence, an entire separation of the cannabigerolic acid, cannabinoid, Cannabidiol, and Delta also 9-Tetrahydrocannabivarin peaks (from 3.5 to 4.5 min) resulted.

Federica Pellati *et al.,* (2018) reported in this work, researchers developed new methods for analyzing bioactive substances in Cannabis sativa L. (hemp). The High-Performance Liquid Chromatography with diode array UV detector technique was employed to ascertain quantitative data on the psychologically inactive cannabinoids found in hemp inflorescences. HS-SPME's extraction of hemp's volatile components was examined by GC-FID.

IV. Hyphenated technique analysis

OierAizpurua-Olaizola *et al.,* (2014) reported Highly efficient liquid chromatography-mass spectrometry can be used to detect as well as quantify cannabinoids in hemp plant. To detect the primary cannabinoids found in extracts prepared from Cannabis sativa L. plants via supercritical fluid extraction, the HPLC-MS/MS approach was extensively improved and validated. Seven small cannabinoids were discovered using UPLC-qToF.

Lorenzo Calvi *et al.,* (2018) reported in this work that, the researchers employed HS-SPME in conjunction with GC-MS and LC-HRMS to evaluate the total quality of therapeutic inflorescence as well as macerated oils. A technique for analysis based on HS-SPME in hyphenation with GC-MS along with High-Resolution Mass-Spectrometry (LC-HRMS) was developed, validated, and used for detailed profiling along with fingerprinting of cannabinoids and

terpenes with two approved medicinal varieties of Cannabis sativa L. inflorescence and macerated oils.

Radmila Pavlovic *et al.,* (2019) reported Phytochemical study of two varieties of Cannabis sativa L. grown in the Italian Alps. Several analytical methods, including Headspace-solid phase microextraction, GC/MS, SDS-PAGE, LC-MS, GC-FID, and HPLC-high-resolution mass spectrometry, can accurately profile two types of altitude-cultivated plants.

Theresa Schmidt *et al.,* (2020) developed a method for identifying and quantifying cannabinol as biomarker for regional cannabis retting in an early sedimentary record using HPTLC-ESI-MS (electrospray ionization mass spectrometry). The detection and quantification of CBN, a cannabinoid that is an unambiguous molecular identity for the Hemp plant and then, as a result, a method of detection for ancient water returning of hemp in sediment samples, using HPTLC-ESI-MS.

Theresa Schmidt *et al.,* (2021) reported A rapid HPTLC-ESI-MS method for differentiating actual cannabinoids from inaccurate cannabinoids in diverse oils. This study used high-performance thin-layer chromatography in hypenation with electrospray ionization mass spectrometry to develop and validate an accurate, simple, dependable, and fast method for analyzing CBN, CBD, and 9-THC in commercially available CBD oils.

Janina K. Bowenetal, (2021) reported the effect of the extraction procedure on the chemical content of cannabis extracts from varieties of plants. 41 compounds were discovered and evaluated with a non-targeted profiling for gas chromatography-mass spectrometry , 15 phytocannabinoids were assessed using a qualitatively targeted assay for ultra-performance liquid chromatography-based tandem mass spectrometry (UPLC-MS/MS), and 24 elements were examined using inductively coupled plasma mass spectrometry.

Federica Pellati *et al.,* (2018) reported novel approaches for the characterization of bioactive chemicals in the hemp plant nonpsychoactive cannabinoids were profiled subjectively and quantitatively in this work utilizing an HPLC ESI-MS with MS2 detection. The cannabis volatile fraction's properties were found by modifying a unique HS-SPME-GC/MS detection method.

CONCLUSION

For thousands of years, both developing and developed nations have employed herbal remedies and their preparations to provide society and communities with primary healthcare. One of the most crucial and fundamental processes in the production of herbal preparations is quality control since the product's quality affects the security and effectiveness of medications. Quality control is mostly utilized for finished products as well as raw materials, excipients, and other ingredients.It is essential for trademark protection, avoiding defective goods, and improving consumer trust. It ensures that the company uses evidence-based research and data rather than subjective experiences to ensure that the services/products fit the standards.

Along with chemically synthesized medicine the quality control as well as standardization of herbal medications is important in their isolated form, extract, in any other herbal or polyherbal formulation which is greatly aided

by spectroscopic and chromatographic techniques. Cannabis sativa is a herbal medicinal plant with a variety of medical properties. The analysis of same is important for its use.

DECLARATION OF INTEREST

The authors declare no conflicts of interests. The authors alone are responsible for the content and writing of this article.

REFERENCES

- Al Hashmi, L.S., Hossain, M.A., Weli, A.M., Al-Riyami, Q. & Al-Sabahi, J.N. (2013) Gas chromatography–mass spectrometry analysis of different organic crude extracts from the local medicinal plant of Thymus vulgaris L. *Asian Pacific Journal of Tropical Biomedicine*, 3, 69–73
- Kuldip, S.D., Sandeep, C. & Jeewan, S.J. (2015) Assessment of Indian medicinal plants for the treatment of asthma. *Journal of Medicinal Plants Research*, 9, 851–862
- Gavali, D.J.B., Pradhan, D.N. & Waghmare, D.N. (2016). *Current Trends in Analytical Methods of Me-Dicinal Plant Drugs*, Vol. 3.
- Kamkin, V., Kamarova, A., Shalabayev, B., Kussainov, A., Anuarbekov, M. & Abeuov, S. (2022) Comparative analysis of the efficiency of medicinal plants for the treatment and prevention of COVID-19. *International Journal of Biomaterials* (edited by S. Ali), 2022, 5943649
- Ganzera, M. & Sturm, S. (2018) Recent advances on HPLC/MS in medicinal plant analysis—An up-date covering 2011–2016. *Journal of Pharmaceutical and Biomedical Analysis*, 147, 211–233
- Agidew, M.G. (2022) Phytochemical analysis of some selected traditional medicinal plants in Ethiopia. *Bulletin of the National Research Centre*, 46, 87
- Sofowora, A., Ogunbodede, E. & Onayade, A. (2013) The role and place of medicinal plants in the strategies for disease prevention. *African Journal of Traditional, Complementary, and Alternative Medicines*, 10, 210–229
- Zhou, J.L., Qi, L.W. & Li, P. (2009) Herbal medicine analysis by liquid chromatography/time-of-flight mass spectrometry. *Journal of Chromatography. A*, 1216, 7582–7594
- Kulkarni, U., Kulkarni, K., Pardeshi, R. & Mane, D. *High Performance Thin Layer Chroma-Tographic Detection of Cannabis in Forensic Interest. Published Online 2018*.
- Ram, G.S., Krishna, C.M., Kumar, D.P., Mohan, K.M. & Babu, G. (2018) Conceptual review on Vijaya (Cannabis sativa linn.): A Forgotten AMBROSIA. *International Journal of Research in Ayurveda and Pharmacy*, 9, 18–27
- Schmidt, T., Kramell, A.E., Oehler, F., Kluge, R., Demske, D., Tarasov, P.E. & Csuk, R. (2020) Identification and quantification of cannabinol as a biomarker for local hemp retting in an ancient sedimentary record by HPTLC-ESI-MS. *Analytical and*

Bioanalytical Chemistry, 412, 2633–2644

- Bowen, J.K., Chaparro, J.M., McCorkle, A.M., Palumbo, E. & Prenni, J.E. (2021) The impact of extraction protocol on the chemical profile of cannabis extracts from a single cultivar. *Scientific Reports*, 11, 21801
- Mirzamohammad, E., Alirezalu, A., Alirezalu, K., Norozi, A. & Ansari, A. (2021) Improvement of the antioxidant activity, phytochemicals, and cannabinoid compounds of Cannabis sativa by sali-cylic acid elicitor. *Food Science and Nutrition*, 9, 6873–6881
- Mano-Sousa, B.J., Maia, G.A.S., Lima, P.L., Campos, V.A., Negri, G., Chequer, F.M.D. & Duarte-Almeida, J.M. (2021) Color determination method and evaluation of methods for the detection of cannabinoids by thin-layer chromatography (TLC). *Journal of Forensic Sciences*, 66, 854–865
- Galand, N., Ernouf, D., Montigny, F., Dollet, J. & Pothier, J. (2004) Separation and identification of cannabis components by different planar chromatography techniques (TLC, AMD, OPLC). *Journal of Chromatographic Science*, 42, 130–134
- Odieka, A.E., Obuzor, G.U., Oyedeji, O.O., Gondwe, M., Hosu, Y.S. & Oyedeji, A.O. (2022) The medicinal natural products of Cannabis sativa Linn.: A review. *Molecules*, 27, 1689
- Ibrahim, E., Hadad, G., Abdel Salam, R. et al. (2018) Recent analytical approaches in quality Con-trol of Cannabis sativa L. and its preparations. Rec Pharm. *Biomedical Science*, 2, 10–22.
- Žampachová, L., Aturki, Z., Mariani, F. & Bednář, P. (2021) A rapid nano-liquid chromatographic method for the analysis of cannabinoids in Cannabis sativa L. extracts. *Molecules*, 26, 1825
- Rodriguez-Morrison, V., Llewellyn, D. & Zheng, Y. (2021) Cannabis inflorescence yield and Can-nabinoid concentration are not increased with exposure to short-wavelength ultraviolet-B radiation. *Frontiers in Plant Science*, 12, 725078
- Jenkins, M.W. (2021) Cannabis sativa & L. Response to narrow bandwidth UV and the combination of blue and red light during the final stages of flowering on leaf level gas-exchange parameters, secondary metabolite production, and yield. *Agricultural Sciences*, 12, 1414–1432.
- Dorado, J., Almendros, G., Field, J.A. & Sierra-Alvarez, R. (2001) Infrared spectroscopy analysis of hemp (Cannabis sativa) after selective delignification by Bjerkandera sp. at different nitrogen levels. *Enzyme and Microbial Technology*, 28, 550–559
- Callado, S.-C. C, Nunez-Sanchez N, Casano S, Ferreiro-Vera C. The potential of near infrared spectroscopy to estimate the content of cannabinoids in Cannabis sativa L.: A comparative study. Talanta. 2018;190:147-157.
- Peschel, W. & Politi, M. (2015) 1 H NMR and HPLC/DAD for Cannabis sativa L. chemotype dis-tinction,

extract profiling and specification. *Talanta*, 140, 150–165

- Gallo-Molina, A.C., Castro-Vargas, H.I., Garzón-Méndez, W.F., Martínez Ramírez, J.A., Rivera Monroy, Z.J., King, J.W. & Parada-Alfonso, F. (2019) Extraction, isolation and purification of tetrahydrocannabinol from the Cannabis sativa L. plant using supercritical fluid extraction and solid phase extraction. *Journal of Supercritical Fluids*, 146, 208–216
- Cirrincione, M., Saladini, B., Brighenti, V., Salamone, S., Mandrioli, R., Pollastro, F., Pellati, F., Protti, M. & Mercolini, L. (2021) Discriminating different *Cannabis sativa* L. chemotypes using attenuated total reflectance – Infrared (ATR-FTIR) spectroscopy: A proof of concept. *Journal of Pharmaceutical and Biomedical Analysis*, 204, 114270
- Gloerfelt-Tarp, F., Hewavitharana, A.K., Mieog, J., Palmer, W.M., Fraser, F., Ansari, O. & Kretzschmar, T. (2023) Using a global diversity panel of Cannabis sativa L. to develop a near infrared-based chemometric application for cannabinoid quantification. *Scientific Reports*, 13, 2253
- Ramos-Guerrero, L., Montalvo, G., Cosmi, M., García-Ruiz, C. & Ortega-Ojeda, F.E. (2022) Classification of various marijuana varieties by Raman microscopy and chemometrics. *Toxics*, 10, 115
- Porcu, S., Tuveri, E., Palanca, M., Melis, C., La Franca, I.M., Satta, J., Chiriu, D., Carbonaro, C.M., Cortis, P., De Agostini, A. & Ricci, P.C. (2022) Rapid in situ Detection of THC and CBD in Canna-bis sativa L. by 1064 nm Raman Spectroscopy. *Analytical Chemistry*, 94, 10435–10442
- da Silveira, P.H.P.M., Ribeiro, M.P., Silva, T.T., Lima, A.M., Lemos, M.F., Oliveira, A.G.B.A.M., Nascimento, L.F.C., Gomes, A.V. & Monteiro, S.N. (2022) Effect of alkaline treatment and graphene oxide coating on thermal and chemical properties of hemp (Cannabis sativa L.) fibers. *Journal of Natural Fibers*, 19, 12168–12181
- Lorensen, M.D.B.B., Hayat, S.Y., Wellner, N., Bjarnholt, N. & Janfelt, C. (2023) Leaves of Cannabis sativa and their trichomes studied by DESI and MALDI mass spectrometry imaging for their contents of cannabinoids and flavonoids. *Phytochemical Analysis*, 34, 269–279
- Huang, S., Qiu, R., Fang, Z., Min, K., van Beek, T.A., Ma, M., Chen, B., Zuilhof, H. & Salentijn, G.I. (2022) Semiquantitative screening of THC analogues by silica gel TLC with an Ag(I) retention zone and chromogenic smartphone detection. *Analytical Chemistry*, 94, 13710–13718
- Fischedick, J.T., Glas, R., Hazekamp, A. & Verpoorte, R. (2009) A Qualitative and Quantitative HPTLC densitometry method for the analysis of cannabinoids in Cannabis sativa L. *Phytochemical Analysis*, 20, 421–426
- Kulkarni, U., Kulkarni, K., Pardeshi, R. & Mane, D. *High Performance*

Thin Layer Chroma-Tographic Detection of Cannabis in Forensic Interest. Published Online 2018.

- Liu, Y., Brettell, T.A., Victoria, J., Wood, M.R. & Staretz, M.E. (2020) High performance thin-layer chromatography (HPTLC) analysis of cannabinoids in cannabis extracts. *Forensic Chemistry*, 19, 100249
- Brighenti, V., Pellati, F., Steinbach, M., Maran, D. & Benvenuti, S. (2017) Development of a new extraction technique and HPLC method for the analysis of non-psychoactive cannabinoids in fibre-type Cannabis sativa L. (hemp). *Journal of Pharmaceutical and Biomedical Analysis*, 143, 228–236
- Zivovinovic, S., Alder, R., Allenspach, M.D. & Steuer, C. (2018) Determination of cannabinoids in Cannabis sativa L. samples for recreational, medical, and forensic purposes by reversed-phase liquid chromatography-ultraviolet detection. *Journal of Analytical Science and Technology*, 9, 27
- Mandrioli, M., Tura, M., Scotti, S. & Gallina Toschi, T. (2019) Fast detection of 10 cannabinoids by RP-HPLC-UV method in Cannabis sativa L. *Molecules*, 24, 2113
- Pellati, F., Brighenti, V., Sperlea, J., Marchetti, L., Bertelli, D. & Benvenuti, S. (2018) New Methods for the Comprehensive Analysis of Bioactive compounds in Cannabis sativa L. (hemp). *Molecules*, 23, 2639
- Aizpurua-Olaizola, O., Omar, J., Navarro, P., Olivares, M., Etxebarria, N. & Usobiaga, A. (2014) Identification and quantification of cannabinoids in Cannabis sativa L. plants by high-performance liquid chromatography-mass spectrometry. *Analytical and Bioanalytical Chemistry*, 406, 7549–7560
- Calvi, L., Pentimalli, D., Panseri, S., Giupponi, L., Gelmini, F., Beretta, G., Vitali, D., Bruno, M., Zilio, E., Pavlovic, R. & Giorgi, A. (2018) Comprehensive quality evaluation of medical Can-Nabis sativa L. inflorescence and macerated oils based on HS-SPME coupled to GC–MS and LC-HRMS (q-exactive Orbitrap®) approach. *Journal of Pharmaceutical and Biomedical Analysis*, 150, 208–219
- Pavlovic, R., Panseri, S., Giupponi, L., Leoni, V., Citti, C., Cattaneo, C., Cavaletto, M. & Giorgi, A. (2019) Phytochemical and ecological analysis of two varieties of hemp (Cannabis sativa L.) grown in a mountain environment of Italian alps. *Frontiers in Plant Science*, 10, 1265
- Schmidt, T., Kramell, A.E., Oehler, F., Kluge, R., Demske, D., Tarasov, P.E. & Csuk, R. (2020) Identification and quantification of cannabinol as a biomarker for local hemp retting in an ancient sedimentary record by HPTLC-ESI-MS. *Analytical and Bioanalytical Chemistry*, 412, 2633–2644
- Schmidt, T., Stommel, J., Kohlmann, T., Kramell, A.E. & Csuk, R. (2021) Separating the true from the false: A rapid HPTLC-ESI-MS method for the

determination of cannabinoids in different oils. *Results in Chemistry*, 3, 100234

- Bowen, J.K., Chaparro, J.M., McCorkle, A.M., Palumbo, E. & Prenni, J.E. (2021) The impact of extraction protocol on the chemical profile of cannabis extracts from a single cultivar. *Scientific Reports*, 11, 21801

IJPPR
INTERNATIONAL JOURNAL OF PHARMACY & PHARMACEUTICAL RESEARCH
An official Publication of Human Journals
ISSN 2349-7203
HUMAN

CURRENT REVIEW ON PHARMACOLOGICAL ACTIVITIES OF *CITRULLUS COLOCYNTHIS* (FRUIT, ROOT & SEED)

Gavarkar Pratibha S*[1], Chavan Rajshri S[2], Patil Suraj R[1]

1. Anandi B. Pharmacy College, Kalambe Tarf Kale, Dist. Kolhapur, India.

2. PDEA's SGR Sable College of Pharmacy, Saswad, Pune, India.

ABSTRACT

Citrullus colocynthis (L.) Schrad (C. colocynthis), often known as Colocynth, is a wild species of the Cucurbitaceae family. The goal of today's research is to look at the phytochemical composition, pharmacological properties, cytotoxicity, and antioxidant activity of various plant elements. Traditional remedies have a higher level of interest as a result of increased health awareness and knowledge of the side effects of synthetic capsules. Medicinal plants provide remedies for a wide range of ailments, as well as basic to advanced living requirements. This has increased demand for herb-based medications by bringing ethnomedicinal studies into the forefront. *Citrullus colocynthis* is an herbaceous plant that contains a variety of nutrients that are important for overall health. in which the anti-diabetic activity is exceptional It appears that more research is needed to evaluate these findings.

Keywords*:* - *Citrullus colocynthis*, health aspects, traditional uses, herbal medicine

INTRODUCTION

PLANT PROFILE:

Synonyms: *Colocynthis vulgaris* Schrad., *Cucumis colocynthis* L. (basionym), *Citrullus pseudocolocynthis* M.Roem. and *Colocynthis officinalis* Schrad(414-2) [1].

Common names: - Arabic: handhal, English: bitter-apple, bitter-cucumber, colocynth, vine-of-Sodom, wild gourd, French: coloquinte, coloquinte, German: bitter-melone, koloquinte, India: tumba, Portuguese: colocíntida, Spanish: alhandal, coloquíntida, Swidish: kolokvint [2, 3].

Plants are often regarded as the most important resources for human medication and food, and organic molecules derived from flora have less side effects than chemical drugs. *Citrullus colocynthis* is a part of the Cucurbitaceae botanical family. It has been given the names coloquinte (French), bitter gourd, bitter apple, bitter cucumber (English), and Koloquinthe (German). Its alternate names all relate to the plant's bitterness. The sour taste of this plant is due to colocynthine, which is a crucial element. *Citrullus colocynthis* is a medicinal plant that is used alone or in combination for medicinal purposes in traditional medicine. The plant's root, leaf, pulp, and seed all have medicinal properties. The pulp of the fruit is the most useful in this regard. *Citrullus colocynthis* is found in Africa and Asia, including Iran's southeast, east, and southwest areas. Because of the importance of *Citrullus colocynthis* dietary and therapeutic properties, this study was carried out to investigate new evidence relating to *Citrullus colocynthis* pharmacological activities [4, 5].

BOTANICAL DISCRIPTION: -

C. colocynthis is a perennial plant with perpetual roots and angular, hard, rough, vine-like stems that extend out from the ground and can climb up. At the leaf axils, they develop a single yellow flower. They're monocious, with lengthy peduncles and a tuberous rootstock that produces trailing or hiking stems [3].

Roots and stem	Perennial roots, stems are angular, tough, and rough vine-like that spread on the ground and may climb up.
Seeds	Yellow to brown in color, smooth in texture, and oval in shape.
Flowers	A single yellow color flower at leaf axils. They are monoecious and have long peduncles.
Fruit	Angular and about 5-10 cm long. They are triangular, rough, and green

CHEMICAL COMPOSITION: -

The quantity of nutrients in plants must be determined in order to properly analyse their effects on humans. The chemical components of *Citrullus colocynthis* (L.) are mostly glycosides, which can be proteolytic enzymes hydrolyzed to create dihydroelatericin B (cucurbitacin L), elatericin B (cucurbitacin I), and elaterin (cucurbitacin E). Extracts of Caffeic acid, chlorogenic acid, and cucurbitacin E-, J-, and L-glucosides are also included. Quercetin extracts another combination from *Citrullus colocynthis*. *Citrullus coloccynthis* was also found to contain phenolic acids, flavonoids, fatty acids, tocopherols, and alkaloids [6].

TRADITIONAL USES: -

For hundreds of years, it has been widely utilized in traditional medicine. The colocynth has a variety of uses in traditional Arabian medicine, including as a laxative, diuretic, and treatment for insect stings. Colocynth powder was occasionally mixed with aloes, unguents, or bandages and applied externally. Troches made from colocynth were once known as "troches of alhandal" and they were used as an emetic. Colocynth sap was once used to treat camel skin outbreaks in ancient Arab veterinary medicine [7].

MEDICINAL PROPERTIES: -

Citrullus colocynthis is a fruit with an abundance of essential nutrients that can be used in medicine formulations to improve health and prevent nutritional deficiencies, according to several studies. *Citrullus colocynthis* has pharmacological capabilities as a result of its abundance of bioactive chemicals, which may help in the treatment of diseased conditions. These bioactive compounds have anti-inflammatory, anti-diabetic, anti-microbial, anti-bacterial, anti-carcinogenic, anti-ulcerogenic, hypolipidemic, hypoglycemia, and anti-oxidant properties, as well as hypolipidemic and hypoglycemic properties [8].

PHARMACOLOGICAL ACTIVITY: -

The species contains antidiabetic, antioxidant, anti-inflammatory, and analgesic properties, as well as anti-cancer and gastrointestinal effects.

ANTIDIBETIC:

Diabetes mellitus is one of the most well-known endocrine disorders in the world, according to current research. *Citrullus colocynthis* (*C. colocynthis*) is one of the most commonly used traditional plants to treat diabetes. It is well-known for its hypoglycemic effect, which is supported by current phytotherapy. Its undesirable consequences include gastrointestinal and urinary tract disturbances. This review article covers a wide range of blood glucose-lowering

studies that have been conducted to date. Roots, fruits, seeds, rinds, and leaves were among the flower parts used in extract management [9].

ANTIOXIDANT: -

The presence of massive amounts of phenolics and flavonoids was discovered during an initial phytochemical screening of the plant. Following that, in step with 100 g of fresh mass, quantification reported the existence of 0.74 percent (m/m) phenolics (calculated as gallic acid) and 0.13 percent (m/m) flavonoids (calculated as catechin equivalents) [10].

ANTI-INFLAMMATORY AND ANALGESIC: -

At various doses, all extracts showed essential analgesic and anti-inflammatory activities without producing any side effects. *Citrullus colocynthis* immature fruit and seed extracts were found to have analgesic and anti-inflammatory activities in this examination. The findings of the tests provide clinical insight on the use of *Citrullus colocynthis* Schrad. as an analgesic and anti-inflammatory agent in the history [11].

ANTICANCER EFFECT: -

In human breast cancer cell growth, the antiproliferative impact of cucurbitacin glycosides derived from *Citrullus colocynthis* leaves was studied. Cucurbitacin B/E glycosides were extracted from the leaves and separated from the extract [12].

GASTROINTESTINAL EFFECT: -

The anti-ulcerogenic activity of the *Citrullus colocynthis* seed methanolic extract was evaluated in Wistar albino rats using a pyloric ligation induced ulcers model. At a dose of 200 mg/kg, *Citrullus colocynthis* (200 mg/kg) demonstrated the maximum inhibition of gastric volume 1.680.18, free acid 39.863.86, and total acidity 61.231.87. At a dose of 200 mg/kg, the extract's greatest percent reduction of ulcerogenicity in a pyloric ligation model was 71.57 percent [5].

CONCLUSION

Citrullus colocynthis is reported as having anti-diabetic, antioxidant, anti-inflammatory, profibrinolytic, analgesic, anti-allergic, and anti-microbial properties in this overview article, although anti-diabetic activity is the most significant. It could also have an impact on the reproductive system and fertility. It appears that more study is needed to investigate the mechanism of this action.

REFERENCES

1. Ali Esmail Al-Snafi, Chemical constituents and pharmacological effects of *Citrullus colocynthis* - A review, Journal of IOSR Journal Of Pharmacy, 2016, 57-67.

2. Mohammad Saeed Kalantari Meybodi, Review on Pharmacological Activities of *Citrullus colocynthis* (L.) Schrad, journal of Asian Journal of Research and Reports in Endocrinology, 2020, 25-26.
3. Qin-Yuan Li , Mahzaib Munawar et al, *Citrullus colocynthis* (L.) Schrad (Bitter Apple Fruit): Promising Traditional Uses, Pharmacological Effects, Aspects, and Potential Applications, Journal of Pharmacology, 2022, 1-2.
4. Mohammad Saeed Kalantari Meybodi, Review on Pharmacological Activities of *Citrullus colocynthis* (L.) Schrad, Journal of Asian Journal of Research and Reports in Endocrinology, 2020, 26-28.
5. Ali Esmail Al-Snaf, Chemical constituents and pharmacological effects of *Citrullus colocynthis* - A review, Journal of IOSR Journal Of Pharmacy, 2016, 60-61.
6. Mohammad Saeed Kalantari Meybodi, Review on Pharmacological Activities of *Citrullus colocynthis* (L.) Schrad, Journal of Asian Journal of Research and Reports in Endocrinology, 2020, 26-27.
7. https://en.m.wikipedia.org/wiki/Citrullus_colocynthis
8. Aparajita Bhasin, Sanjay Singh, Rajesh Garg, Nutritional and medical importance of *Citrullus colocynthis* a review, Journal of plant, 2020 , 3402 -3403.
9. Chenghe Shi et al., A review on antidiabetic activity of *Citrullus colocynthis* Schrad, Acta Pol Pharm., 2014.
10. Sunil Kumar et al., Antioxidant and free radical scavenging potential of *Citrullus colocynthis* (L.) Schrad. methanolic fruit extract, Acta Pharm, 2008.
11. B Marzouk et al, Anti-inflammatory and analgesic activities of Tunisian *Citrullus colocynthis* Schrad. immature fruit and seed organic extracts. Eur Rev Med Pharmacol Sci. 2011.
12. Ali Esmail Al-Snaf, Chemical constituents and pharmacological effects of *Citrullus colocynthis* - A review, Journal of IOSR Journal of Pharmacy, 2016, 61-62.

ISSN 2349-7203
IJPPR
INTERNATIONAL JOURNAL OF PHARMACY & PHARMACEUTICAL RESEARCH
An official Publication of Human Journals
HUMAN

MEDICINAL PLANTS USED IN RHEUMATOID ARTHRITIS

Pratibha S. Gavarkar[1], Rajashree S. Chavan[2]

1. Dept. of Pharmaceutical Chemistry, Anandi Pharmacy College, Kalambe Tarf Kale Tal- Karveer, Dist- Kolhapur, Maharashtra, India.

2. Dept. of Pharmaceutical Chemistry, Seth Govind Raghunath Sable College of Pharmacy, Saswad, Tal- Purandar, Dist- Pune, Maharashtra, India.

ABSTRACT

Rheumatoid arthritis is a chronic, inflammatory disorder that can affect numerous tissues and organs, but predominantly attacks synovial joints. The activity develops an inflammatory response the sheath around the joints and the inflammation of synovial cells. The aim in this review is to assemble all obtained data on anti-arthritic activity of plants and natural products. Different plant species have been recognized as active services of phytochemicals with anti-arthritic properties.

Keywords*:* - Rheumatoid arthritis, anti-arthritic activity, herbal plant, inflammatory

INTRODUCTION

Arthritis is defined as inflammation of the joint. Rheumatoid arthritis (RA) is a ruining inflammatory and autoimmune disease that affects the joints but it cause is quite undetermined. In RA inflammation exhibits in the lining of joints inducing pain, enlargement, joint injury and its defect. It may infrequently comprise other internal organs, such as the nerves, eyes, lungs or heart. But RA is that, as it may mostly attacks the joints. The initial symptoms of RA may be not a detailed or exact, which involves feeling unwell or tired suffering in or around joints, fever and weight loss along with low appetite [1-4].

There is generally a 'stimulation' like an infection or environmental factor, which initiates or activates the genes. When the body subjected to this simulation the immune system responds improperly. Rather than protecting the joint the immune system starts to produce the substances that attack the joints and this result in to the development of rheumatoid arthritis. This paper reviews of some of the habitual and familiar herbs that have a history of human use and their anti-inflammatory or anti-arthritic properties. Primarily herbal plants are used both internally and externally. Plentiful number of herbal drugs is available which are used to reduce chronic joint inflammation [5-8].

In current years, preclinical trials have proved that natural plant extracts and compounds can remarkably relieve RA. Regarding the natural plan extracts and compounds medicines for the treatment of RA represents different systematic rules and functions, examining the potential of natural plant extract and compounds as a medicine for RA treatment will be helpful for RA patients.

NEED OF NATURAL REMEDIES IN RHEUMATOID ARTHRITIS

Since ancient times Indians rely more on natural sources of drugs. Natural remedies are still used in some tribal population, traditional medicinal practitioners are helpful in various diseases. According to WHO, the percentage of people using herbal treatments is about 80%. Also, such natural remedies are used in RA. These herbs can be taken as juice, infusion or with the daily diet to make desirable changes in the disease to beneficence of patients. [2]

EFFECT OF MEDICINAL PLANTS ON RHEUMATOID ARTHRITIS

1) *Boswellia serrata* and *Glycyrrhiza glabra* (liquorice)-

Biological name - *Boswellia serrata*

Common name – Indian frankincense

Family – Burseraceae

Part used - Bark

Biological name – *Glycyrrhiza glabra*

Common name - Liquorice

Family- Leguminosae

Part used - Root, bark

Glycyrrhiza glabra (liquorice) is a herb belongs to bean. Roots and rhizomes of this herb is used from centuries in traditional medicines for its anti-inflammatory, antiulcer, antimicrobial activities. [3] *Boswellia serrata* found in India, north Africa. Its active constituent that is β-boswellic acid in resin portion shows anti-inflammatory and antiarthritic activity.[4]A study conducted in which *Glycyrrhiza glabra* and *Boswellia serrata* combined for synergistic activity on rheumatoid arthritis. They showed good synergistic activity.[3]

2) *Strychnos potatorum* (Linn)

Biological name- *Strychnos potatorum*

Common name - katakam

Family - Loganiaceae

Part used - Seed

This medium sized tree is found in central and south part of India, Sri Lanka and Burma. Powder of seeds of this plant is useful to treat rheumatoid arthritis.[4] Its active constituents are alkaloids, lignin, glycosides, phenols, saponin, sterols and tannins present root, stem bark and seeds are responsible for its activity.[6]

3) *Cinnamomum zeylanicum* L-

Biological name– *Cinnamomum zeylanicum L*.

Common name - cinnamon

Family - lauraceae

Part used – Bark

Cinnamon grows in south India. Its main active constituent is cinnamaldehyde and terpenes. [3]. The Type-A procyanidin polyphenols that is TAPP which obtained by extracting the bark of cinnamon has shown the immunomodulatory effect and anti-inflammatory activity also proved to have effect in rheumatoid arthritis. [7]

4) *Justicia gendarussa* burm. F.-

Biological name- *Justicia gendarussa*

Common name – willow leaved Justicia

Family – Acanthaceae

Part used - leaves

Justicia gendarussa is rarely seen shrub grows in shade a fast growing. The main source country of this plant is China but it also found in forests of India and Sri Lanka. Leaves of the plants have been traditionally used in India in the treatment of different diseases like fever, rheumatism, arthritis. The leaves of this plant contain lignans as main constituents responsible for antiarthritic activity. Also ethanolic extract of the *Justicia gendarussa* found to be affective against rheumatoid arthritis. [5]

4) *Hibiscus platinifolius* Linn-

Biological name – *Hibiscus platinifolius*

Common name – maple leaved mallow

Family - malvaceae

Part used- leaves

Hibiscus platinifolius Linn is flowering plant from India and also Sri Lanka. The anti-arthritic activity of leaves of this plant. It is effective against Freund's complete adjuvant (FCA) and turpentine induced arthritis. Aqueous extract of the *Hibiscus platinifolius* Linn leaves are extracted and used. [1]

CONCLUSION

Rheumatoid arthritis is an autoimmune disease that includes painful inflammations in the joints. Because of great economical value the medicinal plants as natural remedies are used in the treatment of rheumatoid arthritis. It is an evident that plant extract has potential effects on such diseases.

REFERENCES –

1) Kavanaugh A, Cohen S, Cush JJ. The evolving use of tumor necrosis factor inhibitors in rrheumatoid arthritis. J Rheumatol. 2004;31(10):1881–1884.
2) Mishra NK, Bstia S, Mishra G, *et al.* Anti–arthritic activity of *Glycyrrhiza glabra, Boswellia serrata* and their synergistic activity in combined formulation studied in freund's adjuvant induced arthritic rats. J Pharm Educ Res. 2011;2(2):92–98.
3) Sanmugapriya E, Senthamil SP, Venkatarama S. Evaluation of antiarthritic activity of *Strychnos potatorum* Linn seeds in Freund's adjuvant Induced arthritic rat model. BMC Complement Altern Med. 2012;10:56.
4) Suha A, Ahmad D, Eyad Q, *et al.* Anti–Arthritic Activity of the Methanolic Leaf Extract of *Urtica pilulifera* L. on Albino Rats. American Journal of Pharmacology and Toxicology. 2011;6(1):27–32.
5) Surjeet S, Rohit S, Gurdarshan S, et al. Anti–inflammatory and anti–arthritic activity of the rhizome extract of *Polygonum viviparum* L. Spatula DD. 2011;1(4):225–232.
6) Sachin V, Subhash LB, Vishwaraman M, *et al.* Anti–inflammatory and Anti–arthritic activity of type–A procyanidine polyphenols from bark of *Cinnamomum zeylanicum* in rats. Food Science and Human Wellness.2013;2(2):59–67.
7) Mohammed MH, Mohammad SHK, Abul Hasanat, *et al.* Investigation Of *in vitro* anti–arthritic and membrane stabilizing activity of ethanol Extracts of three Bangladeshi plants. The Pharma Innovation Journal. 2015;4(1):76–80
8) Paval J, Kaitheri SK, Potu BK, *et al.* Anti–arthritic potential of the plant *Justicia gendarussa* Burm F. Clinics (Sao Paulo). 2009;64(4):357–362.

ISSN 2349-7203
IJPPR
INTERNATIONAL JOURNAL OF PHARMACY & PHARMACEUTICAL RESEARCH
An official Publication of Human Journals
HUMAN

LAGERSTROEMIA SPECIOSALS

Ms. Pratibha S. Gavarkar[1], Dr. R. S. Chavan[2]

1. Anandi Pharmacy College, Kalambe Tarf Kale, India.
2. Seth Govind Raghunath Sable College of Pharmacy, Saswad, India.

ABSTRACT

Sumatra, especially in the northern Liverworts family Lepidoziasi variety Sumatra Inadequate Report. Therefore, the aim of this study is to explore diversity Taman Eden 100 Natural Tourist Park, Lepidoziaceae in North Sumatra. Was explored the study runs along the hiking trails of the site. Species identification is based on these Morphological characters. Thirteen species of Lepidoziaceae were identified, of which 2 are Genus: Bazania (11 species), and Lepidozia (2 species). There were species of Lepidoziaceae found as epiphyte on tree trunks, decaying wood and soil. The most common species are found the study found Bazaniatridans, while Bazaniapectinata was a rare species.

Keywords*:* - Bazzania, Marchantiophyta, Diversity, Central Java.

INTRODUCTION

Lepidoziaceae is one of the largest family of leaf liverwort, with about 440 species worldwide, With 29 generations, 7 tribes were recorded in Java. This is the largest genus in the family Byzantium, there are about 100 species worldwide. There are species of Lepidoziaceae Distributed from the lowlands to the mountains and abundantly in the tropical forests. There is a family commonly found on tree trunks or tree branches and sometimes on moist soils, rocks and rotten soils Entries. Lepidosis can be distinguished from other families based on morphological characteristics as peanut branching (in Lepidozia, Kurzia and Telarania), Dicotomus branching (in Acromastigum) and Bazania), irregular with basal stolon (in hygrolembidium), rhizoid in tufts from lower base of leaves,the leaves are usually divided into lobes, with lower leaves (ventral leaves) and Gametoasia on small ventral branches [2]. The family has high morphological variability characters, especially of the Bazania genus, are therefore difficult to identify at the species level. The wide morphological variations are affected by environmental changes, including light intensity, Humidity and temperature. Several recent data on the liver of North Sumatra have been recorded. However, the release of the Lepidozygous family is very limited. Just a publication about from North Sumatra to the present Lepidoziasi, which is, has recorded 17 species of Aek.NauliParpat Forest. Furthermore, information on Lepidoziaceae species in Taman Eden 100 no natural park record. Therefore, it is important to do research to create a list species of Lepidoziaceae in Taman Eden 100 Natural Park, North Sumatra. *L. Speciosa* is a species that is widely commercialized as an ornamental fore and azalea. The horticultural acquisition of this species is highly appreciated for its large, attractive, pink to lavender flowers. *L. speciosa* has escaped cultivation and can now have a variety of amenities, including natural waste, fallow lands, open grasslands and amazement. It has diffuse crown and dense root system that has the ability to change soil conditions and prevent the formation of a wide range in the understory. It is currently a member in Belize, Costa Rica, Puerto Rico and Virgin I

Leaves –

Ethyl acetate extract of the leaves of *Lagerstroemia speciosa (LSL)* was investigated for possible antimicrobial-diabetic amylase and glucosidase inhibition. Six penticyclic triterpenes (oleanolic acid, arjunolic acid, asiatic acid, maslinic acid, corosolic acid and 23-hydroxyursolic acid) made LSL connectors. Their composition was determined by spectroscopic analysis and their α-glycosidase and α-amylase inhibitory drug analysis. They demonstrated that-amylase and moderate α-glucosidase were not inhibitory or weakly

inhibitory drugs. Corosolic acid, which seeks the best bioavailability against α-glucosidase (IC50 = 3.53 µg / mL), contributes the most to the α-glucosidase inhibitory regulation of EtOAcextract. The anti-diabetic action of 1% corosolic acid (Glucosol ™) certified extract from the leaves of Lagerstroemia speciosa has been shown in randomized clinical trials involving type II diabetics (non-insulin-dependent diabetes mellitus, NIDDM). Subjects received daily oral doses of Glucosol and blood glucose levels were measured. Taking Glucosol in daily doses of 32 and 48 mg for 2 weeks showed a significant reduction in blood glucose levels. The soft gel capsule formulation shows a 30% reduction in blood glucose levels compared to the hard gelatin capsule formulation (P <0.001) filled with glucosol ™ dry powder, indicating a 30% reduction in blood glucose levels, indicating that the bioavailability of the soft gel formulation is better. Dry powder formulation.

Antimicrobial Effects:

Seed extracts were tested for antibacterial effect against different bacterial organisms, some fractions of seed extracts of Lagerstroemia speciosa showed high antibacterial activity when tested against both Gram-positive and Gram-negative bacteria [42]. The methanolic extracts of Lagerstroemia speciosa leaves and barks were evaluated for their antimicrobial activity against 11 Gram- positive, Gram-negative bacteria and 3 fungi using disk diffusion technique. The average zone of inhibition exhibited by methanolic leaves and barks extracts (500µg/disc) was 10-20 mm and 12-21 mm respectively [43]. The Lagerstroemia speciosa leaf extracts were investigated for antibacterial and antibiofilm activities against potential clinical strains (Staphylococcus aureus, Escherichia coli, P. aeruginosa and Salmonella typhi) by well diffusion technique. The antibacterial property was also investigated against common food borne pathogens (Listeria monocytogenes and Bacillus cereus) at varied concentrations 250 to 1000 µg/ml. The antibiofilm assay was carried out from 250 to 1000µg/ml against P. aeruginosa by coverslip technique. Only minimum inhibition was seen in alcoholic extract for antibacterial activity, whereas all other extracts showed negligible activity. P. aeruginosa biofilm is inhibited to 93.0±2% and 91±2% at higher concentration (1000µg/ml) by methanolic and ethanolic extract respectively [44]. Antibacterial activity of ethanol and water extracts of leaves of Lagerstroemia speciosa were tested by plate agar diffusion method against Gram positive and Gram-negative bacteria. The MIC of ethanol and water extracts of leaves against Staphylococcus aureus: 14 and 15, Bacillus substiles: 12 and 15, Pseudomonas aeruginosa: 14 and 17, and Escherichia coli: 16 and 17 mm respectively. Water extract being the most effective [45]. The antimicrobial effect of the flowers extracts of Lagerstroemia

speciosa was studied against Gram positive bacteria (Bacillus cereus, Bacillusmegaterium, Bacillus subtilis, Staphylococcus aureus, Micrococcus luteus), Gram negative bacteria (Escherichia coli, Pseudomonas aeruginosa, Salmonella paratyphi, Salmonella typhi, Shigellaboydii, Shigelladysenteriae, Vibrio mimicus, Vibrio parahemolyticus) and Fungi (Saccharomyces cerevisiae, Aspergillusniger). Methanolic crude extract possessed an antimicrobial effect against all the tested microorganisms. The largest zone of inhibition (19 mm) was observed for the carbon tetrachloride soluble fraction against Staphylococcus aureus [46]. The antibacterial effect of the methanolic extract of Lagerstroemia speciosa leaves was investigated against Escherichia coli, Salmonella typhimurium, Staphylococcus aureus and Pseudomonas aeruginosa. The extract possessed high antibacterial activity against Escherichia coli (15 mm), Staphylococcus aureus (10 mm), Pseudomonas aeruginosa (10 mm), but had no activity against Salmonella typhimurium

Side effects and safety

The crude ethanol extract is non-toxic in rats, it was well tolerated at a concentration of 500, 1000, 2000, and 3000 mg/kg, no biochemical and histological changes were recorded [89]. In acute toxicity study, no mortality or toxic reaction was recorded in rats after administration of the methanolic crude extract of Lagerstroemia *speciosa* roots (200, 400, 800, 1600 and 3200 mg/kg, orally) [21]. There were no side effects in humans, with the use of the recommended dosages (8-48 mg/day). However, higher doses associated with lowered blood glucose levels, headache, dizziness, and fatigue [90]

Cardiovascular effects

The cardioprotective effect of Lagerstroemia speciosa leave extract (containing 1 % corosolic acid) was evaluated in isoproterenol- induced myocardial injury in mice. Extract pretreatment augmented myocardial antioxidant status and attenuated myocardial oxidative stress. Myocardial apoptosis, as well as MMPs activities, was significantly prevented by the extract pretreatment in isoproterenol-induced myocardial injury in mice. Furthermore, extract pretreatment enhanced the nuclear protein expression of Nrf2 [83].

CONCLUSION

A total of 13 species of Lepidoziasi in the Liverworts family were recorded from Taman Eden 100.Natural Park, North Sumatra, with 2 generations: Bazania (11 species) and Lepidozia (2 species). The most common species reported in the study was Bazaniaerosa. Is an unusual species reported Bazaniapectinata.

REFERENCE

1. Frey W, Stech M 2009 Marchantiophyta, Bryophyta, Anthocerotophyta. Syllabus of Plant Families Part 3. Gebrüder. Borntraeger. Berlin.
2. Gradstein SR 2011 Guide to the Liverworts and Hornworts of Java. Bogor. SeameoBiotrop. Gradstein SR 2017 Nova Hedwigia 105 (1-2) 243-266.
3. Gradstein SR, Churchill SP, Salazar-Allen N 2001. Guide to the Bryophytes of Tropical America. New York: The New York Botani

IJCRT.ORG ISSN : 2320-2882

INTERNATIONAL JOURNAL OF CREATIVE RESEARCH THOUGHTS (IJCRT)

An International Open Access, Peer-reviewed, Refereed Journal

FORMULATION AND EVALUATION OF HERBAL COUGH SYRUP BY USING POMEGRANATE PEELS

[1]POOJA PISAL*, [2]PRANALI A. ZENDE, [3]PRANOTI S. JADHAV, [4]POOJA PETKAR

[1]Assistant professor, [2]Student, [3]Student, [4]Assistant professor

Abstract :

The most common problem suffered by individuals everywhere over many centuries is cough. Coughing is the protective mechanism of the body. Coughs are classified further accordingly which are depending upon factors such as signs and symptoms, duration, type, character, etc. The most commonly used, prepared and popular dosage form to cure cough and cold is syrup. Syrup is a very popular dosage form of cough and cold medications, which eases patient compliance. By adding the decoction of herbal drugs with a base of honey is helpful to the formulation thick and preserve the formulation. The quality of the final herbal cough syrup was evaluated with parameters such as physical appearance colour, odour, taste, pH, and viscosity. It was found that antitussive activity produced by the herbal formulation in the minimum dose was much better than the standard drug.

Keywords : Herbal treatment, Cough, Antimicrobial activity, Honey base.

I. INTRODUCTION -

Health and nutrition are the most important factors in the human resources development of the country. Pomegranate (*Punica granatum*) is one of the oldest fruits and originates from Iran north to the Himalayas in India and is cultivated throughout the Mediterranean region in Asia, Africa and Europe. Early fall is the best time for pomegranates in October and November in the northern hemisphere, but they are usually available in early winter. Pomegranate is also a good source of many essential substances Vitamin B complexes such as pantothenic acid (vitamin B-5), folates, pyridoxine and vitamin K and minerals such as calcium, copper, potassium and manganese[1].

The peels of this fruit make up 26-30% of the total weight of the fruits and they cover the internal membranes. The astringent effect is due to the skin (pericarp). Despite the large number of polyphenolic compounds and beneficial biological effects of pomegranate peel (PP), unfortunately, it is often treated as waste and thrown away. Phenolic compounds such as anthocyanins, ellagic acid glycosides, free ellagic acidification, ellagitannins, punicalagin, punicalin and gallotannins are found deep in the PP. Pomegranate Peel Extract (PPE) is rich in phenols, flavonoids and tannins, which is why it has found an important place in providing by-product pomegranate juice-related preparations to the food industry[2]. They also contain many antioxidants, antivirals, anti-cancer and anti-tumor properties and these antioxidants are equally high, able to protect low-density lipoproteins LDL cholesterol against oxidation and reduces the risk of cancer and heart

disease. It attracts attention because of its obvious wound healing properties and immunomodulatory effects[1].

fig 1 : bioactive components present in the pomegranate peel[2] -

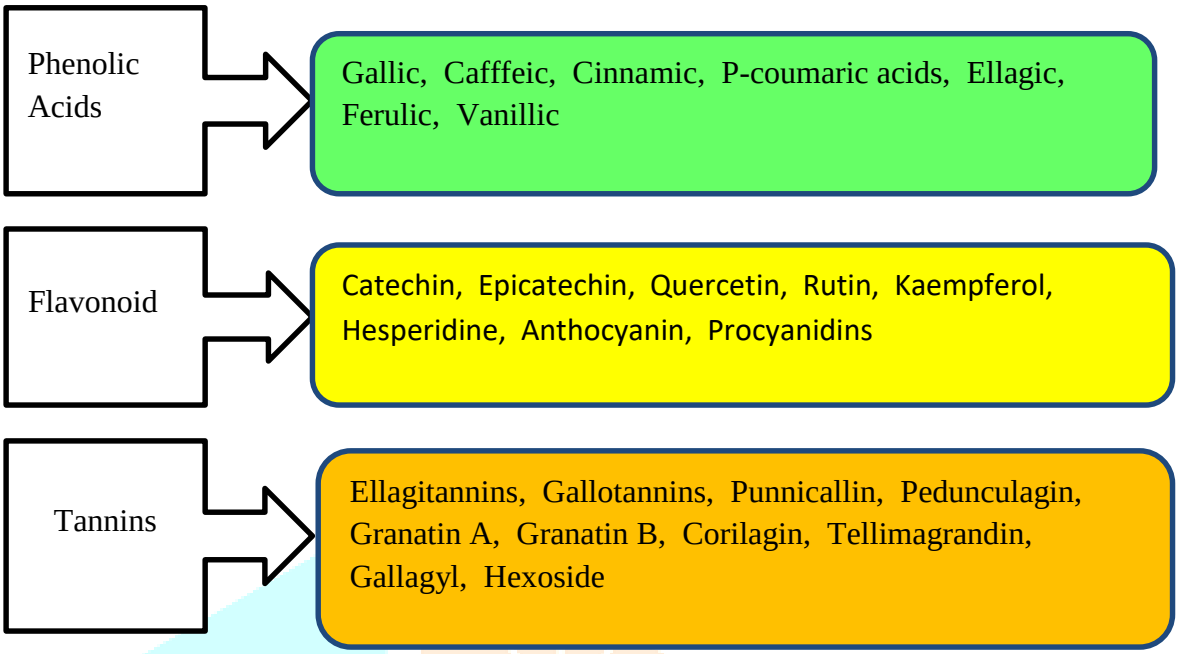

table 1 : classification of cough[3] -

Sr. No.	Types of cough	Properties
1.	Acute cough	Not more than three weeks duration
2.	Chronic cough	More than three weeks
3.	Dry cough	No mucous or secretion
4.	Wet cough	With mucous or secretion
5.	Cough from chest and throat	Productive or non – productive
6.	Paroxysmal	Spasmodic and recurrent
7.	Bovine cough	Soundless cough due to paralysis or larynx
8.	Psychogenic cough	Self – conscious activity of the patient to draw attention

Herbal treatment for cough :

The most popular antitussive is a medicinal plant treatment. Herbal preparations play an important role in improving the health sector. Herbal remedies used for mild to severe health disorders include asthma, tuberculosis, cough, pneumonia, kidney diseases, cancer, diabetes, allergies, lung cancer and viral infections. WHO estimates 80 per cent of the population even use herbal medicines in primary health care standards Medicinal plants have always been used, e.g. with traditional primary providers and especially in Asian countries. The main use of herbal medicines is prescribed chronic health promotion and therapy, for differently conditions that are life-threatening. Most of the synthetic drug treatments used cause a lot of side effects such as vomiting, nausea, sedation, allergies, respiratory infections, change in appetite, irritability,

drowsiness, addiction and overload can damage organs or parts of organs. In recent years, researchers have done focusing mainly on herbal medicines and herbal medicines with less or no side effects during and after treatment[4].

Fig 2.

Fig 3.

Table 2: methods and materials[5] -

Sr. No.	Material	Uses
1	Pomegranate peel	Antitussive
2	Clove	Expectorant
3	Tulsi	Antitussive
4	Fennel	Flavouring agent
5	Black pepper	Preservative
6	Honey	Base

Extraction of pomegranate peels[6] :

The soxhlet extraction meth**o**d is commonly used to extract compound from solid materials, such as pomegranate peel. Here's a basic overview of the process -

- Grind the pomegranate peel into small particles to increase the surface area for extraction.
- Weigh the ground pomegranate peel to accurately determine the amount used in the extraction.
- Place the ground peel into a thimble, which is a small cylindrical container typically made of filter.
- Set up the soxhlet apparatus, consisting of a round bottom flask, a condenser, and a soxhlet extractor. The thimble with the packed peel was placed in the soxhlet extractor.
- Use a suitable solvent (e.g. ethanol, distilled water) in the round bottom flask. The solvent will continuously cycle through the extractor, extracting compounds from the pomegranate peel. Add a mixture of ethanol and water as a solvent in a ratio 1:1.

- Apply heat to the round bottom flask for 12 hours, causing the solvent to evaporate and rise into the soxhlet extractor. The solvent extracts compounds from the pomegranate peel and then drips back into the round bottom flask.
- The process continues in a cyclical manner, with the solvent cyclic through the extraction thimble until a concentrated extract is obtained.
- Collect the extracted solution in a round bottom flask.
- Remove the solvent from the collected solution using techniques like rotary evaporation to obtain the concentrated extract.
- Store the extract in a proper container.

Extraction of Tulsi :

Leaves of *Ocimum sanctum L*. tulsi were collected from different sites and washed with sterile water, 50g of tulsi was placed in the thimble of soxhlet apparatus with 50ml of water and 50 ml of ethanol over 24 hours[7].

Extraction Process of Decoction of Fennel, Clove :

Take 5-7 gm of each herbal ingredient. Herbs were mixed using 500ml of water. Attach reflux condenser and material was boiled carefully by using a water bath for 3 hrs. Boil until the total volume becomes one-fourth part of the previous. Then the liquid was cooled and filtered[7].

Extraction of Black pepper :

The pepper was dried and ground to a fine powder and approximately 10 g was placed in a soxhlet thimble and then extracted using 100 ml of ethanol for 240 minutes[8].

Table 3 : formulation for 15 ml -

Sr. no.	Ingredient	Quantity
1	Pomegranate peel	5ml
2	Clove	1.5 ml
3	Tulsi	3 ml
4	Fennel	1.5 ml
5	Black pepper	1 ml
6	Honey	3 ml

Evaluation parameters :

a) Colour examination [9]:

2ml of prepared syrup was taken on watch glass and it was placed under white tube light. Then colour was observed.

b) Odour examination :
2ml of prepared syrup was taken and smelled by an individual.

c) Taste examination[9]:
Pinch of final syrup was taken and examined the taste buds of the tongue.

d) pH examination[9] :
Steps -
1) The glass electrode is washed with distilled water and cleaned.
2) Place the electrode in the pH 7 buffer solution and set the pH meter to 7 by turning the calibration knob on the meter .
3) The electrode was removed, washed with distilled water and cleaned.
4) The inserted electrode was in a buffer solution of pH 4. Adjust the value.
5) The electrode was then placed in the final syrup and the pH was monitored .

e) Density examination[9] :
Steps –
1) Cleaned the specific gravity bottle.
2) The bottle was cleaned at least two times with distilled water.
3) Measured the weight of empty dry bottle syrup with stopper (w1).
4) The bottle was filled with final syrup and the stopper, wipe out excess syrup from outside the tube.
5) Measure the weight in grams of syrup(w2).
6) Calculate weight in grams of syrup(w3).
7) Formula of density :

$$\text{density of liquid under test (syrup)} = \frac{\text{weight of syrup under test}}{\text{volume of final syrup under test}}$$

f) Viscosity examination[10] :

Steps-

1) An organic solvent such as acetone.
2) Mount the viscometer in a vertical position on a suitable stand.
3) Fill water in a dry viscometer up to mark G.
4) Count time required, in seconds for water to flow from mark A to mark B.
5) Repeat step 3 at least 3 times to obtain accurate reading.
6) Rinse the viscometer with test liquid and then fill it up to mark A, and find out the time required for liquid to flow to mark B.
7) Determination of densities of liquid as mentioned in the density determination experiment

Formula:

$$\text{viscosity} = \frac{\text{density of test liquid} \times \text{time required to flow test liquid}}{\text{density of water} \times \text{time required to flow water}} \times \text{viscosity of water}$$

g) Determination of antimicrobial activity[11] :

The agar plate method was used to examine the antimicrobial activity of the herbal cough syrup. The test compound (50µL) was introduce in the well. The plate was incubated over night at room temperature. The antimicrobial spectrum of the extract was determine for the bacterial species in terms of zone sizes around the well.

Fig 4 : MIC against E.Coli

Result :

The results obtained in this study suggest that herbal formulations prepare and possess anti-microbial activity, the component of herbal cough formulation was selected due to their reported action that plays preventive and curative role in the prevention of cough. The syrup prepared passes all physical parameters and shows significant anti-microbial activity.

Table 4 : Result of Physicochemical parameters of developed herbal syrup -

Sr.no.	Parameter	Observation value
1.	Color	Reddish brown
2.	Odour	Sweet aromatic
3.	Taste	Sweet
4.	pH	5.9
5.	Viscosity	0.029 P
6.	Density	0.77 g/cm^3

Table 5: The antimicrobial activity and MIC of the prepared extract

Test bacteria	Zone of inhibition (mm)	
	50µL	Positive
E-coli	3	13

Conclusion :

In conclusion, our study showed that Pumica granatum showed antitussive activity and a satisfactory result was found. Pumica granatum has no adverse effects comparable to chemical drugs. Hence, it has the potential to be used as a cheap, non-toxic formulation for standard antitussive activity. This is an in-vitro study, the data of which can be useful for further studies on animals and then eventually on human beings. Pumica granatum has no adverse effects comparable to chemical drugs. Hence, it has the potential to be used as a cheap, non-toxic formulation for standard antitussive activity. This study will help us understand cough and measures to prevent cough. This study helps us understand the effectiveness of herbal cough syrups compared to chemical-based syrups This is an in-vitro study, the data of which can be useful for further studies on animals and then eventually on human beings.

Acknowledgement :

The authors express gratitude to the Principal, Dr. R.S . Chavan, Seth Govind Raghunath Sable College of Pharmacy, Saswad, Department of Chemistry for providing facilities required for the article, also thankful to Ms. Pooja Pisal for providing consistent support and timely guidance.

Reference

1 Sayeeda Fathima, Yamuna Devi Puraikalan, 2015, Developement of food products using pomegranate skin, International Journal of Science and Research (IJSR), Page no- 1756-1757.

2 Yaxian Mo, Jiagi Ma, Wentao Gao, leizhang Jiangui Li, Jingaming and Jiachen zang, 09 June 2022 Volume – 09, Pomegranate peel as a source of bioactive compounds: a mini review on their physiological function.

3 Ankush Ganpat patil, Kaivalya Gajanan, Mirajkar, Prnav Laxamn Savekar, Chetana V. Bugadikattikar, Somesh S. Shintre, 2020, Formulation and evaluation of ginger macerated honey base herbal cough syrup, Internantional journal of innovative science and research technology page no. 582-588, Classification of cough.

4 Pratikeshwar Panda, Arpita Sahu 2023, Formulation and evaluation of cough syrup, Asian Journal of herbal pharmaceutical research and development, page no 28-32 (herbal treatment for cough).

5 S.C Kushwaha, M.B.Bira and Pradyuman Kumar, Nov-Dec 2013, Nutritional composition of detanninated and fresh pomegranate peel powder (material and methods) Page no- 38-41.

6 Jing chen chuhling Liao, Xiaolu Ouyang, Ibrahim Kahramanoglu, Yudi Gan, and 4 Nov 2020, Antimicrobial activity of pomegranate peel and its application on food preservation (the extract process of pomegranate peel).

7 Miss. Priya D. Khode, Rupali R. Singanjude, Urwashi D. Lanjewar, Formulation and Evaluation of herbal Cough Syrup, Journal of Critical Reviews, Vol 06, Issue 03, 2019.

8 H. G., Matena, Z.N., Kariuki and B.C., Ongarora OPTIMIZATION OF PIPERINE EXTRACTION FROM BLACK PEPPER (PIPER NIGRUM) USING DIFFERENT SOLVENTS FOR CONTROL OF BEDBUGS.

9 Dr. Javesh K. Patil, Dipali R. Mali*, Komal R. More and Shraddha M. Jain. FORMULATION AND EVALUATION OF HERBAL SYRUP, World Journal of Pharmaceutical Research Volume 8, Issue 6, 1061-1067.

10 Krishna Suresh Gupta, Yatin Nitin Gorhekar , Pratiksha Subhash Gharat , Maheshwari Ashok Gawari , Saroj Changdev Firke Formulation and Evaluation of Herbal Syrup , International Journal of Research Publication and Reviews Vol 4, no 6, pp 3300-3304 June 2023

11 Vikash Sharma, Saurabh Singh , Arushi Dixit and Alka Saxena FORMULATION AND EVALUATION OF HERBAL COUGH SYRUP FROM SEEDS EXTRACT OF HEDGE MUSTARD , INTERNATIONAL JOURNAL OF RESEARCH IN PHARMACY AND CHEMISTRY 2020, 10(1), 1-10